Advanced Solid State Physics

Version 2009:
Michael Mayrhofer-R., Patrick Kraus, Christoph Heil, Hannes Brandner,
Nicola Schlatter, Immanuel Mayrhuber, Stefan Kirnstötter,
Alexander Volk, Gernot Kapper, Reinhold Hetzel
Version 2010: Martin Nuss
Version 2011: Christopher Albert, Max Sorantin, Benjamin Stickler
Version 2016: Andreas Jeindl, Lukas Hoermann

TU Graz, SS 2016

Lecturer: Univ. Prof. Ph.D. Peter Hadley

Contents

1 Introduction

1.1 What is Solid State Physics

Solid state physics is (still) the study of how atoms arrange themselves into solids and what properties these solids have.

The atoms arrange in particular patterns because the patterns minimize the energy in a binding, which is typically with more than one neighbor in a solid. An ordered (periodic) arrangement is called **crystal**, a disordered arrangement is called **amorphous**.

All the macroscopic properties like electrical conductivity, color, density, elasticity and more are determined by and can be calculated from the microscopic structure.

1.2 Schrödinger Equation

The framework of most solid state physics theory is the **Schrödinger equation** of non relativistic quantum mechanics:

$$i\hbar\frac{\partial\Psi}{\partial t} = \frac{-\hbar^2}{2m}\nabla^2\Psi + V(\mathbf{r},t)\Psi \qquad (1)$$

The most remarkable thing is the great variety of **qualitativly different solutions** to Schrödinger's equation that can arise. In solid state physics you can calculate all properties with the Schrödinger equation, but the equation is intractable and can be only solved with approximations.

For solving the equation numerically for a given system, the system and therewith Ψ are discretized into cubes of the relevant space. To solve it for an electron, about 10^6 elements are needed. This is not easy, but possible. But let's have a look at an other example:
For a gold atom with 79 electrons there are (in three dimensions) $3 \cdot 79$ terms for the kinetic energy in the Schrödinger equation. There are also 79 terms for the potential energy between the electrons and the nucleus. With the interaction of the electrons there are additionally $\frac{79 \cdot 78}{2}$ terms. So the solution for Ψ would be a complex function in 237(!) dimensions. For a numerically solution we have to discretize each of these 237 axis, let's say in 100 divisions. This would give $100^{237} = 10^{474}$ hyper-cubes, where a solution is needed. That's a lot, because there are just about 10^{68} atoms in the Milky Way galaxy!
Out of this it is possible to say:

The Schrödinger equation explains everything but can explain nothing.

Out of desperation: The model for a solid is simplified until the Schrödinger equation can be solved. Often this involves neglecting the electron-electron interactions. Back to the example of the gold atom this means that the resulting wavefunction is considered as a product of hydrogen wavefunctions. Because of this it is possible to solve the new equation exactly. The total wavefunction for the electrons must obey the Pauli exclusion principle. The sign of the wavefunction must change when two electrons are exchanged. The antisymmetric N electron wavefunctioncan can be written as a **Slater determinant**:

$$\Psi(\mathbf{r_1}, \mathbf{r_2}, ..., \mathbf{r_N}) = \frac{1}{\sqrt{N!}} \begin{vmatrix} \Psi_1(\mathbf{r_1}) & \Psi_1(\mathbf{r_2}) & \dots & \Psi_1(\mathbf{r_N}) \\ \Psi_2(\mathbf{r_1}) & \Psi_2(\mathbf{r_2}) & \dots & \Psi_2(\mathbf{r_N}) \\ \vdots & \vdots & \ddots & \vdots \\ \Psi_N(\mathbf{r_1}) & \Psi_N(\mathbf{r_2}) & \dots & \Psi_N(\mathbf{r_N}) \end{vmatrix} \tag{2}$$

Exchanging two columns changes the sign of the determinant. If two columns are the same, the determinant is zero. There are still $N!$, in the example 79! ($\approx 10^{100} = 1$ *googol*) terms.

2 Quantisation

For the quantization of a given system with **well defined equations of motion** it is necessary to **guess a Lagrangian** $L(q_i, \dot{q}_i)$, i.e. to construct a Lagrangian by inspection. q_i are the positional coordinates and $\dot{q}_i$ the generalized velocities.

With the **Euler-Lagrange equations**

$$\frac{d}{dt}\frac{\partial L}{\partial \dot{q}_i} - \frac{\partial L}{\partial q_i} = 0 \tag{3}$$

it must be possible to come back to the equations of motion with the constructed Lagrangian.[1]

The next step is to **get the conjugate variable** p_i:

$$p_i = \frac{\partial L}{\partial \dot{q}_i} \tag{4}$$

Then the **Hamiltonian** has to be derived with a Legendre transformation:

$$H = \sum_i p_i \dot{q}_i - L \tag{5}$$

Now the **conjugate variables have to be replaced by the given operators in quantum mechanics**. For example the momentum p with

$$p \to -i\hbar\nabla.$$

Now the Schrödinger equation

$$H\Psi(q) = E\Psi(q) \tag{6}$$

is ready to be evaluated.

2.1 Harmonic Oscillator

The first example how a given system can be quantized is a one dimensional harmonic oscillator. It's assumed that just the equation of motion

$$m\ddot{x} = -kx$$

with m the mass and the spring constant k is known from this system. Now the Lagrangian L must be constructed by inspection:

$$L(x, \dot{x}) = \frac{m\dot{x}^2}{2} - \frac{kx^2}{2}$$

---

[1] There is no standard procedure for constructing a Lagrangian like in classical mechanics where the Lagrangian is constructed with the kinetic energy T and the potential U:

$$L = T - U = \frac{1}{2}m\dot{x}^2 - U$$

The mass m is the big problem - it isn't always as well defined as for example in classical mechanics.

It is the right one if the given equation of motion can be derived by the Euler-Lagrange eqn. (3), like in this example. The next step is to get the conjugate variable, the generalized momentum p:

$$p = \frac{\partial L}{\partial \dot{x}} = m\dot{x}$$

Then the Hamiltonian has to be constructed with the Legendre transformation:

$$H = \sum_i p_i \dot{q}_i - L = \frac{p^2}{2m} + \frac{kx^2}{2}.$$

With replacing the conjugate variable p with

$$p \to -i\hbar \frac{\partial}{\partial x}$$

because of position space[2] and inserting in eqn. (6) the Schrödinger equation for the one dimensional harmonic oscillator is derived:

$$-\frac{\hbar^2}{2m}\frac{\partial^2 \Psi(x)}{\partial x^2} + \frac{kx^2}{2}\Psi(x) = E\Psi(x)$$

2.2 Magnetic Flux

The next example is the quantization of magnetic flux in a superconducting ring with a Josephson junction and a capacitor parallel to it (see fig. 1). The equivalent to the equations of motion is here the equation for current conservation:

$$C\ddot{\Phi} + I_C sin\left(\frac{2\pi\Phi}{\Phi_0}\right) = -\frac{\Phi - \Phi_e}{L_1}$$

What are the terms of this equation? The charge Q in the capacitor with capacity C ist given by

$$Q = C \cdot V$$

with V as the voltage applied. Derivate this equation after the time t gives the current I:

$$\dot{Q} = I = C \cdot \dot{V}$$

With Faraday's law $\dot{\Phi} = V$ (Φ as the magnetic flux) this gives the first term for the current through the capacitor

$$I = C \cdot \ddot{\Phi}.$$

The current I in a Josephson junction is given by

$$I = I_c \cdot sin\left(\frac{2\pi\Phi}{\Phi_0}\right)$$

---

[2] position space: Ortsraum

with the flux quantum Φ_0, which is the second term. The third term comes from the relationship between the flux Φ in an inductor with inductivity L_1 and a current I:

$$\Phi = L_1 \cdot I$$

With the applied flux Φ_e and the flux in the ring this results in

$$I = \frac{\Phi - \Phi_e}{L_1},$$

which is the third term.

In this example it isn't as easy as before to construct a Lagrangian. But luckily we are quite smart and so the right Lagrangian is

$$L(\Phi, \dot{\Phi}) = \frac{C\dot{\Phi}^2}{2} - \frac{(\Phi - \Phi_e)^2}{2L_1} + E_j cos\left(\frac{2\pi\Phi}{\Phi_0}\right).$$

The conjugate variable is

$$\frac{\partial L}{\partial \dot{\Phi}} = C\dot{\Phi} = Q.$$

Then the Hamiltonian via a Legendre transformation:

$$H = Q\dot{\Phi} - L = \frac{Q^2}{2C} + \frac{(\Phi - \Phi_e)^2}{2L_1} - E_j cos\left(\frac{2\pi\Phi}{\Phi_0}\right)$$

Now the replacement of the conjugate variable, i.e. the quantization:

$$Q \to -i\hbar\frac{\partial}{\partial\Phi}$$

The result is the wanted Schrödinger equation for the given system:

$$-\frac{\hbar^2}{2C}\frac{\partial^2\Psi(\Phi)}{\partial\Phi^2} + \frac{(\Phi - \Phi_e)^2}{2L_1}\Psi(\Phi) - E_j cos\left(\frac{2\pi\Phi}{\Phi_0}\right)\Psi(\Phi) = E\Psi(\Phi)$$

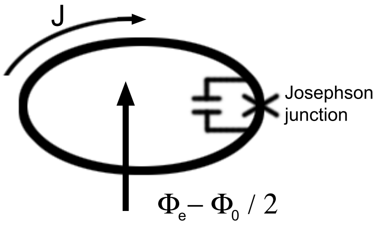

Figure 1: Superconducting ring with a capacitor parallel to a Josephson junction

2.3 Charged particle in a magnetic field (with spin)

For now we will neglect that the particle has spin, because in the quantisation we will treat the case of a constant magnetic field pointing in the z-direction. In this simplified case there is no contribution to the force from the spin interaction with the magnetic field (because it only adds a constant to the Hamiltonian which does not affect the equation of motion).
We start with the equation of motion of a charged particle (without spin) in an EM-field, which is given by the Lorentz force law.

$$\mathbf{F} = m\frac{\partial^2 \mathbf{r}(t)}{\partial t^2} = q(\mathbf{E} + \mathbf{v} \times \mathbf{B}) \tag{7}$$

One can check that a suitable Lagrangian is

$$L(\mathbf{r}, t) = \frac{m\mathbf{v}^2}{2} - q\phi + q\mathbf{v} \cdot \mathbf{A} \tag{8}$$

where ϕ and $\mathbf{A}$ are the scalar and vector Potential, respectively. From the Lagrangian we get the generalized momentum (canonical conjugated variable)

$$\begin{aligned} p_i &= \frac{\partial L}{\partial \dot{r}_x} = mv_x + qA_x \\ \mathbf{p} &= m\mathbf{v} + q\mathbf{A} \\ \mathbf{v}(\mathbf{p}) &= \frac{1}{m}(\mathbf{p} - q\mathbf{A}) \end{aligned} \tag{9}$$

The conjugated variable to position has now two components, the first therm in eqn.(9) $m\mathbf{v}$ which is the normal momentum. The second term $q\mathbf{A}$ which is called the field momentum. It enters in this equation because when a charged particle is accelerated it also creates a Magnetic field. The creation of the magnetic field takes some energy, which is then conserved in the field. When one then tries to stop the moving particle one has to overcome the kinetic energy plus the energy that is conserved in the magnetic field, because the magnetic field will keep pushing the charged particle in the direction it was going (this is when you get back the energy that went into creating the field, also called self inductance).

To construct the Hamiltonian we have to perform a Legendre transformation from the velocity $\mathbf{v}$ to the generalized momentum $\mathbf{p}$.

$$\begin{aligned} H &= \sum_{i=1}^{3} p_i v_i(p_i) - L(\mathbf{r}, \mathbf{v}(\mathbf{p}, t) \\ H &= \mathbf{p} \cdot \frac{1}{m}(\mathbf{p} - q\mathbf{A}) - \frac{1}{2m}(\mathbf{p} - q\mathbf{A})^2 + q\phi - \frac{q}{m}(\mathbf{p} - q\mathbf{A}) \cdot \mathbf{A} \end{aligned}$$

Which then reduces to

$$H = \frac{1}{2m}(\mathbf{p} - q\mathbf{A})^2 + q\phi \tag{10}$$

Eqn.(10) is the Hamiltonian for a charged particle in an EM-field without Spin. The QM Hamiltonian of a single Spin in a magnetic field is given by

$$H = -\hat{\mathbf{m}} \cdot \mathbf{B} \tag{11}$$

where

$$\hat{\mathbf{m}} = \frac{2g\mu_B}{\hbar}\hat{\mathbf{S}} \tag{12}$$

$\mu_B = \frac{g\hbar}{2m}$ the Bohr Magnetron and $\hat{\mathbf{S}}$ is the QM Spin operator. By Replacing the momentum and location in the Hamiltonian by their respective QM operators we obtain the QM Hamiltonian for our System

$$\hat{H} = \frac{1}{2m}(\hat{\mathbf{p}} - q\mathbf{A}(\hat{\mathbf{r}}))^2 + q\phi(\hat{\mathbf{r}}) - \frac{2g\mu_B}{\hbar}\hat{\mathbf{S}} \cdot \mathbf{B}(\hat{\mathbf{r}}) \tag{13}$$

We consider the simple case of constant magnetic field pointing in the z-direction $\mathbf{B} = (0, 0, B_z)$ and $\phi = 0$. Plugging this simplifications in eqn.(13) yields

$$\hat{H} = \frac{1}{2m}(\hat{\mathbf{p}} - q\mathbf{A}(\hat{\mathbf{r}}))^2 - \frac{2g\mu_B}{\hbar}B_z\hat{S}_z \equiv \hat{H}_1 + \hat{S} \tag{14}$$

We see that the Hamiltonian consists of two non interacting parts $\hat{H}_1 = \frac{1}{2m}(\hat{\mathbf{p}} - q\mathbf{A}(\hat{\mathbf{r}}))^2$ and $\hat{S} = -\frac{2g\mu_B}{\hbar}B_z\hat{S}_z$. The state vector of an electron consists of a spacial part and a Spin part

$$|\Psi\rangle = |\psi_{Space}\rangle \otimes |\chi_{Spin}\rangle$$

Where the Symbol $\otimes$ denotes a so called tensor product. The Schroedinger equation reads

$$\begin{aligned}(\hat{H}_1 \otimes \hat{\|} + \hat{S} \otimes \hat{\|})|\psi_{Space}\rangle \otimes |\chi_{Spin}\rangle &= E|\psi_{Space}\rangle \otimes |\chi_{Spin}\rangle \\ \hat{H}_1|\psi\rangle \otimes |\chi\rangle + |\psi\rangle \otimes \hat{S}|\chi\rangle &= E|\psi\rangle \otimes |\chi\rangle \end{aligned} \tag{15}$$

From eqn.(14), we see that the Spin part is essentially the S_z operator. It follows that the Spin part of the state vector is $|\chi\rangle = |\pm z\rangle$. Thus, we have

$$\hat{S}|\chi\rangle = -\frac{2g\mu_B}{\hbar}B_z\hat{S}_z|\pm z\rangle = \mp g\mu_B B_z|\pm z\rangle \tag{16}$$

where we used $\hat{S}_z|\pm z\rangle = \pm\frac{\hbar}{2}$. Using eqn.(16), we can rewrite the Schroedinger equation, eqn.(15), resulting in

$$\begin{aligned} &\hat{H}_1|\psi\rangle \otimes |\pm z\rangle \mp |\psi\rangle \otimes g\mu_B B_z|\pm z\rangle = E|\psi\rangle \otimes |\pm z\rangle \\ &\qquad \hat{H}_1|\psi\rangle \otimes |\pm z\rangle = (E \pm g\mu_B B_z)|\psi\rangle \otimes |\pm z\rangle \equiv E'|\psi\rangle \otimes |\pm z\rangle \end{aligned} \tag{17}$$

Where we define $E' = E \pm g\mu_B B_z$. In order to obtain a differential equation in space variables, we multiply eqn.(17) by $\langle \mathbf{r}| \otimes \langle\sigma|$ from the left.

$$\begin{aligned} &(\langle \mathbf{r}| \otimes \langle\sigma|)(\hat{H}_1|\psi\rangle \otimes |\pm z\rangle) = E'(\langle \mathbf{r}| \otimes \langle\sigma|)(|\psi\rangle \otimes |\pm z\rangle) \\ &\qquad \langle \mathbf{r}|\hat{H}_1|\psi\rangle\langle\sigma|\pm z\rangle = E'\langle \mathbf{r}|\psi\rangle\langle\sigma|\pm z\rangle \end{aligned} \tag{18}$$

Canceling the Spin wave function $\langle\sigma|\pm z\rangle$ on both sides of eqn.(18) and plugging in the definition $\hat{H}_1 = \frac{1}{2m}(\hat{\mathbf{p}} - q\mathbf{A}(\hat{\mathbf{r}}))^2$ from eqn.(15) yields

$$\frac{1}{2m}(\hbar\nabla + q\mathbf{A}(\mathbf{r}))^2\psi(\mathbf{r},t) = E'\psi(\mathbf{r},t) \tag{19}$$

For a magnetic field $\mathbf{B} = (0, 0, B_z)$ we can choose the vector potential $\mathbf{A}(\mathbf{r}) = B_z x\mathbf{y}$ (this is called Landau gauge). Using the Landau gauge and multiplying out the square leaves us with

$$\frac{1}{2m}(-\hbar^2(\frac{\partial^2}{\partial x^2} + \frac{\partial^2}{\partial y^2} + \frac{\partial^2}{\partial z^2}) + 2i\hbar q B_z x\frac{\partial}{\partial y} + q^2B_z^2x^2)\psi = E'\psi \tag{20}$$

In eqn.(20) only x appears explicitly, which motivates the ansatz

$$\psi(\mathbf{r},t) = e^{i(k_z z + k_y y)}\phi(x) \tag{21}$$

After plugging this ansatz into eqn.(20), we get

$$\frac{1}{2m}(-\hbar^2\phi'' + \hbar^2(k_y^2 + k_z^2)\phi - 2\hbar q B_z k_y x\phi + q^2B_z^2x^2\phi) = E'\phi \tag{22}$$

By completing the square we get a term $-\hbar^2k_y^2$ which cancels with the one already there and we are left with

$$\begin{aligned} &\frac{1}{2m}(-\hbar^2\phi'' + \hbar^2k_z^2\phi + (qB_z x - \hbar k_y)^2\phi) = E'\phi \\ &\qquad \frac{1}{2m}(-\hbar^2\phi'' + q^2B_z^2(x - \frac{\hbar k_y}{qB_z})^2\phi) = (E' - \frac{\hbar^2k_z^2}{2m})\phi \equiv E''\phi \\ &\qquad -\frac{\hbar^2}{2m}\phi'' + \frac{1}{2}m\frac{q^2B_z^2}{m^2}(x - \frac{\hbar_y}{qB_z})^2 = E''\phi \end{aligned} \tag{23}$$

We see that the z-part of the Energy $E_z = \frac{\hbar^2k_z^2}{2m}$ is the same as for a free electron. This is because a constant magnetic field pointing in the z-direction leaves the motion of the particle in the z-direction unchanged. Comparing eqn.(23) to the equation of a harmonic oscillator

$$-\frac{\hbar}{2m}\phi'' + \frac{1}{2}m\omega^2(x - x_o)^2 = E\phi \tag{24}$$

with energies $E_n = \hbar\omega(n + \frac{1}{2})$, we obtain

$$\begin{aligned}
E''_n &= \hbar\frac{qB_z}{m}(n + \frac{1}{2}) \\
E'_n &= \hbar\frac{qB_z}{m}(n + \frac{1}{2}) + \frac{\hbar^2 k_z^2}{2m} \\
E_n &= \hbar\frac{qB_z}{m}(n + \frac{1}{2}) + \frac{\hbar^2 k_z^2}{2m} \mp g\mu_B B_z
\end{aligned} \tag{25}$$

Where each energy level E_n is split into two levels because of the term $\mp g\mu_B B_z$. Where the minus is for Spin up (parallel to $\mathbf{B}$), which lowers the energy because the Spin is aligned and plus for Spin down (anti parallel). It should be noted that $\omega_c = \frac{qB_z}{m}$ is also the classical angular velocity of an electron in a magnetic field. Rewriting eqn.(25) by using the cyclotron frequency ω_c and $\mu_B = \frac{q\hbar}{2m}$, we end up with

$$\begin{aligned}
E_n &= \frac{\hbar^2 k_z^2}{2m} + \hbar\omega_c(n + \frac{1}{2}) \mp \frac{g}{2}\omega_c \\
E_n &= \frac{\hbar^2 k_z^2}{2m} + \hbar\omega_c(n + \frac{1 \mp g}{2})
\end{aligned} \tag{26}$$

2.4 Dissipation

Quantum coherence is maintained until the decoherence time. This depends on the strength of the coupling of the quantum system to other degrees of freedom. As an example: Schrödinger's cat. The decoherence time is very short, because there is a lot of coupling with other, lots of degrees of freedom. Therefore a cat, which is dead and alive at the same time, can't be investigated.

In solid state physics energy is exchanged between the electrons and the phonons. There are Hamiltonians H for the electrons (H_e), the phonons (H_{ph}) and the coupling between both (H_{e-ph}). The energy is conserved, but the entropy of the entire system increases because of these interactions.

$$H = H_e + H_{ph} + H_{e-ph}$$

3 Photons

3.1 Thermodynamic Properties of Bosons (missing)

3.2 Photons in vacuum (missing)

3.3 Photonic Crystals

3.3.1 Plane Waves in Crystals

A crystal lattice is a periodic arrangement of lattice points. If a plane wave hits the crystal, it scatters from every point in it. The scattered waves typically travel as spherical waves away from the points. There are certain angles where all of these reflections add constructively, hence they generate a diffraction peak in this direction. In fig. 2 one point is defined as the origin. An incoming radio wave scatters from the origin and goes out into a direction where a detector is positioned. Another ray scatters in some general position **r** and then also travels out towards the detector. The beam that goes through the origin has by definition phase 0. The beam that goes through the point **r** travels an extra length $(r\cos\theta + r\cos\theta')$.

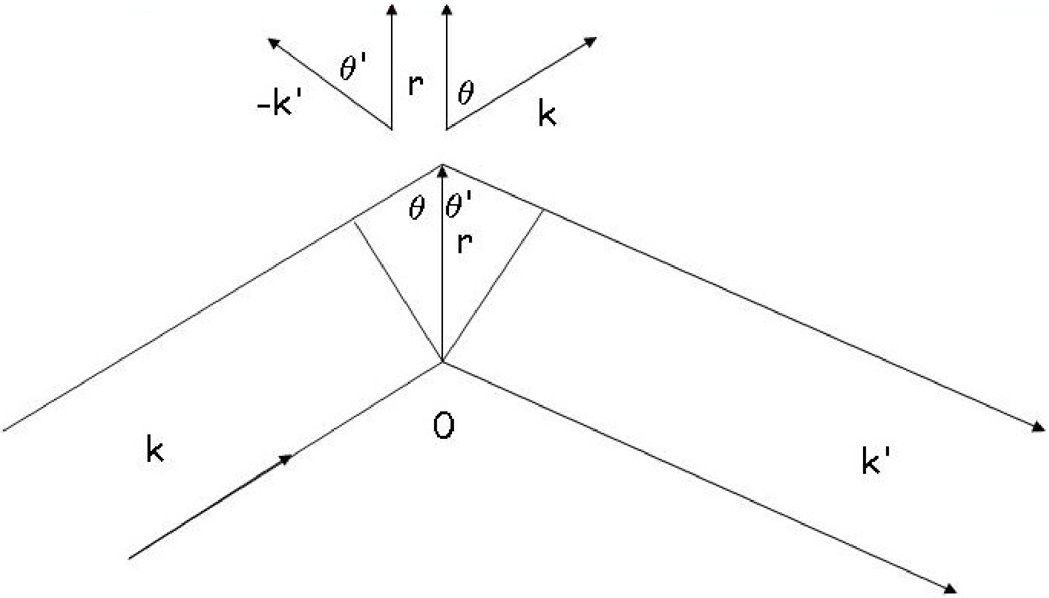

Figure 2: Scattering amplitude.

The phase of the beam scattered at **r** is $(\frac{2\pi}{\lambda}(r\cos\theta + r\cos\theta')) = (k - k')r$. So the phase factor is $\exp(i(\mathbf{k} - \mathbf{k}')\mathbf{r})$. If the phase difference is 2π or 4π, then the phase factor is 1 and the rays add coherently. If the phase is π or 3π, then the phase factor is -1 and the rays add destructively.

Now consider a scattering amplitude F.

$$F = \int dVn(\mathbf{r}) \exp\left(i(\mathbf{k} - \mathbf{k}')\mathbf{r}\right) = \int dVn(\mathbf{r}) \exp\left(-i\Delta\mathbf{kr}\right) \tag{27}$$

The amplitude of the scattered wave at $\mathbf{r}$ is assumed to be proportional to the electron density $n(\mathbf{r})$ in this point. A high concentration of electrons in $\mathbf{r}$ leads to more scattering from there, if there are no electrons in $\mathbf{r}$ then there is no scattering from that point. In eq. (27) the 3rd term is rewritten because of $\Delta\mathbf{k} = \mathbf{k}' - \mathbf{k} \rightarrow \mathbf{k} - \mathbf{k}' = -\Delta\mathbf{k}$.

Now we expand the electron density $n(\mathbf{r})$ in a fourier series (this is possible because the periodicity of $n(\mathbf{r})$ is the same as for the crystal).

$$n(\mathbf{r}) = \sum_{\mathbf{G}} n_{\mathbf{G}} \exp\left(i\mathbf{G}\cdot\mathbf{r}\right) = \sum_{\mathbf{G}} n_{\mathbf{G}} \left(\cos\left(\mathbf{G}\cdot\mathbf{r}\right) + i\sin\left(\mathbf{G}\cdot\mathbf{r}\right)\right) \tag{28}$$

To expand in terms of complex exponentials the factor $n_{\mathbf{G}}$ has to be a complex number, because a real function like the electron density does not have an imaginary part. If the fundamental wavelength of the periodic structure is a then there would be a vector $\mathbf{G} = \frac{2\pi}{a}$ in reciprocal space. So we just sum over all lattice vectors in reciprocal space which correspond to a component of the electron density.

We combine the scattering amplitude F and the electron density $n(\mathbf{r})$ and get

$$F = \sum_{\mathbf{G}} \int dVn_{\mathbf{G}} \exp\left(i\left(\mathbf{G} - \Delta\mathbf{k}\right)\cdot\mathbf{r}\right)$$

Thus, the phase factor depends on $\mathbf{G}$ and on $\Delta\mathbf{k}$. If the condition $\mathbf{G} - \Delta\mathbf{k} = 0$ is fullfilled for every position $\mathbf{r}$, the phase factor is 1. For all other values of $\Delta\mathbf{k}$ it's a complex value which is periodic in $\mathbf{r}$, so the integral vanishes and the waves interfere destructively. We obtain the **diffraction condition**

$$\mathbf{G} = \Delta\mathbf{k} = \mathbf{k}' - \mathbf{k}$$

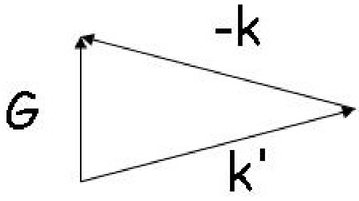

Figure 3: Geometric interpretation of the diffraction condition

Most of the time in diffraction scattering is elastic. In this case the incoming and the outgoing wave have the same energy and because of that also the same wavelength. That means $|\mathbf{k}| = |\mathbf{k}'|$ because of $\frac{2\pi}{\lambda} = k$. So for elastic scattering the difference between $\mathbf{k}$ and $\mathbf{k}'$ must be a reciprocal lattice vector $\mathbf{G}$ (as shown in fig. 3). We apply the law of cosines and get a new expression for the diffraction condition.

$$k^2 + G^2 - 2kG\cos\left(\theta\right) = k^2 \qquad \rightarrow \qquad 2\mathbf{k}\cdot\mathbf{G} = G^2 \qquad \xrightarrow{:4} \qquad \mathbf{k}\cdot\frac{\mathbf{G}}{2} = \left(\frac{G}{2}\right)^2$$

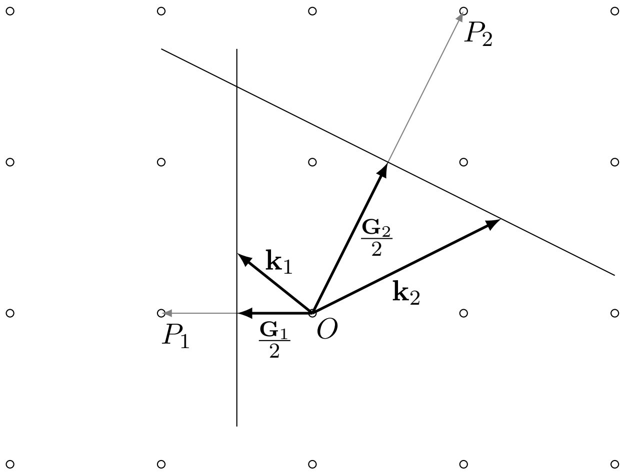

Figure 4: Brillouin zone

The geometric interpretation can be seen in Fig. 4. The origin is marked as 0. The point C is in the direction of one of the wave vectors needed to describe the periodicity of the electron density. We take the vector $\mathbf{G_C}$ half way there and draw a plane perpendicular on it. This plane forms part of a volume.

Now we take the inner product of $\mathbf{G_C}$ with some vector $\mathbf{k_1}$. If this product equals $\frac{G^2}{2}$ then $\mathbf{k_1}$ will fall on this plane and the diffraction condition is fullfilled. So a wave will be diffracted if the wavevector $\mathbf{k}$ ends on this plane (or in general on one of the planes).

The space around the origin which is confined by all those planes is called the **1st Brillouin zone**.

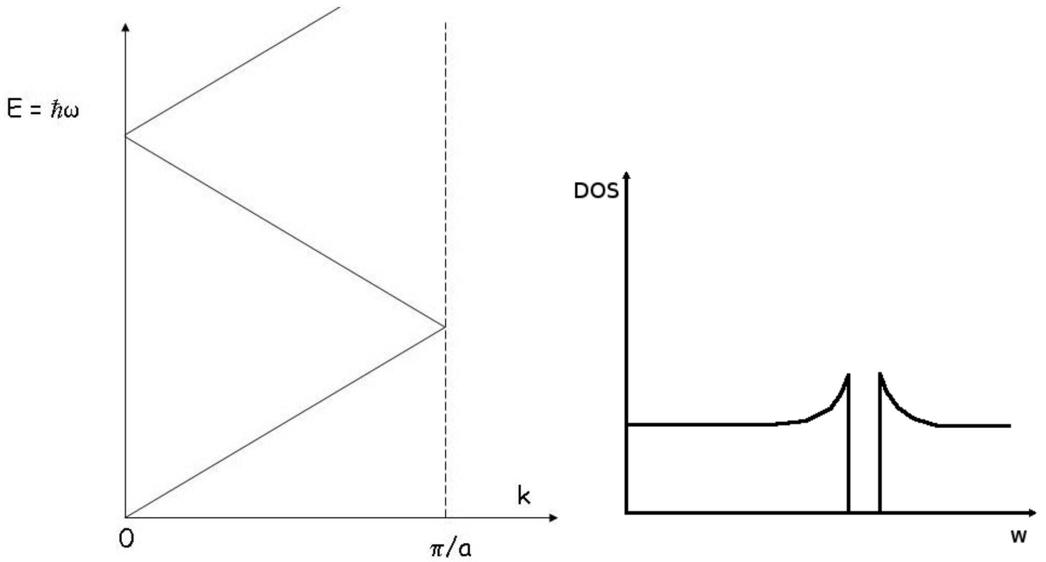

(a) (b)

Figure 5: a) Dispersion relation for photons in vacuum (potential is zero!); b) Density of states in terms of ω for photons (potential is nonzero!).

3.3.2 Empty Lattice Approximation (Photons)

What happens to the dispersion relationship of photons when there is a crystal instead of vacuum? In the Empty Lattice Approximation a crystal lattice is considered, but no potential. Therefore diffraction is possible. The dispersion relation in vacuum is seen in fig. 5(a).

The slope is the speed of light. If we have a crystal, we can reach diffraction at a certain point. The first time we do that is when k reaches $\frac{\pi}{a}$. Then we are on this plane which is the half way to the first neighboring point in reciprocal space. In a crystal the dispersion relation is bending over near the brillouin zone boundary and then going on for higher frequencies. With photons it happens similar to what happens with electrons. Close to the diffraction condition a gap will open in the dispersion relationship if a nonzero potential is considered (with the Empty Lattice Approximation no gap occurs, because the potential is assumed to be zero), so there is a gap of frequencies where there are no propagating waves. If you shoot light at a crystal with these frequencies, it would get reflected back out. Other frequencies will propagate through.

Because of the gap in the dispersion relationship for a nonzero potential, it also opens a gap in the density of states. In terms of $\mathbf{k}$ the density of states is distributed equally. The possible values of $\mathbf{k}$ are just the ones you can put inside with periodic boundary conditions. In terms of ω (how many states are there in a particular range of ω) it is first constant followed by a peak resulting of the dispersion relation' bending over. After that there is a gap in the density of states and another peak (as seen in fig. 5(b)).

The **Empty Lattice Approximation** can be used to guess what the dispersion relationship looks like. So we know **where diffraction is going to occur** and **what the slope is**. This enables us to **tell where the gap occurs in terms of frequency**.

3.3.3 Central Equations

We can also take the **central equations** to do this numerically. Now we have the wave equation with the speed of light as a function of r, which means we assume for example that there are two materials with different dielectric constants (so there are also different values for the speed of light inside the material).

$$c^2(r)\nabla^2 u = \frac{d^2u}{dt^2}$$

This is a linear differential equation with periodic coefficients. The standard technique to solve this is to expand the periodic coefficients in a fourier series (same periodicity as crystal!):

$$c^2(r) = \sum_{\mathbf{G}} U_{\mathbf{G}} \exp\left(i\mathbf{G}\cdot\mathbf{r}\right) \tag{29}$$

This equation describes the modulation of the dielectric constant (and so the modulation of the speed of light). $U_{\mathbf{G}}$ is the amplitude of the modulation. We can also write

$$u(r,t) = \sum_{\mathbf{k}} c_{\mathbf{k}} \exp\left(i(\mathbf{k}\cdot\mathbf{r} - \omega t)\right). \tag{30}$$

Putting the eqns. (29) and (30) into the wave equation gives us

$$\sum_{\mathbf{G}} U_{\mathbf{G}} \exp\left(i\mathbf{G}\cdot\mathbf{r}\right) \sum_{\mathbf{k}} c_{\mathbf{k}} k^2 \exp\left(i(\mathbf{k}\cdot\mathbf{r} - \omega t)\right) = \sum_{\mathbf{k}} c_{\mathbf{k}} \omega^2 \exp\left(i(\mathbf{k}\cdot\mathbf{r} - \omega t)\right) \tag{31}$$

On the right side we have the sum over all possible **k**-vectors and on the left side the sum over all possible **k**- and **G**-vectors. It depends on the potential how many terms of **G** we have to take. Eqn. (31) must hold for every **k**, so we take a particular value of **k** and then search through the left side of eq. (31) for other terms with the same wavelength. So we take all those coefficients and write them as an algebraic equation:

$$\sum_{\mathbf{G}} (\mathbf{k}-\mathbf{G})^2 U_{\mathbf{G}} c_{\mathbf{k}-\mathbf{G}} = c_{\mathbf{k}} \omega^2$$

The vectors **G** describe the periodicity of the modulation of the material. So we only do not know the coefficients and ω yet and we can write this as a matrix equation.

We look at a simple case with just a cosine-potential in x-direction. This means the speed of light is only modulated in the x-direction. Looking at just 3 relevant vectors of **G** and with

$$c^2(r) = U_0 + U_1 \exp\left(iG_0 r\right) + U_1 \exp\left(-iG_0 r\right)$$

we get

$$\begin{pmatrix} (\mathbf{k}+\mathbf{G_0})^2 U_0 & \mathbf{k}^2 U_1 & 0 \\ (\mathbf{k}+\mathbf{G_0})^2 U_1 & \mathbf{k}^2 U_0 & (\mathbf{k}-\mathbf{G_0})^2 U_1 \\ 0 & \mathbf{k}^2 U_1 & (\mathbf{k}-\mathbf{G_0})^2 U_0 \end{pmatrix} \cdot \begin{pmatrix} c_{k+G} \\ c_k \\ c_{k-G} \end{pmatrix} = \omega^2 \begin{pmatrix} c_{k+G} \\ c_k \\ c_{k-G} \end{pmatrix} \tag{32}$$

as the matrix equation. **G** and U come from the modulation of the material, k is just the value of **k**. So what we do not know are the coefficients and ω. The coefficients have to do with the eigenvectors

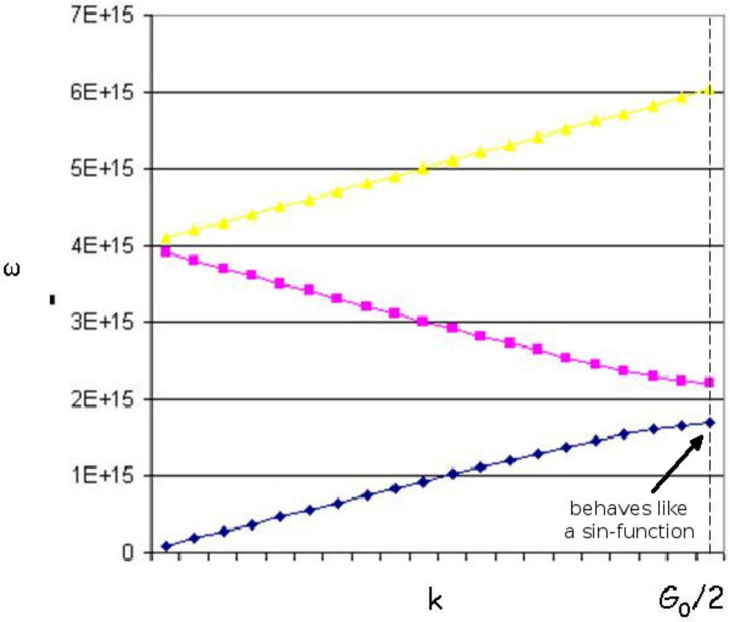

Figure 6: Dispersion relation for photons in a material.

of the matrix and ω^2 are the eigenvalues of the matrix. We just need to choose numbers for them and find the eigenvalues. Solving this over and over for different values of $\mathbf{k}$ we get a series of ω that solves the problem and gives us then the entire dispersion relationship.

So take some value of $\mathbf{k}$, diagonalize the matrix, find the eigenvalues (ω^2), take the square root of these three values and plot them in fig. 6. Then the next step is to increase the value of $\mathbf{k}$ a little bit and do the calculation again, so we have the next three points. This has to be done for all the points between zero and the brillouin zone boundary (which is half of the way to a first point $\mathbf{G}$ out of the origin).

At low values for $\mathbf{k}$ we get a linear dispersion relation, so the slope is the average value of the speed of light of the material. But when we get close to the brillouin zone boundary, the dispersion relationship bends over and then there opens a gap. So light with a wavelength close to that bragg condition will just get reflected out again (this is called a **Bragg reflector**).

After that the dispersion relationship goes on to the left side and then there is another gap (although it is harder to see). Fig. 6 only shows the first three bands. To calculate higher bands, you need to include more k values.

3.3.4 Estimate the Size of the Photonic Bandgap

Sometimes we do not need to know exactly what the dispersion relationship looks like, we just want to get an idea how big the band gap is. Then the way to calculate is to reduce the matrix that needs to be solved to a two-by-two matrix, which means that we only take one fourier coefficient into account.

$$\begin{pmatrix} (\mathbf{k}-\mathbf{G_0})^2U_0 & k^2U_1 \\ (\mathbf{k}-\mathbf{G_0})^2U_1 & k^2U_0 \end{pmatrix} \cdot \begin{pmatrix} c_{k-G} \\ c_k \end{pmatrix} = \omega^2 \begin{pmatrix} c_{k-G} \\ c_k \end{pmatrix}$$

For $k = \frac{G}{2}$ it is

$$\frac{G_0^2}{4} \begin{pmatrix} U_0 & U_1 \\ U_1 & U_0 \end{pmatrix} \cdot \begin{pmatrix} c_{k+G} \\ c_k \end{pmatrix} = \omega^2 \begin{pmatrix} c_{k+G} \\ c_k \end{pmatrix}$$

Finding the eigenvalues of a two-by-two matrix is easy, we can do that analytically. As a result for the eigenvalues we get the two frequencies

$$\omega = \frac{G_0}{2}\sqrt{U_0 - U_1} \qquad \text{and} \qquad \omega = \frac{G_0}{2}\sqrt{U_0 + U_1}.$$

So we can estimate how large the gap is. Further we know that very long wavelengths do not see the modulation, so the speed of light in this region is the average speed. If we know the modulation and where the brillouin zone boundary is, we can **analytically figure out** what the **size of the gap** is.

3.3.5 Density of States

From the dispersion relationship we can determine the density of states. This means how many states are there with a particular frequency. When we have light travelling through a periodic medium, the density of states is different than in vacuum. So some of those things calculated for vacuum, like the radiation pressure or the specific heat, are now wrong because of the different density of states.

In vacuum the density of states in one dimension is just constant, because in the one-dimensional k-space the allowed values in the periodic boundary conditions are just evenly spaced along k. The allowed wave that fits in a one-dimensional box of some length L is evenly spaced in k. So in this region the allowed states is a linear function so it is evenly spaced in ω too.

In a material we start out with a constant density of states. When we get close to the brillouin zone boundary, it is still evenly spaced in terms of k. But the density of states increases at the brillouin zone boundary and then drops to zero, because there are no propagating modes in this frequency range (photons with these frequencies will get reflected back out). After the gap, the density of states bunches again and then gets kind of linear (see fig. 5(b)).

In fig. 6 it looks a bit like a sin-function near the brillouin zone boundary, so $\omega \approx \omega_{max}|\sin\frac{ka}{2}|$. So we get $k = \frac{2}{a}\sin^{-1}\left(\frac{\omega}{\omega_{max}}\right)$. The density of states in terms of ω is

$$D(\omega) = D(k)\frac{dk}{d\omega}.$$

The density of states in terms of k is a constant. The density of states in ω is

$$D(\omega) \propto \frac{1}{\sqrt{1 - \frac{\omega^2}{\omega_{max}^2}}} \tag{33}$$

It looks like the plot in fig. 7(a).

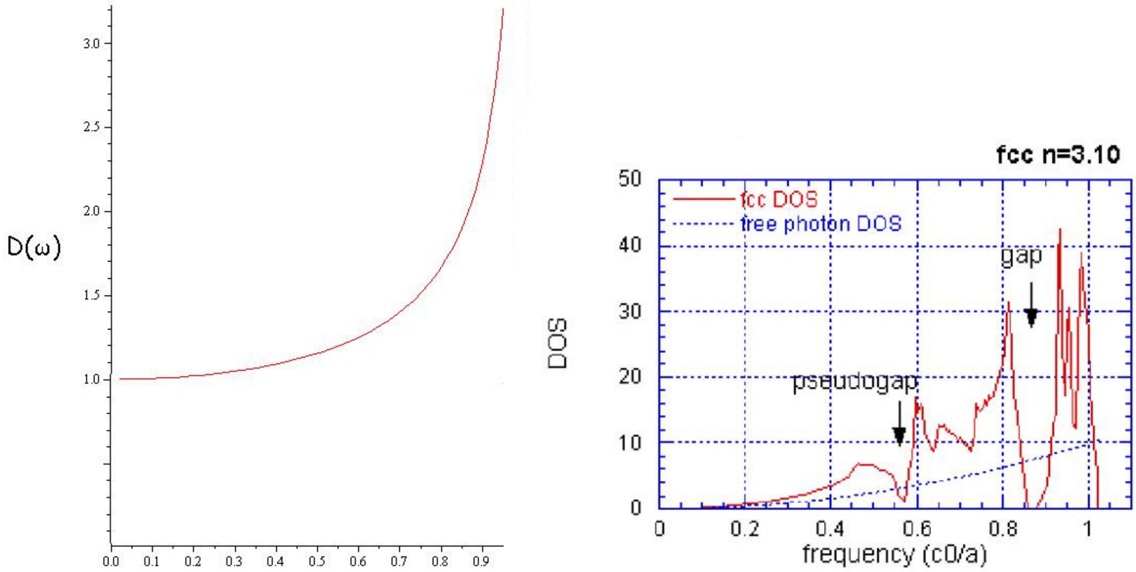

(a) (b)

Figure 7: a) Density of states for photons in one dimension in a material in terms of ω; b) Density of states of photons for voids in an fcc lattice

3.3.6 Photon Density of States

Now we have a three-dimensional density of states calculated for an fcc crystal. There are holes in some material and the holes have an fcc lattice. The material has a dielectric constant of 3, the holes have 1 (looks like some kind of organic material). So we have a lot of holes in the material, a large modulation and we calculate the density of states. The little line in fig. 7(b) is the vacuum density of states. But we have this periodic modulation and when there is a band we can get a gap. The peaks are typically near edges and near the gaps because there the states pile up.

If we have a strange function for the density of states and we want to calculate the corresponding planck radiation law, we just have to plug it in because the planck radiation law is the energy times the density of states times the Bose-Einstein factor (see chapter **??**).

4 Electrons

4.1 Thermodynamic properties of Fermions (missing)

4.2 Review of the free Electron Fermi Gas

The density of states $D(E)$ of an electron gas is $D(E) = D(k)\frac{dk}{dE}$, as stated previously. The energy of a free electron regardless of the numbers of dimensions considered is always:

$$E = \hbar\omega = \frac{\hbar^2 k^2}{2m}$$

But the density $D(k)$ is of course dependent on the number of dimensions:

$$D(k)_{1-D} = \frac{2}{\pi}, \qquad D(k)_{2-D} = \frac{k}{\pi}, \qquad D(k)_{3-D} = \frac{k^2}{\pi^2}$$

So computing the derivative $\frac{dk}{dE}$ and expressing everything in terms of E leads us to these equations:

$$D(E)_{1-D} = \frac{1}{\hbar\pi}\sqrt{\frac{2m}{E}}, \qquad D(E)_{2-D} = \frac{m}{\hbar^2\pi}, \qquad D(E)_{3-D} = \frac{(2m)^{\frac{3}{2}}}{2\hbar^3\pi^2}\sqrt{E}$$

4.2.1 Fermi Energy

We assume a system of many electrons at temperature $T = 0$, so our system has to be in the lowest possible energy configuration. Therefore, we group the possible quantum states according to their energy and fill them up with electrons, starting with the lowest energy states. When all the particles have been put in, the **Fermi energy** is the energy of the highest occupied state. The mathematical definition looks like this

$$n = \int_0^{E_F} D(E)dE \tag{34}$$

where n is the electron density, $D(E)$ the density of states in terms of the energy and E_F is the Fermi Energy.

Performing the integral for the densities of states in 1, 2, and 3 dimensions and plugging in these Fermi energies in the formulas for the density of states gives us (N is the number of electrons and L is the edge length of the basic cube, see also chapter **??**):

1-D:

$$E_F = \frac{\hbar^2\pi^2}{8m}\left(\frac{N}{L}\right)^2, \qquad D(E) = \sqrt{\frac{2m}{\hbar^2\pi^2 E}} = \frac{n}{2\sqrt{E_F E}} \quad \left[\frac{1}{Jm}\right]$$

2-D:

$$E_F = \frac{\hbar^2\pi N}{mL^2}, \qquad D(E) = \frac{m}{\hbar^2\pi} = \frac{n}{E_F} \quad \left[\frac{1}{Jm^2}\right]$$

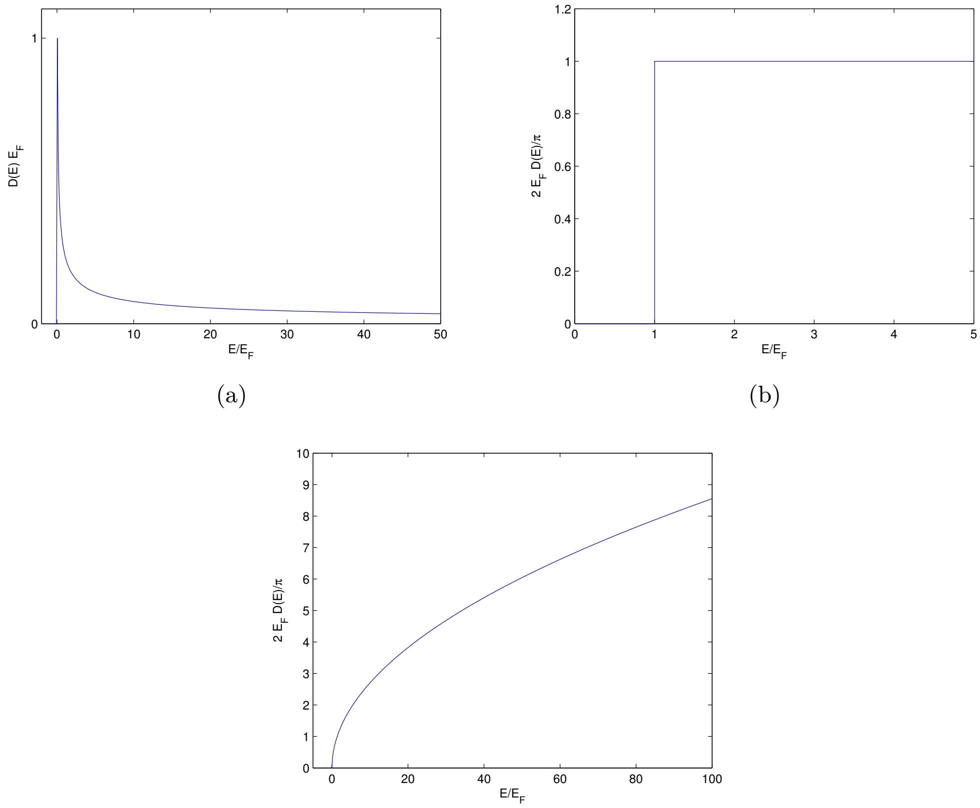

(a) (b)

(c)

Figure 8: a) Density of states of an electron gas in 3 dimensions; b) Density of states of an electron gas in 2 dimensions; c) Density of states of an electron gas in 1 dimension

3-D:

$$E_F = \frac{\hbar^2}{2m}\left(\frac{3\pi^2 N}{L^3}\right)^{\frac{2}{3}}, \qquad D(E) = \frac{\pi}{2}\left(\frac{2m}{\hbar^2\pi^2}\right)^{\frac{3}{2}} = \frac{3n}{2E_F^{\frac{3}{2}}}\sqrt{E}\ \left[\frac{1}{Jm^3}\right]$$

4.2.2 Chemical Potential

The Fermi Energy is of course a theoretical construct, because $T = 0$ can't be reached, so we start to ask ourselves what happens at non-zero temperatures. In case of non-zero temperatures one has to take the Fermi-statistic into account. With this in mind, we adapt eqn. (34) for the electron density

$$n = \int_0^\infty D(E) f(E) dE \tag{35}$$

where $f(E)$ is the Fermi-function, so the equation for n reads as:

$$n = \int_0^\infty \frac{D(E)dE}{e^{\frac{E-\mu}{k_B T}} + 1}$$

In this equation, μ stands for the **chemical potential**, which can be seen as the change of the characteristic state function per change in the number of particles. More precisely, it is the thermodynamic conjugate of the particle number. It should also be noted, that for $T = 0$, the Fermi Energy and the chemical potential are equal.

4.2.3 Sommerfeld Expansion

When you calculate the thermodynamic quantities the normal way you get stuck analytically at the density of states $D(E)$ of the dispersion relationship. From this point on you have to work numerically. The Sommerfeld-Expansion allows you to calculate analytically the leading order term(s) as a function of temperature, which are enough in a lot of cases. The number of electrons n and the internal energy u are:

$$n = \int_{-\infty}^{\infty} D(E) f(E) dE \qquad u = \int_{-\infty}^{\infty} E \cdot D(E) f(E) dE$$

with $f(E)$ as the fermi function and E as the energy. We would like to perform integrals of the form:

$$\int_{-\infty}^{\infty} H(E) f(E) dE$$

$H(E)$ stands for an arbitrary function which is multiplied by the fermi function. Such an integral appears if you want to calculate the total number of states or for instance μ, the chemical potential, which is inside the fermi-function. We integrate by parts:

$$\int_{-\infty}^{\infty} H(E) f(E) dE = K(\infty) f(\infty) - K(-\infty) f(-\infty) - \int_{-\infty}^{\infty} K(E) \frac{df(E)}{dE} dE$$

with

$$K(E) = \int_{-\infty}^{E} H(E') dE' \qquad i.e. \qquad H(E) = \frac{dK(E)}{dE} \tag{36}$$

The fermi function $f(E)$ at $T = 0$ K looks like a step function at the chemical potential. The last term with the integral includes the derivation of the fermi function, which is a peak around the chemical potential. The fermi function vanishes for $E \to \infty$, $f(-\infty) = 1$ and $H(-\infty) = 0$. With eqn. (36):

$$\int_{-\infty}^{\infty} H(E)f(E)dE = -\int_{-\infty}^{\infty} K(E)\frac{df(E)}{dE}dE$$

Then K(E) is expanded around $E = \mu$ with a Taylor series (everywhere else the derivation is zero):

$$K(E) \approx K(\mu) + \frac{dK}{dE}_{E=\mu}(E-\mu) + \frac{1}{2}\frac{d^2K}{dE^2}_{E=\mu}(E-\mu)^2 + ...$$

Solving the integral this way is similar that you say that just the states near the fermi surface contribute to the physical properties of the electrons. Only states near the fermi sphere contribute to the measurable quantities.

With

$$x = \frac{E-\mu}{k_B T}$$

$$\int_{-\infty}^{\infty} H(E)f(E)dE = K(\mu)\int_{-\infty}^{\infty}\frac{e^x}{(1+e^x)^2}dx + k_B T\frac{dK}{dE}_{E=\mu}\int_{-\infty}^{\infty}\frac{x \cdot e^x}{(1+e^x)^2} + ...$$

where every odd term is zero (x, x^3, x^5) and the other ones are just numbers. If you put in these terms you get

$$n = \int_{-\infty}^{\infty} H(E)f(E)dE = K(\mu) + \frac{\pi^2}{6}(k_B T)^2\frac{dH(E)}{dE}_{E=\mu} + \frac{7\pi^4}{360}(k_B T)^4\frac{d^3H(E)}{dE^3}_{E=\mu} + ...$$

Sommerfeld Expansion: Chemical Potential 3D

It is possible to get the chemical potential out of the Sommerfeld expansion. If $H(E) = D(E)$, which you get out of the dispersion relationship, you can get $K(E)$ which is just the integral of $H(E)$ over all energies. You get the non-linear relationship of the μ and the T (E_F as the fermi energy):

$$n = \frac{n\mu^{1/2}}{E_F^{3/2}} + \frac{\pi^2}{8}(k_B T)^2\frac{n\mu^{-1/2}}{E_F^{3/2}} + ...$$

Dividing both sides by n gives:

$$1 = \frac{\mu^{1/2}}{E_F^{3/2}} + \frac{\pi^2}{8}(k_B T)^2\frac{\mu^{-1/2}}{E_F^{3/2}} + ...$$

Sommerfeld Expansion: Internal energy

In this case $H(E) = D(E)E$. So we get the expression for the internal energy:

$$u = \int_{-\infty}^{\infty} H(E)f(E)dE = \frac{3n}{5E_F^{3/2}}\mu^{3/2} + \frac{3\pi^2}{8}(k_B T)^2\frac{n}{E_F^{3/2}}\mu^{1/2}$$

Sommerfeld Expansion: Electronic specific heat

If you differentiate the internal energy once you get the specific heat c_V. So you see that the specific heat is linear with the temperature.

$$c_V = \frac{du}{dT} = \frac{3\pi^2}{4}(k_B T)\frac{n}{E_F^{3/2}}\mu^{1/2} + ...$$

If you take a metal and measure the specific heat at a certain temperature T, some of the energy goes into the electrons ($\propto T$) and some into the phonons ($\propto T^3$), because both are present in a metal:

$$c_V = \gamma T + AT^3$$

$\frac{C}{T}$ is plotted versus T^2 to get a line (see fig. 9). The slope of the line is the phonon constant A and the interception with the y-axis gives γ, the constant for the electrons.

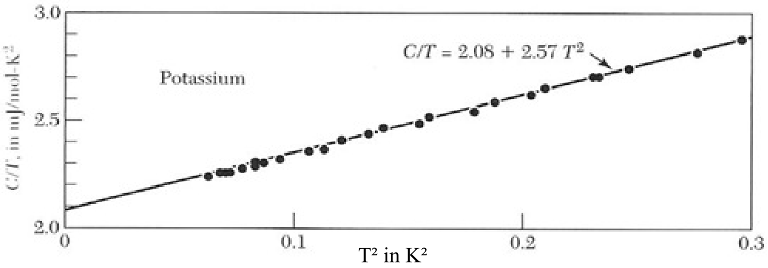

Figure 9: Plot of the specific heat to get the constants

Typically metals are given an **effective mass** m^*, which was reasonable when comparing the calculated free electron case (mass m_e, γ) with the results measured ($\gamma_{observed}$) (The effective mass is a way to parameterize a system - interaction was neglected). What was really done with this was specifying a derivative of the Sommerfeld expansion. So because of history we are talking about effective mass, but we mean this derivative in the Sommerfeld expansion.

$$\frac{m^*}{m_e} = \frac{\gamma_{observed}}{\gamma} \qquad and \qquad m^* = \frac{2}{9}\frac{dH}{dE}_{E=\mu} \cdot m_e$$

	1-D, free particle $i\hbar\frac{d\Psi}{dt} = -\frac{\hbar^2}{2m}\Delta\Psi$	2-D, free particle $i\hbar\frac{d\Psi}{dt} = -\frac{\hbar^2}{2m}\Delta\Psi$	3-D, free particle $i\hbar\frac{d\Psi}{dt} = -\frac{\hbar^2}{2m}\Delta\Psi$
Eigenfunct. sol.	$A_k e^{i(kx-wt)}$	$A_{\mathbf{k}} e^{i(\mathbf{k}\cdot\mathbf{x}-wt)}$	$A_{\mathbf{k}} e^{i(\mathbf{k}\cdot\mathbf{x}-wt)}$
Disp. relation	$E = \hbar\omega = \frac{\hbar^2 k^2}{2m}$	$E = \hbar\omega = \frac{\hbar^2 k^2}{2m}$	$E = \hbar\omega = \frac{\hbar^2 k^2}{2m}$
DOS $D(k)$	$D(k) = \frac{2}{\pi}$	$D(k) = \frac{k}{\pi}$	$D(k) = \frac{k^2}{\pi^2}$
$D(E) = D(k)\frac{dk}{dE}$	$D(E) = \frac{1}{\pi\hbar}\sqrt{\frac{2m}{E}} = \frac{n}{2\sqrt{E_F E}}$	$D(E) = \frac{m}{\pi\hbar^2} = \frac{n}{E_F}$	$D(E) = \frac{(2m)^{\frac{3}{2}}}{2\pi^2\hbar^3}\sqrt{E} = \frac{3n}{2E_F^{\frac{3}{2}}}\sqrt{E}$
Fermi energy	$E_F = \frac{\pi^2\hbar^2 n^2}{8m}$	$E_F = \frac{\pi\hbar^2 n}{m}$	$E_F = \frac{\hbar^2}{2m}(3\pi^2 n)^{\frac{2}{3}}$
Chem. pot.	...	...	...

Table 1: Calculated thermodynamic quantities for free electrons

Sommerfeld Expansion: Entropy, Free Energy, Pressure

We can also calculate the entropy for the system. The specific heat is divided by temperature T and we get the derivation of the entropy (with constant N and V). So we get an entropy density s which is linear with the temperature

$$s = \frac{3\pi^2}{4} k_B^2 T \frac{n}{E_F^{3/2}} \mu^{1/2} + ...$$

The Helmholtz free energy can be calculated with:

$$f = u - T \cdot s$$

Also other thermodynamic quantities: The pressure P can be calculated with:

$$P = -\left(\frac{\partial U}{\partial V}\right)_N = \frac{2}{5} n E_F \qquad with \qquad E_F = \frac{\hbar^2}{2m}\frac{3\pi^2 N}{V}$$

This pressure comes from the kinetic energy of the electrons, not from the e-e interaction, which was neglected in this calculation. The bulk modulus B (how much pressure is needed to change the volume) is:

$$B = -V\frac{\partial P}{\partial V} = \frac{5}{3}P = \frac{10}{9}\frac{U}{V} = \frac{2}{3} n \cdot E_F$$

We can put all the calculated thermodynamic quantities into a table for free electrons (1d-, 2d-, 3d-Schrödinger equation - see table 1). We started our calculation with the eigenfunction solution ($A_k \cdot e^{i(kx-wt)}$), which we put into the Schrödinger equation to get the dispersion relationship($E = \hbar\omega$). To get the density of states $D(k)$ we have to know how many waves fit in a box with periodic boundary conditions. After that we calculate the density of states for energy $D(E) = D(k)\frac{dk}{dE}$ from that we can get the Fermi energy. Until now everything can be calculated analytically, so now we go over to the Sommerfeld equation to get the chemical potential (and internal energy, specific heat, entropy, Helmholtz free energy, bulk modulus, etc. like seen before).

4.3 Electronic Band Structure Calculations

In this section the band structure is calculated. In the sections before this was done for the free electron gas (1d, 2d, 3d), now the electrons are put in a periodic potential and the properties are evaluated.

4.3.1 Empty Lattice Approximation

The empty lattice approximation is the easiest one for most materials. We know from previous experiments that gaps will appear in the DOS for solids in a periodic potential. We also know that if we have a metal, the electrons are almost free - the dispersion-relationship is a parabola. But at the Brillouin zone boundary there will be some diffraction that will cause a gap. That's the same for the next boundary. For most materials that gap is approximately 1 eV big (The energy where the gap occurs can be calculated with $k = \frac{\pi}{a}$ and $E = \frac{\hbar^2 k^2}{2m}$). After the 1^{st} Brillouin zone the dispersion curve would move on to higher **k**-vectors, but we map it back into the 1^{st} Brillouin zone (see fig. 10). This helps saving paper, but the more important reason is that the crystal lattice conserves the momentum (i.e. if a photon excites an electron) by absorbing or giving momentum to the electrons (the whole crystal starts to move with the opposite momentum of the electron). The third reason is the symmetry (the Hamiltonian H commutes with the symmetry operator S). You can take any atom and pick it up and put it down on another atom. So the empty lattice approximation just tells you that you can draw the parabola and then draw another one just one reciprocal lattice vector shifted. So you can draw the dispersion relationship in the first Brillouin zone. The dispersion relationships are always symmetric in k_x and k_{-x}, so they are in y- and z-direction.

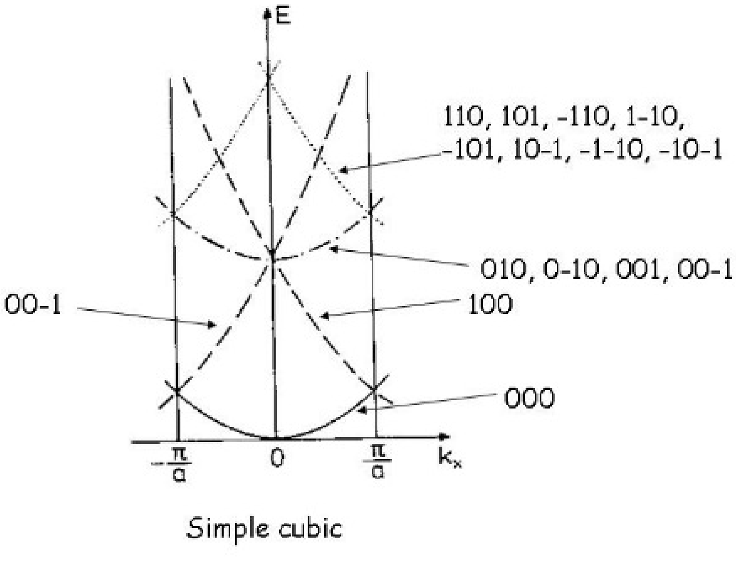

Figure 10: Dispersion relationship for a simple cubic lattice in 3D for the empty lattice approximation

If you have a simple cubic metal the curve plotted in fig. 11 shows the dispersion relation for the empty lattice approximation. It starts at Γ, where k is zero, to different directions for example to M at the 110 direction. This complicated looking thing is just the free electron model, where k starts at zero and grows with k^2. If there is a potential, gaps will be formed.

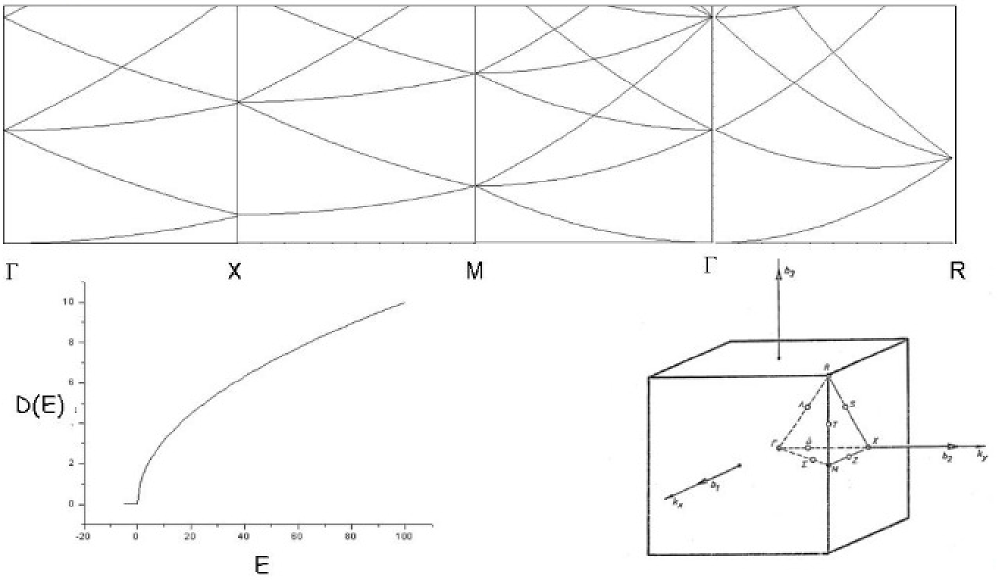

Figure 11: Dispersion relationship for a simple cubic lattice for the empty lattice approximation

You can do the same for fcc (most metals). Fig. 12 is an equivalent kind of drawing for fcc. Again it starts at Γ where k is zero and goes to X (to the y direction, in this crystal x, y and z direction have the same symmetry (6 symmetry related directions)) or L (is closer in k space to Γ because the reciprocal lattice to fcc is bcc and in bcc there are 8 nearest neighbors which are in the 111 direction).

If you make a calculation you get nearly the same band structure like in the empty lattice approximation and additionally you get the gaps at the Brillouin zone boundaries like expected. So this is a good first approximation for the real band structure.

If you compare two materials, for example the group 4 elements, you see that the structures are always repeating in various crystals. You just look at the valence electrons (C, Si, Ge all have 4 valence electrons), the other, inner electrons do not contribute to most of the material properties.

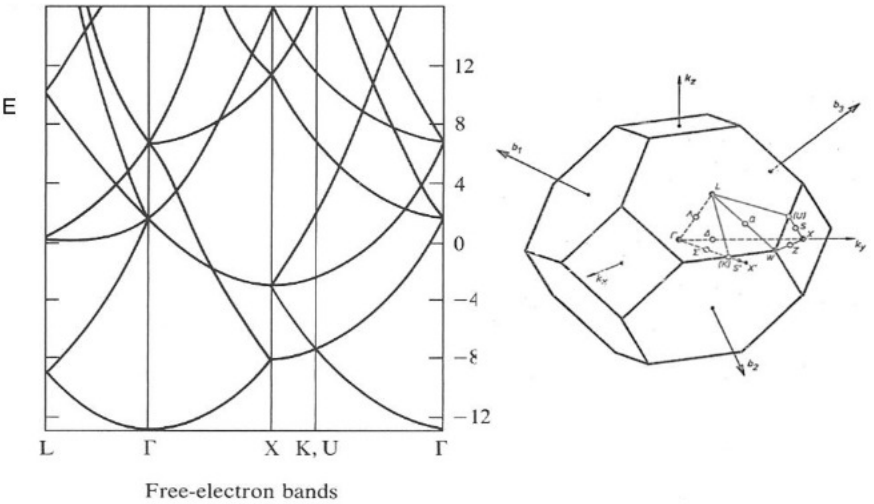

Figure 12: Dispersion relationship for a fcc for the empty lattice approximation

4.3.2 Plane Wave Method - Central Equations

Now we want to talk about the Schrödinger equation with a periodic potential (in the free electron model the potential was zero), i.e. electrons moving through a crystal lattice. Such calculations are called band structure calculations (there are bands and bandgaps). Now the plane wave method is used (simple method, numerically not very efficient). We will end up with something that's called the central equations.

We start with the Schrödinger equation, which is a linear differential equation with periodic coefficients.

$$\frac{-\hbar^2}{2m}\nabla^2\Psi + U(\mathbf{r})\Psi = E\Psi$$

When the function $U(\mathbf{r})$ is periodic, it can be written as a Fourier- series (potential as a sum of plane waves, $\mathbf{G}$ as a reciprocal lattice vector). For Ψ a former solution is assumed, which is also periodic, but in the scale of the crystal (i.e. 1 cm). So the boundary conditions don't matter.

$$U(\mathbf{r}) = \sum_{\mathbf{G}} U_{\mathbf{G}} e^{i\mathbf{G}\mathbf{r}}$$

$$\Psi = \sum_{\mathbf{k}} C_{\mathbf{k}} e^{i\mathbf{k}\mathbf{r}}$$

These are put in the Schrödinger equation to get an algebraic equation out of a differential equation:

$$\sum_{\mathbf{k}} \frac{\hbar^2 k^2}{2m} C_{\mathbf{k}} e^{i\mathbf{k}\mathbf{r}} + \sum_{\mathbf{G}}\sum_{\mathbf{k}} U_{\mathbf{G}} C_{\mathbf{k}} e^{i(\mathbf{G}+\mathbf{k})\cdot\mathbf{r}} = E\sum_{\mathbf{k}} C_{\mathbf{k}} e^{i\mathbf{k}\mathbf{r}} \tag{37}$$

We know $\frac{\hbar^2 k^2}{2m}$ and we know which $\mathbf{G}$ vectors correspond to the potential. The coefficients $C_{\mathbf{k}}$ are unknown, but there are linear equations for the C's. It can be written in a matrix - there is a different matrix for every k in the first Brillouin zone:

$$\left(\frac{\hbar^2 k^2}{2m} - E\right) C_{\mathbf{k}} + \sum_{\mathbf{G}} U_{\mathbf{G}} C_{\mathbf{k}-\mathbf{G}} = 0 \tag{38}$$

By solving these equations we get both, the coefficients C and the energy. This is done for every k to get the band structure. Before starting to calculate, a potential must be chosen.

Example: FCC-Crystal
We make an example for an fcc crystal. We need to express this periodic potential ($U(\mathbf{r}) = \sum_{\mathbf{G}} e^{i\mathbf{G}\mathbf{r}}$) mathematically. For example with a Heaviside stepfunction Θ and a delta function:

$$\Theta(1 - \frac{|\mathbf{r}|}{b}) \cdot \sum_{j=fcc} \delta(\mathbf{r} - \mathbf{r}_j)$$

Now we have a mathematical expression for this hard sphere potential. The Fourier transform of this function is equal to the right side of eqn. (39) because the Fourier transform of the convolution of two functions is the product of the Fourier transforms of the two functions. The Fourier transformation of the fcc lattice is a bcc lattice. The Fourier transform of this stepfunction is a Bessel function, which is zero most of the time, the other time it is the amplitude of the Bessel function. The horizontal lines in fig. 13 of the Bessel function correspond to the coefficients($U_{\mathbf{G}}$).

$$\widehat{\Theta\left(1 - \frac{|\mathbf{r}|}{b}\right) \sum_{j=fcc}} \delta(\mathbf{r} - \mathbf{r}_j) = \widehat{\Theta\left(1 - \frac{|\mathbf{r}|}{b}\right)} \sum_{j=bcc} \delta(\mathbf{r} - \mathbf{r}_j) \tag{39}$$

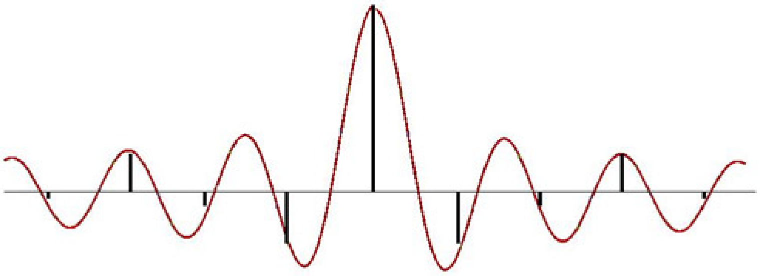

Figure 13: Bessel function with coefficients $U_{\mathbf{G}}$

Now to the relationship between real space lattices and reciprocal space lattices. For a bcc in real you get an fcc in reciprocal space. That's the same for fcc in real space, there you get a bcc in reciprocal space. For simple cubic, tetragonal and orthorhombic lattices in real space you get the same in reciprocal space.(for a tetragonal lattice: a, a, b in real space the reciprocal lattice is: $\frac{2\pi}{a}, \frac{2\pi}{a}, \frac{2\pi}{b}$ - which is also tetragonal). An hcp in real space is an hcp rotated by 30 degrees in reciprocal space.

It turns out that hard spheres have these nasty Bessel function - behaviour. So we want to try cubic atoms, because the Fourier transform is much easier. But an even nicer form to use is a gaussian. The Fourier transform of a gaussian is a gaussian. It does not have oscillations, and it also looks more like an atom, for example it could be the s-wave function of an atom.

Now back to the Central equations (1 dim). These are the algebraic equations we get when we put the Fourier- series in the Schrödinger equation:

$$\left(\frac{\hbar^2 k^2}{2m} - E\right) C_k + \sum_G U_G C_{k-G} = 0$$

The central equations couple coefficients k to other coefficients that differ by a reciprocal lattice wavevector $\mathbf{G}$. So we choose a k and already know $\hbar$ and m, we only do not know the energy E. The points of the bravais lattice in reciprocal space are G_0, $2G_0$ and so on. Thus we know the G_0's so the energies are the eigenvalues of a matrix. We make a matrix like this:

$$\begin{bmatrix} \ddots & & & & & & \\ & \frac{(\hbar^2(k-2G_0))^2}{2m} - E & U_{G_0} & U_{2G_0} & & & \\ & U_{-G_0} & \frac{(\hbar^2(k-G_0))^2}{2m} - E & U_{G_0} & U_{2G_0} & & \\ & U_{-2G_0} & U_{-G_0} & \frac{\hbar^2 k^2}{2m} - E & U_{G_0} & U_{2G_0} & \\ & & U_{-2G_0} & U_{-G_0} & \frac{(\hbar^2(k+G_0))^2}{2m} - E & U_{G_0} & U_{2G_0} \\ & & & U_{-2G_0} & U_{-G_0} & \frac{(\hbar^2(k+2G_0))^2}{2m} - E & U_{G_0} \\ & & & & & & \ddots \end{bmatrix} \begin{bmatrix} \vdots \\ C_{k+2G_0} \\ C_{k+G_0} \\ C_k \\ C_{k-G_0} \\ C_{k-2G_0} \\ \vdots \end{bmatrix} = 0 \tag{40}$$

The minimum of nearest neighbors in a 1 dimensional problem is one. You get a matrix (2 by 2), which can be solved and plotted. What you get is the dispersion relationship with the energy over k (it starts parabolic, then bends over to the Brillouin zone boundary, then there's a gap, and then the second band - see fig. 14).

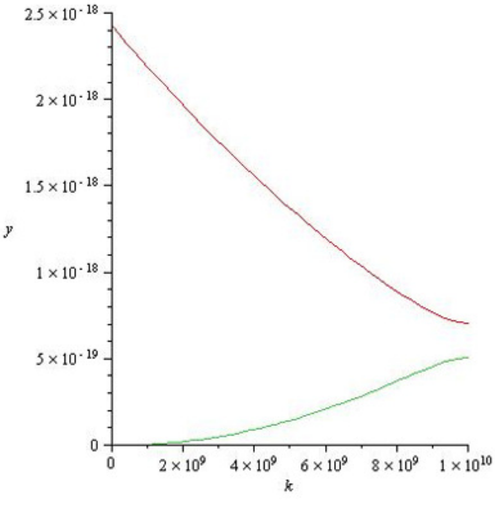

Figure 14: Dispersion relation $E(k)$ evaluated with Central Equations

You can also expand the matrix and take more terms (two to the right and one to the left). Everything is coupled to it's two nearest neighbors (just a linear chain). For this 4 by 4 matrix you get four energies (four bands). Thus by making the matrix bigger, higher energies can be calculated.

Example: Simple Cubic
At first we have to figure out what the Fourier- series is for simple cubic. Just take the nearest neighbors in k space. So choose gaussian atoms and put them on a simple cubic lattice and make them pretty wide in real space so they are quite narrow in k-space. Then only the nearest neighbors are relevant. For the potential only take contribution by the nearest neighbors (6 for sc). They will correspond to these six terms:

$$U(\mathbf{r}) = U_0 + U_1(e^{i\frac{2\pi x}{a}} + e^{-i\frac{2\pi x}{a}} + e^{i\frac{2\pi y}{a}} + e^{-i\frac{2\pi y}{a}} + e^{i\frac{2\pi z}{a}} + e^{-i\frac{2\pi z}{a}})$$

This is the reciprocal space expansion for the simple cubic. When we put this in the known algebraic equations (37) and (38) we get a matrix and can solve it. There you get a 7 by 7 matrix. The term in the middle of the matrix is always the central atom. This central atom is always connected equally to the nearest neighbors. The terms in the diagonal represent the nearest neighbors (in this case 6) in ± x, ± y and ± z direction. The smallest G is $\frac{2\pi}{a}$, then one step further in this direction $(k_x + \frac{4\pi}{a})$. We can neglect the other interactions instead of the nearest neighbors because the gaussian function falls exponentially.

So if you can construct this matrix you can calculate the band structure for an electron moving in a periodic potential. If you increase the amplitude there will appear gaps in the band structure where we thought they would appear in the empty lattice approximation, but you can't tell what the band structure would really be.

The next issue is band structure, where we try to calculate the dispersion relationship $E(k)$ for electrons. Typically it starts out like a parabola and then bends over and continues on, so there opens a gap like you see in fig. 15. In the density of states there are a lot of states in the range of the bands and no states at the gaps.

Important differences for the DOS and the Fermi energy between the different types of materials:
A metal has partially filled bands with a high density of electron states at the Fermi energy. A semimetal has partially filled bands with a low density of electron states at the Fermi energy. An insulator has bands that are completely filled or completely empty with a bandgap greater than 3 eV. The Fermi energy is about in the middle of the gap. A semiconductor has a Fermi energy in a gap which is less than 3 eV wide. Some electrons are thermally excited across the gap. The difference between a semimetal and a semiconductor is that a semiconductor looses all its conductivity during cooling down. A semimetal does not loose all the conductivity. In fig. 15 you can see the dispersion relation and the density of states over the energy. At the right you can see the Fermi energies of the several possibilities.

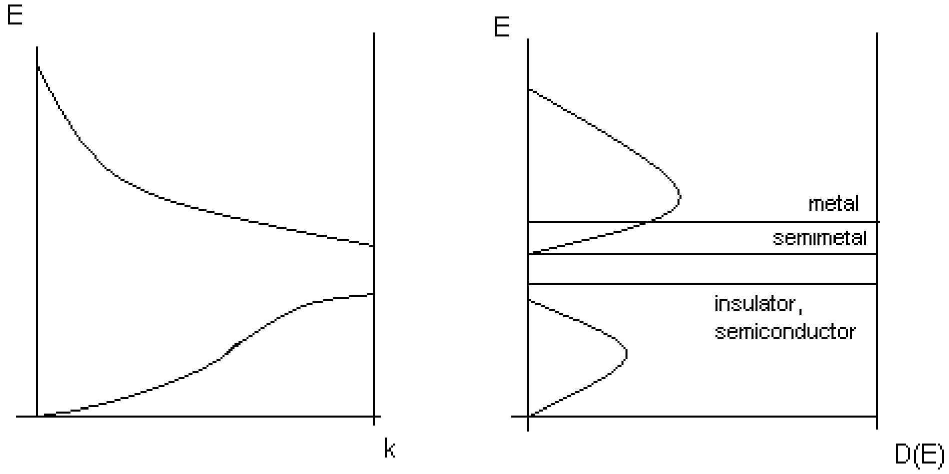

Figure 15: Dispersion relation and the density of states over the energy.

4.3.3 Tight Binding Model

The tight binding model is another method for band structure calculations. Starting with the atomic wavefunction we imagine a crystal where the atoms are much further apart than in a normal crystal (the internuclear distances are big). They are still in the same arrangement (for example an fcc structure) but the bond lengths are shorter. Therefore they don't really interact with each other. The atomic wavefunctions are the electron states. If you bring the atoms together they will start to form bonds. The energies will shift. In fig. 16 at the left side the atoms are far apart (they are all in the ground state, all same energy, 1s) and to the right side the atomic wavefunctions start to overlap and they start to form bonds. The states split into bands which we are calculating. If the lattice constant gets smaller the band gets wider and there is more overlap between the wavefunctions (a little bit like making a covalent bond). If two atoms with given wavefunctions are brought together, they interact in a way that the wavefunction splits into a bonding state (goes down in energy) and an antibonding state (goes up in energy). We consider a 1-dimensional crystal and look at the Coulomb potential of every atom in it. The total potential is the sum over all potentials. Adding a lot of Coulomb potentials together gives a periodic potential:

$$V(\mathbf{r}) = \sum_n \nu(\mathbf{r} - na\mathbf{x}) \qquad\qquad n = ... - 1, 0, +1....$$

The Hamiltonian then is

$$H = \frac{-\hbar^2}{2m}\nabla^2 + \sum_n \nu(\mathbf{r} - na\mathbf{x}).$$

The atomic wavefunction is chosen as a basis. The wavefunction one on every lattice site is taken as a basis to do the calculation. The wavefunction Ψ_{qn} is labeled by two letters. n labels the position and q labels which excited state it is (1s,2p,..). Knowing the wavefunction and the Hamiltonian we can form the Hamiltonian matrix. If we solve every matrix element numerically we get the eigenfunctions (of the Hamiltonian) and the eigenvalues (energies).

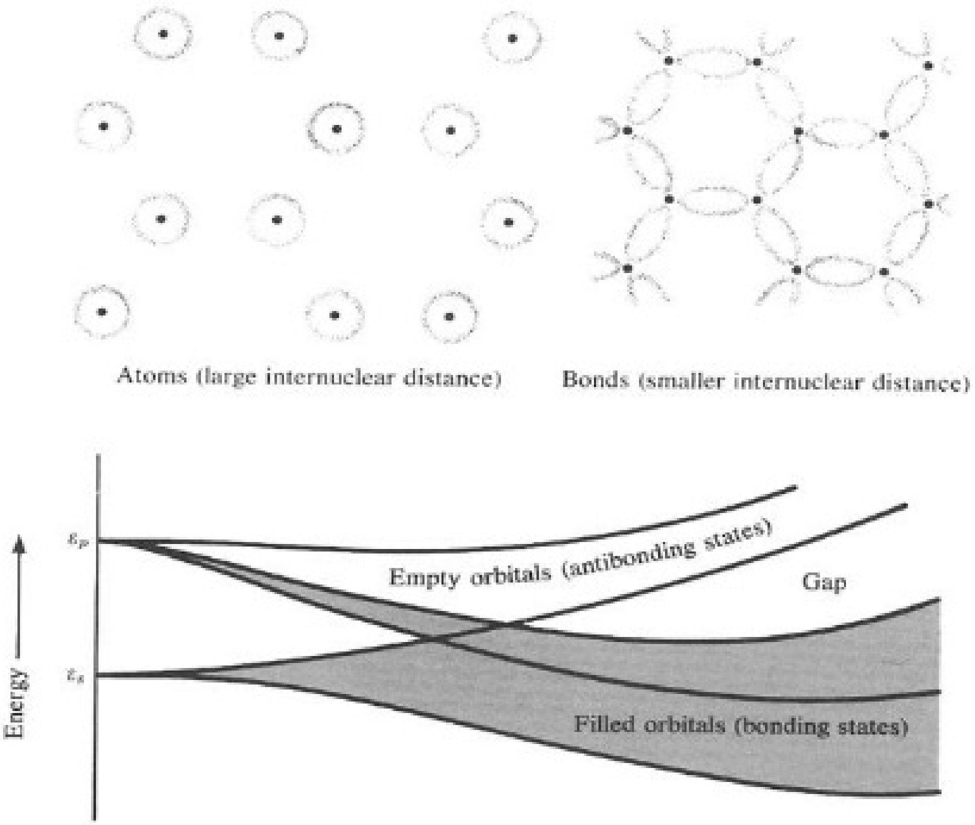

Figure 16: Tight binding model.

$$\begin{bmatrix} \langle \Psi_{1,1} | H | \Psi_{1,1} \rangle & \langle \Psi_{1,1} | H | \Psi_{1,2} \rangle & \dots & \langle \Phi_{1,1} | H | \Phi_{M,N} \rangle \\ \langle \Psi_{1,2} | H | \Psi_{1,1} \rangle & \langle \Psi_{1,2} | H | \Psi_{1,2} \rangle & \dots & \langle \Phi_{1,2} | H | \Phi_{M,N} \rangle \\ \vdots & & \ddots & \vdots \\ \langle \Psi_{M,N} | H | \Psi_{1,1} \rangle & \langle \Psi_{M,N} | H | \Psi_{1,2} \rangle & \dots & \langle \Phi_{M,N} | H | \Phi_{M,N} \rangle \end{bmatrix} \tag{41}$$

$$\langle \Psi_{1,2} | H | \Psi_{3,4} \rangle = \left\langle \Psi_{1,2} \left| \frac{-\hbar^2}{2m} \nabla^2 + V(r) \right| \Psi_{3,4} \right\rangle \tag{42}$$

If you make these calculations for a 1-dimensional problem (see eqn. (43)), you always get the same number ($\epsilon = \langle \Psi_{q,n} | H | \Psi_{q,n} \rangle$) for the terms down the diagonal because the wavefunctions are the same only the position is different. One step away from the main diagonal you get a term $-t$ and $t = -\langle \Psi_{q,n} | H | \Psi_{q,n+1} \rangle$ between the wavefunctions of two neighboring atoms (small number). This is the overlap of two neighboring atoms. One step further there are just zeros, because the 2nd nearest neighbors are too far apart. The $-t$'s in the corners are associated with the periodic boundary conditions.

$$\begin{bmatrix} \epsilon & -t & 0 & 0 & & -t \\ -t & \epsilon & -t & 0 & \cdots & 0 \\ 0 & -t & \epsilon & -t & & 0 \\ 0 & 0 & -t & \epsilon & & \vdots \\ & \vdots & & & \ddots & -t \\ -t & 0 & 0 & \cdots & -t & \epsilon \end{bmatrix} \begin{bmatrix} 1 \\ e^{i2\pi j/N} \\ e^{i4\pi j/N} \\ e^{i6\pi j/N} \\ \vdots \\ e^{i2\pi(N-1)j/N} \end{bmatrix} = (\epsilon - t\cdot(e^{i2\pi j/N} + e^{i2(N-1)\pi j/N})) \begin{bmatrix} 1 \\ e^{i2\pi j/N} \\ e^{i4\pi j/N} \\ e^{i6\pi j/N} \\ \vdots \\ e^{i2\pi(N-1)j/N} \end{bmatrix} \tag{43}$$

This kind of matrix has a known solution as showed in eqn. (43). It looks like plane waves. The first term of the wavefunction is 1, the next term has a phase factor j, which shows the position in the chain. It is just an integer and N is the total number of atoms. The next elements always grow with the same phase factor. If you multiply this vector by the matrix you get three terms and the vector as you see below. So these terms are the eigenvalues of the matrix:

$$\epsilon - t\left(e^{\frac{i2\pi j}{N}} + e^{\frac{-i2\pi j}{N}}\right) = \epsilon - 2t\cos\left(\frac{2\pi j}{N}\right)$$

They can be translated from j to k by $\frac{2\pi j}{N} = ka$. So the dispersion relationship is

$$E(k) = \epsilon - 2t\cos(ka),$$

which is shown in fig. 17.

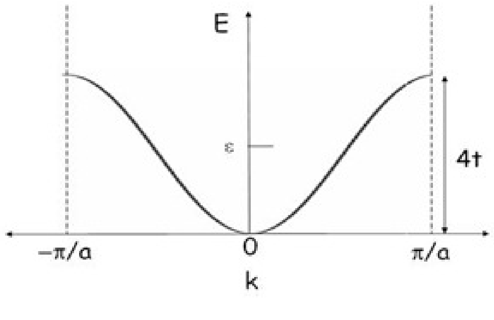

Figure 17: Dispersion relation for the tight binding model

Example: Square Well Potential

A square well potential can be solved by the tight binding model by looking for a solution for a finite potential well. A finite potential well has an exponential decay at the potential wall. In a 1-dimensional case we could take the lowest energy solution and put it at the bottom of everyone. With the tight binding model it is possible to calculate the dispersion relationship for electrons moving in a periodic potential like this. That problem is interesting because it is analytically solvable (Kronig Penney Model). Therefore the tight binding solution can be compared to the the exact solution.

To get an idea about the solution, a graphically overview (fig. 18) can be quite useful. Solutions occur that are a lot like the solutions of two wells that form a covalent bond. With a small potential well between the two waves there is an overlap of the two wavefunctions. So you get a bonding and an antibonding solution. We have more wells next to each other, you get the lowest total energy solution when you take them all with a symmetric wavefunction (Take the basic solution. To get the next solution multiply the first by one). For an antibonding solution you multiply the solution by $-1(e^{\frac{i\pi}{a}})$ then by $1(e^{\frac{i2\pi}{a}})$ and so on. So the k-vector is $\frac{\pi}{a}$. You have the basic solution and just multiply by the phase factor. If k is zero you multiply by 1,1,1,.. and if $k = \frac{\pi}{a}$ you get +1,−1,+1,−1.... and in between you get a complex factor which is not in the figure because it's hard to draw. In fig. 18 it is shown how the solutions look like.

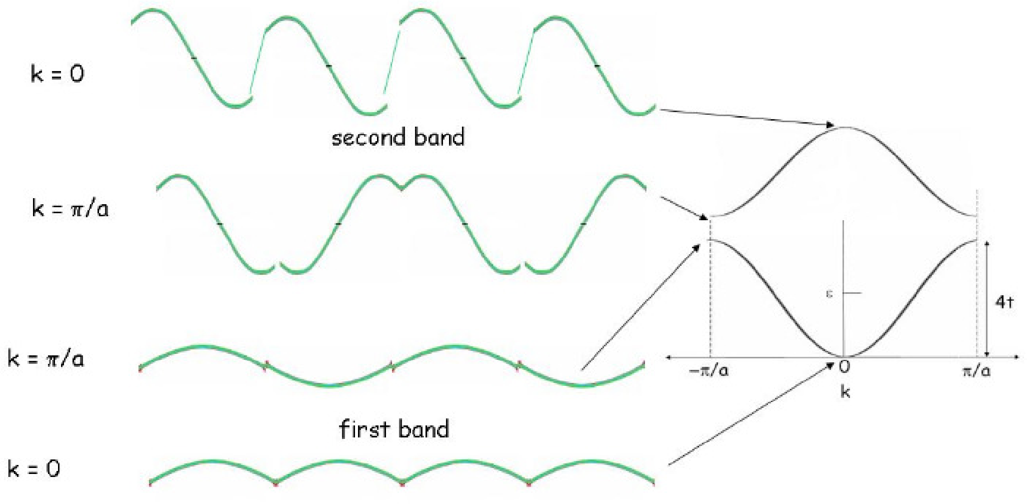

Figure 18: Solution of the square well potential.

Easier way to do the calculation:
Back to the linear chain model we used for phonons (see chapter 10.2.1). Now we are talking about mechanical motion, not about electrons. There are masses connected by springs which we handle with Newton's law:

$$m\frac{d^2u_s}{dt^2} = C(u_{s+1} - 2u_s + u_{s-1}).$$

If we write Newton's law in terms of a matrix equation it looks like shown in eqn. (44). In the diagonal you always get the $2C$ and one step away the C. The masses further away are not coupled with each other, so we get zero. For periodic boundary conditions we get the C in the corners.

$$-w^2m\begin{bmatrix} A_1 \\ A_2 \\ A_3 \\ A_4 \end{bmatrix} = \begin{bmatrix} -2C & C & 0 & C \\ C & -2C & C & 0 \\ 0 & C & -2C & C \\ C & 0 & C & -2C \end{bmatrix}\begin{bmatrix} A_1 \\ A_2 \\ A_3 \\ A_4 \end{bmatrix} \tag{44}$$

The matrix is exactly the same as before in the tight binding model. The easy way to solve the tight bindig model is to write down the Hamiltonian and then write down plane waves times the wave functions. This solves the Schrödinger equation. We know that plane waves times the atomic wavefunctions is the answer in the tight binding model. Taking that and putting it into the Schrödinger equation we get the dispersion relationship.

In the tight binding method we want to find the wavefunctions for electrons in a crystal, and we know the wavefunctions of the electrons on isolated atoms. When the atoms are pretty far apart, the atomic wavefunctions are good solutions for the electron wavefunctions of the whole system. We try to write a basis for the crystal wavefunctions in terms of the atomic wavefunctions and we get the big hamiltonian matrix. Then you have to diagonalize the matrix and the best solution you can make for electrons moving in a periodic crystal is

$$\Psi_k = \frac{1}{\sqrt{N}}\sum_{l,m,n} e^{i(l\mathbf{k}\mathbf{a_1}+m\mathbf{k}\mathbf{a_2}+n\mathbf{k}\mathbf{a_3})}\Psi(\mathbf{r} - l\mathbf{a_1} + m\mathbf{a_2} + n\mathbf{a_3}). \tag{45}$$

It is the atomic wavefunction, one on every side (one on every atom) times a phase factor (the same we used for phonons) that looks like a plane wave. Now we calculate the dispersion curve by calculating the energy of this particular solution:

$$E_k = \frac{\langle\Psi_k\,|H|\,\Psi_k\rangle}{\langle\Psi_k|\Psi_k\rangle}. \tag{46}$$

If you guess a wavefunction and the Hamiltonian you can calculate the corresponding energy. This does not mean that it is the lowest possible wavefunction. The calculation goes over a lot of terms for the calculation of the matrix elements. But the wavefunction falls exponentially with the distance, so the interaction is just important between nearest neighbors and next nearest neighbors. Therefore three atoms apart the interaction is zero (so the product of these two wavefunctions is zero). Our calculations now are just for the nearest neighbors. In this part of the calculations (the mean diagonal elements) the phase factor cancels out.

$$\epsilon = \frac{\int d^3\mathbf{r}\Psi^*(\mathbf{r})H\Psi(\mathbf{r})}{\langle\Psi_k|\Psi_k\rangle}$$

Now to the m nearest neighbors. They are all equivalent in the crystal (so there is one kind of atom, and one atom per unit cell). ρ is the distance to the nearest neighbor. The factor is because there is a little bit of overlap between two nearest neighbors:

$$t = -\frac{\int d^3\mathbf{r}\Psi^*(\mathbf{r}-\rho_\mathbf{m})H\Psi(\mathbf{r})}{\langle\Psi_k|\Psi_k\rangle}$$

In the definition of t there is a minus because t is negative most of the time (but a negative t is not a must!). If all m nearest neighbors are equivalent there are mN terms like $te^{i\mathbf{k}\rho_\mathbf{m}}$. All these terms have a phase factor because there is a difference in the phase factor (the phase factor changes by moving through the crystal, this is because there are differences when it moves for example in the y-direction or in the x-direction) a_1, a_2 and a_3 are the primitive lattice vectors in real space.

If you have a wavefunction like in eqn. (45) and you calculate the energy like in (46) you get this general formula to calculate the total energy with the sum over the phase factors. Equation (47) is the basic formula to calculate the dispersion relationship.

$$E = \epsilon - t\sum_m e^{i\mathbf{k}\vec{\rho}_m} \tag{47}$$

$\vec{\rho}_m$ is the distance to the nearest neighbors.

Doing this for a simple cubic crystal structure, all the atoms have 6 nearest neighbors (two in x-, two in y- and two in z-direction). So we take the sum over the six nearest neighbors for the calculation of the energy (eqn. (47)). The next equation is just for the nearest neighbors and the first term is for example in plus x-direction with $\rho = a$ (which is the same in each direction in a simple cubic). The second term goes in the minus x-direction with $\rho = a$ and so on for the y- and z-direction. And then you see that you can put it together to a cosinus term, you get an energy versus k dispersion relationship (for just the nearest neighbor terms). That looks like

$$E = \epsilon - t(e^{ik_xa} + e^{-ik_xa} + e^{ik_ya} + e^{-ik_ya} + e^{ik_za} + e^{-ik_za}) = \epsilon - 2t(cos(k_xa) + cos(k_ya) + cos(k_za)). \tag{48}$$

For a bcc crystal there are one atom in the middle and eight nearest neighbors at the edges. In this case the formula consists of 8 terms and looks like

$$E = \epsilon - t(e^{i(k_x\frac{a}{2}+k_y\frac{a}{2}+k_z\frac{a}{2})} + e^{i(k_x\frac{a}{2}+k_y\frac{a}{2}-k_z\frac{a}{2})} + ... = \epsilon - 8t\left(\cos\left(\frac{k_xa}{2}\right) + \cos\left(\frac{k_ya}{2}\right) + \cos\left(\frac{k_za}{2}\right)\right).$$

This is the dispersion relationship for a bcc crystal in the tight binding model.

In an fcc crystal there are 12 nearest neighbors, so the formula has twelve terms and looks like:

$$E = \epsilon - t(e^{i(k_x\frac{a}{2}+k_y\frac{a}{2})} + e^{i(k_x\frac{a}{2}-k_y\frac{a}{2})} + ..) =$$

$$= \epsilon - 4t\left(\cos\left(\frac{k_xa}{2}\right)\cos\left(\frac{k_ya}{2}\right) + \cos\left(\frac{k_xa}{2}\right)\cos\left(\frac{k_za}{2}\right) + \cos\left(\frac{k_ya}{2}\right)\cos\left(\frac{k_za}{2}\right)\right)$$

Fig. 19 shows the dispersion relationship of a simple cubic. It starts from Γ to X because in the x-direction there is a nearest neighbor. It starts like a parabola, close to the brillouin zone boundary it turns over and hits with about 90 degrees. M is in the 110 direction and R is in the 111 direction. So the energy is higher at the corner and at the edge of the cube. That is what we expected to happen from the empty lattice approximation. At the bottom we can calculate the effective mass $m^* = \frac{\hbar^2}{2ta^2}$ which is the second derivation of the dispersion relation. So if the overlap between the atomic wavefunctions is small (that means a small t) the effective mass is high. This makes it difficult to move the electron through the crystal. This also means that we get very flat bands because of eqn. (48). In fig. 19 you see just one band. If you want to have the next band you have to take the next atomic state (2s instead of 1s) and redo the calculation.

If you know k_x, k_y and k_z you can calculate the energy and you can plot the fermi sphere, which looks like a ball. If you go to higher energies there are no more possible states left, so you get a hole at the brillouin zone boundaries. If you increase the energy the hole becomes bigger and bigger and at one point there will be no more solutions in this band (from the atomic wavefunction you chose), if you took a very high energy. For a metal the fermi surface then separates into the occupied and the unoccupied states in a band.

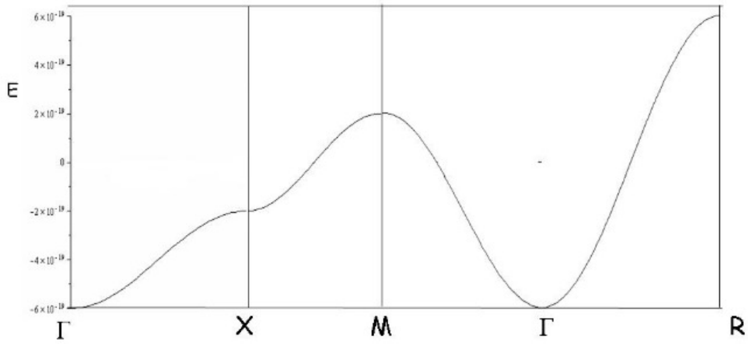

Figure 19: Dispersion relationship for a simple cubic.

In fig. 20 the dispersion relationship for an fcc crystal is shown. It is just plotted from Γ (centre) to L (111-direction) and to X (100-direction). The energies here are switched around because the nearest neighbors are in the 111-direction and there is the lowest energy. The facts about the overlap and the effective mass are also true for fcc. Out of the dispersion relationship it is possible to calculate k_x, k_y and k_z for a constant energy. The solutions are surfaces with constant energy, this is what is shown in fig. 21. The surface with the energy equal to the Fermi energy is with a good approximation (tight binding) the fermisurface.

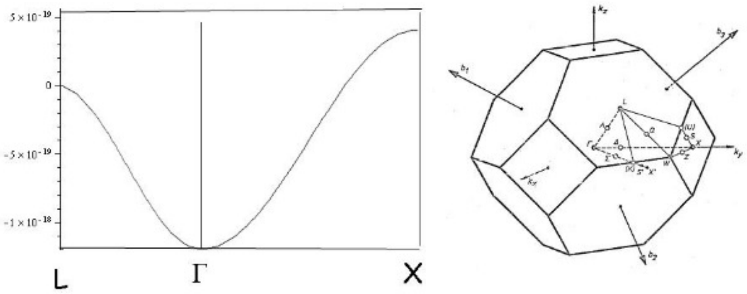

Figure 20: Dispersion relationship for an fcc crystal.

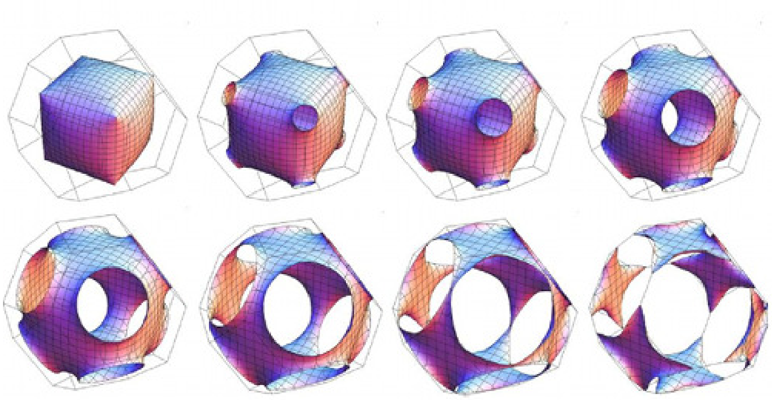

Figure 21: Surfaces of constant energy for a fcc crystal calculated with the Tight Binding approximation.

Now the same for bcc crystals. Here the nearest neighbors are in the 111 direction, and so is the lower energy. You can see that in fig. 22 the brillouin zone is a rhombic dodecahedron. There are corners with three lines to it and corners with four lines to it. One corner is the N point (closest point) of the lowest energy. Here the fermi surface shows unexpected behavior, see fig. 23. At a certain energy it is shaped like a cube. Then it breaks up and the states are getting fewer at higher energies.

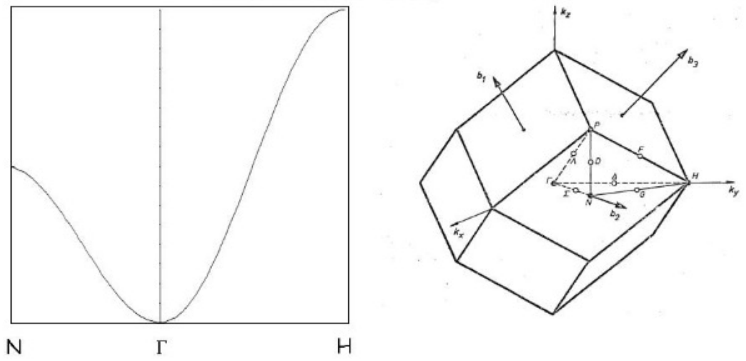

Figure 22: Dispersion relationship for a bcc crystal.

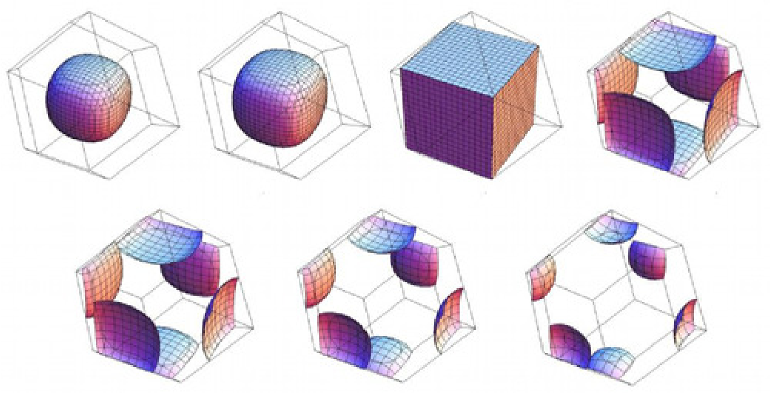

Figure 23: Surfaces of constant energy for a bcc crystal calculated with the Tight Binding approximation.

How to calculate the Fermi Energy: One possibility to calculate the fermi energy of a certain material is to construct it straightforward out of the density of states. To get the density of states we first need the dispersion relationship. By calculating the energy for every **k**-value we can look how many states there are at a certain energy. The curve we get, when we integrate this density of states gives us the total number of states over the energy. Assuming that you know how many electrons belong to the material you can read the fermi energy out of that curve.
An example is given in fig. 24 for the transition metal Osmium. The energy, where the curve for the total number of states reaches the number of electrons determines the fermi energy for Osmium.

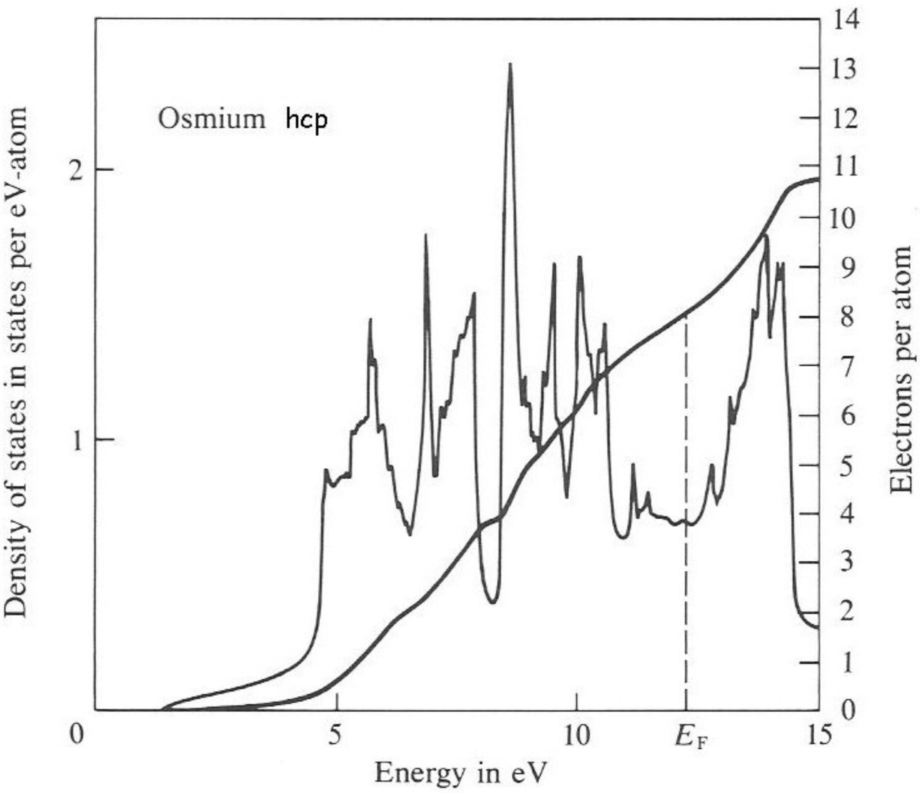

Figure 24: Density of states of the transition metal Osmium plus its integrated signal

4.4 Materials

4.4.1 Graphene

This part ist about graphene, which is one of the forms of carbon and has **2 atoms per unit cell**. Other forms of carbon are diamond (a pretty hard material) and graphite (a very soft material). In graphite there is a hexagonal lattice of carbon, and then the layers are just stepped. So graphene is a single layer of graphite and it turns out that this causes quite different electronic properties. If we look at the crystal structure in the left of fig. 25, we see that one of the carbon atoms has its bond to

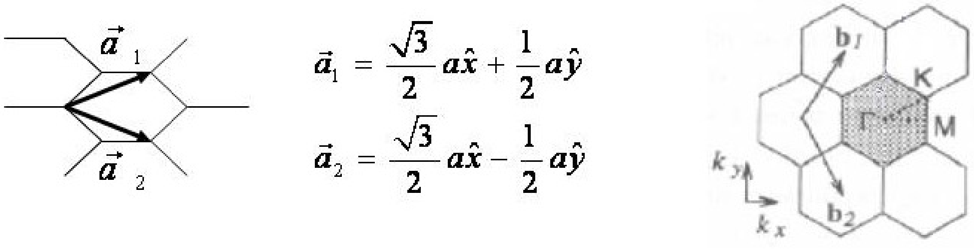

$$\vec{a}_1 = \frac{\sqrt{3}}{2}a\hat{x} + \frac{1}{2}a\hat{y}$$

$$\vec{a}_2 = \frac{\sqrt{3}}{2}a\hat{x} - \frac{1}{2}a\hat{y}$$

Figure 25: Lattice, primitive lattice vectors and reciprocal lattice of of graphene

the left and the other one to the right. So there are two inequivalent positions in the unit cell. The reciprocal lattice is also a hexagonal lattice (can be seen in the right of fig. 25). Trying to calculate the tight binding model, we see that there is a correlation in between the tight binding model and phonon calculations. In phonon calculations we had two atoms per unit cell and got an acoustical branch and an optical branch. Now we get two bands in the dispersion relationship, a lower energy branch and a higher energy branch.

The wavefunction is calculated by taking the two wavefunctions $\mid \psi_a >$ and $\mid \psi_b >$ of the atoms a and b of the unit cell and coupling them together like we were making a covalent bond. To calculate the energy shift (in a covalent bond) we describe the state of the whole system in terms of these two wavefunctions and construct the hamiltonian matrix:

$$\begin{vmatrix} \langle \psi_a \mid H \mid \psi_a \rangle - E & \langle \psi_a \mid H \mid \psi_b \rangle \\ \langle \psi_b \mid H \mid \psi_a \rangle & \langle \psi_b \mid H \mid \psi_b \rangle - E \end{vmatrix} = \begin{vmatrix} \varepsilon - E & -t \\ -t^* & \varepsilon - E \end{vmatrix} = 0 \quad \rightarrow \quad E = \varepsilon \pm |t| \tag{49}$$

It is only a two-by-two matrix, so it is easy to solve. ε is the energy eigenvalue without interaction and t is the overlap integral between the atoms a and b (so the nearest neighbour matrix elements). For the eigenenergy E we get two solutions, one for the bonding state and one for the anti-bonding state.

Now we do the same thing for two carbon sublattices. We also get the same kind of answer like in eqn. (49), but this is just the calculation for $\mathbf{k} = 0$. So there are also two eigenvalues for $\mathbf{k} = 0$. For $k \neq 0$ we have to redo the calculation multiplied by a phase factor. So we get

$$\begin{vmatrix} \varepsilon - E & -tf(\mathbf{k}) \\ -tf^*(\mathbf{k}) & \varepsilon - E \end{vmatrix} = 0$$

with the phase factor

$$f(\mathbf{k}) = \exp\left(\frac{ik_x a}{2}\right)\left(1 + \exp\left(-i\left(\frac{\sqrt{3}k_x a}{2} - \frac{k_y a}{2}\right)\right) + \exp\left(-i\left(\frac{\sqrt{3}k_x a}{2} + \frac{k_y a}{2}\right)\right)\right),$$

which depends on $\mathbf{k}$ (and is the sum over the three nearest neighbours). We plug the phase factor in the matrix equation

$$\begin{vmatrix} \varepsilon - E & t\left(1 + \exp\left(-i\left(\frac{\sqrt{3}k_x a}{2} - \frac{k_y a}{2}\right)\right) + \exp\left(-i\left(\frac{\sqrt{3}k_x a}{2} + \frac{k_y a}{2}\right)\right)\right) \\ t\left(1 + \exp\left(+i\left(\frac{\sqrt{3}k_x a}{2} - \frac{k_y a}{2}\right)\right) + \exp\left(+i\left(\frac{\sqrt{3}k_x a}{2} + \frac{k_y a}{2}\right)\right)\right) & \varepsilon - E \end{vmatrix} = 0$$

and after some calculation (using the trigonometric identities $\cos(a \pm b) = \cos(a)\cos(b) \mp \sin(a)\sin(b)$ and $\cos(2a) = 2\cos^2(a) - 1$) we get

$$E = \varepsilon \pm t\sqrt{1 + 4\cos\left(\frac{\sqrt{3}k_x a}{2}\right)\cos\left(\frac{k_y a}{2}\right) + 4\cos^2\left(\frac{k_y a}{2}\right)}.$$

So again we get two solutions (eigenenergies) for every $\mathbf{k}$ from this matrix. The energy E is the atomic energy ε plus the overlap integral t times some function of $\mathbf{k}$. When we plot that function at $\mathbf{k} = 0$ it starts to rise like a parabola (see fig. 26). The two solutions (for the bonding and the anti-bonding state) are just mirror images of each other. In the upper direction there is the energy. The solutions touch at six points and the fermi energy also cuts through this point. So we have a fermi surface which consists of six points. At the fermi surface the dispersion relationship is linear (usually it has some curvature like a parabola).

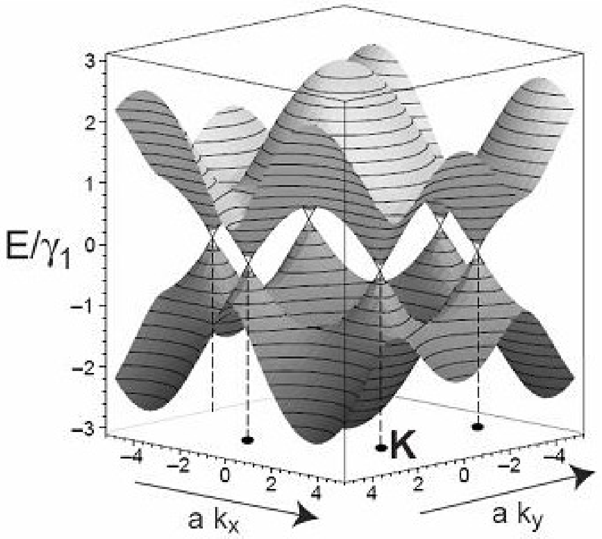

Figure 26: Plot energy versus k_x and k_y (2 dimensions).

4.4.2 Carbon nanotubes

Carbon nanotubes are made of a sheet of **graphene** rolled up into a tube. There are three different types of carbon nanotubes, as we can see in fig. 27.

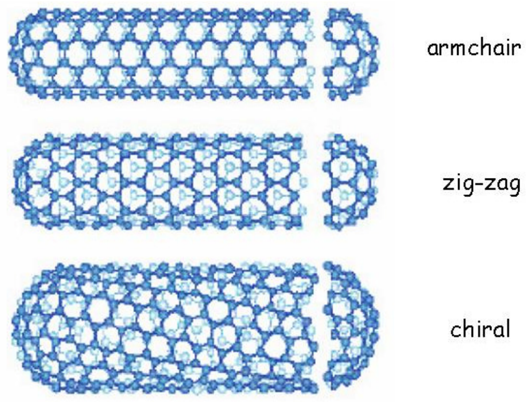

Figure 27: Different types of carbon nanotubes.

- Armchair: Looks like an armchair.
- Zig-Zag: Going around (along the diameter) the tube it makes zig-zag.
- Chiral: Atomic rows do not go straight on the tube, they twist around (chiral can vary).

Carbon nanotubes can also have different diameters. A terminology to specify what kind of nanotube we have is to take a plane of graphene like in fig. 28. We choose an origin and count along over the primitive lattice vectors to another point of the lattice with an equivalent site. Then we cut the

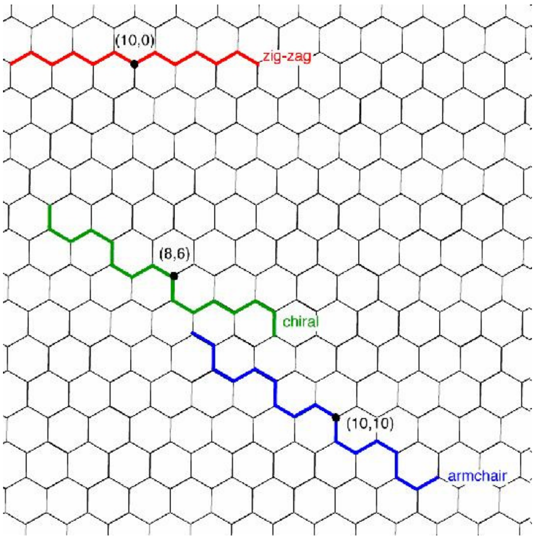

Figure 28: How to specify the kind of a nanotube.

graphene out perpendicular to this line and role it up so that the end point falls on the origin we defined.

Now we calculate the band structure, the dispersion relationship for carbon nanotubes. With carbon nanotubes there are periodic boundary conditions around the short distance (around the diameter of the tube). So there are only certain k_y-values, in the direction k_x we also use periodic boundary conditions but the length L in this direction is much larger, hence there are more values for k_x then for k_y. In fig. 29 there is a plot in k-space and on the left this issue is shown for the first brillouin zone (which goes from $-\pi/a$ to π/a). If we have a (10,10) tube going around the diameter we only have 10 values for k_y. That means there are fewer allowed k-vectors. But the tight binding problem does not change with respect to the problem solved for graphene. For carbon nanotubes the calculation is the same except there are only certain values for k_y. In fig. 29 on the right side the highest bonding

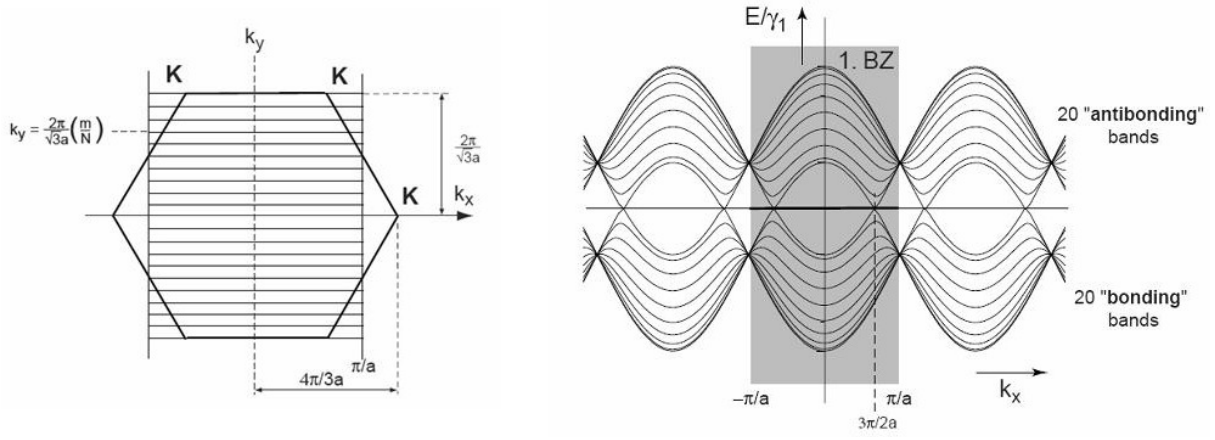

Figure 29: Metallic (10,10) armchair tube.

band line corresponds to $k_y = 0$ and it touches the band above at a certain k_x point. If we increase k_y a little bit what happens is that we miss this point where the two bands meet and then we get something that looks like a semiconductor. But this (10,10) armchair tube is metallic because we went through the points where the two solutions meet.

From the dispersion relationship we can calculate the density of states. For a metallic tube the dispersion relationship is constant around the fermi energy and that gives a constant density of states like in fig. 30. The next allowed value of k_y has a maximum and that results in a Van Hove singularity in the density of states (because there are a lot of states in this energy range). If we have a semiconducting nanotube (as seen on the right in fig. 30) the bands do not meet and the density of states is zero, there is a gap. But we also have this Van Hove singularity on both sides because of the maxima and the minima in the bands.

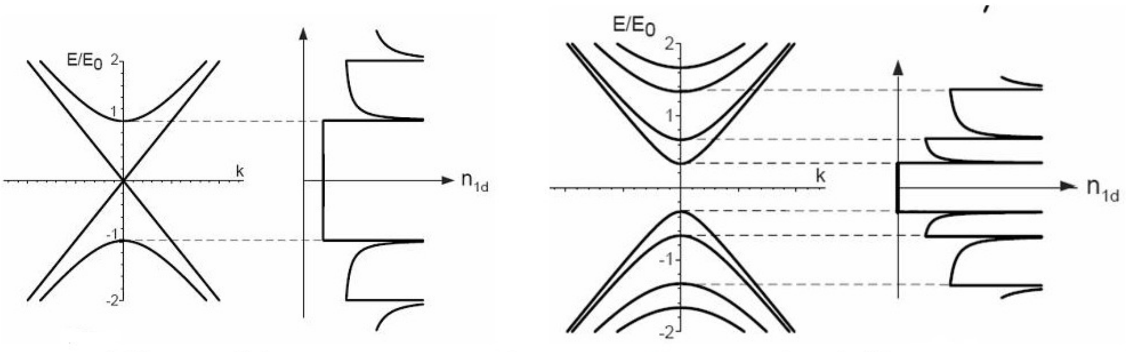

metallic m-n=3Z

semiconducting

Figure 30: Dispersion relationship and density of states for both a metallic and a semiconducting carbon nanotube.

The formula $m - n = 3Z$ (for a (m, n)-nanotube) says that if $\frac{m-n}{3}$ is an integer the tube will be metallic, otherwise semiconducting (for example a (10,0) nanotube: $10 - 0 = 10$ can not be divided by three so this should be a semiconducting tube).

Other Nanotubes

Carbon is not the only material which makes tubes, others are:

- Tungsten disulfide
- Boron nitride
- Silicon
- Titanium dioxide
- Molybdenum disulfide

Boron nitride for example has the same bond lengths in all directions and so all the directions are the same, therefore we get get the same phase factors and band structures with the tight binding model as for graphene (as we see in fig. 31). But because there are two different types of atoms per unit cell the energy of the bonding and antibonding state is never the same - there is always a band gap - boron nitride is always a semiconductor.

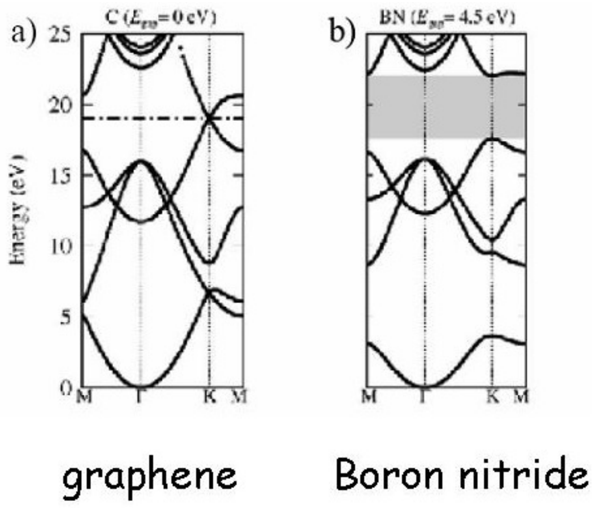

Figure 31: Band structure of graphene and Boron nitride.

4.4.3 Metals

In a metal there are a bunch of bands that are electrically inert. They are occupied by electrons but far away from the fermi energy so that the electrons do not participate in the properties of the metal (conductivity, specific heat). Hence they are called **inert bands**. Bands way above the fermi energy are just empty and electrically inactive too. The interesting band is the one that is partly filled. The electrons at this level will contribute to the magnetism, the heat capacity, the electrical conductivity and the thermal conductivity of the material. Fig. 32 is drawn for about room temperature. At room temperature $k_B T$ (the thermal energy) tends to be much smaller than the fermi energy and the fermi function is pretty sharp.

In fig. 33 the periodic table is shown with the tagged d- and f-band metals. For calculating the band structure of these metals with the tight binding model only the d- and f-band electrons are interesting, because these are the only electrons which interact with electrons of their neighbor atoms. The resulting band then is called d respectively f, hence also the metals are called d- and f-band metals.

Fig. 34 displays the band structure of the transition metals (the dotted line is the fermi energy). From the left to the right the electron density increases and so the fermi energy moves up to the d bands. But in every point the fermi energy hits the band somewhere. In the d bands the band width is very small, which means that the matrix element we calculated in the tight binding model is fairly small. That gives fairly flat bands and if we want to approximate something like parabolas it ends up that we need a high effective mass (so in something with flat bands the electrons do not move through so good). For example in copper the fermi energy cuts through the s band and all the d bands are filled. So in copper all the narrow bands that have a high effective mass just are not contributing any more

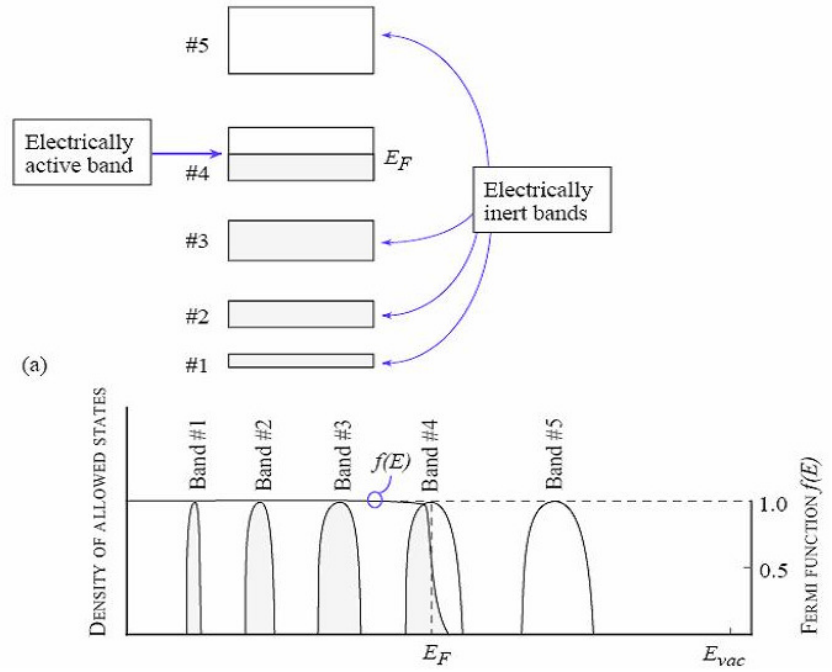

Figure 32: Bands in a metal.

and the fermi energy has moved up. The s band makes copper a good conductor. Fig. 35 shows the dispersion relationship and the density of states of copper. The density of states of the d band has some peaks in it. These peaks correspond to places in the dispersion relationship where there are a lot of states at that energy.

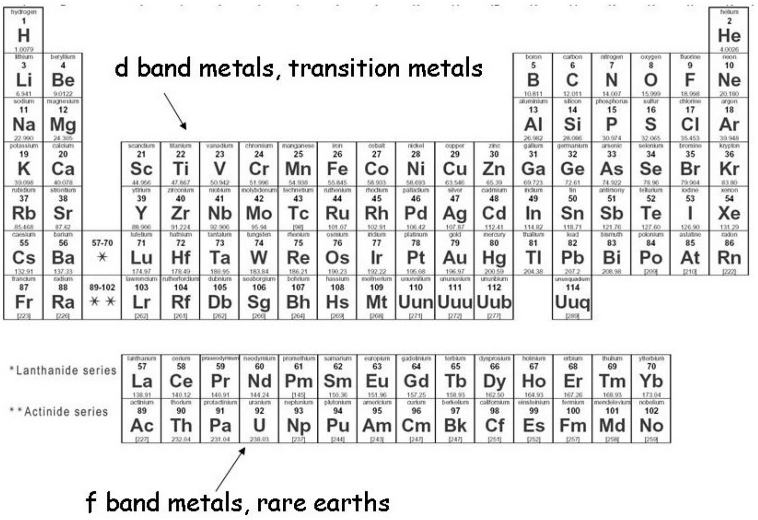

1 H																		2 He
3 Li	4 Be												5 B	6 C	7 N	8 O	9 F	10 Ne
11 Na	12 Mg												13 Al	14 Si	15 P	16 S	17 Cl	18 Ar
19 K	20 Ca		21 Sc	22 Ti	23 V	24 Cr	25 Mn	26 Fe	27 Co	28 Ni	29 Cu	30 Zn	31 Ga	32 Ge	33 As	34 Se	35 Br	36 Kr
37 Rb	38 Sr		39 Y	40 Zr	41 Nb	42 Mo	43 Tc	44 Ru	45 Rh	46 Pd	47 Ag	48 Cd	49 In	50 Sn	51 Sb	52 Te	53 I	54 Xe
55 Cs	56 Ba	57-70 *	71 Lu	72 Hf	73 Ta	74 W	75 Re	76 Os	77 Ir	78 Pt	79 Au	80 Hg	81 Tl	82 Pb	83 Bi	84 Po	85 At	86 Rn
87 Fr	88 Ra	89-102 **	103 Lr	104 Rf	105 Db	106 Sg	107 Bh	108 Hs	109 Mt	110 Uun	111 Uuu	112 Uub		114 Uuq				

*Lanthanide series	57 La	58 Ce	59 Pr	60 Nd	61 Pm	62 Sm	63 Eu	64 Gd	65 Tb	66 Dy	67 Ho	68 Er	69 Tm	70 Yb
**Actinide series	89 Ac	90 Th	91 Pa	92 U	93 Np	94 Pu	95 Am	96 Cm	97 Bk	98 Cf	99 Es	100 Fm	101 Md	102 No

Figure 33: Periodic table.

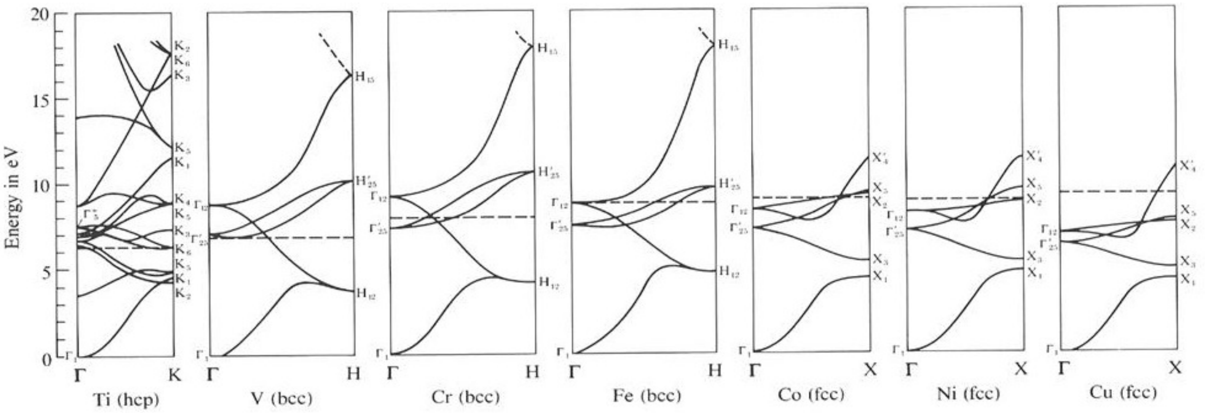

Figure 34: Transition metals.

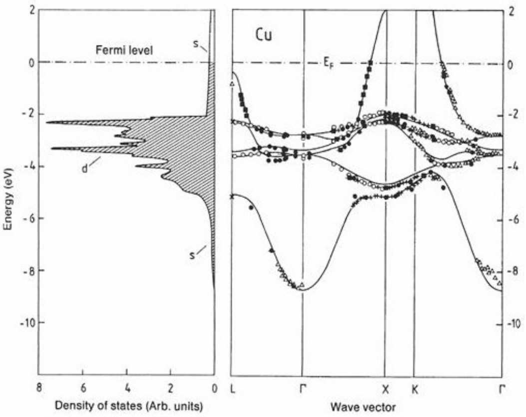

Figure 35: Dispersion relationship and density of states of copper.

4.4.4 Semimetal

A semimetal is a metal where the fermi energy is in the band but the electron density is pretty low. The right plot in fig. 36 is a bit more a metal than a semimetal. So in a semimetal there are just a few states in the upper band. This can happen if there is something that's almost a semiconductor but in one direction in k-space the bands overlap in energy. That means that a semimetal is a metal but with a low electron density. A classical example of a semimetal is bismuth.

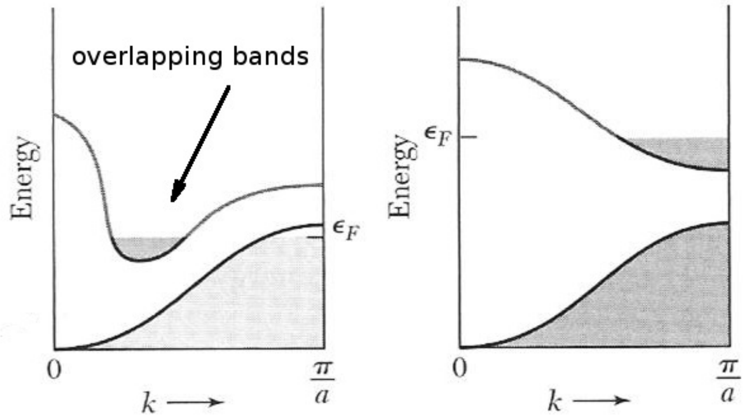

Figure 36: Two kinds of a semimetal.

4.4.5 Semiconductors

In a semiconductor bands that are filled are also electrically inert. But now the fermi energy falls in between two bands in a gap. These two bands are called valence band and conduction band. It is only a semiconductor if the gap is less than 3eV. The value of 3eV comes through the fact that for low temperatures some electrons are excited thermally above the gap from the valence band into the conduction band and we measure some kind of conductivity. If the gap is bigger there are zero electrons excited into the conduction band at low temperatures. In fig. 37 we see the fermi energy dropping in the gap leaving a few holes in the valence band and a few electrons in the conduction band.

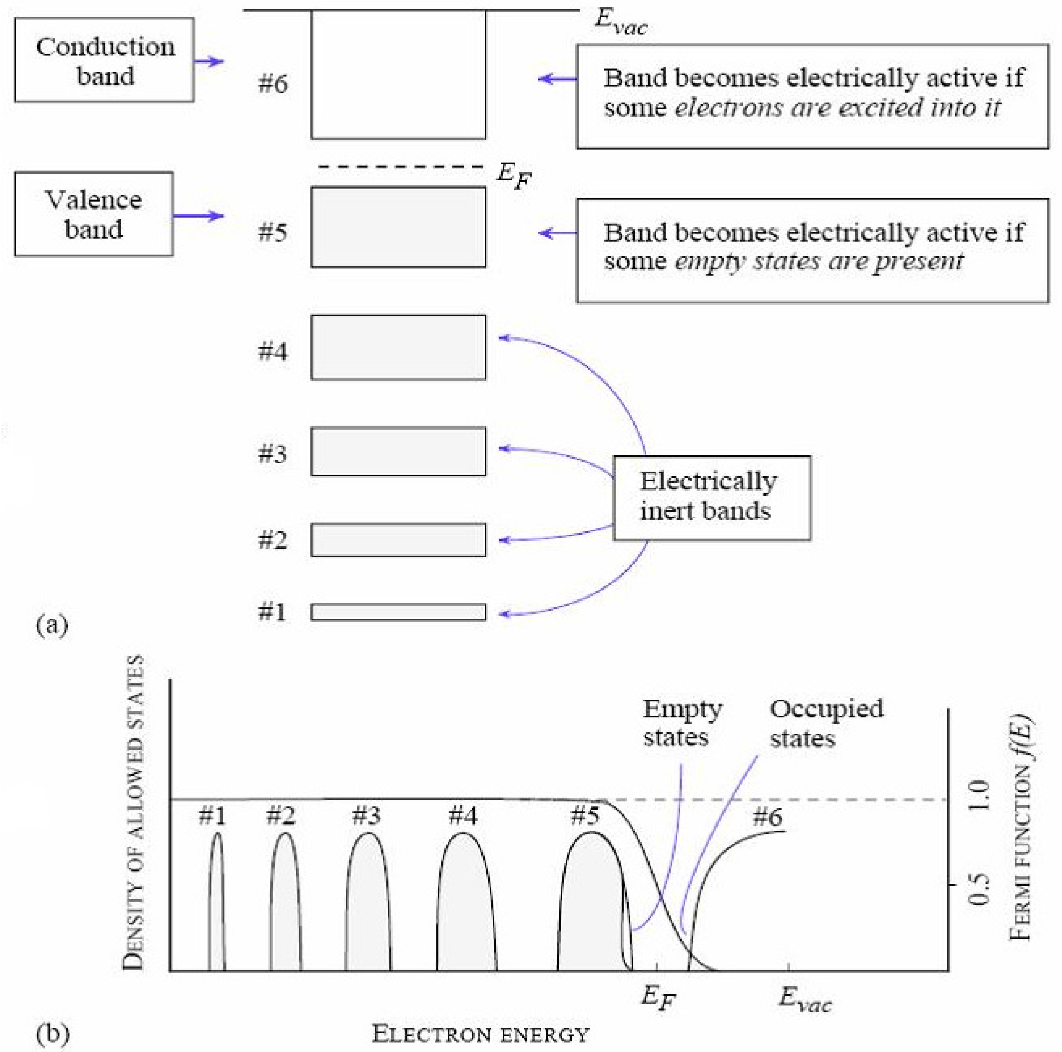

Figure 37: Bands in a semiconductor.

Direct and Indirect Bandgaps Generally semiconductors can be divided into two types. There are semiconductors with direct bandgaps (fig. 38 (a)) and those with indirect bandgaps (fig. 38 (b)). In semiconductors with direct bandgaps the top of the valence band and the bottom of the conduction band are at the same **k**-value, which is not the case in semiconductors with indirect bandgaps, as fig. 38 shows.

The main differences occur in the relaxation from an excited state. After an electron is excited into the conduction band by a photon with an energy, which is high enough, it will occupy the lowest possible energy state in the conduction band. The generated hole in the valence band will occupy the highest possible energy state. If those two positions are at different **k**-values, which is the case in semiconductors with indirect bandgaps, the particle produced in the relaxation has to carry both the difference in energy and momentum. Since photons can only carry a very little amount of momentum, this relaxation will produce phonons. That's the reason why light emmitting devices are built using semiconductors with direct bandgaps like Gallium-Arsenite, and solar cells, which shouldn't emmit

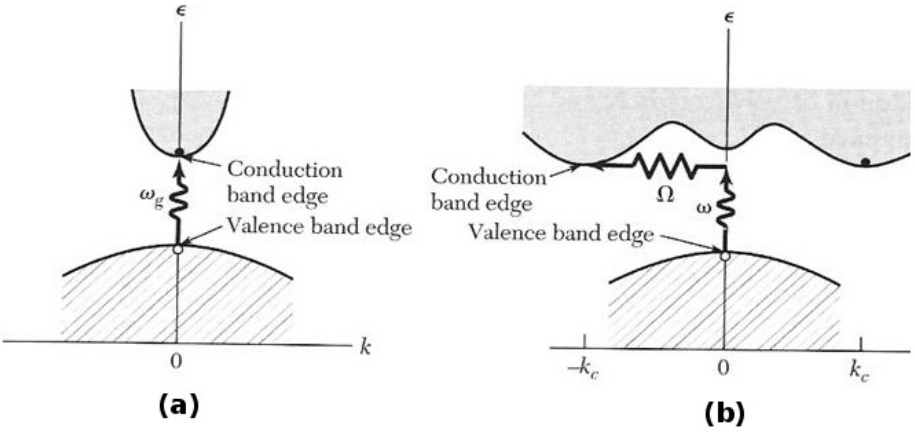

Figure 38: Top of the valence band and bottom of the conduction band in semiconductors with direct (a) and indirect (b) bandgaps

light, can be built using semiconductors with indirect bandgaps like Silicon.

5 Magnetism and Response to Electric and Magnetic Fields

Physical quantities in solids can be calculated the following way:
Solve the Schroedinger equation → get the dispersion relation → calculate the density of states → use this to get the Gibbs free energy → take certain derivatives to get quantities as the specific heat, pressure, piezoelectric constants, piezomagnetic constants, etc.

The main problem seems to be calculating the microscopic states, as anything else is a straight forward calculation. However, to get the microscopic states, one uses different types of models. Until now, we often used the free electron model, and the electric field and the magnetic field were expected to be zero. Because of this, the piezoelectric and the piezomagnetic constants turned out to be zero too, when calculating the free energy.
As we want to know, how a material responses to an electric or a magnetic field, the simplifications mentioned above, have to be corrected.

5.1 Magnetic Fields

When a charged particle (in most cases a free electron) moves through a magnetic field, there is a force on this particle, perpendicular to the velocity. Remember that this force can change the direction of the electron, but the magnetic field does no mechanical work, because of the electron moving perpendicular to the force.

$$\mathbf{F} = -e\mathbf{v} \times \mathbf{B} \tag{50}$$

$$evB_z = \frac{mv^2}{R} \tag{51}$$

$$v = w_c R \tag{52}$$

$$w_c = \frac{eB_z}{m} \tag{53}$$

with w_c the angular frequency or cyclotron frequency.

When the particle is moving in a circle around a located position, it is moving around the origin in k-space as shown in fig. 39.

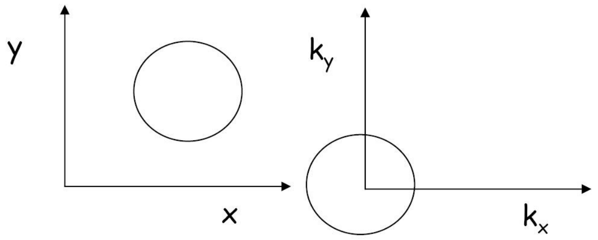

Figure 39: Particle moving on a circle in cartesian coordinates and in k-space. Something moving on a circle at a located position, moves around the origin in k-space, because the x- and y-velocity keep going to zero and that's the path taken in k-space.

Usually when a charge is accelerated (which it is, when moving on a circle), it emits electromagnetic radiation. For solids, a similar thing would be to put a metal into a magnetic field. The electrons at the fermi surface are moving quite fast and there is also a perpendicular force on them when the metal is in the field, but they are not emitting radiation. The reason for this is that they simply can't get into a state with lower kinetic energy (all filled up) like a free electron does.

The problem of getting the magnetic field into the Schroedinger equation is that the force depends on the velocity as shown below.

$$\mathbf{F} = q(\mathbf{E} + \mathbf{v} \times \mathbf{B}) \tag{54}$$

So, one has to construct a Lagrangian, which is a function of velocity. Normally one guesses the Lagrangian and looks if the right force comes out, but luckily in this case the Lagrangian was guessed before to be

$$L = \frac{1}{2}mv^2 - qV(\mathbf{r},t) + q\mathbf{v} \cdot \mathbf{A}(\mathbf{r},t). \tag{55}$$

So by putting this Lagrangian into the Euler-Lagrange equations (eqn. (56)), we obtain the Lorentz force law[3]:

$$\frac{d}{dt}\left(\frac{\partial L}{\partial \dot{x_i}}\right) - \frac{\partial L}{\partial x_i} = 0 \tag{56}$$

$$\begin{aligned}
&\frac{d}{dt}\left(\frac{\partial L}{\partial v_x}\right) - \frac{\partial L}{\partial x} = 0 \\
&\frac{d}{dt}\left(\frac{\partial L}{\partial v_x}\right) = \frac{d}{dt}(mv_x + qA_x) = m\frac{dv_x}{dt} + q\frac{dA_x}{dt} \\
&= m\frac{dv_x}{dt} + q\left(\frac{dx}{dt}\frac{\partial A_x}{\partial x} + \frac{dy}{dt}\frac{\partial A_x}{\partial y} + \frac{dz}{dt}\frac{\partial A_x}{\partial z} + \frac{\partial A_x}{\partial t}\right) \\
&= m\frac{dv_x}{dt} + q\left(v_x\frac{\partial A_x}{\partial x} + v_y\frac{\partial A_x}{\partial y} + v_z\frac{\partial A_x}{\partial z} + \frac{\partial A_x}{\partial t}\right) \\
&\frac{\partial L}{\partial x} = -q\frac{\partial V}{\partial x} + q\left(v_x\frac{\partial A_x}{\partial x} + v_y\frac{\partial A_y}{\partial x} + v_z\frac{\partial A_z}{\partial x}\right) \\
&m\frac{dv_x}{dt} = -q \underbrace{\left(\frac{\partial V}{\partial x} + \frac{\partial A_x}{\partial t}\right)}_{\text{x component of electric field}} \underbrace{+q\left(v_y\left(\frac{\partial A_y}{\partial x} - \frac{\partial A_x}{\partial y}\right) + v_z\left(\frac{\partial A_z}{\partial x} - \frac{\partial A_x}{\partial z}\right)\right)}_{\text{x component of }\mathbf{v}\text{ x }\mathbf{B}}
\end{aligned}$$

With the calculation above in all three dimensions, $\mathbf{E} = -\nabla V - \frac{\partial \mathbf{A}}{dt}$ and $\mathbf{B} = \nabla \times \mathbf{A}$, eqn. (54) is obtained, which proves eqn. (55) to be the right Lagrangian to solve this problem.

So with eqn. (55) the momentum can be calculated as

$$p_x = \frac{\partial L}{\partial v_x} = mv_x + qA_x \tag{57}$$

---

[3] Der Beweis fuer die Richtigkeit der Lagrangefunktion ist nicht pruefungsrelevant, wird aber der Vollstaendigkeit halber wiedergegeben. Man sollte aber wissen, dass genau diese Lagrangefunktion das Problem beschreibt.

In this case, beside the kinetic momentum, there is an additional part, which is called the field momentum. When a charged particle is moving, there is a current flowing, which causes a magnetic field. So when the particle is decelerated, the inductance of the magnetic field keeps pushing it forward, so that there is more energy needed to stop the particle than just the kinetic energy.
With this information the Hamiltonian can be constructed:

$$H = \mathbf{v} \cdot \mathbf{p} - L$$

$$H = \frac{1}{2m} \left(\mathbf{p} - q\mathbf{A}(\mathbf{r}, t)\right)^2 + qV(\mathbf{r}, t)$$

Finally, with the substitution $\mathbf{p} \to -i\hbar\nabla$, the Schroedinger equation for electrons in an electromagnetic field is obtained:

$$i\hbar\frac{\partial\Psi}{\partial t} = \frac{1}{2m} \left(-i\hbar\nabla - q\mathbf{A}(\mathbf{r}, t)\right)^2 \Psi + qV(\mathbf{r}, t)\Psi \tag{58}$$

5.2 Magnetic Response of Atoms and Molecules

Sometimes it is a good approximation to treat a solid as a noninteracting gas of magnetic atoms or molecules. The Schroedinger equation reads as follows:

$$\frac{1}{2m} \left(-i\hbar\nabla - q\mathbf{A}\right)^2 \Psi + V(\mathbf{r})\Psi = E\Psi$$

It is possible to separate the Hamiltonian into two parts:

$$H_0 = \frac{-\hbar^2}{2m}\nabla^2 + V(\mathbf{r})$$

$$H_1 = \frac{1}{2m}\left(i\hbar\nabla \cdot \mathbf{A} + i\hbar q\mathbf{A} \cdot \nabla + q^2A^2\right) + g\mu_B S_z B_z$$

with g the g-factor which is for the spin of an electron ∼ 2.
H_0 is the Hamiltonian for zero magnetic field and H_1 contains the additional parts that come from the magnetic field plus an extra term for the spin (in non-relativistic quantum mechanics one just adds the term for the spin, there is no logical approach for that). The vector potential can be chosen so that

$$\nabla \times \mathbf{A} = B_z\hat{z} \quad \text{(this means that } \mathbf{B} \text{ points into the z-direction).}$$

$$\nabla \cdot \mathbf{A} = 0 \quad \text{(Coulomb gauge)}$$

$$\to \mathbf{A} = \begin{bmatrix} -\frac{1}{2}yB_z \\ \frac{1}{2}xB_z \\ 0 \end{bmatrix}$$

The second part of the Hamiltonian can be written as

$$H_1 = \frac{-i\hbar eB_z}{4m}\left(-y\frac{\partial}{\partial x} + x\frac{\partial}{\partial y}\right) + \frac{e^2B_z^2}{8m}\left(x^2 + y^2\right) + g\mu_B S_z B_z$$

The first part of H_1 can be identified as the angular momentum operator:

$$L_z = -i\hbar \left(x\frac{\partial}{\partial y} - y\frac{\partial}{\partial x} \right)$$

To get the energy associated with H_1, it is necessary to calculate the matrix elements $\langle \Psi | H_1 | \Psi \rangle$. It turns out, that in most cases spherical symmetric waves are of specific interest. For those waves one can write the expectation value of $\mathbf{r}^2$ as $\langle \mathbf{r}^2 \rangle = \langle \mathbf{x}^2 \rangle + \langle \mathbf{y}^2 \rangle + \langle \mathbf{z}^2 \rangle = 3\langle \mathbf{x}^2 \rangle = \frac{3}{2}\left(\langle \mathbf{x}^2 \rangle + \langle \mathbf{y}^2 \rangle \right)$.
So when we use waves of the described form and calculate the matrix elements, we get for the energy (using the Bohr magneton $\mu_B = \frac{e\hbar}{2m_e}$):

$$E_1 = \left(\langle L_z \rangle + g\langle S_z \rangle \right)\mu_B B_z + \frac{e^2 B_z^2}{12m}\left\langle \mathbf{r}^2 \right\rangle .$$

The right-side term depends on the average position of the electrons. It also doesn't matter from which side one applies the magnetic field, there is always an increase in energy. So this part stands for the **diamagnetic** response. This is because the energy in a magnetic problem is calculated by

$$E = -\boldsymbol{\mu} \cdot \mathbf{B},$$

so only when the magnetic moment and the magnetic field are antiparallel the energy increases.
The left side-term depends on the orbital angular momentum and the spin angular momentum, which can either be positive or negative. So it is on the magnetic quantum number (for angular momentum $l = 1 \rightarrow m_l = -1, 0, 1$) whether the energy increases or decreases. A good example is the Zeeman effect, where the two states for spin +1/2 and -1/2 split up and one goes up in energy and one goes down. Now the state that goes down in energy has a lower energy and therefore is more likely to be occupied. This leads to a magnetization of the system because there are still both states, but the lower one is more likely to be occupied than the upper one and there the magnetic moments are aligned with the magnetic field which is responsible for the **paramagnetic** effect.

5.2.1 Diamagnetic Response

At the beginning, we need the formula for the diamagnetic moment:

$$\mu = -\frac{\partial E}{\partial B} = -\frac{e^2 B_z}{6m}\left\langle \mathbf{r}^2 \right\rangle$$

This description is often used in ionic crystals, where the two atoms have an electric closed shell configuration. For a filled shell with L=0 and S=0 the paramagnetic part vanishes and one is left with the diamagnetic part. Then the magnetic moment can be calculated like described above.
The minus sign indicates, that the magnetic moment is opposite to the applied field. The energy can be calculated as $E = -\boldsymbol{\mu} \cdot \mathbf{B}$ and always increases with an applied field.
It is not easy to synthesize magnetic molecules, because stable molecules have a closed shell configuration. However there are molecules that do not have a closed shell configuration (e.g. OH), which are called radicals in chemistry. Those molecules are not charged but very reactive in order to get the stable closed shell configuration.
When there are many electrons, $\langle \mathbf{r}^2 \rangle$ can be substituted by $Z^2 a^2$ (with Z = number of valence electrons

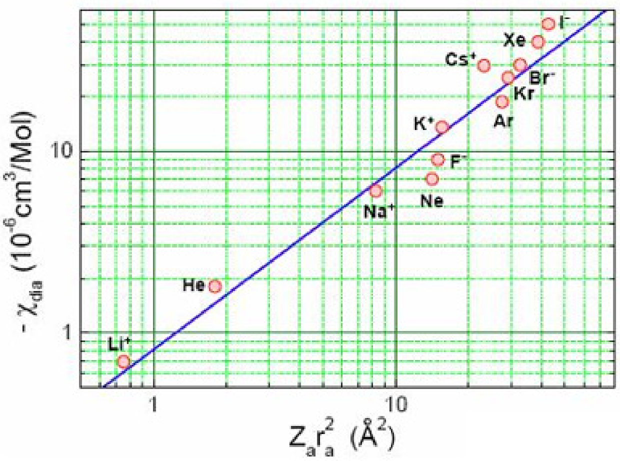

Figure 40: Magnetic behavior of molecules and ions with closed electron shell configuration. The blue line is the expected behavior for diamagnets.

and a = ionic radius). Then it is possible to write the magnetic susceptibility as

$$\chi_{dia} = -\mu_0 \frac{N}{V} \frac{e^2 B_z}{6m} Z^2 a^2.$$

Fig. 40 shows the magnetic response for some molecules and ions with closed shell configuration, where the blue line is the expected behavior for diamagnetism, calculated with the formula above.

5.2.2 Paramagnetic Response

Whenever there is a non-zero angular momentum in the z-direction (spin), there are more than one states (remember different magnetic quantum numbers), which split into different energy levels due to the Zeeman effect. So first one has to figure out what the energies of these different states are and then a partition function[4] has to be constructed (lower states are occupied more likely).
Again the energy can be calculated as $E = -\boldsymbol{\mu} \cdot \mathbf{B}$, but now using $\boldsymbol{\mu} = -g_J \mu_B \mathbf{J}$, with $\mathbf{J}$ the total angular momentum ($\mathbf{J} = \mathbf{L} + \mathbf{S}$).

Brillouin functions
The average magnetic quantum number can be calculated as following:

$$\langle m_J \rangle = \frac{\sum_{-J}^{J} m_J e^{-E(m_J)/k_BT}}{\sum_{-J}^{J} e^{-E(m_J)/k_BT}} = \frac{\sum_{-J}^{J} m_J e^{-m_J g_J \mu_B B/k_BT}}{\sum_{-J}^{J} e^{-m_J g_J \mu_B B/k_BT}} = -\frac{1}{Z}\frac{dZ}{dx}$$

Z is the partition function and $x = g_J \mu_B B / k_B T$.

$$Z = \sum_{-J}^{J} e^{-m_J x} = \frac{sinh\left((2J+1)\frac{x}{2}\right)}{sinh\left(\frac{x}{2}\right)}$$

The total magnetization then reads

$$\begin{aligned} M &= -\frac{N}{V} g_J \mu_B \langle m_J \rangle = \frac{N}{V} g_J \mu_B \frac{1}{Z}\frac{dZ}{dx} \\ &= \frac{N}{V} g \mu_B J \left(\frac{2J+1}{2J} coth\left(\frac{2J+1}{2J}\frac{g\mu_B JH}{k_BT}\right) - \frac{1}{2J} coth\left(\frac{1}{2J}\frac{g\mu_B JH}{k_BT}\right)\right). \end{aligned}$$

It is possible to plot the temperature dependence of the magnetization for different values of the total angular momentum as depicted in fig. 41. When no magnetic field is applied, x equals zero and the magnetization is zero too. For very low temperatures or very high fields, the saturation region is reached and (nearly) all spins get aligned.
For high temperatures there is a linear region, because here the Curie law holds. ($m = \chi H \Rightarrow m \propto \frac{H}{T} \Rightarrow \chi \propto \frac{1}{T}$) So it turns out, that for $\mu B << k_B T$ the susceptibility can be written as $\chi \approx \frac{\mu_0 M}{B} = \frac{C}{T}$ with the Curie constant C.

5.3 Free Particles in a Weak Magnetic Field

When calculating the paramagnetic response (called **Pauli paramagnetism**) of free electrons to a magnetic field, it turns out to be much smaller than it would be for individual atoms. This happens because free electrons fill up all states to the fermi surface and only those electrons, which are at the fermi surface participate in paramagnetism. As said before, the two states for spin up and spin down split up in a magnetic field and the state with spin parallel to the field has the lower energy (see fig. 42). So one has to calculate the number of electrons that fill up those states in order to get the magnetization (eqn. (59)).

---

[4] Zustandssumme

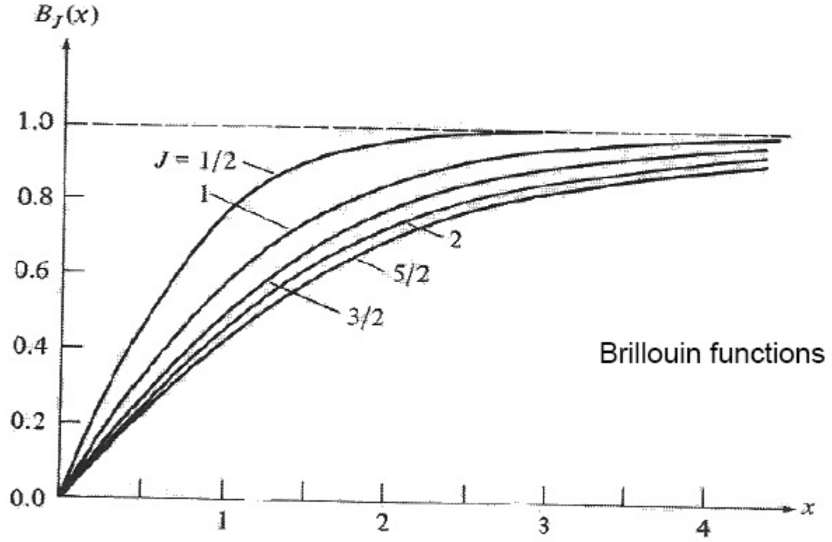

Figure 41: Magnetization for different values of the total angular momentum at variable values of magnetic field and temperature.

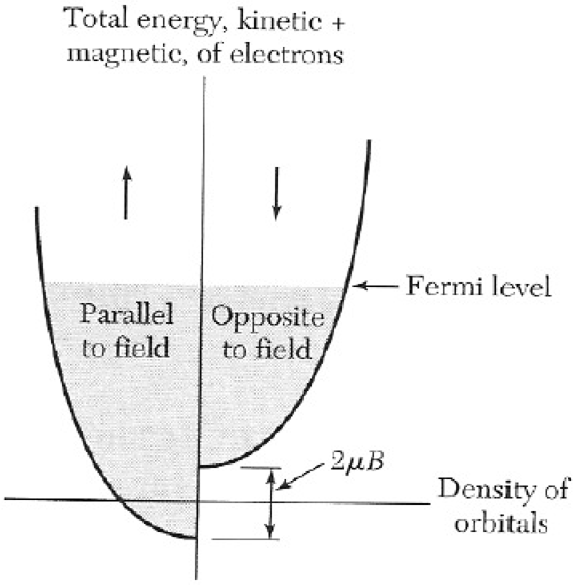

Figure 42: Energy versus density of states for spins parallel and antiparallel to the direction of the applied magnetic field.

$$N_+ = \frac{1}{2}\int_{-\mu_B}^{E_F} D(E+\mu_0\mu_B B)dE \approx \frac{1}{2}\int_0^{E_F} D(E)dE + \frac{1}{2}\mu_0\mu_B B D(E_F)$$

$$N_- = \frac{1}{2}\int_{\mu_B}^{E_F} D(E-\mu_0\mu_B B)dE \approx \frac{1}{2}\int_0^{E_F} D(E)dE - \frac{1}{2}\mu_0\mu_B B D(E_F)$$

Here N_+ is the number of spins parallel to the magnetic field and N_- is the number of spins opposite to the magnetic field. One can see, as mentioned above, that the only difference occurs at the fermi-surface and that there is the same number of electrons for both spin orientations in the fermi sphere. Now the magnetization can be calculated.

$$M = \mu_B(N_+ - N_-) \tag{59}$$

$$M = \mu_0\mu_B^2 D(E_F)B \tag{60}$$

So in this case the magnetization can be calculated as a function of the magnetic field. The susceptibility can be obtained by taking the derivative and it turns out to be temperature independent.

$$\frac{\chi}{\mu_0} = \frac{dM}{dB}$$

$$\chi_{Pauli} = \mu_B^2 D(E_F)$$

So, Pauli paramagnetism is much smaller than atomic paramagnetism and it is temperature independent. However, the Pauli paramagnetism is $\frac{2}{3}$ times bigger than the diamagnetic part.

5.3.1 Landau Levels, Landau diamagnetism

The first thing to do is to find the microscopic states for free electrons in a magnetic field. So we take the Schroedinger equation with zero electric field (V=0).

$$\frac{1}{2m}(-i\hbar\nabla - q\mathbf{A})^2\Psi(\mathbf{r}) = E\Psi(\mathbf{r})$$

Using the Landau gauge $\mathbf{A} = B_z x\hat{\boldsymbol{y}}$ one gets

$$\frac{1}{2m}\left(-\hbar^2\nabla^2 + i2\hbar q B_z x\frac{d}{dy} + q^2B_z^2x^2\right)\Psi = E\Psi.$$

So y and z don't appear in the Hamiltonian and so the solution can be written as a product of functions of x,y and z (separating variables) and has the form

$$\Psi = e^{ik_y y}e^{ik_z z}g(x).$$

The equation for g(x) is

$$\frac{1}{2m}\left(-\hbar^2\frac{\partial^2 g(x)}{\partial x^2} + \hbar^2k_y^2 + \hbar^2k_z^2 - 2\hbar q B_z k_y x + q^2B_z^2x^2\right)g(x) = Eg(x).$$

Let's complete the square

$$\frac{1}{2m}\left(-\hbar^2\frac{\partial^2 g(x)}{\partial x^2} + q^2B_z^2\left(x - \frac{\hbar k_y}{qB_z}\right)^2\right)g(x) = \left(E - \frac{\hbar^2k_z^2}{2m}\right)g(x).$$

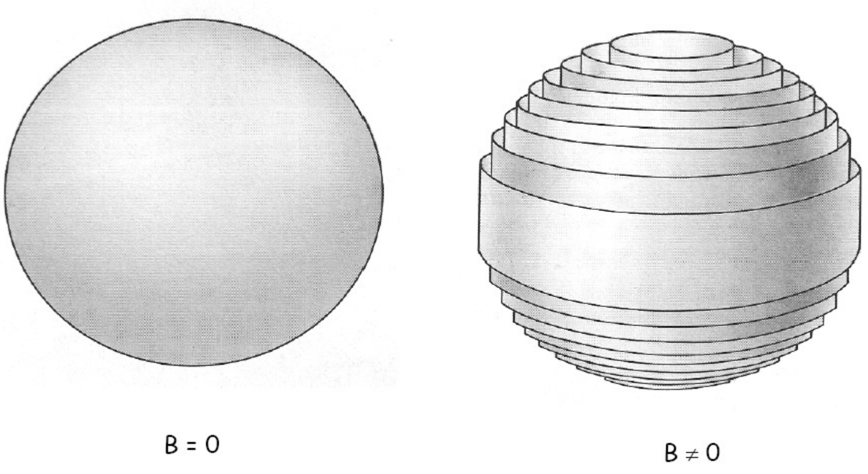

Figure 43: Left: Fermi sphere for zero applied magnetic field. Right: Split of Fermi sphere into different Landau levels when magnetic field is applied.

This is the equation for a harmonic oscillator

$$\frac{-\hbar^2}{2m}\frac{\partial^2 g(x)}{\partial x^2} + \frac{1}{2}m\omega^2(x-x_0)^2 g(x) = Eg(x)$$

$$E_{k_z,n} = \frac{\hbar^2 k_z^2}{2m} + \hbar\omega_c\left(n+\frac{1}{2}\right)$$

$$\omega_c = \frac{qB_z}{m}$$

The equation holds for a magnetic field in the z-direction because then the electrons can have kinetic energy in the z-direction without being pushed in this direction. So the oscillation just takes place in the x-y-plane, where the electrons move in a circle with the cyclotron frequency. Because of this, the value in kinetic energy in the z-direction is not restricted, but only discrete values in the x-y-plane are allowed (going with n), because there $k_x^2 + k_y^2$ has to be a constant when the electrons move in a circle.
So the harmonic motion is quantized and n labels the Landau level.

$$E_n = \hbar\omega_c\left(n+\frac{1}{2}\right) = \frac{\hbar^2}{2m}(k_x^2 + k_y^2)$$

Fig. 43 shows the splitting of the fermi sphere in cylinders, corresponding to the different Landau levels. Note that the cylinders have a certain height because the energy in z-direction gets smaller when the energy in the x-y plane gets bigger. Of course, there would be states at cylinders even with infinite height, but those would not be occupied. Here only occupied states are depicted and we know that they are within a fermi-sphere.

There are two limits where one can solve this problem:

High temperatures / Landau diamagnetism (weak magnetic fields)

For high temperatures the split gets smaller, so the states are close together. This calculation is called Landau diamagnetism. Usually the calculation is done in a grand-canonical ensemble.

We can use the grand-canonical potential Ω to obtain the Gibbs-free energy G and then get the magnetization by taking the derivative.

$$\Omega = -k_B T \ln Z_G$$

$$G = \Omega + \mu N$$

$$M = -\frac{\partial G}{\partial H}$$

$$\chi = -\frac{\partial^2 G}{\partial H^2}$$

In this case, the logarithm of the partition function can be calculated as shown below. After that, the discrete energies have to be plugged in and after that it is necessary to sum over all Landau levels and put in the degeneracy of the levels. This is a difficult calculation[5] so only the result is presented here (equ. 63).

$$\Omega = -k_B T \sum_k 2 \ln\left(1 + e^{\beta(\mu - E_k)}\right) \tag{61}$$

$$E_n = \left(n + \frac{1}{2}\right)\hbar\omega_c \tag{62}$$

$$\Omega = -k_B T \frac{Am}{\pi\hbar^2}\hbar\omega_c \sum_n \ln\left(1 + e^{\beta(\mu - E_n)}\right) \tag{63}$$

The factor containing A comes from the degeneracy of the Landau levels. The result, that is obtained by evaluating the sum, shows that the susceptibility is about a third of the susceptibility for Pauli paramagnetism.

$$\Omega(H) \approx \Omega(0) + \frac{1}{3}\mu_B^2 D(E_F) H^2 \qquad (k_B T >> \hbar\omega_c)$$

$$\chi = -\frac{\partial^2 G}{\partial H^2}$$

$$\chi \approx -\frac{1}{3}\mu_B^2 D(E_F)$$

$$\chi_{Landau} \approx -\frac{1}{3}\chi_{Pauli}$$

Low temperatures / Landau diamagnetism (strong magnetic fields)

In this limit the energy associated with the steps between the Landau levels are much bigger than $k_B T$ ($k_B T << \hbar\omega_c$). Equation (63) stays valid, but when one evaluates it in this limit, the solution turns out to be proportional to a cosine:

$$\Omega \propto \sum_{k=1}^{\inf} \cos\left(\frac{e\hbar k}{m E_F H} - \frac{\pi}{4}\right)$$

---

[5] the calculation can be looked up in the internet: http://physics.ucsc.edu/~peter/231/magnetic_field/magnetic_field.html

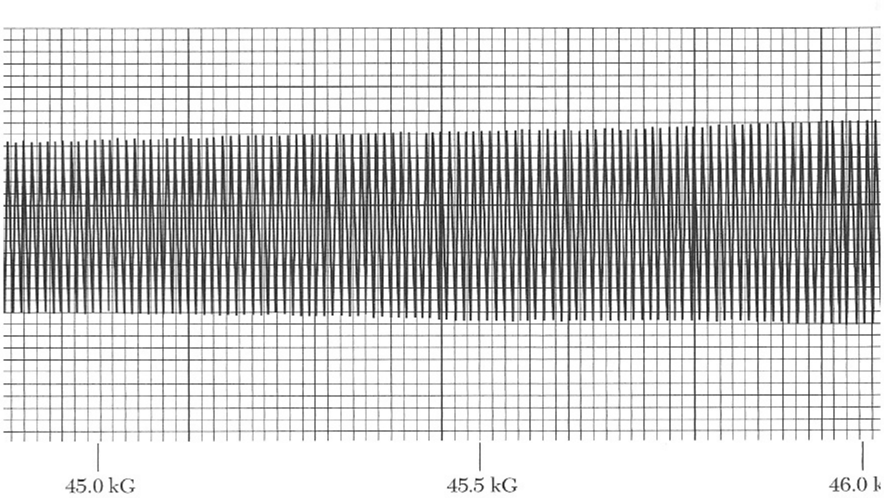

Figure 44: De Haas-van Alphen effect for gold as a good approximation for a free electron gas. The magnetic moment is plotted as function of B.

So, when one calculates the magnetization by taking the derivative as shown above, the magnetization will oscillate. This is the De Haas-van Alphen effect. Fig. 44 shows this effect, using gold as a good approximation for a free electron gas. As one can see, the magnetic moments oscillate in dependence of the magnetic field applied.

One can think about that, using the picture of the cylinders of the Landau levels. The diameter of those cylinder increases with the magnetic field and then the cylinders move through the fermi surface. This causes a big change in the density of states at that point, which leads to large consequences for all thermodynamic quantities. So the effect can not only be seen in the magnetization, but in all thermodynamic quantities, as they are all functions of the free energy.

5.3.2 Quantum Hall Effect (incomplete)

Another effect is the Quantum Hall Effect. In this case, one varies the magnetic field and measures the resistivity (green line in fig. 45). There are oscillations in conductivity, called Shubnikov-De Haas oscillations. The red line depicted in the figure shows the Hall voltage (measured perpendicular to the applied voltage and the applied field), for a 2-dimensional electron gas (electrons on a surface). Here we can see steps in this voltage and a constant voltage for regions where the resistivity drops to zero. Normally electrons travel for a while and then they get scattered off in different directions, which causes the resistance. When there is a high magnetic field of the right amplitude applied, the electrons move at the edge of the sample, they don't get scattered any more. Electrons in the middle of the sample might also move in circles, but then they don't participate in the conduction process.

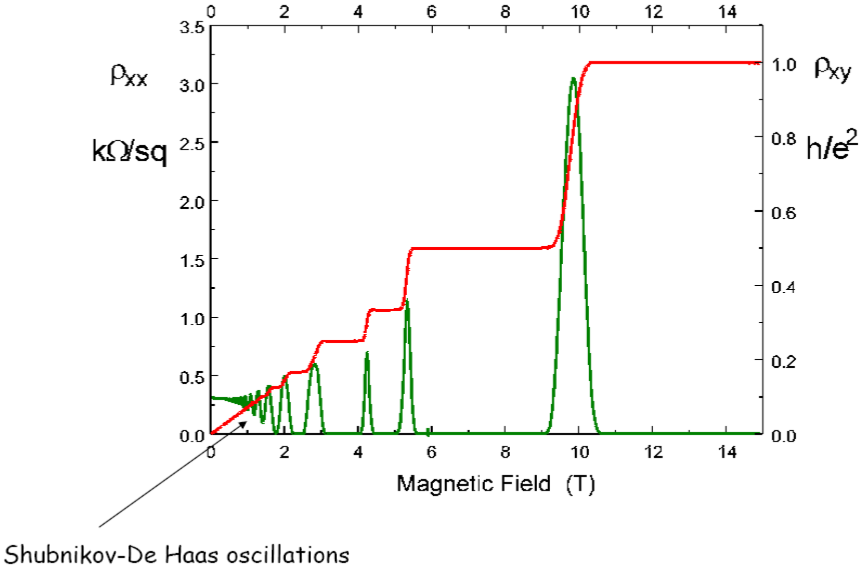

Figure 45: Conductivity (green line) and Hall voltage (red) line over magnetic field.

5.3.3 Measurements of the Fermi surface (missing)

5.4 Ferromagnetism

A ferromagnetic material shows spontaneous magnetization below a certain critical temperature T_c. Below that temperature the magnetic moments in the solid (i.e. spins, magnetic moments due to electron movement,...) align in a preferential direction by themselves. From a classical point of view this is in deed very puzzling because two neighboring magnetic moments should align antiparallel to minimize their energy in their mutual magnetic fields. Ferromagnetism is a quantum effect which is classically seen due to electric interaction as we shall see in the following. Imagine a two electron system described by the stationary Schrödinger equation

$$-\frac{\hbar^2}{2m}(\nabla_1^2 + \nabla_2^2) + V_1(r_1) + V_2(r_2) + V_{1,2}(r_1, r_2)\Psi = E\Psi \tag{64}$$

. Neglecting the electron-electron interaction term $V_{1,2}$ enables us to use the product wavefunction

$$\Psi(r_1, s_1, r_2, s_2) = \psi(r_1)\chi(s_1) \cdot \psi(r_2)\chi(s_2) \tag{65}$$

. Because electrons are fermions the wavefunction has to be antisymmetric under an exchange of the two particles so the possible solutions are either symmetric in spin χ_S and antisymmetric in position ψ_A or vice versa (figure 46). With this picture in mind one sees that ferromagnetism will emerge if the energy of the symmetric spin state (antisymmetric in position) is lower than the energy of the antisymmetric spin state (symmetric in position). It is now somehow plausible to see how two spins may align parallel. Because then their wavefunction is antisymmetric in position and therefore the electrons are farther away from each other resulting in a more favourable configuration from an electrostatic point of view. After this rough semiclassical picture of how one can understand the

Figure 46: Possible states for a two electron-spin system.

emergence of ferromagnetism a short overview of a mathematical theory of ferromagnetism shall be given. The *Heisenberg model* consists of the hamiltonian

$$\hat{H} = -\sum_{i,j} J_{i,j}\hat{\vec{S}}_i \cdot \hat{\vec{S}}_j - g\mu_B B \sum_i \hat{\vec{S}}_i \tag{66}$$

. The first term describes the exchange interaction between spins which raises or decreases the energy depending on their alignment. One should not forget that this exchange interaction is of electric nature as described above. The second term accounts for the interaction with an external magnetic field. We will simplify this model by considering only nearest neighbor interaction (subscript nn). Further we will remoe the nonlinearity in S by replacing the $\hat{\vec{S}}_{nn}$ operator by its expectation value. Thereby introducing the mean field hamiltonian

$$\hat{H}_{mf} = \sum_i \hat{\vec{S}}_i (\sum_{nn} J_{i,nn} < \vec{S} > + g\mu_B B) \tag{67}$$

. It is possible to rewrite the first term as a magnetic field due to the neigboring spins.

$$\vec{B}_{mf} = \frac{1}{g\mu_B} \sum_{nn} J_{i,nn} < \vec{S} > \tag{68}$$

The magnetization is given as magnetic moment per volume

$$\vec{M} = \frac{g\mu_B N}{V} < \vec{S} > \tag{69}$$

. Eliminating $< \vec{S} >$ yields

$$\vec{B}_{mf} = \frac{V}{Ng^2\mu_B^2} n_{nn} J\vec{M} \tag{70}$$

where n_{nn} is the number of nearest neighbors. So one can use mean field theory to transform the exchange energy which is coming from Coulomb interaction into a magnetic field of neighboring spins. This additional magnetic field may now be used for statistical considerations to calculate the magnetization as a function of temperature. The magnetization is the magnetic moment of the electrons times the differnce in spin occupation (see figure 47).

$$M = (N_1 - N_2)\mu \tag{71}$$

We can calculate N_1 and N_2 in thermal equilibrium

$$\frac{N_1}{N} = \frac{e^{\frac{\mu B}{k_B T}}}{e^{\frac{\mu B}{k_B T}} + e^{\frac{-\mu B}{k_B T}}} \tag{72}$$

$$\frac{N_2}{N} = \frac{e^{-\frac{\mu B}{k_B T}}}{e^{\frac{\mu B}{k_B T}} + e^{\frac{-\mu B}{k_B T}}} \tag{73}$$

Combining these equations leads to a magnetization of

$$M = (N_1 - N_2)\mu \tag{74}$$

$$M = N\mu \frac{e^{\frac{\mu B}{k_B T}} - e^{\frac{-\mu B}{k_B T}}}{e^{\frac{\mu B}{k_B T}} + e^{\frac{-\mu B}{k_B T}}} \tag{75}$$

$$M = N\mu tanh(\frac{\mu B}{k_B T}) \tag{76}$$

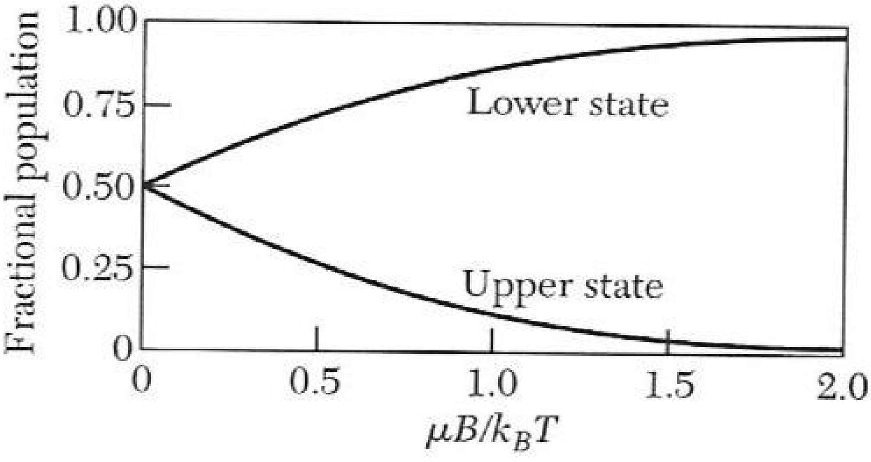

Figure 47: Equilibrium spin population. [from Kittel]

In this result for the magnetization we can plug in the magnetic field from the mean field calculation

$$M = M_s tanh(\frac{T_c}{T}\frac{M}{M_s}) \tag{77}$$

with the saturation magnetization

$$M_s = \frac{Ng\mu_B}{2V} \tag{78}$$

and the Curie temperture

$$T_c = \frac{n_{nn}J}{4k_B} \tag{79}$$

. A well known approximation to this implicit equation is the Curie-Weiss law which is valid for $B << T$ (see figure 48). Expanding the hyperbolic tangent around T_c yields

$$\vec{M} = \frac{\chi}{\mu_0}\vec{B},\ T > T_c \tag{80}$$

$$\chi = \frac{C}{T - T_c} \tag{81}$$

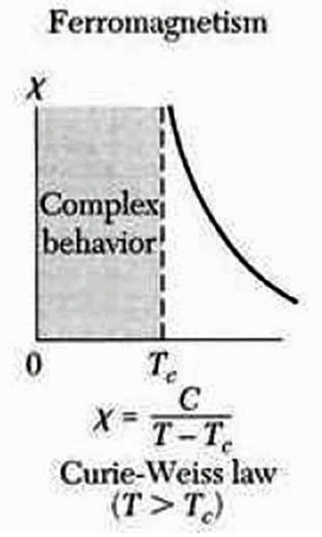

Figure 48: Curie-Weiss law. [from Kittel]

Summing up

- Ferromagnetic materials show spontaneous magnetization without an external field below the critical temperature.
- The emerging order can only be explained quantum mechanically (Pauli principle, exchange interaction).
- A mathematical basis is the Heisenberg hamiltonian. It can be solved in mean field theory. This is done in treating the exchange energy as an additional magnetic field resulting from the nearest neighbors.
- Using a statistical approach for the occupation of the spin levels and the magnetic field obtained from the mean field calcualtion one can find a relation between the magnetization and temperature.

6 Linear Response Theory

What we want to look at is the linear response of a solid to a time dependent force for example electric field or stress. Linear response means that the response of the solid is proportional to the force. An other important consideration is causality. Causality requires that effects follow causes this means that e.g. a bell rings when you hit it and not the other way around. This will lead us to the Kramers-Kronig relations and the fluctuation dissipation theorem.

6.1 Greens functions

To start with the linear response theory we first look at an ordinary **linear** differential equation:

$$L\, g(t,t') = \delta(t-t') \tag{82}$$

Where g is called Green's function, which is the solution to a linear differential equation to a δ-function driving force (Be careful: the name Green's function has different meanings!). For instance a damped spring-mass system:

$$m\frac{d^2g}{dt^2} + b\frac{dg}{dt} + kg = \delta(t) \tag{83}$$

with m the mass, b the damping and k the spring constant. This differential equation has the solution

$$g(t) = \frac{1}{b}\exp(\frac{-bt}{2m})\sin(\frac{\sqrt{4mk-b^2}}{2m}t), \quad t > 0 \tag{84}$$

Where $g(t)$ is the Green's function for this system which is a decaying sinusoidal function. Green's functions are also called impulse response functions.

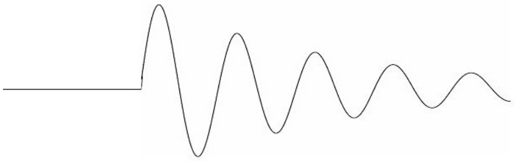

Figure 49: Example of a response $g(t)$ to $\delta(t)$ driving force (eqn. (84))

The advantage of Green's functions is that every function can be written as a sum over δ peaks:

$$f(t) = \int \delta(t-t')f(t')dt'$$

This means that the solution to a linear differential equation $Lu(t) = f(t)$ can be found by a superposition of Green's functions.

$$u(t) = \int g(t-t')f(t')dt'$$

For the damped spring-mass system from above (eq. (83)) this gives us

$$u(t) \;=\; \int -\frac{1}{b}\exp\left(\frac{-b(t-t')}{2m}\right)\sin\left(\frac{\sqrt{4mk-b^2}}{2m}(t-t')\right)f(t')dt' \;.$$

But keep in mind this is only possible if the response of the system is linear to the impulse.

6.2 Generalized susceptibility

We now assume we have such a situation where we have a linear differential equation $Lu(t) = f(t)$ with a driving force $f(t)$. We also assume that the driving force is sinusoidal, $f(t) = A\exp(i\omega t)$. Because the response of the system is linear, the response will also be sinusoidal with the same frequency ω as the driving force. The general solution in terms of the Green's function then is

$$u(t) \;=\; \int g(t-t')f(t') \;=\; \int g(t-t')A\exp(i\omega t')dt'$$

We define the generalized susceptibility which is the response of the system divided by the driving force

$$\chi(\omega) \;=\; \frac{u}{f} \;=\; \frac{\int g(t-t')A\exp(i\omega t')dt'}{A\exp(i\omega t)} \tag{85}$$

Since the integral is over t', the factor with t can be put in the integral.

$$\chi(\omega) \;=\; \frac{u}{f} \;=\; \int g(t-t')A\exp(-i\omega(t-t'))dt'$$

This equation looks similar to a Fourier transformation. If the variables are changed to $\tau = t-t'$

$$\chi(\omega) \;=\; A\cdot\int g(\tau)\exp(-i\omega\tau)d\tau \tag{86}$$

we see that the susceptibility is proportional to the Fourier transform of the Green's function. This is useful because if we now know the Green's function we know the response of the system at all frequencies. (Without loss of generality[6] the proportionality factor A can be neglected.)

6.3 Kramers-Kronig relations

Any function $g(t)$ can be written as the sum of an even component $E(t)$ and an odd component $O(t)$

$$g(t) \;=\; E(t)+O(t) \tag{87}$$

If $g = 0$ for $t < 0$, which is the case for the response function for a system (causality), this requires that

$$O(t) \;=\; sgn(t)E(t). \tag{88}$$

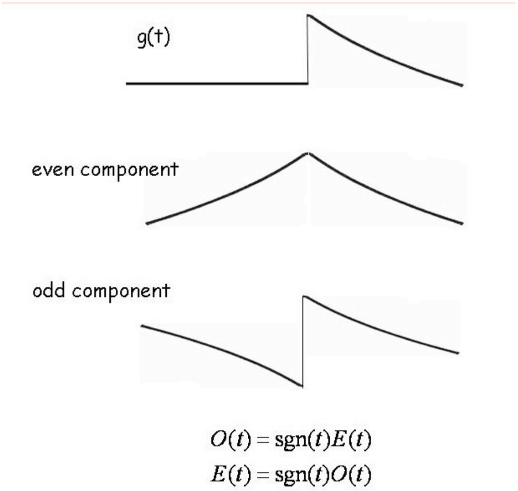

Figure 50: Response $g(t)$ of a system to a $\delta(t)$ driving force splitted into an even and an odd component

Therefore the impulse response function is completely specified by either it's even components or its odd components.
The Green's function written as the sum of its even and odd component and put in eq. (86) leads to:

$$\boxed{\chi''(\omega) \;=\; \frac{1}{\pi}\int_{-\infty}^{\infty}\frac{\chi'(\omega')}{\omega'-\omega}d\omega'} \tag{89}$$

$$\boxed{\chi'(\omega) \;=\; -\frac{1}{\pi}\int_{-\infty}^{\infty}\frac{\chi''(\omega')}{\omega'-\omega}d\omega'} \tag{90}$$

Since the even component of the Green's function is related to the odd component also the real part of the susceptibility is related to the imaginary part of the susceptibility. For example if the real part χ' is known, the inverse Fourier transform gives the even component $E(t)$ of the Green's function. By knowing $E(t)$ the odd component can be determined with $O(t) = sgn(t)E(t)$. The Fourier transformation of $O(t)$ leads to χ''. The relationship between the real part and the imaginary part of the susceptibility is called the **Kramers-Kronig relation:**

$$\chi''(\omega) \;=\; \frac{1}{\pi}\int_{-\infty}^{\infty}\frac{\chi'(\omega')}{\omega'-\omega}d\omega' \tag{91}$$

$$\chi'(\omega) \;=\; -\frac{1}{\pi}\int_{-\infty}^{\infty}\frac{\chi''(\omega')}{\omega'-\omega}d\omega' \tag{92}$$

This relation is very useful because if you measure e.g. the response of a solid to a light wave you can either measure the depth which the light wave is penetrating into the material or the polarisation caused by the light wave and calculate the other one. Or you measure both and check with the Kramers-Kronig relationship if it is right.

---

[6] ohne Beschränkung der Allgemeinheit

"If you calculated a linear response and want to tell everybody else about it, put it in the Kramers-Kronig relation to see if it is right. Because if you publish a response and then somebody else says: 'Oh, but it violates causality' - it looks stupid."

The form (eqn. (89) and (90)) of the Kramers-Kronig relations should be used for mathematical calculations. For experimental data the second form of the Kramers-Kronig relation should be used (eqn. (93) and eqn. (94)) which is derived in the following part. First step is to split the integral and change the sign of ω:

$$\begin{aligned} &\Longrightarrow \\ \chi'(\omega) &= -\frac{1}{\pi}\int_{-\infty}^{0}\frac{\chi''(\omega')}{\omega'-\omega}d\omega' - \frac{1}{\pi}\int_{0}^{\infty}\frac{\chi''(\omega')}{\omega'-\omega}d\omega' \\ &\Longrightarrow \\ \chi'(\omega) &= -\frac{1}{\pi}\int_{0}^{\infty}\frac{\chi''(\omega')}{\omega'+\omega}d\omega' - \frac{1}{\pi}\int_{0}^{\infty}\frac{\chi''(\omega')}{\omega'-\omega}d\omega' \end{aligned}$$

With the relationship

$$\frac{1}{\omega'+\omega}+\frac{1}{\omega'-\omega} = \frac{2\omega'}{\omega'^2-\omega^2}$$

the second form of the Kramers-Kronig relation is derived:

$$\boxed{\chi'(\omega) = \frac{2}{\pi}P\int_{0}^{\infty}\frac{\omega'\chi''(\omega')}{\omega'^2-\omega^2}d\omega'} \tag{93}$$

$$\boxed{\chi''(\omega) = -\frac{2\omega}{\pi}P\int_{0}^{\infty}\frac{\chi'(\omega')}{\omega'^2-\omega^2}d\omega'} \tag{94}$$

Here P represents the **Principle part**, which is important because at a particular point $\omega' = \omega$ the integral gets undefined (singularity). With this Principle part it is possible to integrate around this singularity.

6.4 Dielectric function

One way to calculate the dielectric functions is to measure the index of refraction n and the extinction coefficient K (this coefficient tells how quickly a wave dies out). Taking the square of the following relationship

$$\sqrt{\mu_0\epsilon_0\epsilon(\omega)} = n(\omega)+iK(\omega)$$

gives the dielectric function:

$$\epsilon(\omega) = \frac{n^2 - K^2 + 2inK}{\mu_0\epsilon_0} = \epsilon'(\omega) + i\epsilon''(\omega) \tag{95}$$

Important to mention is that $n^2 - K^2$ and $2nK$ are related by the Kramers-Kronig relation.

Bound electrons
Insulators do not have free electrons, which means that their charge is bound. The electrons can be modeled to be coupled by a spring to the ions and as a result it's possible to describe this function as a harmonic oscillator. A hit of this function with a δ-function will give the response function (Green's function) for this linear harmonic oscillator:

$$m\frac{d^2g}{dt^2} + b\frac{dg}{dt} + kg = \delta(t)$$

$$g(t) = -\frac{1}{b}exp\left(\frac{-bt}{2m}\right) sin\left(\frac{\sqrt{4mk - b^2}}{2m}t\right) \qquad t > 0$$

The solutions (assumption) for the displacement and the force have the form $x(\omega)e^{-i\omega t}$ and $F(\omega)e^{-i\omega t}$.

$$m\frac{d^2x}{dt^2} + b\frac{dx}{dt} + kx = F(t)$$

$\Longrightarrow$

$$-\omega^2 m x(\omega) - i\omega b x(\omega) + kx(\omega) = F(\omega)$$

The generalized susceptibility $\chi(\omega)$ is

$$\chi = \frac{F(\omega)}{x(\omega)} = \frac{F}{-\omega^2 m - i\omega b + k} = \frac{F}{m}\frac{\omega_0^2 - \omega^2 + i\omega b}{(\omega_0^2 - \omega^2)^2 + \omega^2 b^2} \tag{96}$$

with

$$\omega_0 = \sqrt{\frac{k}{m}}.$$

Fig. 51 shows an expected response of a mass spring system. At low frequencies (below the resistant frequency) the mass will move in phase, at much higher frequencies the system will oscillate out of phase. **The Fourier transform of the impulse response function is the generalized susceptibility.**

6.5 Dielectric Response of Insulators

Fig. 52 shows the real (dotted line) and the imaginary part of a dielectric response of an insulator. The peak of the imaginary part indicates energy losses at a particular frequency.

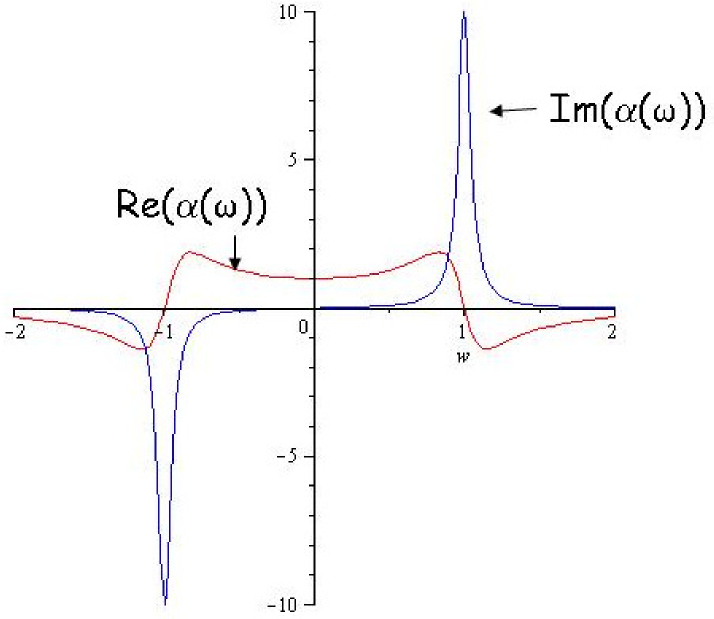

Figure 51: Response of a mass spring system

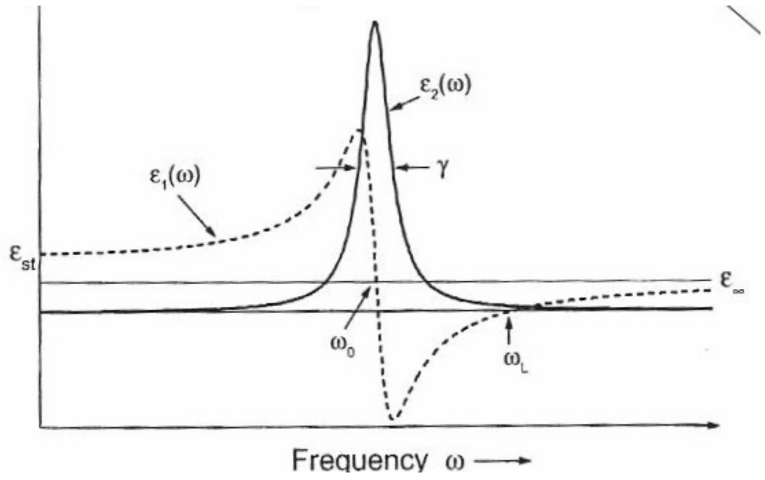

Figure 52: Dielectric response of an insulator. The dotted line represents the real part, the solid line the imaginary part.

Calculation of the dielectric constant:

$$\epsilon = 1 + \chi = 1 + \frac{P}{\epsilon_0 E} \tag{97}$$

with

$$P = nex$$

The +1 in eqn. (97) shifts the response function in the positive direction, which means that in comparison to fig. 52 the dielectric constant of insulators goes to +1 instead to zero at higher frequencies. As a result **an insulator reflects incoming waves at particular frequencies where the dielectric constant is below 0.**

With eqn. (96) and the static dielectric constant $\epsilon_{st} = \epsilon(\omega = 0)$ we get

$$\epsilon(\omega) = \epsilon_\infty + \frac{(\epsilon_{st} - \epsilon_\infty)\, \omega_0^2\, (\omega_0^2 - \omega^2 + i\omega b)}{(\omega_0^2 - \omega^2)^2 + \omega^2 b^2} \tag{98}$$

Now it is possible to do some quantum calculations. There is a coupling between electromagnetic waves and electron states. When light hits the crystal, absorption is possible, which means that an electron of the filled state goes to an empty state. With Fermi's golden rule it is possible to calculate the transition rate of this process. The couplings of the initial state and the final state has to do with the dipole moment, which means that the oscillator strength (eqn. (99)) is proportional to the tunneling rate.

$$\epsilon = 1 + \chi = 1 + \frac{P}{\epsilon_0 E} = 1 + \frac{ne^2}{\epsilon_0 m} \sum_{i,k} \frac{f_{ik}}{\omega_{ik}^2 - \omega^2} \tag{99}$$

with the Oscillator strength f_{ik}:

$$f_{ij} = \frac{2m}{\hbar} \omega_{ik} |(r_{ik})|^2$$

Fig. 53 shows an example of such calculations with two harmonic oscillators (2 frequencies). For real materials it's common that there are more than one residents.

Another example would be an infrared absorption of very thin materials, which is shown in fig. 54. Every peak stands for a certain mode with a certain frequency. At theses frequencies there is a resident and as a result an energy loss (absorption).

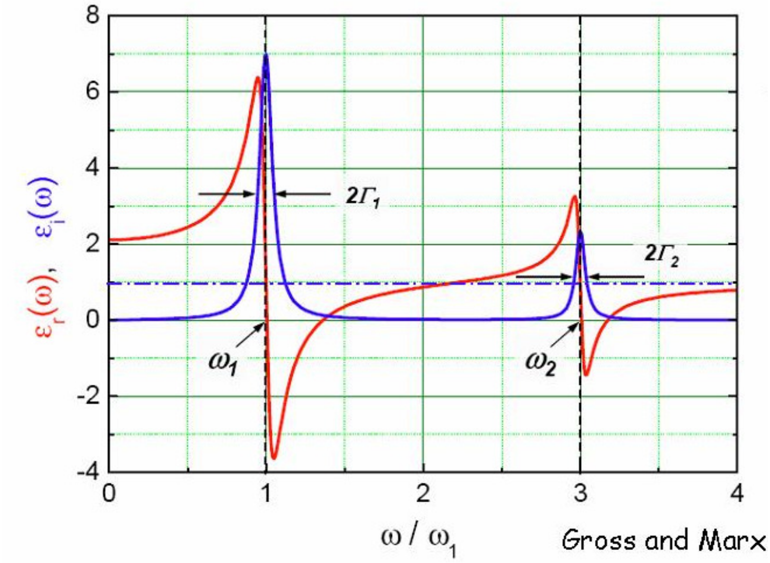

Figure 53: Example of a quantum calculation with two harmonic oscillators

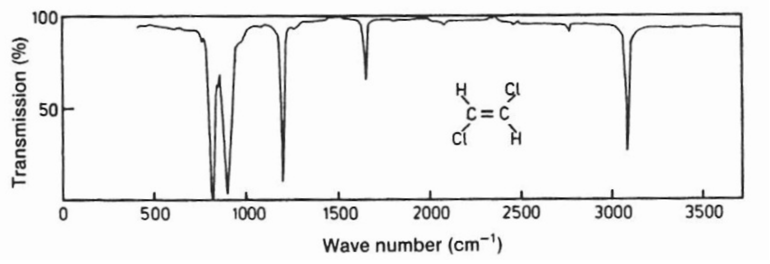

Figure 54: Infrared absorption of a thin material

6.6 Dielectric function of semiconductors

A common approximation for the real part of the dielectric function of a semiconductor is:

$$\epsilon'(\omega) = 1 + \frac{\omega_p^2}{\omega_g^2 - \omega^2} \tag{100}$$

with ω_g the gap frequency ($E_g = \hbar\omega_g$).
Fig. 55 shows the real part of the dielectric function for a semiconductor. The imaginary part would be a peak around this resident. When ω_g gets smaller and smaller, in the end the band gap gets smaller and smaller and as a result a metal observes.

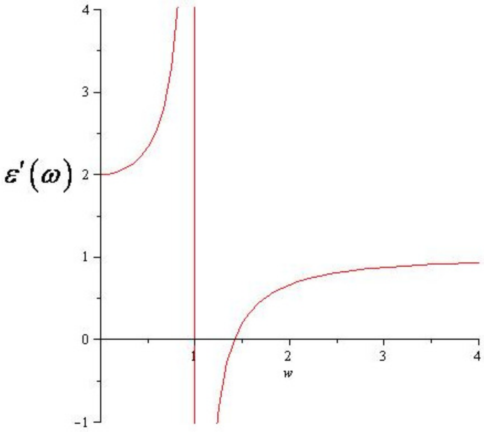

Figure 55: Real part of a dielectric function of a semiconductor. The imaginary part would have a peak around the residents.

Fig. 56 and 57 show some experimental functions of semiconductors. As discussed above, it is very simple to see the real part (has negative components) and the imaginary part (peaks around the residents). It is very interesting that the peaks of the real part aren't very strict, which is common for semiconductors. One explanation for that property is, that semiconductors do have two atoms per unit cell, so they have two coupled modes which splits the peaks.

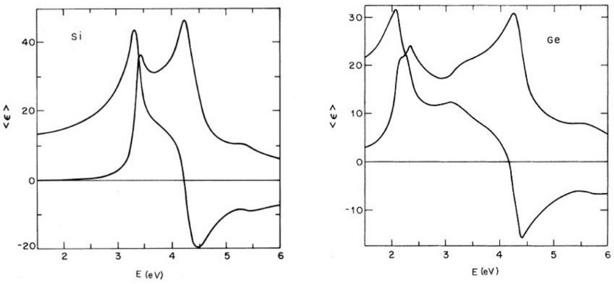

Figure 56: Real and imaginar part of a dielectric function of the semiconductors Germanium and Silicon. The imaginary part has two peaks around the resident.

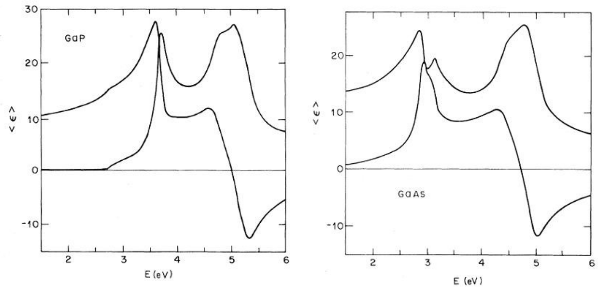

Figure 57: Real and imaginar part of a dielectric function of the semiconductors Galium-Phosphor and Galium-Arsenid. The imaginary part has two peak around the resident.

6.7 Excursus: Dielectrics

Dielectrics seem to be really boring materials for electronics, because an ideal dielectric doesn't conduct. But experimentally everything conducts, if the voltage is high enough. What we exactly want to have is that they don't conduct at DC and that they have low losses at AC. It is not possible to have zero losses at AC, because the dielectric constant always has a real part and an imaginary part. The real part corresponds to the out-of-phase components of the electric field and the current. The imaginary part corresponds to the in-phase components, which is the dissipative part, so there always have to be losses.

Sometimes low dielectric constants are needed for transporting signals (CMOS) and sometimes high dielectric constants are needed for supercapacitors. This kind of capacitors is used to store the won energy of braking a car and to give it back when accelerating.

It is possible to use the complex dielectric function to describe the AC losses, but that is not done in practice. Instead of that, we start with an ideal capacitor, where the current leads the voltage by 90°. Because of the complex dielectric part, this angle will not be exactly 90°, so we add an offset angle $90° - \delta$. As we see in eqn. (101), the power loss depends on the tangent of this offset angle and it gets bigger, when the frequency gets higher.

$$\text{Power loss} = \frac{w\epsilon_1 V_0^2}{2}\tan(\delta) \qquad (101)$$

Loss tangents are really small numbers (about 10^{-5} to 10^{-2}, so it doesn't matter if someone speaks about the loss tangent or someone speaks about the angle δ, because they are nearly the same near zero ($\tan(\delta) \sim \delta$, $\delta \ll 1$).

Barium titanate is a material which is used in capacitors as a dielectric. It can appear as white powder or as a transparent crystal. The unit cell is a cube, where the Barium atoms sit on the corners. There is one titanium in the middle and the oxygens sit on the faces of the cube. This structure is called a perovskit.

In fig. 58 we can see, that the dielectric constant has several peaks at different temperatures, which will be explained in the chapter of structural phase transistions. In addition, the dielectric constant depends on the applied voltage. The developer of an electronic element has to think about the temperatures inside the element, when the device is working. A typical temperature for the processor of a mobile phone is about 100° C, which leads to an ϵ_r of approximately 2000, which is not a bad value for a dielectric.

When the temperature is increased, it leads to a structural phase transition, which will be discussed in chapter 11.3.

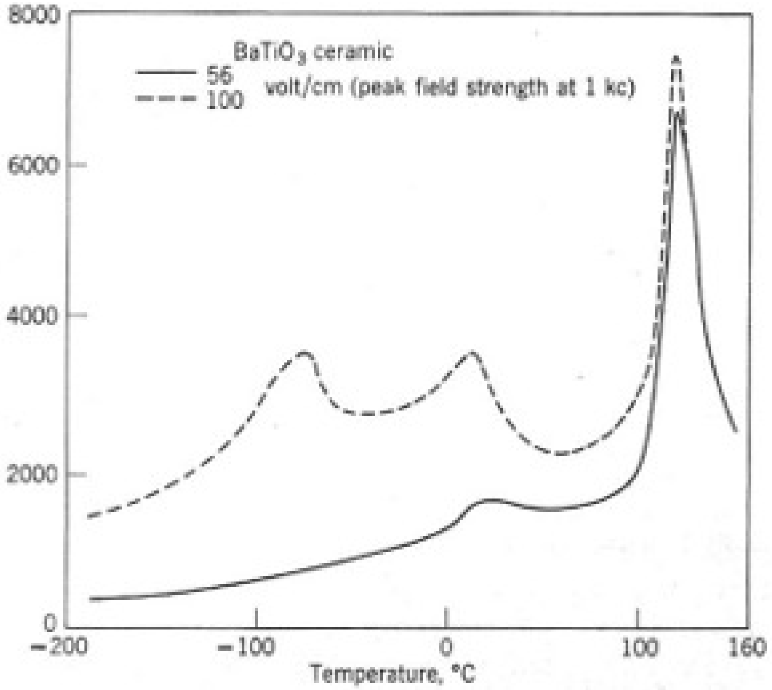

Figure 58: Dependence of the dielectric constant of the temperature and the voltage

6.7.1 Polarizability

There are different sources of polarizability. Four of them are discussed in this chapter:

- Electronic polarizability

- Ionic polarizability
- Orientation polarizability
- Space charge polarizability

Electronic polarizability:

We think of an atom. There we have the positive protons somewhere in the middle and the negative electrons are moving around the protons. The resulting dipole moment is zero. If an electric field is applied, the protons and electrons will move in opposite directions and so a dipole moment is induced. Of course, if the applied field is oscillating, the generated dipoles will oscillate too.

For gases the polarization is easy to describe mathematically. It's just proportional to the electric field and the count of atoms with the polarization α as constant of proportionality:

$$\mathbf{P} = N\alpha\mathbf{E} = N\mathbf{p} \tag{102}$$

In solids and liquids the local field depends on the applied field and the field induced by the neighboring dipoles. There are three types of fields to observe. The applied field, the local microscopic field around the atom and the macroscopic field, which is the mean electric field over many atoms, but smaller compared to the wavelength of light. It has to be said, that every material has a polarization, because everything consists of atoms.

Ionic polarizability:

The effect of ionic polarizability only appears in ionic substances. The positive and negative ions are pushed in different directions by an electric field and local dipole moments are induced.

Orientation (dipolar) polarizability:

It is easy to understand this effect when we think of a gas with permanent dipole moments. In such a gas at high temperatures and zero field, all the dipoles are oriented randomly. If a field is applied, the average of the dipoles will show in the direction of the field. The theory is very similar to the theory of paramagnetism. There the spins get oriented by an external field and at low temperatures and high fields there will be saturation. If we do the same calculation for the polarization as for the paramagnetism, we see that the susceptibility χ diverges at low temperatures:

$$\chi \propto \frac{1}{T} \tag{103}$$

For gases and liquids this effect is easy to describe, because there the dipole moments can arrange freely. However, in solids the moments are bound and so another model is needed to describe this effect here. The theory is based on ion jumps in solid crystals which have defects. In such defects double charged ions are attracted and trapped. In fig. 59 the double charged ion is marked with a bold border. Now it could happen, that this ion changes its position with a single charged ion and what happens is that the polarization changes the direction.

Space charge polarizability:

This effect is often observed in insulators with different phases in them and these different phases have different dielectric constants. If one phase has a much higher resistivity than the others, the whole

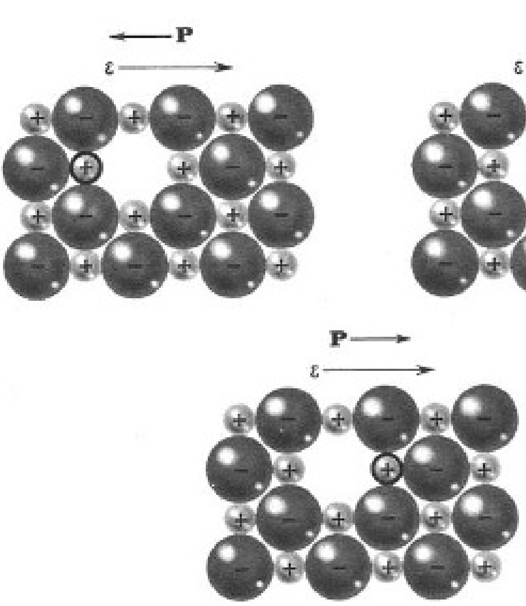

Figure 59: A solid crystal with a defect, where a double charged ion is attracted and trapped. When this ion swaps the position with another ion, the polarization will change the direction

material will be an insulator. Between these phases there are other phases, which conduct a little bit. So the whole thing looks like a chain of resistors and capacitors and this has a specific AC response.

Total polarizability:

In fig. 60 the parts of the different polarizabilities are shown in dependence of the frequency. First it has to be said, that the part of the space charge polarizability is not from big technical interest and so it is not plotted, but it would be at low frequencies.

The important thing is, that if the frequency is increased, there is a point where one can observe a behaviour that can also be seen when the charges in an atom oscillate naturally. The oscillations are so fast, that they get out of phase and the polarizability gets negative. This is a typical response of a mass-spring system. When the applied force oscillates at low frequencies, the masses move with the force and at high frequencies the masses move out of phase to the applied force.

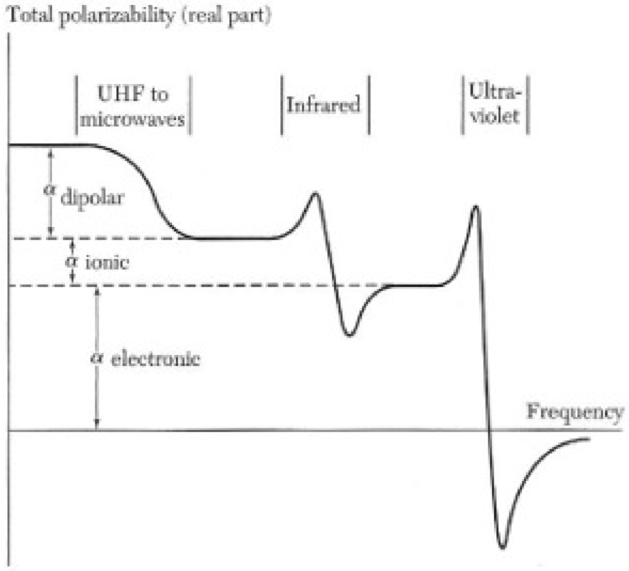

Figure 60: Diagram of the different polarizability parts of the total polarizability

6.8 Collisionless Metal

In collisionless metals electrons travel ballistically which means that the scattering time and the mean free path are infinite. The relationship between velocity v and the electric field E is:

$$\frac{m}{-e}\frac{dv(t)}{dt} = E(t) \tag{104}$$

So if an oscillating field influences the material, the electrons start to oscillate but they oscillate out of phase . The derivative of the velocity is proportional to the electric field (eqn. (104)).
To solve this problem, the solution of a harmonic oscillator is assumed ($E(\omega)e^{-i\omega t}$, $v(\omega)e^{-i\omega t}$). From eqn. (104):

$$(\frac{i\omega m}{e})v(\omega) = E(\omega)$$

The conductivity:

$$j = \sigma E \Rightarrow \sigma = \frac{j}{E} = \frac{-nev(\omega)}{E(\omega)} = \frac{ine^2}{\omega m} \tag{105}$$

So σ is purely imaginary because the motion of the electrons is **out of phase**, but of course there must be a real part. With the Kramers-Kronig relation it is possible to calculate the real part:

$$\sigma''(\omega) = \frac{1}{\pi}\int_{-\infty}^{\infty}\frac{\sigma'(\omega')}{\omega'-\omega}d\omega' \tag{106}$$

$$i\sigma''(\omega) = \frac{-nev(\omega)}{E(\omega)} = \frac{ine^2}{\omega m} \tag{107}$$

To calculate the real part we guess the solution (the reason for this is that it is easier)

$$\sigma'(\omega) \;=\; \frac{\pi n e^2}{m}\delta(\omega) \tag{108}$$

Equation (108) in eqn. (106) gives:

$$\sigma''(\omega) \;=\; \frac{ne^2}{m}\int_{-\infty}^{\infty}\frac{\delta(\omega')}{\omega'-\omega}d\omega' \tag{109}$$

After integrating this and comparing with eqn. (107) the real part is derived. Now its possible to write the imaginary and the real part of the conductivity:

$$\sigma(\omega) \;=\; \frac{ne^2}{m}(\pi\delta(\omega)+\frac{i}{\omega}) \tag{110}$$

Furthermore it is possible to calculate the dielectric constant $\epsilon(\omega)$. For the dielectric constant the susceptibility is needed:

$$\chi(\omega) \;=\; \frac{P(\omega)}{\epsilon_0 E(\omega)} \;=\; \frac{nex(\omega)}{\epsilon_0 E(\omega)} \;=\; \frac{nev(\omega)}{\epsilon_0 E(\omega)(-i\omega)} \tag{111}$$

with eqn. (105):

$$\Rightarrow \chi(\omega) \;=\; \frac{\sigma(\omega)}{i\omega\epsilon_0} \;=\; \frac{ne^2}{i\omega\epsilon_0 m}(\pi\delta(\omega)+\frac{i}{\omega}) \tag{112}$$

We used:

$$x(\omega,t) \;=\; x(\omega)e^{-i\omega t} \Rightarrow v(\omega,t) \;=\; x(\omega)e^{-i\omega t}(-i\omega) \Rightarrow x(\omega) \;=\; \frac{v(\omega,t)}{-i\omega}e^{i\omega t} \;=\; \frac{v(\omega)}{-i\omega}$$

So the dielectric constant is derived:

$$\epsilon(\omega) \;=\; 1+\chi(\omega) \;=\; 1+\frac{ne^2}{i\omega\epsilon_0 m}(\pi\delta(\omega)-\frac{i}{\omega}) = 1-\frac{\omega_p^2}{\omega^2}+i\omega_p^2\pi\delta(\omega) \tag{113}$$

with the Plasma frequency:

$$\omega_p^2 = \frac{ne^2}{m\epsilon_0}$$

Fig. 61 shows the real part of the dielectric constant:

$$\epsilon(\omega) = 1-\frac{\omega_p^2}{\omega^2} \tag{114}$$

At the Plasma frequency ω_p the dielectric constant is zero. Below zero (so below the Plasma frequency) the material reflects and above zero (above the Plasma frequency) the material transmits incoming waves.

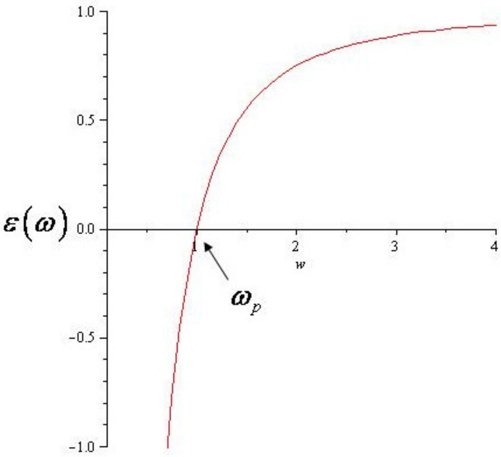

Figure 61: Real part of the dielectric constant of a collisionless material. Below the plasma frequency the material reflects, above the plasma frequency the material transmits incoming waves.

6.9 Diffusive Metals

In diffusive metals, there is one component which is out of phase and one component which is in phase (eqn. 115):

$$\underbrace{\frac{m}{-e}\frac{dv(t)}{dt}} - \underbrace{\frac{v(t)}{\mu}} = E(t) \tag{115}$$

The first term is the initial term (out of phase), the second term is the scattering term (in phase). Again, the solution of a harmonic oscillator is assumed ($E(\omega)e^{-i\omega t}$; $v(\omega)e^{-i\omega t}$):

$$\left(\frac{i\omega m}{e} - \frac{1}{\mu}\right)v(\omega) = E(\omega) \tag{116}$$

As before we calculate the conductivity:

$$\sigma(\omega) = \frac{j(\omega)}{E(\omega)} = \frac{-nev(\omega)}{E(\omega)} = ne\left(\frac{-i\omega m}{e} + \frac{1}{\mu}\right)^{-1}$$

$\Longrightarrow$

$$\sigma(\omega) = ne\left(\frac{e\mu}{e - i\mu\omega m}\right) = ne\mu\left(\frac{1}{1 - i\omega\tau}\right) = ne\mu\left(\frac{1 + i\omega\tau}{1 + \omega^2\tau^2}\right) \tag{117}$$

For low frequencies (the probability for the electrons to get scattered is high) it is possible to neglect $\frac{i\omega\tau}{\omega^2\tau^2}$ and as a result the conductivity is:

$$\sigma(\text{low } \omega) = ne\mu$$

The solution for high frequencies is the **same** as for collisionless metals:

$$\sigma(\text{high } \omega) = \frac{ine^2}{\omega m}$$

with

$$\mu = \frac{e\tau}{m}$$

With σ it's possible to calculate the susceptibility:

$$\chi(\omega) = \frac{P(\omega)}{\epsilon_0 E(\omega)} = \frac{nex(\omega)}{\epsilon_0 E(\omega)} = \frac{nev(\omega)}{i\omega\epsilon_0 E(\omega)} = \frac{\sigma(\omega)}{i\omega\epsilon_0} = \frac{ne\mu}{i\omega\epsilon_0}\left(\frac{1+i\omega\tau}{1+\omega^2\tau^2}\right) \tag{118}$$

And again the dielectric constant:

$$\epsilon(\omega) = 1+\chi = 1-\frac{ne\mu}{\omega\epsilon_0}\left(\frac{\omega\tau - i}{1+\omega^2\tau^2}\right) \tag{119}$$

$\Longrightarrow$

$$\epsilon(\omega) = 1-\omega_p^2\left(\frac{\omega\tau^2 - i\tau}{\omega+\omega^3\tau^2}\right) \tag{120}$$

Fig. 62 shows the real part of the dielectric function:

$$\epsilon'(\omega) = 1-\frac{\omega_p^2}{\omega^2+\frac{1}{\tau^2}} \tag{121}$$

For diffusive metals the real part of the dielectric constant does not diverge.

The imaginary part depends on ω! When τ goes to infinity the imaginary part of the dielectric constant can be:

$$\begin{aligned}\epsilon''(\omega) &= 0 \text{ for } \omega > 0\\ \epsilon''(\omega) &= \infty \text{ for } \omega = 0\end{aligned}$$

6.9.1 Dielectric Function

Fig. 63 shows the dielectric functions of different metals. These dielectric function were explained by different theories or measurements. Fig. 63 contains three types:
The first type is called reflection electron energy loss spectra (REELS). Electrons (or light) are shot at the surface of a crystal and the measurement of the energy of the reflected electrons will give the dielectric constant. Furthermore, the surface of the crystal must be very clean because light does not penetrate the surface very deep.
The second type is called Palik, which is an optical measurement method.
The third plot is calculated via density functional theory (DFT). In this theory it is very simple to calculate things like dispersion relationships or the density of states. Its possible to get software packages which calculate all these things more or less exactly.

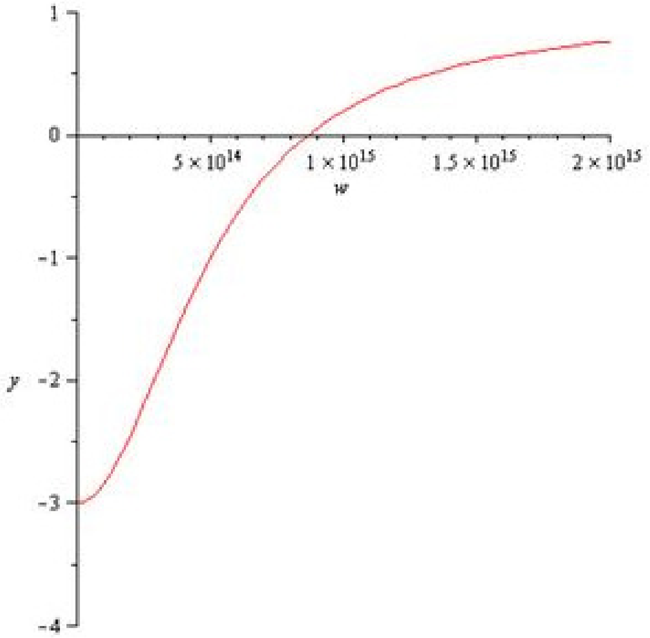

Figure 62: Real part of the dielectric constant of an diffusive material.

6.10 Annotation: Skin depth

The skin depth is an important property in microwave engineering and is related to the high frequency properties of metal. In this case high frequency means that the frequency is still below the plasma frequency so waves do not propagate in the material. With ω the frequency and τ the scattering time we can say that below $\omega\tau \ll 1$ electromagnetic waves penetrate into a material to a certain depth which is called the skin depth.
With the curl of Ohm's law ($\mathbf{J} = \sigma\mathbf{E}$), Faraday's law ($\nabla\times\mathbf{E} = -\frac{d\mathbf{B}}{dt}$), Ampere's law ($\nabla\times\mathbf{B} = \mu_0\mathbf{J}$) and the vector identity $\nabla\times\nabla\times\mathbf{B} = \nabla\underbrace{(\nabla\cdot\mathbf{B})}_{=0} - \nabla^2\mathbf{B}$ the following equation can be obtained:

$$\frac{1}{\sigma\mu_0} = \nabla^2\mathbf{B} = \frac{d\mathbf{B}}{dt} \tag{122}$$

Once again we assume harmonic solutions $B_0 = \exp\left[i(kx-\omega t)\right]$, with this the equation for k can be calculated to be:

$$k = \sqrt{i\omega\sigma\mu_0} = \sqrt{\frac{\omega\sigma\mu_0}{2}} + i\underbrace{\sqrt{\frac{\omega\sigma\mu_0}{2}}}_{exp.decay} \tag{123}$$

The inverse (units) of the component which is describing the exponential decay is a length, the skin depth

$$\delta = \sqrt{\frac{2}{\mu_0\sigma\omega}}\ . \tag{124}$$

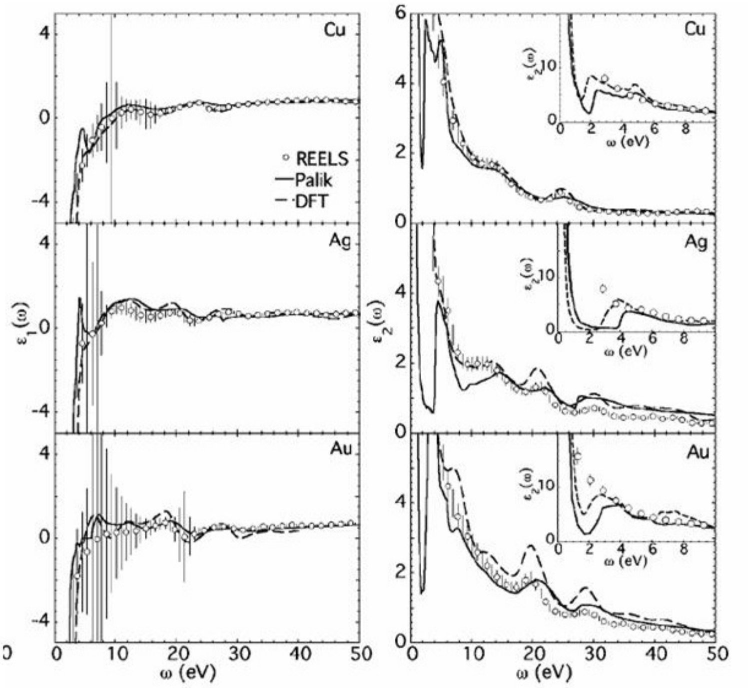

Figure 63: Real (right) and imaginary (left) part of the Dielectric function of different materials.

In microwave engineering (GHz) the surface resistance of a transmission line is an important property, it's dependent on the skin depth. The resistance of a transmission line can be written as

$$R = \frac{l}{\sigma w t}$$

with l the length, w the width and t the thickness of the transmission line. For high frequencies the skin depth gets smaller than the thickness, so the resistivity depends on the skin depth, hence also dependent on the frequency ω.

$$R \approx \frac{1}{\sigma\delta} \approx \sqrt{\omega}$$

6.11 Annotation: Inter- and Intraband Transition

Transition can take place from a filled into an empty state. For an insulator only interband transition is possible, because they only have full valence bands and empty conduction bands.
For metals and semiconductors either inter- or intraband transitions are allowed. Intraband transition means that transition in the same band is possible. When there are regions, where the conduction band and the valence band are parallel, peaks in the absorption will be observed. Parallel bands means, that a photon can excite a lot of states in the conduction and in the valence band. This effect is shown in fig. 64. At every maximum (particular energy, e.g. Λ or X in fig. 64) the bands are parallel. This measurement is very important to understand the band structure.

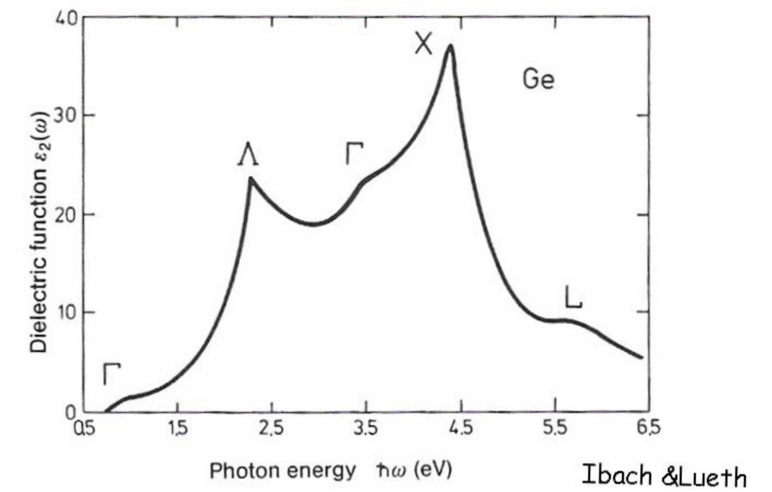

Figure 64: Plot of the dielectric function over the photon energy. At every maximum the valence and the conduction bands are parallel

The condition for absorption is:

$$\hbar\omega = E_c(\mathbf{k}) - E_v(\mathbf{k})$$

7 Transport Regimes

7.1 Ballistic Transport

The formulas for ballistic transport are the same as for electrons in vacuum, because ballistic means there are no obstacles and no scattering. Newton's law with the force $\mathbf{F} = -e\mathbf{E}$ is

$$\mathbf{F} \;=\; m\mathbf{a} \;=\; -\,e\mathbf{E} \;=\; m\frac{d\mathbf{v}}{dt}\ . \tag{125}$$

This is a differential equation for the velocity $\mathbf{v}$. The velocity can be determined to be

$$\mathbf{v} \;=\; \frac{-e\mathbf{E}t}{m} + \mathbf{v}_0$$

and is proportional to the time t, the position $\mathbf{x}$ is given by

$$\mathbf{x} \;=\; \frac{-e\mathbf{E}t^2}{2m} + \mathbf{v}_0 t + \mathbf{x}_0\ .$$

If the electrons are put into an magnetic field they move on a spiral. For a magnetic and an electric field the electrons move perpendicular to both fields[7].

7.2 Drift-Diffusion

For the diffusive transport the electrons are also accelerated at the beginning like the ballistic electrons, but after a time t_0 the electrons scatter and have a velocity $\mathbf{v}_0$ which is randomly distributed. Hence the average velocity after the scattering event is $\langle\mathbf{v_0}\rangle \;=\; 0$. Newton's law for an electron in an electric field is (again)

$$\mathbf{F} \;=\; m\mathbf{a} \;=\; -\,e\mathbf{E} \;=\; m\frac{d\mathbf{v}}{dt},$$

and the velocity $\mathbf{v}$ can be calculated as

$$\mathbf{v} \;=\; -\,\frac{e\mathbf{E}(t-t_0)}{m} + \mathbf{v}_0.$$

With the average velocity after a scattering event is being zero the drift velocity $\mathbf{v}_d$ which is the average velocity of the electrons is:

$$\mathbf{v}_d \;=\; \langle\mathbf{v}\rangle \;=\; \frac{-e\mathbf{E}\tau_{SC}}{m} \;=\; \frac{-e\mathbf{E}l}{mv_F} \;=\; -\,\mu\mathbf{E} \tag{126}$$

where μ is the mobility of the electrons and $\tau_{SC} \;=\; \langle t - t_0\rangle$ is the average time between scattering events. This means that the drift velocity is not proportional to the time any more only proportional to τ_{SC} and the electric field, therefore also the current density $j \;=\; nqv$ is proportional to the electric field which is Ohm's law.
Without an electric field the average electron position in a magnetic field is zero, the electrons only

---

[7] In an electric and magnetic field electrons move with a drift velocity $\mathbf{v} \;=\; \frac{\mathbf{E}\times\mathbf{B}}{B^2}$

move on circular paths. However if the electrons are in an electric and magnetic field the average electron position moves on a straight line at the Hall angle to the fields (in contradiction to the ballistic transport where the electrons move perpendicular to the electric and magnetic field).
The described Drift-Diffusion above is valid for low frequencies, if the frequency of the electric field is high the probability that the electrons scatter gets smaller. This is because the mean free path is much longer than the distances the electrons travel before the electric field changes the direction. Therefore the transport gets more ballistic.
In an insulator in an electric field no current is flowing, although the insulator gets polarized. For an insulator in a changing electric field the polarisation gets changed and therefore a current is flowing which is out of phase with respect to the electric field. In the high frequency regime the transport in metals gets to be ballistic transport because of the unlikely electron scattering as mentioned above. Therefore metals act like insulators, because the ballistic electrons move out of phase with respect to the fast changing electric field which is a similar behaviour to an insulator.

7.3 Diffusive and Ballistic Transport

We now try to get a uniform picture of the transport e.g. if the frequency is so high that there is some scattering of electrons but also ballistic transport. In this frequency regime metals can be described by a dielectric constant which sounds weird, because normally only insulators have a dielectric constant. But for this particular frequency range the electric field changes faster than the electrons scatter and therefore the electrons move out of phase just like they do in an insulator (polarization current). Hence a dielectric constant is also useful to describe a metal in this frequency range.
In general the polarization and the electric displacement are connected to the electric field via a matrix χ:

$$P_i(\omega,k) = \sum_j \varepsilon_0 \chi_{ij}(\omega,k) E_j(\omega,k) \tag{127}$$

$$D_i(\omega,k) = \sum_j \varepsilon_0 \varepsilon_{ij}(\omega,k) E_j(\omega,k) \tag{128}$$

The polarization and the electric displacement are both linear to the electric field which is linear response theory. The susceptibility ($\chi = \frac{P}{\varepsilon_0 E}$) and the dielectric constant ($\varepsilon = \frac{D}{\varepsilon_0 E}$) can be thought of as generalized susceptibilities as above (see chapter 6) and therefore must satisfy the Kramers-Kronig relations.
The displacement is related to the polarization like

$$\mathbf{D} = \varepsilon_0 \mathbf{E} + \mathbf{P},$$

with this equation, eqn. (127) and (128) the dielectric constant can be written as

$$\varepsilon(\omega,k) = 1 + \chi(\omega,k)\ .$$

Often this relation is written

$$\varepsilon(\omega) = 1 + \chi(\omega)\ .$$

This is the low - frequency (wavelength longer than the lattice constant) approximation which is important e.g. for optics.
In an insulator in a changing electric field there are no free electrons to produce a current but there is a displacement current which is the derivation of the displacement by time.

$$\mathbf{J}_D = \frac{\partial \mathbf{D}}{\partial t} = \varepsilon_0 \varepsilon \frac{\partial \mathbf{E}}{\partial t} \tag{129}$$

For a sinusoidal electric field $E(\omega) = \exp(i\omega t)$, the displacement current is

$$\mathbf{J}_D = i\omega\varepsilon_0\varepsilon(\omega)E(\omega), \tag{130}$$

hence the displacement current and the electric field are 90° out of phase. The displacement current and Ohm's law ($\mathbf{J} = \sigma\mathbf{E}$) put into Faraday's law ($\nabla \times \mathbf{H} = \mathbf{J} - \frac{\partial \mathbf{D}}{\partial t}$) gives

$$\nabla \times \mathbf{H} = \sigma(\omega)\mathbf{E}(\omega) - i\omega\varepsilon_0\varepsilon(\omega)\mathbf{E}(\omega) \tag{131}$$

To describe this equation in a simpler way we could define a complex conductivity σ or a complex dielectricity ε. Both is possible and both is being done. A complex conductivity is often used for high frequencies when insulators start to act like metals and a complex dielectric constant is used for very high frequencies when dielectrics act like metals with poor conductivity.

$$\tilde{\sigma}(\omega) = \sigma(\omega) - i\omega\varepsilon_0\varepsilon(\omega) \tag{132}$$

$$\tilde{\varepsilon}(\omega) = \varepsilon(\omega) + i\frac{\sigma(\omega)}{\varepsilon_0\omega} \tag{133}$$

We now look at the response of metals, including the inertial term (eqn. (125)) and the ohmic term (eqn. (126)), the relation between the electric field an the velocity of an electron is

$$\underbrace{\frac{m}{-e}\frac{dv(t)}{dt}}_{Ballistic} - \underbrace{\frac{v(t)}{\mu}}_{Diff.} = E(t) \tag{134}$$

The same equation written as a function of $g(t)$, the Green's function

$$\frac{m}{-e}\frac{dg(t)}{dt} - \frac{g(t)}{\mu} = \delta(t)$$

The solution to this differential equation for $t > 0$ is

$$g = \mu\exp(\frac{-et}{m\mu}),\ t > 0 \tag{135}$$

At $t = 0$ the velocity jumps up and then decays, if there would be only the ballistic part the velocity would also jump up at $t = 0$ but then stay at the same level all the time because there is no drag force or scattering.
To get the generalized susceptibility the Fourier transform of $g(t)$ is needed, which is an Lorentzian for an exponential decay.

$$G(\omega) = \mu\frac{1 - i\omega\tau}{1 + \omega^2\tau^2},\ \tau = \frac{m\mu}{e}$$

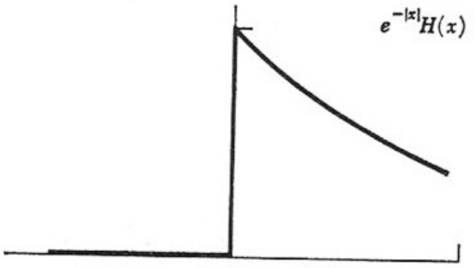

Figure 65: response $g(t)$ to $\delta(t)$ driving force

The generalized susceptibility is the response divided by the driving force

$$\chi(\omega) \;=\; \frac{v(\omega)}{E(\omega)} \;=\; \mu\frac{1-i\omega\tau}{1+\omega^2\tau^2} \tag{136}$$

The frequency dependent conductivity is

$$\sigma(\omega) \;=\; \frac{j(\omega)}{E(\omega)} \;=\; \frac{nev(\omega)}{E(\omega)} \;=\; ne\mu\frac{1-i\omega\tau}{1+\omega^2\tau^2} \tag{137}$$

If we think of low frequencies the conductivity is $\sigma(\omega) \;=\; ne\mu$ which is the same result we got for diffusive transport. For high frequencies the conductivity is $\sigma \;=\; -i\frac{ne\mu}{\omega\tau}$, hence the current again is out of phase with respect to the electric field and the metal acts like an insulator.
The polarization is the number of charges multiplied with the displacement, for harmonic solutions the displacement is $x \;=\; \int v(\omega,t)dt \;=\; \frac{v(\omega)}{i\omega}$

$$P(\omega) \;=\; -nex(\omega) \;=\; \frac{-nev(\omega)}{i\omega} \tag{138}$$

The electrical susceptibility is given by the polarization divided by the electric field

$$\chi(\omega) \;=\; \frac{P(\omega)}{\epsilon_0 E(\omega)} \;=\; \frac{-nev(\omega)}{i\epsilon_0\omega E(\omega)} \;=\; \frac{ne}{i\epsilon_0\omega}(\frac{i\omega m}{e}+\frac{1}{\mu})^{-1} \tag{139}$$

The dielectric constant can be calculated with $\varepsilon(\omega) \;=\; 1+\chi(\omega)$ and by using the definition of the plasma frequency $\omega_P^2 \;=\; \frac{ne^2}{\varepsilon_0 m}$ and the mobility $\mu \;=\; \frac{e\tau}{m}$:

$$\varepsilon(\omega) \;=\; 1-\frac{\omega_P^2}{\omega^2+i\frac{\omega_P^2\varepsilon_0}{\sigma(\omega)}\omega} \tag{140}$$

For low damping (large σ) the dielectric constant can be approximated by the following equation

$$\varepsilon(\omega) \;\approx\; 1-\frac{\omega_P^2}{\omega^2}, \tag{141}$$

this is what's shown in fig. 66(a). At the plasma frequency the dielectric constant is zero and for higher frequencies ε gets positive, thus the metal acts like an insulator, but what happens if the dielectric

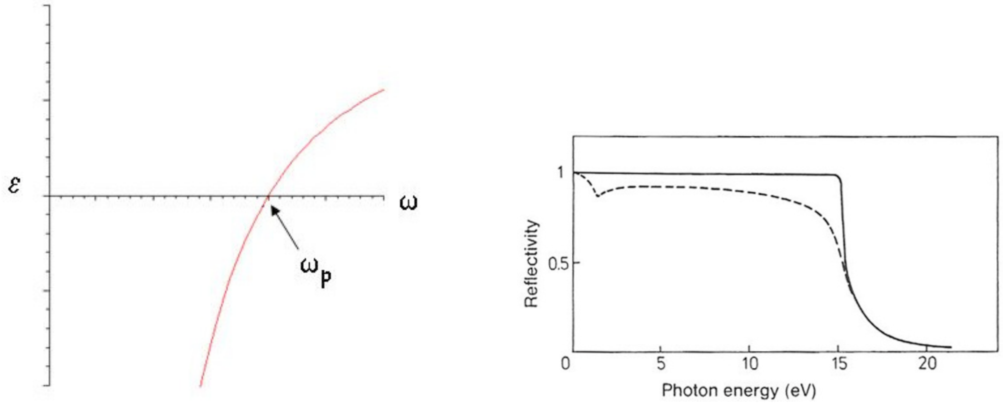

(a) (b)

Figure 66: a) Dielectric constant ε vs. ω. The dielectric constant is positive for frequencies above the plasma frequency; b) Reflectivity of Aluminium, at about 15 eV it drops, this is where the frequency of the light is the plasma frequency.

constant is negative?
For a negative dielectric constant there is no propagating wave solution to the wave-equation only damped solutions, but because the wave and it's energy has to go somewhere the wave gets reflected out of the material. In the following fig. 66(b) the reflectivity for Aluminium is shown. For photon energies $0-15$ eV aluminium is shiny, in the ultraviolet the reflectivity drops and the light goes through the aluminium. To remind you: the plasma frequency is depending on the electron density, this behaviour is used to make transparent contacts for solar cells. There a semiconductor with a low electron density is used, so visible light can pass through it. However for DC the semiconductor is still conducting.

Dispersion relation general
With Amperes law, Faraday's law and the electric displacement as $\mathbf{D} = \varepsilon \mathbf{E}$ as well as $\mathbf{B} = \mu \mathbf{H}$ the following equation which is a more general dispersion relation for ω and k can be derived (for plane waves):

$$\varepsilon(\omega, k)\mu_0\varepsilon_0\omega^2 = k^2 \tag{142}$$

On the left side (for positive ε) is $c^2\omega^2$, with c the speed of light in the material, therefore the waves are travelling at the speed of light in the material. From the Diffusion-Ballistic regime we now that the dielectric constant for a metal can be negative.

$$\varepsilon \approx 1 - \frac{\omega_P^2}{\omega^2}$$

Hence k (eqn. (142)) can get complex and a complex k means that the wave decays exponentially, this shows fig. 67. This phenomenon is similar to electrons shooten into a semiconductor with an energy in-between the band gap of the semiconductor, which are reflected because there are no allowed states. For metals there is a forbidden frequency gap for light.

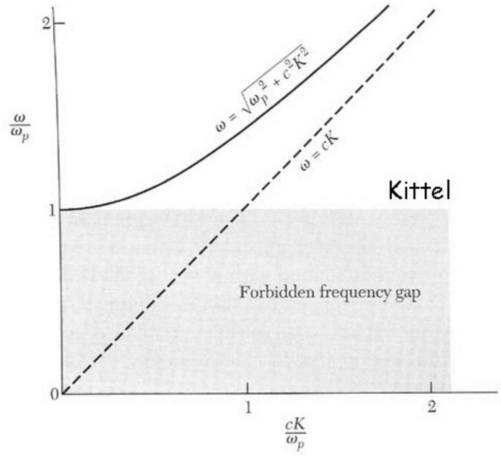

Figure 67: Dispersion relation ω vs. k

7.4 Boltzmann equation (missing)

8 Crystal Physics

The main subject of Crystal Physics is how the symmetries of the crystal affect the physical properties. Knowledge of the symmetries can ease the measurements of the properties. If we take a simple cubic crystal for example, repetition of a measurement after a rotation of 90° wouldn't make much sense. Tensors, with which one can describe such properties must take that symmetry into account. Knowing the structure of the tensors, we would know how many independent properties we would have to measure to be able to explain the whole behavior of the crystal.

8.1 Stress and Strain

To give an example for a physical property that is related to a certain tensor we will look at the stress and strain relation in solids. If we apply a force to a crystal, it will most likely be deformed. The former right-angled basis vectors **x**, **y**, and **z** will move to not-right-angled ones **x'**, **y'** and **z'**, as shown in fig. 68. This distortion of the material is described by the strain matrix ϵ_{ij}.

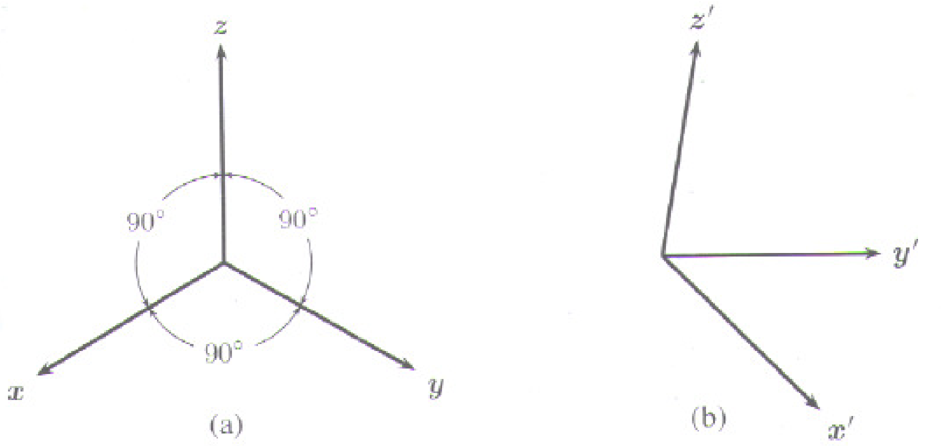

Figure 68: Shift of the basis vectors because of strain, former right angled vectors (a) get displaced (b)

$$\begin{aligned}\mathbf{x}' &= (1 + \epsilon_{xx})\mathbf{x} + \epsilon_{xy}\mathbf{y} + \epsilon_{xz}\mathbf{z}\\ \mathbf{y}' &= \epsilon_{yx}\mathbf{x} + (1 + \epsilon_{yy})\mathbf{y} + \epsilon_{yz}\mathbf{z}\\ \mathbf{z}' &= \epsilon_{zx}\mathbf{x} + \epsilon_{zy}\mathbf{y} + (1 + \epsilon_{zz})\mathbf{z}\end{aligned}$$

The strain matrix enables us to describe shear, the distortion in a different direction than the force acts.

Correspondingly, stress describes the forces per unit area applied to the material. We can find nine independent forces Xx, Xy, Xz, Yx, Yy, Yz, Zx, Zy and Zz as shown in fig. 69. The capital letter describes the direction of the force, the small ones the, to the plane on which the force acts on,

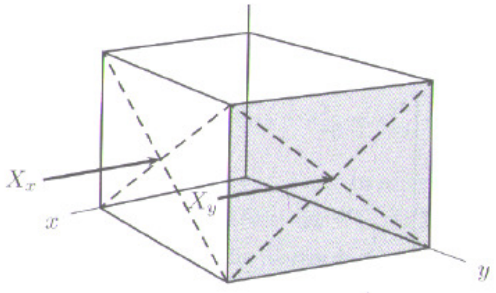

Figure 69: Forces applyable in the x-direction

orthogonal direction. We can define a stress tensor:

$$\sigma_{kl} = \begin{bmatrix} \frac{Xx}{Ax} & \frac{Xy}{Ay} & \frac{Xz}{Az} \\ \frac{Yx}{Ax} & \frac{Yy}{Ay} & \frac{Yz}{Az} \\ \frac{Zx}{Ax} & \frac{Zy}{Ay} & \frac{Zz}{Az} \end{bmatrix}$$

The relationship between those two can be described with a rank four stiffness tensor

$$\epsilon_{ij} = s_{ijkl}\sigma_{kl}$$

Of course, this relationship exists in two directions, the inverse of the stiffness tensor is called the compliance tensor

$$\sigma_{ij} = c_{ijkl}\epsilon_{kl}$$

Most physical properties can be connected to each other via tensors, as we will see in chapter 8.2. One further example is the electric susceptibility χ, which connects the electric field to the electric polarisation. Since both properties are vectors, the susceptibility is a rank two tensor, a matrix. So if we want to relate two properties, like the strain and the electric field, we know that since the electric field is a vector and the strain is a matrix, we will need a tensor of rank three.

8.2 Statistical Physics

As usual in statistical physics we start out with a microcannonical ensemble. There, the internal energy is described by the extrinsic variables (Just to remind you: Extrinsic variables scale with the size of the system). We can take the total derivative:

$$dU = \frac{\partial U}{\partial S}dS + \frac{\partial U}{\partial \epsilon_{ij}}d\epsilon_{ij} + \frac{\partial U}{\partial P_k}dP_k + \frac{\partial U}{\partial M_l}dM_l \tag{143}$$

Or, using the intrinsic variables:

$$dU = TdS + \sigma_{ij}d\epsilon_{ij} + E_kdP_k + H_ldM_l$$

For every system, on which we would like to perform experiments, using the extrinsic variables as the independent ones isn't a good idea. Usually in an experiment we hold the temperature under control. To realize this, we can make a Legendre transformation to get the free energy F:

$$F = U - TS$$

But in an experiment we usually are also in control of the stress, the electric and the magnetic field we apply to the material. So it is a good idea to perform a couple of additional Legendre transformations to get the generalized Gibbs free energy:

$$G = U - TS - \sigma_{ij}\epsilon_{ij} - E_k P_k - H_l M_l$$

By taking the total derivative and using eqn. (143), we are left with:

$$dG = -SdT - \epsilon_{ij}d\sigma_{ij} - P_k dE_k - M_l dH_l$$

or, using the definition of a total derivative

$$dG = \left(\frac{\partial G}{\partial T}\right) dT + \left(\frac{\partial G}{\partial \sigma_{ij}}\right) d\sigma_{ij} + \left(\frac{\partial G}{\partial E_k}\right) dE_k + \left(\frac{\partial G}{\partial H_l}\right) dH_l$$

we can identify

$$\begin{array}{llll} -\left(\frac{\partial G}{\partial T}\right) = S & & -\left(\frac{\partial G}{\partial \sigma_{ij}}\right) = \epsilon_{ij} \\ -\left(\frac{\partial G}{\partial E_k}\right) = P_k & & -\left(\frac{\partial G}{\partial H_l}\right) = M_l \end{array}$$

So if we know the Gibbs free energy of a system in dependence of the intrinsic variables, we can determine the extrinsic ones with a simple derivation. But calculating the Gibbs free energy is the difficult part. Remembering the course on statistical physics, we know how to calculate the free energy of a canonical ensemble:

$$Z = \sum_j exp\left(\frac{-E_j}{k_B T}\right) \qquad F = -k_B T ln(Z)$$

Here the sum over j sums over all microscopic states corresponding to a macroscopic state. But there occurs the energy of the states in the sum. We can get the energy by solving the system quantum mechanically. Calculating the Gibbs free energy is very similar, but the energy in the partition function also depends on the magnetic and the electric fields. The calculations for the hamiltonians of electrons in electromagnetic fields are part of chapter **??**.

By taking the total derivative of the extrinsic variables we can get to materials constants or physical properties. As an example we take the total derivative of the strain:

$$d\epsilon_{ij} = \left(\frac{\partial \epsilon_{ij}}{\partial \sigma_{kl}}\right)_1 d\sigma_{kl} + \left(\frac{\partial \epsilon_{ij}}{\partial E_k}\right)_2 dE_k + \left(\frac{\partial \epsilon_{ij}}{\partial H_l}\right)_3 dH_l + \left(\frac{\partial \epsilon_{ij}}{\partial T}\right)_4 dT$$

Where the single derivations represent:

1. Elastic deformation (stiffness tensor)

2. Reciprocal piezo-electric effect

3. Reciprocal piezo-magnetic effect

4. Thermal dilatation

8.3 Crystal Symmetries

Intrinsic Symmetries
As seen in chapter 8.2, we can get the stiffness tensor by taking the derivative of the strain in respect to the stress.

$$\frac{d\epsilon_{ij}}{d\sigma_{kl}} = s_{ijkl}$$

The strain itself is calculated out of the Gibbs free energy:

$$-\left(\frac{\partial G}{\partial \sigma_{ij}}\right) = \epsilon_{ij}$$

So the stiffness tensor can be written as the second derivative of the Gibbs free energy in respect to two different elements of the stress matrix:

$$-\left(\frac{\partial G}{\partial \sigma_{ij}\partial \sigma_{kl}}\right) = s_{ijkl}$$

Because of Schwarz' theorem[8] we get the same result if we can change the order of the derivatives:

$$-\left(\frac{\partial G}{\partial \sigma_{kl}\partial \sigma_{ij}}\right) = s_{klij} \overset{!}{=} s_{ijkl}$$

This way we can find those symmetries for a lot of different properties, for example the electric and the magnetic susceptibility:

$$-\left(\frac{\partial G}{\partial E_j \partial E_k}\right) = \left(\frac{\partial P_k}{\partial E_j}\right) = \chi_{kj} = -\left(\frac{\partial G}{\partial E_k \partial E_j}\right) = \left(\frac{\partial P_j}{\partial E_k}\right) = \chi_{jk}$$

$$-\left(\frac{\partial G}{\partial H_k \partial H_l}\right) = \left(\frac{\partial M_l}{\partial H_k}\right) = \psi_{lk} = -\left(\frac{\partial G}{\partial H_l \partial H_k}\right) = \left(\frac{\partial M_k}{\partial H_l}\right) = \psi_{kl}$$

---

[8] Hermann Schwarz, 1864 till 1951

Direct and reciprocal effects

In the exact same way we can find relationships between direct and reciprocal effects. As an example we look at the direct and the reverse piezoelectric effect. This effect describes how the electric polarisation of a crystal changes, when we apply stress to it.

$$\left(\frac{\partial P_k}{\partial \sigma_{ij}}\right) = d_{kij}$$

Again following back to the derivatives of the Gibbs free energy leads us to an interesting solution:

$$-\left(\frac{\partial^2 G}{\partial \sigma_{ij} \partial E_k}\right) = \left(\frac{\partial P_k}{\partial \sigma_{ij}}\right) = -\left(\frac{\partial^2 G}{\partial E_k \partial \sigma_{ij}}\right) = \left(\frac{\partial \epsilon_{ij}}{\partial E_k}\right) = d_{kij}$$

The same tensor elements used for the direct piezoelectric effect are also used in the tensor for the reverse piezoelectric effect. An interesting use of this symmetry is to track down systematical errors in a measurement. We could measure the piezoelecric effect by squeezing a crystal and measure the polarisation as well as applying an electric field to it and measure the strain. If we perform both measurements and don't get the same solution there must be a systematic error in at least one of the two measurements.

Groups

Crystals can have translational, rotational, inversion and reflectional symmetries. Those of them, where one point of the crystal remains the same, can be written as a matrix. The matrices of those symmetry operations to one crystal form the group of this crystal. The groups, which contain only operations where one point of the crystal remains the same, are called **point groups**. (There are 32 of them.) If we also include translational symmetries, where no point in the crystal remains at it's incident position, we get the 230 **space groups**.

Fig. 70 shows the symmetries in a crystal with point group C2 and C4. For C2 we can define the symmetry operations

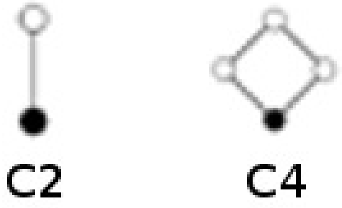

Figure 70: Illustration of the crystal symmetries in the point groups C2 and C4

$$E = \begin{bmatrix} 1 & 0 & 0 \\ 0 & 1 & 0 \\ 0 & 0 & 1 \end{bmatrix}, \; C_2 = \begin{bmatrix} -1 & 0 & 0 \\ 0 & -1 & 0 \\ 0 & 0 & 1 \end{bmatrix}$$

where the first one is the identity and the second one rotates the crystal by 180°. As we can easily verify, those two operations form a group. C4 contains a few more operations.

$$E = \begin{bmatrix} 1 & 0 & 0 \\ 0 & 1 & 0 \\ 0 & 0 & 1 \end{bmatrix}, C_4 = \begin{bmatrix} 0 & -1 & 0 \\ 1 & 0 & 0 \\ 0 & 0 & 1 \end{bmatrix}, C_2 = \begin{bmatrix} -1 & 0 & 0 \\ 0 & -1 & 0 \\ 0 & 0 & 1 \end{bmatrix}, C_4^3 = \begin{bmatrix} 0 & 1 & 0 \\ -1 & 0 & 0 \\ 0 & 0 & 1 \end{bmatrix},$$

C4 contains the operations for rotations by 90°, 180°, 270° and the identity. The next step is to find out how these symmetries affect the properties of the tensors.

As an example we want to find out how a 180° rotational symmetry affects the polarisation tensor. Since both the electric field and the polarisation can be described as vectors, this is a rank two tensor, a matrix:

$$\begin{bmatrix} P_x \\ P_y \\ P_z \end{bmatrix} = \begin{bmatrix} \chi_{xx} & \chi_{xy} & \chi_{xz} \\ \chi_{yx} & \chi_{yy} & \chi_{yz} \\ \chi_{zx} & \chi_{zy} & \chi_{zz} \end{bmatrix} \begin{bmatrix} E_x \\ E_y \\ E_z \end{bmatrix}$$

If we perform a crystal symmetry operation on both the electric field and the polarisation, the equation must hold:

$$U\mathbf{P} = \chi U\mathbf{E} \qquad \text{with } U = \begin{bmatrix} -1 & 0 & 0 \\ 0 & -1 & 0 \\ 0 & 0 & 1 \end{bmatrix}$$

Now we multiply with the inverse of U from the left

$$U^{-1}U\mathbf{P} = U^{-1}\chi U\mathbf{E}$$

This can only be true if the susceptibility matrix is invariant under the symmetry operation

$$\chi = U^{-1}\chi U$$

which would mean

$$\chi = \begin{bmatrix} \chi xx & \chi xy & -\chi xz \\ \chi yx & \chi yy & -\chi yz \\ -\chi zx & -\chi zy & \chi zz \end{bmatrix}$$

This is fulfilled if χxz, χyz, χzx and χzy are equal to zero. Further we know from the intrinsic symmetries explained above, that $\chi_{ij} = \chi_{ji}$. Thus the susceptability tensor of a crystal with only the 180° rotational symmetry looks like this:

$$\chi = \begin{bmatrix} \chi xx & \chi xy & 0 \\ \chi xy & \chi yy & 0 \\ 0 & 0 & \chi zz \end{bmatrix}$$

Those symmetries and the point- and space groups can be looked up in tables[9]. Since it would be far too complicated to write all symmetry operations of one group in such a table, these tables often only contain the generating matrices. Those matrices describe the symmetry operations with which all other symmetry operations of this group can be constructed. Another quite important thing is that especially in those tables, tensors with a rank higher than two have to be displayed. To simplify the high

---

[9] i.e. the very own of this course at http://lamp.tu-graz.ac.at/ hadley/ss2/crystalphysics/crystalclasses/crystalclasses.html

number of indices, crystallographers very often combine pairs of two indices using the following scheme:

$$\begin{array}{ccc} 11 \rightarrow 1 & 12 \rightarrow 6 & 13 \rightarrow 5 \\ & 22 \rightarrow 2 & 23 \rightarrow 4 \\ & & 33 \rightarrow 3 \end{array}$$

So if we got a third rank tensor element g_{36} it would be g_{312}, if it's a fourth rank tensor it would be g_{3312}.
Another interesting consequence of those symmetry operations is, that in all crystals, which have inversion symmetry, all rank three tensors equal zero, that means, those crystals don't show effects described by a rank three tensor. Examples are piezoelectricity, piezomagnetism and the piezo-caloric effect.

8.4 Example - Birefringence [10]

A fairly interesting example is an effect called birefringence. If we look on a piece of newspaper through a calcite crystal, we will see all letters doubled. This effect occurs from the fact that different polarisations of light have different velocities in calcite. To explain this, the index of refraction in calcite must be a matrix. If we follow that clue, we find, that the electric susceptibility has to be a matrix too. To look up the form of this second rank tensor, we first need to know the point group of calcite. After some research we can get the point group in two ways. The first possibility is to look up the crystal structure of calcite, the second one to explicitly look for the point group of it. In both cases we can look it up in a table and find out the structure of second rank tensors in trigonal structures (like calcite has).:

$$g_{ij} = \begin{bmatrix} g_{11} & 0 & 0 \\ 0 & g_{11} & 0 \\ 0 & 0 & g_{33} \end{bmatrix}$$

Which is exactly what we expected. There are two independent constants, so the index of refraction has to be a matrix.

---

[10] Birefringence = Doppelbrechung

9 Electron-electron interactions, Quantum electronics

9.1 Electron Screening

For a single electron in vacuum Gauss's law is

$$\nabla \cdot \mathbf{E} = \frac{-e\delta(r)}{\varepsilon}\ . \tag{144}$$

If you use the relationship

$$\mathbf{E} = -\nabla V \tag{145}$$

between the electric field E and the electrostatic potential V and plug it into Gauss's law, you get the Poisson equation

$$\nabla^2 V = \frac{e\delta(r)}{\varepsilon}\ . \tag{146}$$

The solution of this differential equation is

$$V = \frac{-e}{4\pi\epsilon r}\ . \tag{147}$$

If a single electron is put in a metal and fixed, the other mobile electrons will react to the electric field whereas the uniformly distributed positive ions will stay at their position. Before the single electron was put in, the electrons where uniformly distributed too. The electrons far away are still where they were before but now the electrons near the fixed negative charge are repelled. The poisson equation now looks like

$$\nabla^2 V = \frac{e\delta(r)}{\varepsilon} + \frac{-\rho_{reaction}}{\varepsilon}\ . \tag{148}$$

Now we want to know how $\rho_{reaction}$ looks like. Based on observations we can say that the potential goes to zero far away from the extra added electron. The reaction goes to zero far away too, therefore we assume in the simplest approximation that $\rho_{reaction}$ is proportional to V. So we can rewrite eqn. (148) as

$$\nabla^2 V - k^2 V = \frac{e\delta(r)}{\varepsilon} \tag{149}$$

which is the Helmholtz equation where the solution is well known. The proportionality constant is typically chosen to be k^2 with k as a wave vector because the dimension of the factor is $\frac{1}{length^2}$. The Helmholtz equation in 3-d is

$$\left(\nabla^2 - k^2\right) g = \delta(\mathbf{r}) \tag{150}$$

where g is the appropriate Green's function

$$g = \frac{-\exp\left(-k\left|\mathbf{r} - \mathbf{r}'\right|\right)}{4\pi\left|\mathbf{r} - \mathbf{r}'\right|}\ . \tag{151}$$

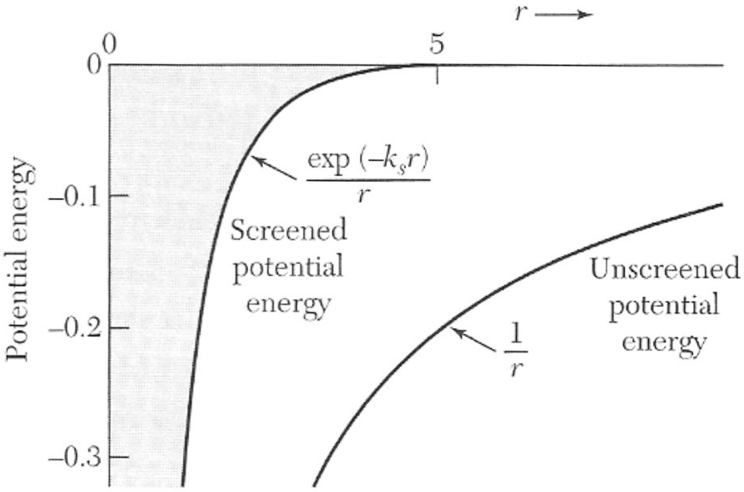

Figure 71: Unscreened and screened potential.

So the resulting potential is

$$V = \frac{-\exp\left(-k\left|\mathbf{r}-\mathbf{r}'\right|\right)}{4\pi\varepsilon\left|\mathbf{r}-\mathbf{r}'\right|} \,. \tag{152}$$

Fig. 71 shows the unscreened and the screened Coulomb potential. The distance how far the screened potential can reach, the screening length, is determined by k_s. The Thomas-Fermi approximation is one possible way to calculate it, where

$$k_s^2 = \frac{3e^2 n}{\varepsilon_0 E_F} \,. \tag{153}$$

The so-called Thomas-Fermi screening length depends mostly on the electron density n in the metal. If the electron density is large, k_s becomes large and the screening length is small and vice versa. This means that a metal with a large electron density can screen the potential of the extra electron better than a metal with a small electron density.

The actual screening of a point charge looks different to an exponential decay. For example fig. 72 shows an STM picture of GaAs doped with Si on Ga-sites. Around the dopants there are the screening clouds of electrons. But the charge goes up and down and makes these oscillations which are called Friedel oscillations. The reason for these oscillations is that the electrons that shield the point charge (δ-distribution) have a certain wave number k. But the ones with the highest wave number (shortest wavelength) are around k_F. Therefore you can't build structures with electron waves that are smaller than this wavelength and so the reaction distribution oscillates around the point charge.

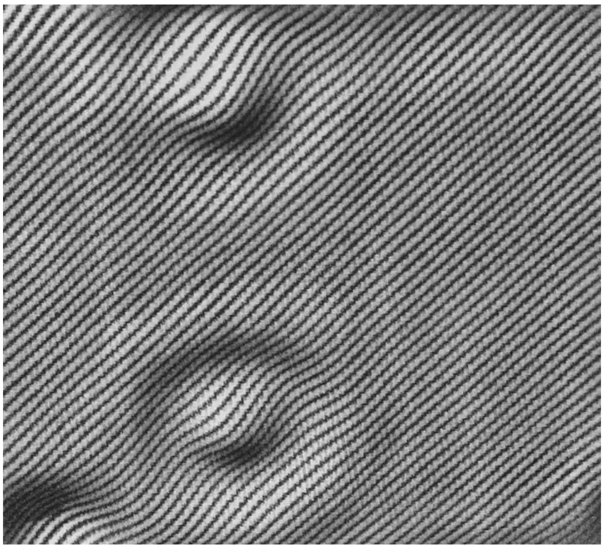

Figure 72: STM picture of GaAs doped with Si at Ga-sites.

9.2 Single electron effects

9.2.1 Tunnel Junctions

A tunnel junction looks like in fig. 73 where two metals are separated with an insulating barrier where a bias voltage is applied. The tunnel junction can be described by a Hamiltonian

$$H = H_l + H_r + H_T$$

that consists of the Hamiltonian H_l and H_r of the electrons on the left and right side, and of the tunnelling-Hamiltonian which describes the tunnelling from left to right and contains the height and width of the barrier. Fermi's golden rule gives the rate of electrons tunnelling through the barrier

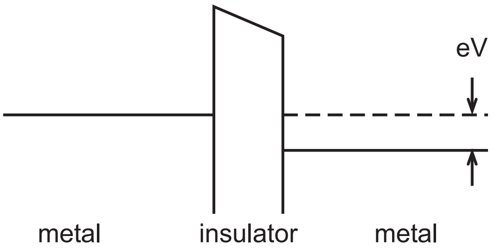

Figure 73: Tunnel junction.

$$\Gamma_{l\to r} = \frac{2\pi}{\hbar} \left|\langle l\,|H_T|\,r\rangle\right|^2 \ \delta(E_l - E_r) \ . \tag{154}$$

The δ-function shows you that the energy of the electron has to be the same before and after the tunnelling. Therefore only electrons in the energy range between the dashed and the solid line can tunnel through the barrier because below all the states on the right side are filled and above there are no electron states occupied on the left side. So we should integrate over pairs of states where the one on the left is occupied and the one on the right is empty. The tunnelling rate finally looks like

$$\Gamma_{L\to R} = \int \frac{2\pi}{\hbar} \left|\langle l\left|H_T\right| r\rangle\right|^2 \; D_L(E_L)f(E-E_L)D_R(E_R)(1-f(E-E_R))dE \tag{155}$$

where $D_{L,R}$ are the density of states of the metal on the left and right side and $f(E-E_L)$ is the Fermi function that describes the occupation of the states on the left and $(1-f(E-E_R))$ is the Fermi function of the empty states on the right. The density of states for a metal is approximately constant, especially for small voltage ranges this approximation is okay. So we can pull the density of states out of the integral and get

$$\Gamma_{L\to R} = \frac{2\pi t^2 D_L(E_L)D_R(E_R)}{\hbar} \int f(E-E_L)(1-f(E-E_R))dE \tag{156}$$

with t as the transfer integral (overlap of the states on the left and right side). (We assume the same for the transfer integral as for the density of states.) The integral over the Fermi function of the occupied states on the left times the Fermi function of the empty states on the right can be calculated with e.g. Matlab which leads us to

$$\Gamma_{L\to R} = \frac{2\pi t^2 D_L(E_L)D_R(E_R)}{\hbar} \frac{E_R-E_L}{\exp\left(-\frac{E_R-E_L}{k_BT}\right)-1} \ . \tag{157}$$

The difference in energy equals the electron charge times the applied voltage on the tunnel junction:

$$E_R - E_L = eV \ .$$

The final solution for the tunnel rate looks like this

$$\Gamma_{L\to R} = \frac{V}{eR}\frac{1}{\exp\left(-\frac{eV}{k_BT}\right)-1} \ . \tag{158}$$

At low temperatures the exponential term can be neglected and the tunnel rate only depends on $\frac{V}{R}$ but at high temperatures electrons are thermally activated across the barrier and the temperature dependent term becomes important again. A tunnel rate from right to left can be calculated equivalently. If you bias the tunnel junction so that the electrons will move from left to right, at finite temperature there are still some electrons that can move in the opposite direction because the Fermi function allows some electrons on the right to occupy states that are empty on the left. The resulting tunnelling current is the difference of the tunnelling rates times the electron charge

$$I_{L\to R} = -\left|e\right|(\Gamma_{L\to R} - \Gamma_{R\to L}) \ . \tag{159}$$

The temperature dependent parts cancel out and the current only depends on V and R:

$$I_{L\to R} = \frac{V}{R} \tag{160}$$

with R as

$$R = \frac{\hbar}{2\pi e^2 D_l(E_l)D_r(E_r)t^2} \tag{161}$$

So the tunnelling current is proportional to the applied voltage.

If you combine two tunnel junctions you get a single electron transistor.

9.2.2 Single Electron Transistor

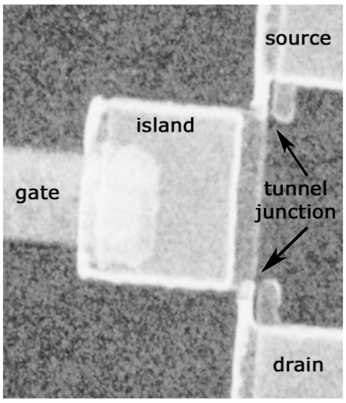

Figure 74: Single electron transistor.

In fig. 74 you can see a single electron transistor with its three gold electrodes and an island (size of 1 μm) where only one electron at the time can tunnel on. The gate electrode is not connected to the island but there is a thick insulating layer between the gold and the island where no tunnelling can take place. But an applied voltage can induce a polarisation to the island which pulls the electrons on the left side that causes a change in the bias across the tunnel junctions. The total capacitance of the island is about 1 μF. If an electron tunnels on the island the voltage changes. For a capacitor the formula $Q = CV$ has to be used with $Q = e$ which leads to a voltage change of $\Delta V = 10^{-4}$ V.

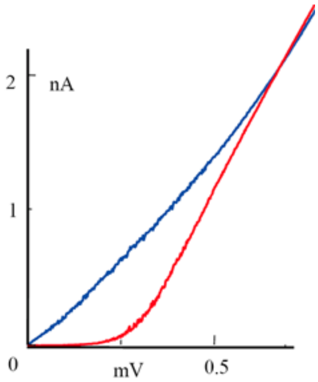

Figure 75: I vs V: blue line: without Coulomb blockade; red line: with Coulomb blockade.

If you apply a bias less than ΔV across the whole thing no tunnelling will happen because there is a Coulomb blockade. But a voltage change on the gate can suppress the Coulomb blockade and the current will be linear to the applied voltage as you would expect for a tunnel junction. At other voltages there is still the Coulomb blockade and the current will increase only at a certain voltage (see fig. 75). For the model with the little crystals it means that at low bias voltages none of the electrons will tunnel and the material will become an insulator.

We will discuss the single electron transistor (SET) now in more detail. In experiments a SET has usually two gates. One where the signal comes in and one to tune whether the Coulomb blockade is suppressed or at its maximum. Figure 76 shows the set up and its circuit.

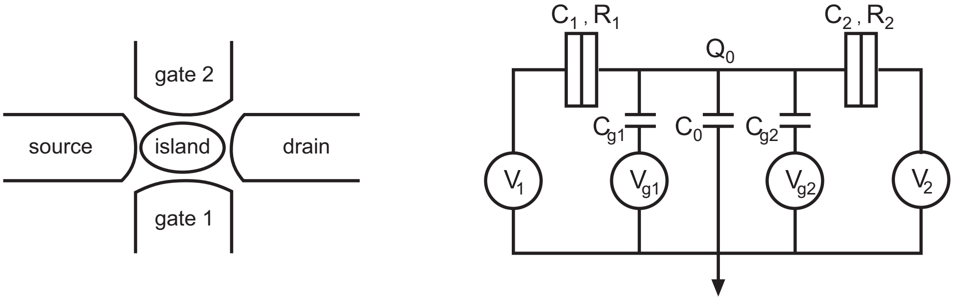

Figure 76: Single electron transistor with two gates and its circuit.

The total charge Q on the island is

$$Q = C_1(V - V_1) + C_2(V - V_3) + C_{g1}(V - V_{g1}) + C_{g2}(V - V_{g2}) + C_0 V \tag{162}$$

but Q needs to be an integer number n times electron charge plus a background charge Q_0 that is caused by electric field lines that can come from any other electronic device.

So the voltages that the island is allowed to have are

$$V(n) = (-ne + Q_0 + C_1V_1 + C_2V_2 + C_{g1}V_{g1} + C_{g2}V_{g2})/C_\Sigma \tag{163}$$

with C_Σ as the total capacitance of the island:

$$C_\Sigma = C_1 + C_2 + C_{g1} + C_{g2} + C_0 \quad . \tag{164}$$

The energy needed to add an infinitesimal charge dq to an island at voltage $V(n)$ is $V(n)dq$. The energy needed to add a whole electron at a given number of electrons on the island is therefore:

$$\Delta E = \int_0^{-e} V(n)dq = -eV(n) + \frac{e^2}{2C_\Sigma} \tag{165}$$

The extra term $\frac{e^2}{2C_\Sigma}$ is the charging energy that comes from the fact that every time you add a fraction of an electron to the island the voltage changes.

The energy needed to remove a whole electron is analog as above:

$$\Delta E = \int_0^{e} V(n)dq = eV(n) + \frac{e^2}{2C_\Sigma} \tag{166}$$

The charging energy is still the same because the sign of the charge vanishes when it's being squared.

You can take these formulas to calculate the energy that is needed for the four possible tunnel events: an electron can tunnel from the first electrode on the island or from the island on the first electrode and from the island on the second electrode or from the second electrode on the island. The relating change in energy is as follows:

$$\begin{aligned}
\Delta E_{1R}(n) &= eV_1 - e(-ne + Q_0 + C_1V_1 + C_2V_2 + C_{g1}V_{g1} + C_{g2}V_{g2})/C_\Sigma + \frac{e^2}{2C_\Sigma} && (167)\\
\Delta E_{1L}(n) &= -eV_1 + e(-ne + Q_0 + C_1V_1 + C_2V_2 + C_{g1}V_{g1} + C_{g2}V_{g2})/C_\Sigma + \frac{e^2}{2C_\Sigma} && (168)\\
\Delta E_{2R}(n) &= -eV_2 + e(-ne + Q_0 + C_1V_1 + C_2V_2 + C_{g1}V_{g1} + C_{g2}V_{g2})/C_\Sigma + \frac{e^2}{2C_\Sigma} && (169)\\
\Delta E_{2L}(n) &= eV_2 - e(-ne + Q_0 + C_1V_1 + C_2V_2 + C_{g1}V_{g1} + C_{g2}V_{g2})/C_\Sigma + \frac{e^2}{2C_\Sigma}\ . && (170)
\end{aligned}$$

If the change in energy is negative the electron will tunnel. Figure 77 shows a plot where all four of them are plotted as a function of the bias and the gate voltage. All other voltages are held constant. The shaded regions show where none of the tunnel events can decrease the energy which is called the Coulomb blockade regime. The region labelled with 0 determines the bias and gate voltage range where no electron is allowed to tunnel on or off the island. But if you increase the gate voltage you come to a region where one electron can tunnel on the island because the positive gate voltage pulls one electron on it. The higher the gate voltage the more electrons can tunnel. But if you increase the bias voltage nothing happens until you get to the region that is labelled with 0, 1 which shows us that at a given number n of electrons either n or $n+1$ electrons are allowed on the islands. It depends now on the number of electrons on the island which tunnel processes decrease or increase the energy.

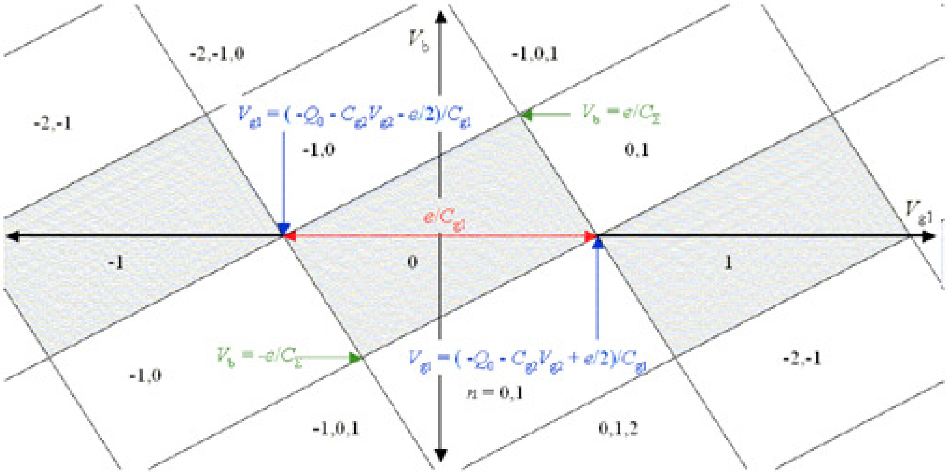

Figure 77: Coulomb blockade; shaded region: Coulomb blockade is active - none of the four tunnel events decrease the energy; the number in the region says how many electrons are allowed to tunnel on the island.

This illustration is important to interpret experimental data (see fig. 78). In the Coulomb blockade regime there is no current flowing but if you increase the bias voltage you get into a regime where there is a current that changes periodically with the change of the gate voltage (instead of linear compared to usual transistors).

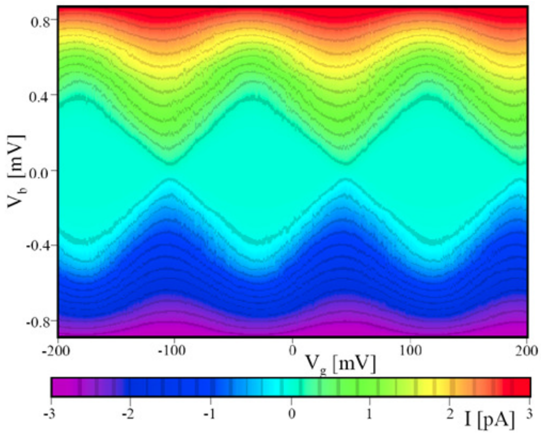

Figure 78: Experimental data: current as a function of V_b and V_G.

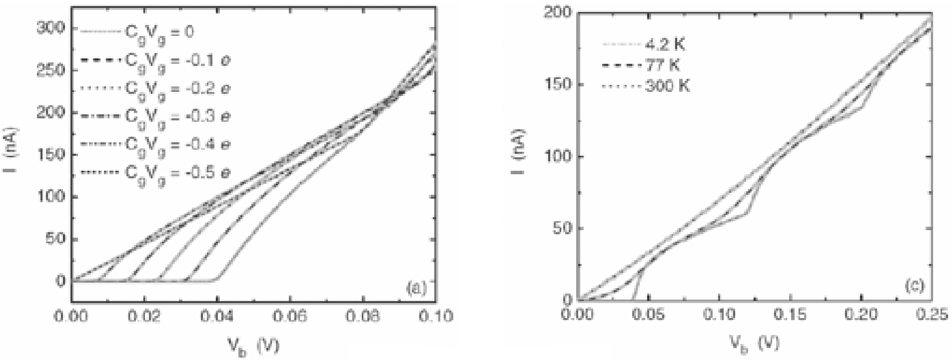

Figure 79: Coulomb staircase.

Figure 79 shows the so-called Coulomb staircase at different gate voltages and different temperatures. The first picture shows the current depending on the bias voltage at different gate voltages. The second one shows that at high temperatures like room temperature the Coulomb staircase disappears and the current-bias voltage line looks like the one of a resistor. We can say that the staircase gets washed out when you increase the temperature which can be explained with the thermal fluctuations. Because at high temperatures the thermal energy is bigger than the charging energy

$$\frac{e^2}{2C_\Sigma} \ll k_B T \tag{171}$$

and the thermally activated electrons can tunnel easily on the island.

But the Coulomb blockade can also be suppressed by quantum fluctuations. The Heisenberg uncertainty relation for energy looks like

$$\Delta E \cdot \Delta t \sim \hbar \tag{172}$$

and the average time of a quantum fluctuation of the order of the charging energy is then

$$\Delta t \sim \frac{\hbar 2C_\Sigma}{e^2} \ . \tag{173}$$

Now we have a look at the charging time of the capacitance which is RC_Σ. If this charging time is much faster than a quantum fluctuation

$$RC_\Sigma < \frac{\hbar 2C_\Sigma}{e^2} \tag{174}$$

the system has time to move an electron on the island. The capacitance cancels out and we can calculate the critical resistance:

$$R < \frac{2\hbar}{e^2} \approx 8\ k\Omega \tag{175}$$

If the resistance is smaller than 8 $k\Omega$ the Coulomb blockade can be suppressed by quantum fluctuation otherwise it can not be suppressed. But all the calculations were not very precise and we used the uncertainty relation so one generally says that if the resistance between the crystals in a material is below the resistance quantum

$$\frac{h}{e^2} \approx 25.5\ k\Omega\ , \tag{176}$$

quantum fluctuations can suppress the Coulomb blockade. If it is above, you get an insulator at low temperatures.

The critical resistance can also be related to the dimensions of the crystals:

$$R_{crit} \approx \frac{h}{e^2} = \frac{\rho l}{wt}\ , \tag{177}$$

with w as width, l as length, t as thickness and ρ as the resistivity of the crystal. If we assume that the crystals are squared which means that $w = l$ and that they have about the thickness of a regular crystal $t \approx 0.2\ nm$, the resistivity then has to be $\rho = 500\ \mu\Omega\ cm$. In general you can say that materials with resistivities $>\ 1\ m\Omega\ cm$ tend to be a Mott insulator.

Another way to check if you have a Mott insulator is to look at the formula of the conductivity that just depends on the mean free path and the electron density:

$$\sigma = \frac{ne^2 l}{\hbar(3\pi^2 n)^{1/3}}\ . \tag{178}$$

By measuring the conductivity and knowing the electron density you can calculate the mean free path and if it is smaller than the size of an atom the free electron model is wrong and electron-electron interactions need to be considered.

Disorder plays also a role in the Mott transition because it favours the insulating state. As you can see in fig. 80 a linear chain of islands with uniform tunnel barriers below the resistance quantum characterizes a metal. But if there are random tunnel barriers and some of them have resistances above the resistance quantum, the whole section between them form an island. Although these islands are metallic in between those barriers, the Coulomb blockade effect at the barrier forces the material to go into the insulating state.

The Mott transition is also relevant for high-temperature superconductors. They have a conductivity which is 100 times worse than the conductivity of a metal like copper or aluminium but as you cool them down they become superconductors. But if you change the charge doping (oxygen concentration) they

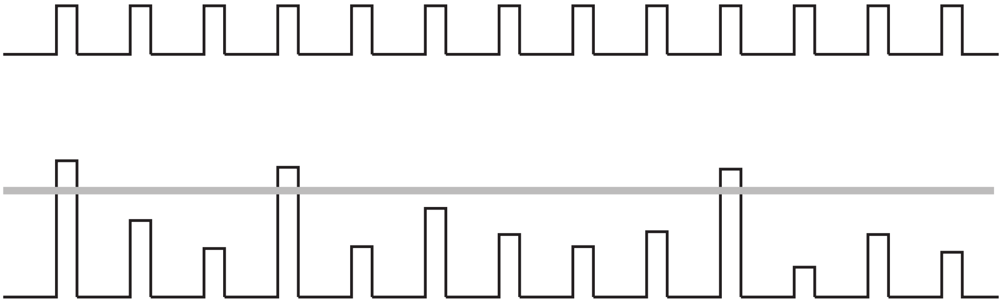

Figure 80: Uniform tunnel barrier;
Random tunnel barriers, some with resistance above the resistance quantum.

make a transition to a Mott insulating anti-ferromagnet. And for a anti-ferromagnet the resistivity goes up as the temperature goes down.

Another example for a Mott insulator is shown in fig. 81. It shows the conductivity of Si doped with P, which is a donor in Si, at low temperature. If the doping is above $\sim 4 \cdot 10^{18}\ cm^{-3}$ it's acting like a metal and it's a so-called degenerate semiconductor but if the doping is below $\sim 4 \cdot 10^{18}\ cm^{-3}$ it acts like an insulator because the donors freeze out. This transition is also a Mott transition.

9.3 Electronic phase transitions

9.3.1 Mott Transition[11]

The simple models that we use to describe metals or semiconductors neglect the electron-electron interactions. And it often happens that materials that supposed to be a metal (based on the independent electron models) are actually insulators. Mott showed that electron-electron interactions can cause an insulating state where electrons can be better described as localized than extended over the whole crystal. The Mott transition is a transition from a metallic to an insulating state that takes place because of the electron-electron interaction. The electron screening is related to the Mott transition. If the screening length is very short, in some sense the electron electron interactions are not that important. But if it is long, the electron-electron interactions become more important. This also means that metals with a low electron density go more likely through a Mott transition than metals with a high electron density.

A simple model to describe a Mott insulator is showed in fig. 82. The material is considered to be consisting of coupled metal crystals connected by tunnel junctions. For strong coupling, if the crystals are close together, the material is a metal. For weak enough coupling the material is an insulator. By changing the tunnel coupling you can go from a metal to an insulator. The tunnel coupling is characterized by a resistance. If crystals are arranged in a two dimensional square array the critical resistance R equals $\hbar/e^2 = 25.5\ k\Omega$. If the resistance of the tunnel coupling is below this value, the material acts like a metal at low temperatures, if it is above, it acts like an insulator (see fig. 83). If the coupling is strong and the material is cooled down the crystals come closer together

---

[11] Nevill Francis Mott won the Nobel prize in physics 1977

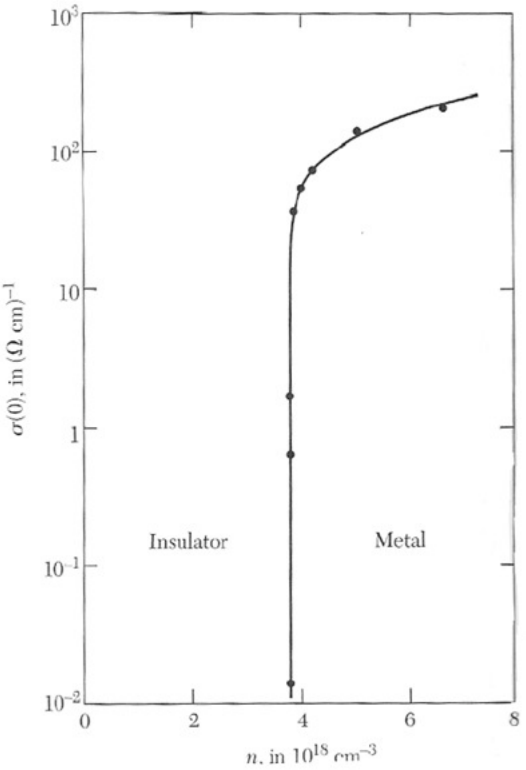

Figure 81: Semiconductor at low temperature: P in Si.

and become one big crystal and the conductivity gets better. If they are weakly coupled the electrons get localized on the crystals as they are cooled down and the material becomes an insulator. In order to understand the Mott transition, we start with the description of a tunnel junction.

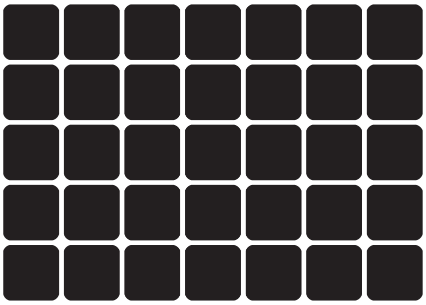

Figure 82: Small crystals as a model to describe a Mott insulator.

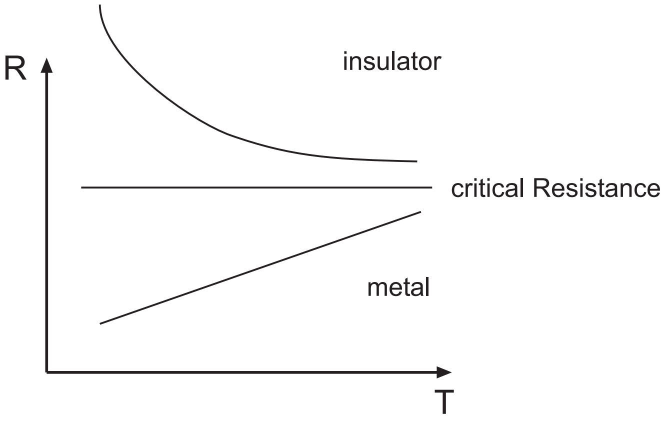

Figure 83: T vs. R;
starting with resistance above the critical resistance - insulator
starting with resistance below the critical resistance - metal.

9.3.2 Peierls Transition

The transition at low temperature from a metal state to an insulator state is called Peierls transition. This Peierls transition gain from an electron-phonon interaction and happens in **quasi-one dimensional metals**. Those materials are three dimensional crystals with a certain chain length structure which have much better conductivity in one direction than in the other one.
One way to understand this theory is to consider a one dimensional lattice of atoms with a lattice constant a as shown in fig. 84 a. Fig. 84 b shows a periodic distortion of this one dimensional lattice with a periodicity of 2 a (new lattice constant). This kind of distortion is called **dimerization**.

If N is the number of atoms per unit cell there are 2 N states in each band:
In a one dimensional conductor it is possible to label the electronic states with **spin** and **k-vector**. Every k state corresponds to a certain translational symmetry. So if there are N atoms in a row with periodic boundary conditions, there are N translational symmetries.

On the one hand every **k** vector corresponds to a symmetry, on the other hand there are 2 values of spin (up and down) for every state, which gives all in all 2 N states for every band. If the crystal is

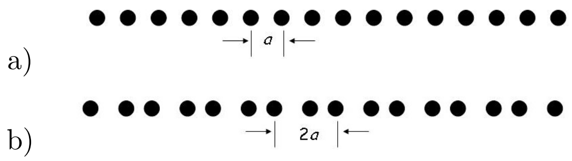

Figure 84: a) One dimensional lattice of atoms with lattice constant a
b) Periodic distortion of a one dimensional lattice with lattice constant 2 a.

getting bigger the number of states in each band does not change because there is an increase of the symmetry and also an increase of the k states so again: 2 N states.

Last but not least it is very important how many atoms are in the unit cell. If there is an even number of atoms, the material will be an insulator or a semiconductor (because there are just filled and empty bands), if there is an odd number of atoms per unit cell, the material will be a metal.

Fig. 85 shows dispersion relations of a material which has one electron per unit cell (band is half filled). The left plot shows a periodic function (one dimensional lattice of atoms), the right plot a periodic distortion. The dispersion relation of the normal periodic function looks like a parabola, the dispersion relation on the right side shows a particular gap at $k = \frac{\pi}{2a}$. The gap arises because the energy on the left side of $k = \frac{\pi}{2a}$ decreases, while the energy on the right side of $k = \frac{\pi}{2a}$ increases (fig. 86).

So all in all for small displacements the system **decreases** the energy because there is an increase of the elastic energy (Δ^2) and a decrease of the electronic energy with Δ. The linear term always wins for small displacements.

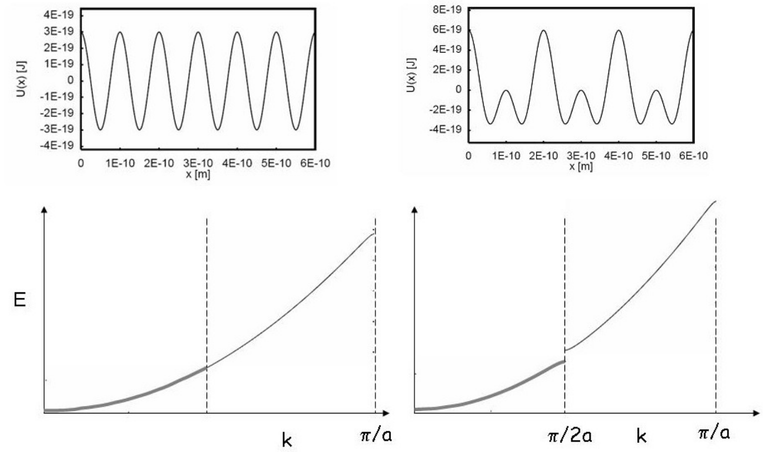

Figure 85: Material with one elctron per unit cell. left: peridoc function, right: periodic distortion of a one dimensional lattice

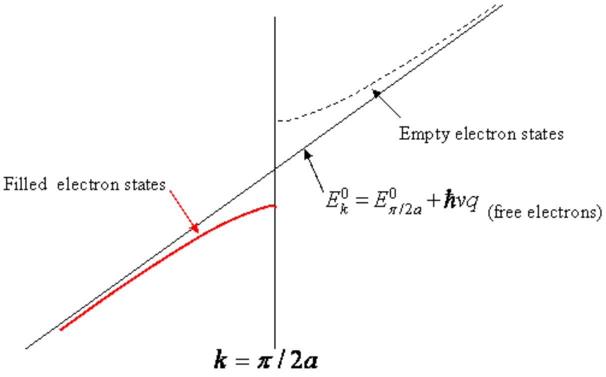

Figure 86: Plot of the band gap at $k = \frac{\pi}{2a}$

One example for a Peierls transition is shown in fig. 87. Due to two different types of bonds (single and double) the lattice is dimerized and as a result a Peierls transition can be observed.

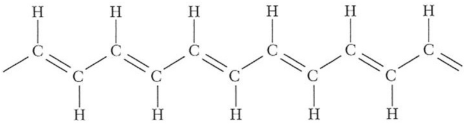

Figure 87: Structure of polyacetylene. The lattice gets dimerized because of the single and double bonds. Furthermore Peierls transition is possible

Another example for a Peierls transition would be $NbSe_3$. This certain crystal is a very good conductor in one direction and because of the Peierls transition it gets an insulator when the system cools down. If the material is an insulator the electron density forms a wave and as a result, dimerized regions can be observed. This wave starts to slide if an electric field affects on the material. Fig. 88 shows the current versus voltage for such a material at low temperatures. At a particular point (high electric field) the current starts to increase, that's the point where the electron density wave starts to slide.

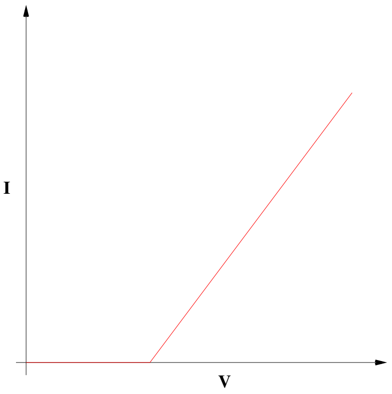

Figure 88: Current flow of $NbSe_3$. If an electric field affects on the material the current increases and the charge density wave starts to slide.

10 Quasiparticles

In many-body quantum mechanics it is convenient to simplify problems because the initial equations may be too difficult to solve. However it is often possible to calculate the groundstate (at zero temperature). In linearizing the underlying equations, neglecting fast osciallating terms,... one can derive a handy theory for low-lying excitations which can be built in the language of second quantization using elementary harmonic oscillators. These quasiparticles will serve as elementary exitations. In this framework it is possible to excite the system to higher energy by adding quanta of quasiparticles. Or to lower its energy by removing these quanta until the groundstate is reached again. Because the concept of quasiparticles is a low energy theory it is not valid for high excitations. For example a crystal in which the ion lattice undergoes tiny vibrations is said to inhibit phonons. For a crystal which gets macroscopically distorted it makes no sense to speak of phonons. By investigating the properties of individual quasiparticles, it is possible to obtain a great deal of information about low-energy systems, including the flow properties and heat capacity. Most many-body systems possess two types of elementary excitations. The first type, the quasiparticles, correspond to single particles whose motions are modified by interactions with the other particles in the system. The second type of excitation corresponds to a collective motion of the system as a whole. These excitations are called collective modes.

10.1 Particle-like quasiparticles

10.1.1 Fermi Liquid Theory

The use of the free electron model is a very successful way to describe metals. With the electron density it is possible to calculate the magnitude of the energy of the electron-electron interaction (calculation of the Coulomb-energy and sum over all local electrons). The only way to solve the Schrödinger equation, is to neglect the electron-electron interactions.

Landau was very concerned about this explanation and tried to find another solution for this problem. He tried to go back and reconstruct the theory with including the electron-electron interaction. He was interested about the proper normal modes of an electron interacting system which he called **quasiparticles**.

One easy example for this would be a system of phonons, in fact, masses which are connected by a spring. If just one of these masses would be pulled to a side, it would oscillate forward and backward with some particular frequency. But if you connect them all together and one of them would be pulled to a side, the energy will spread out and all other masses also will start to oscillate. There won't be a periodic solution for this problem anymore.

A model for a crystal would be a lot of springs which connect all phonons and these phonons will be pulled up and down with a certain $\mathbf{k}$ vector. The solution are modes which are eigenmodes of the system. This model is ideal for phonons because they have a specific wavelength, frequency and energy.

Landau now includes the electron-electron interaction to find the eigenmodes of the system (these eigenmodes are called quasiparticles).

If there are just weak interactions (in border case the electron-electron interaction is zero $\Rightarrow$ free electron model) the free electron model is almost right. So there is a correspondence between the free electrons and the quasiparticles. The number of quasiparticles is the same as the number of the free

electrons. This is also true for phonons:
In a system of N atoms the number of variables which describe the motion is $3N$ (x, y and z components). So there are also $3N$ phonons (there are as many phonons as primitive lattice vectors in the first Brillouin zone). As a result the number of modes for phonons is conserved and furthermore there is also conservation in the electron case. The number of quasiparticles is the same as the number of free electrons. **This quasipartcicles can have the same spin, charge and k vectors as the electrons**.

10.1.2 Polarons

A polaron is the simplest kind of quasiparticle which describes the interaction between electrons and phonons. The combination of the electrons and the screening field around them defines the polaron. In ionic crystals this effect is very important because the Coulomb-interactions between the ions and the electrons are very high. Therefore in covalent crystals this effect just has a small impact because the interactions between neutral atoms and electrons are very weak.

There are two types of polarons. The first one is called **large polaron** and was described by Fröhlich: This polaron looks like an electron which moves through the crystal with a particular effective mass. The electron pushes the negative ions away and pulls on the positive ions (the whole system is still moving). The polarization field is spread out and as a result the energy of the whole system does not change dramatically. The second type are **small polarons** which were described by Holstein. This type is similar to a mott insulator. The electrons get trapped from the ions and at high temperature (thermal activation) the electrons hop from one place to another. At low temperature the electrons are tunneling very slowly through the crystal.

10.1.3 Bipolarons

One way to describe superconductivity is via Bipolarons. Bipolarons consist of two polarons which bind together. The reason is that they reduce the polarization field (sharing of the polarization field). The bipolarons have two electrons with spin $\frac{1}{2}$ but the total spin is integer so they are bosons.

10.1.4 Excitons

An exciton is a bound state of an electron and a hole in a semiconductor or an insulator. The generation of an exciton is comparable to the principle of a solar cell. A photon comes in and creates an electron-hole pair in the pn-junction. These electrons and holes get separated because of an electric field and so an electric current starts to flow. If we just have a pure semiconductor (undoped) there is no field to push the electrons and the holes away from each other, because there is just a coulomb force which holds them together. What happens here, is comparable to the hydrogen atom, where we have a light electron moving around a heavy proton. Here the mass of electrons and holes is almost the same, but not exactly.

We remember that an incoming photon with an energy, which is higher than the band gap, can move an electron to the conduction band and a hole is generated in the valence band. Now we think about

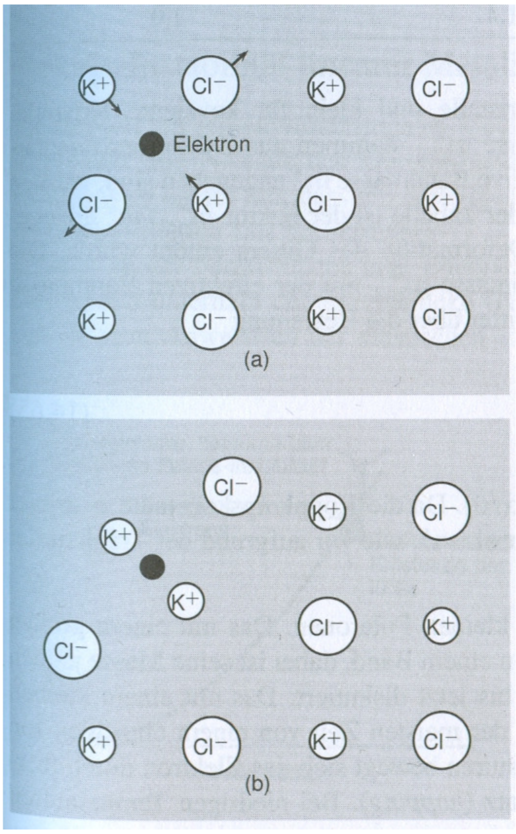

Figure 89: a) electron in ionic crystal (KCL). Forces are symbolized by arrows. b) Electron in a kind of equilibrium. The ions change there position so the effective mass of the electron increases

photons with energies less than the band gap. These are the photons that can create bound electron-hole-pairs. Excitons are not very stable and so they will decay after a little amount of time and a photon is emitted again. Another possibility to loose their energy is to interact with electrons or phonons. This process can be seen in the optical absorption.

Mott Wannier Excitons

There are two types of excitons. One of them is called the Mott Wannier exciton. The important thing about them is that their size is much bigger than the lattice constant.

To calculate the binding energy of excitons we can use the formula of the hydrogenic model with the effective masses of electrons and holes.

$$E_{n,K} = E_g - \frac{\mu^* e^4}{32\pi^2\hbar^2\epsilon^2\epsilon_0^2 n^2} + \underbrace{\frac{\hbar K^2}{2(m_h^* + m_e^*)}}_{\text{kinetic energy}} \tag{179}$$

The quantum number n again defines the energy level and here an additional term appears, which belongs to the kinetic energy of the exciton. When we calculate the energies, we draw them on the same axis as the dispersion relationship with the valence band and the conduction band. The result is, that there are additional states near the conduction band for the excitons, which can be seen in fig. 90.

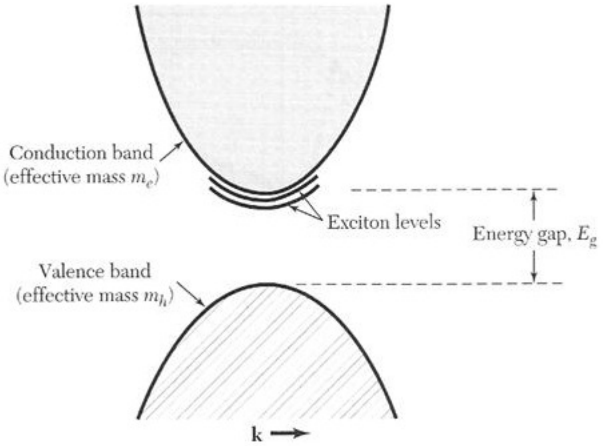

Figure 90: Dispersion relationship for a semiconductor with the energy levels of excitons

The result of an interesting experiment to see excitons is shown in fig. 91. Normally, light should go right through a semiconductor, if the energy is less than the energy gap, so that no electrons are taken from the valence to the conduction band, but in fig. 91 we see a number of absorption peaks. These peaks appear when the incoming photons can excite excitons. Another experiment was done with Gallium Arsenide (GaAs). In fig. 92 we see that the absorption has a peak, when the photon energy is smaller than the energy gap. This happens again because of the excitation of excitons.

The concentration of the created excitons in an insulator depends on the intensity of the incoming light. When we have a look at fig. 93 we see that at low temperatures and low concentrations, which means low intensity of light, a free exciton gas is generated. The material still remains to be an insulator, because excitons are uncharged particles and are uninvolved by an external electric field. When the intensity of light gets bigger, more and more excitons are created and they start to overlap, which has influence on the screening of the electrons (Mott criterion in fig. 93). So there are no more bound states and the result is a gas of unpaired electrons and holes, which means that the insulator becomes a semiconductor.

Frenkel excitons

In contrast to a Mott Wannier exciton, a Frenkel exciton is localized on an atom or molecule in a crystal. For example solid krypton has a band gap of 11.7 eV but the lowest atomic transition in the solid is at 10.17 eV. So it is possible to excite an atom to a higher state without bringing electrons from the valence band to the conduction band. When an exciton is created in an ideal molecular crystal at one site, it can move to another site, because in a perfect crystal all the sites are equivalent. That's the working principle of organic solar cells.

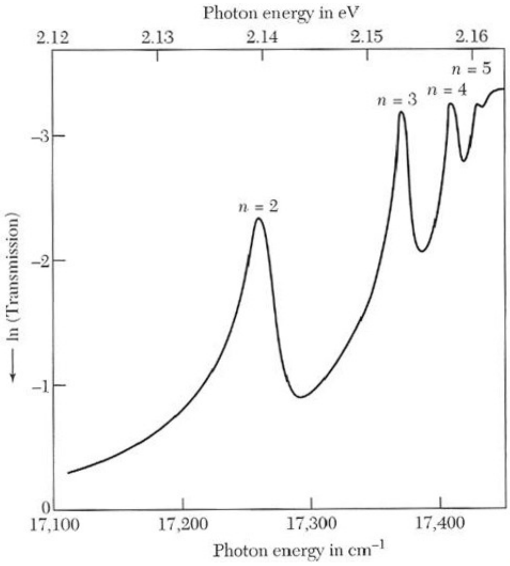

Figure 91: Absorption experiment to show the excitation levels of excitons

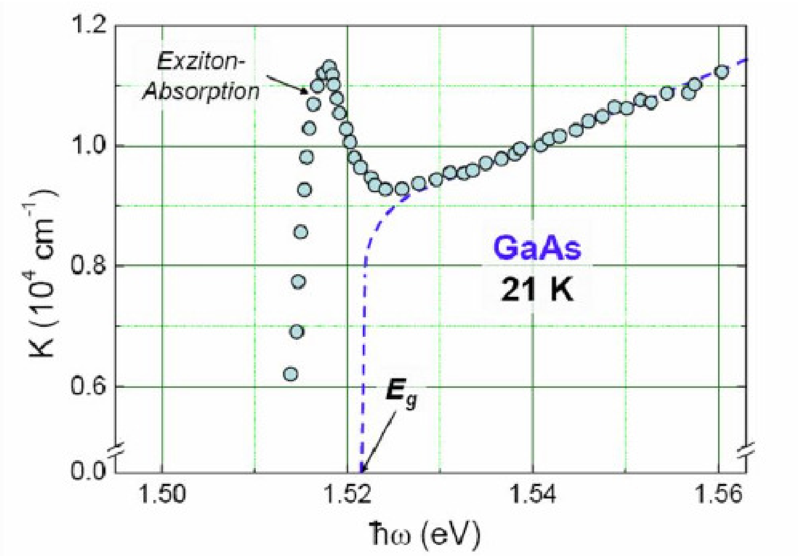

Figure 92: Result of an experiment to show the existence of excitons

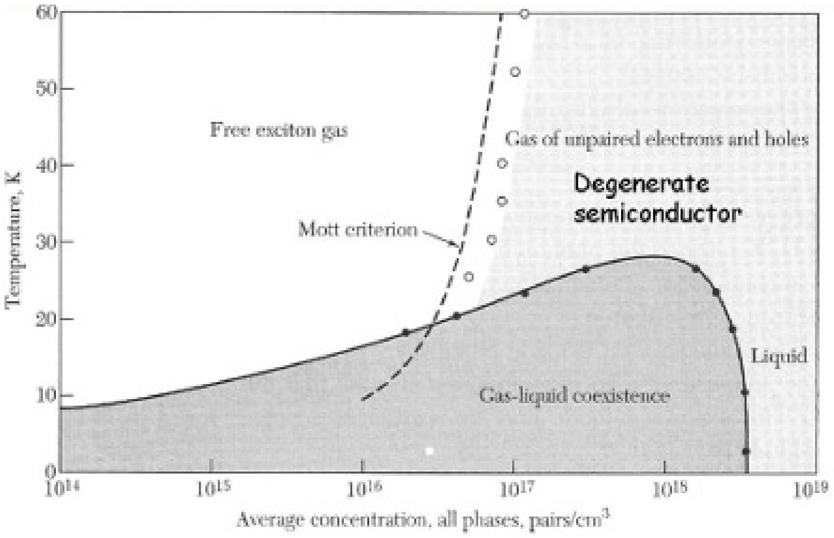

Figure 93: Phase diagram for photoexcited electrons and holes in unstressed silicon

It is possible to describe this movement with a hamiltonian:

$$H\psi_j = E_0\psi_j + t(\psi_{j-1} + \psi_{j+1}) \tag{180}$$

The exciton has an energy at a specific site and there is also some coupling to the neighboring sites. This is the same problem as for a linear chain of phonons, spinons or the tight binding model. The solutions of such problems are plane waves, which should be already known from the tight binding model:

$$\psi_k = \sum_j e^{ijka}\psi_j \tag{181}$$

$$E_k = E_0 + 2t \cdot cos(ka) \tag{182}$$

In fig. 94 we see the energy dependence of the wave vector **k**. Remember that the solution has similarity with the tight binding model beside the sign.

Frenkel excitons occur in organic solar cells, organic light emitting diodes and in photosynthesis. They can transport energy but no charge.

10.2 Collective modes

10.2.1 Phonons

In the long wavelength limit (at low frequencies), sound obeys the wave equation:

$$c^2\nabla^2 u(x,t) = \frac{\partial^2 u(x,t)}{\partial t^2} \tag{183}$$

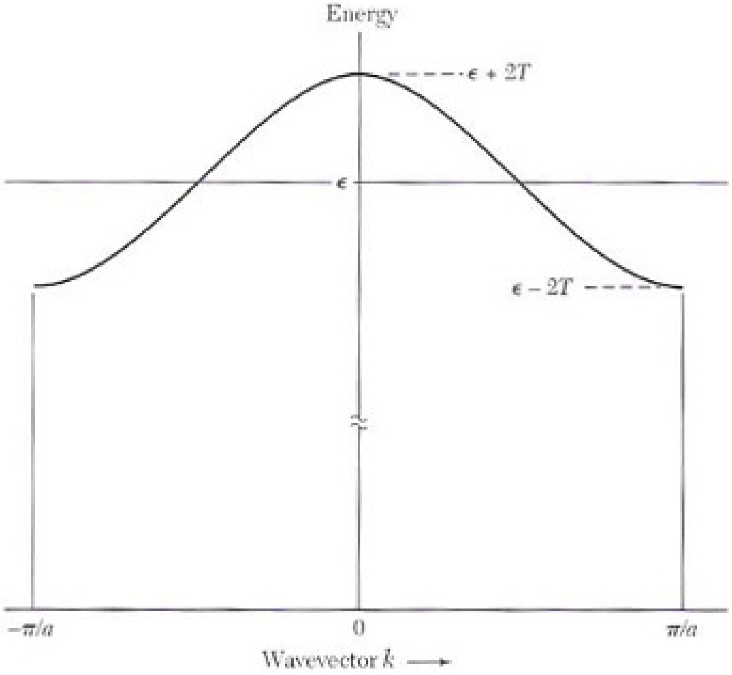

Figure 94: Solution of the energy, when frenkel excitons move through a perfect crystal

By substituting the speed of light with the speed of sound we can make use of all the previously stated formulas with which we computed the properties of photons, to compute the properties of phonons in the long wavelength limit.

Linear Chain

We will now take a closer look at two simple models, the first being the **Linear Chain**. In this model, we have a chain of identical masses, which are connected to their neighbors by a linear force.

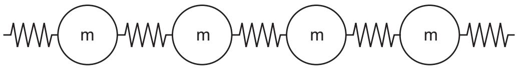

Figure 95: Linear chain of atoms

Thus, **Newtons law** for the s^{th} mass reads as follows:

$$m\frac{\partial^2 u_s(x,t)}{\partial t^2} = C(u_{s+1} - 2u_s + u_{s-1})$$

with a spring constant C and the lattice constant a.
By assuming harmonic solutions like

$$u_s = A_k e^{i(ksa-\omega t)}$$

we obtain the following equation:

$$-\omega^2 m = C(e^{ika} - 2 + e^{-ika})$$

With using the Euler identities this equation simplifies to

$$-\omega^2 m = 2C(1 - cos(ka)).$$

Hence, the solutions for ω are:

$$\omega = \sqrt{\frac{4C}{m}} \left| sin\left(\frac{ka}{2}\right) \right|$$

Now it is possible to draw the **dispersion relation** for this 1-dimensional chain.

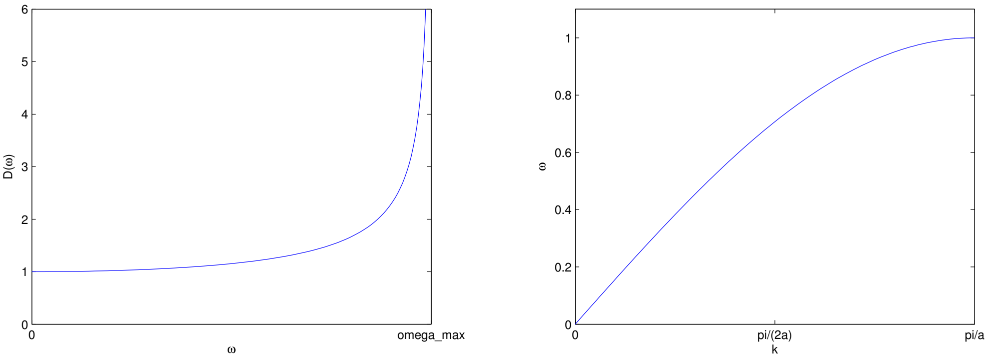

(a) (b)

Figure 96: a) Dispersion relation of a 1-dimensional chain of atoms; b) Density of states for a 1-dimensional chain of atoms

The **Debye-frequency**, which is the highest frequency of the normal mode, can be computed very easily: The shortest wavelength we can create in our chain is $\lambda = 2a$ and k can be expressed like $k = \frac{2\pi}{\lambda}$, so $k_D = \frac{\pi}{a}$. This k_D also gives us the **Brillouin zone boundaries**. It also should be noted, that for phonons, there are as many normal modes as there are degrees of freedom in the crystal, therefore our 1-dimensional chain can only have 1 normal mode.

The **density of states** $D(\omega)$ can be obtained the same way as for photons, by computing $D(\omega) = D(k)\frac{dk}{d\omega}$ which leads us to fig. 96(a).

Chain of two different types of atoms

Now we generalize our assumption a bit, as we take two different masses M_1 and M_2 into account, so every atom of mass M_1, to which we assign the position vectors u_s, is coupled to two atoms of masses M_2 with position vectors v_s and vice versa.

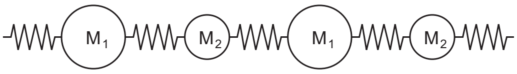

Figure 97: Linear chain of two different types of atoms

Hence, Newton's law has to be altered as follows:

$$M_1 \frac{\partial^2 u_s(x,t)}{\partial t^2} = C(v_{s-1} - 2u_s + v_s)$$

$$M_2 \frac{\partial^2 v_s(x,t)}{\partial t^2} = C(u_s - 2v_s + u_{s+1})$$

As before, we assume harmonic solutions for u_s and v_s

$$u_s = ue^{i(ksa-\omega t)}$$

$$v_s = ve^{i(ksa-\omega t)}$$

to obtain the equations:

$$-\omega^2 M_1 u = C(v(1+e^{-ika}) - 2u)$$

$$-\omega^2 M_2 v = C(u(1+e^{ika}) - 2v)$$

These equations can be written in a matrix

$$\begin{pmatrix} \omega^2 M_1 - 2C & C(1+e^{-ika}) \\ C(1+e^{ika}) & \omega^2 M_1 - 2C \end{pmatrix} \begin{pmatrix} u \\ v \end{pmatrix} = \mathbf{0}$$

In order for this equation to be true, the determinant of the matrix has to vanish, which leads to the following equation (once again the Euler identities were used):

$$M_1 M_2 \omega^4 - 2C(M_1 + M_2)\omega^2 + 2C^2(1 - cos(ka)) = 0$$

And for ω the following equation must hold:

$$\omega^2 = C\left(\frac{1}{M_1} + \frac{1}{M_2}\right) \pm C\sqrt{\left(\frac{1}{M_1} + \frac{1}{M_2}\right)^2 - \frac{4\sin^2(ka)}{M_1 M_2}} = 0$$

As one can see in fig. 98(a), there are two solutions for ω^2 and therefore also two branches if we plot $\sqrt{2C\left(\frac{1}{M_1} + \frac{1}{M_2}\right)}$, an optical and an acoustical branch (without loss of generality we assumed $M_1 > M_2$).

The density of states for this chain can be seen in fig. 98(b). If both masses are the same, we have the same case as in fig. 96(a), where the optical branch vanishes and the Brillouin zone boundaries are at $\frac{\pi}{a}$ (a is the distance between two atoms). However, if the masses are only slightly different, the Brillouin zone gets smaller ($\frac{\pi}{2a}$), because the lattice constant is now $2a$ instead of a. The dispersion relation now looks like as shown in fig. 99, because the branches from the neighboring zones reach in and there is an optical branch once more.

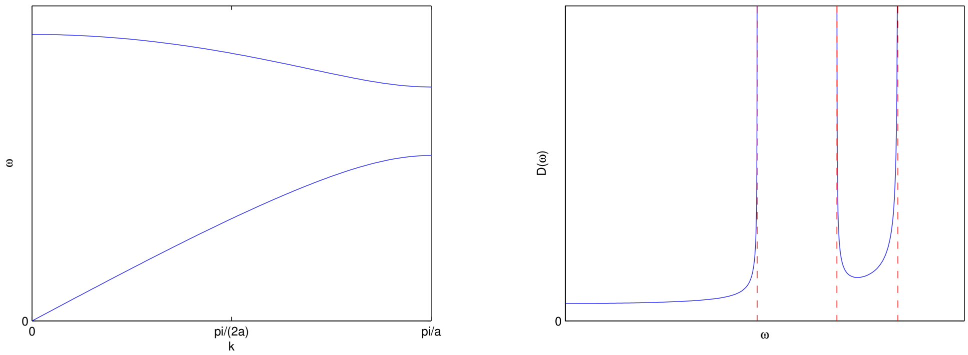

(a) (b)

Figure 98: a) Density of states for a 1-dimensional chain of two different types of atoms; b) Dispersion relation of a 1-dimensional chain of two different types of atoms

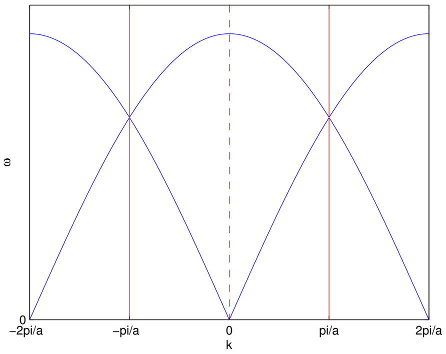

Figure 99: Dispersion relation of a 1-dimensional chain of two different types of atoms with similar masses

10.2.2 Polaritons

A polariton is a combined wave between light and sound. In fig. 100(a) the photon dispersion is drawn into a plot of the phonon dispersion. As you can see, the photon dispersion crosses the optical phonon branch close to $k = 0$. At this point photons and phonons have the same wavelength and frequency and thus the same energy. At this point, the optical phonons will couple to the photons and this coupling is described by a polariton. Polaritons can only occur in materials where there more than two atoms per unit cell, otherwise there would not be any optical phonons!

We will start the calculation to couple light and sound with Maxwell's equation for light propagating in a medium:

$$\nabla^2 E = \mu_0 \frac{\delta^2 D}{\delta t^2}, \tag{184}$$

assuming a plane wave we get

$$k^2 E = \mu_0 \omega^2 (\varepsilon_0 E + P) \ . \tag{185}$$

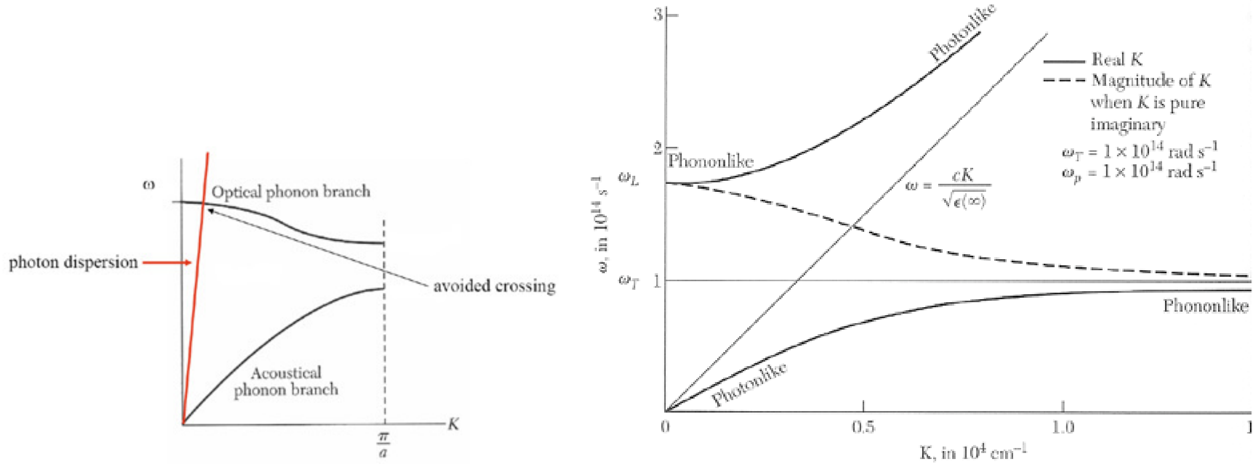

(a) (b)

Figure 100: a) Phonon dispersion and photon dispersion; b) Dispersion relationship of polaritons.

The photon dispersion can also be written as

$$k^2 = \mu_0 \varepsilon_0 \varepsilon(\omega)\omega^2 \ . \tag{186}$$

Now we need to describe the motion of the atoms. We think of the atoms as masses connected by springs but the atoms also have a charge that reacts to an electric field so Newton's law for the atoms is

$$m\frac{d^2x}{dt^2} = -eE - CX \ . \tag{187}$$

Around the crossing point the dispersion of the optical phonons is very flat and we can assume that the transverse optical phonons have the frequency

$$\omega_T = \sqrt{\frac{C}{m}} \ . \tag{188}$$

We solved the differential equation for the position of the atoms but the position is related to the polarization like this:

$$P = -Nex \tag{189}$$

If we solve this equation for x and plug it into eqn. (187) we get

$$\frac{\omega^2 mP}{Ne} = -eE + \frac{m\omega_T^2 P}{Ne} \tag{190}$$

$$-\omega^2 P + \omega_T P = \frac{Ne^2 E}{m} \tag{191}$$

With eqn. (185) and eqn. (191) we have two equations for the relation between the electric field and the polarization. (The electric field of the light wave is coupled to the polarization of the atoms.) We can solve this system of equations by calculating

$$\begin{vmatrix} \mu_0\varepsilon_0\omega^2 - k^2 & \mu_0\omega^2 \\ Ne^2 \ / \ m & \omega^2 - \omega_T^2 \end{vmatrix} = 0 \ , \tag{192}$$

which gives us a new dispersion relationship between k and ω that is shown in fig. 100(b). There are two solutions for every k, one for the upper branch and one for the lower branch. In the frequency range between ω_T and ω_L there are no waves at all allowed in the crystal. This means that light Bragg reflects off the sound wave and sound Bragg reflects off the light wave.

In fig. 101 you can see the reflectance of NaCl. At the frequency range of the gap in the polariton dispersion relationship the reflectance of NaCl is very high as expected. The dielectric constant as a function of ω now looks like

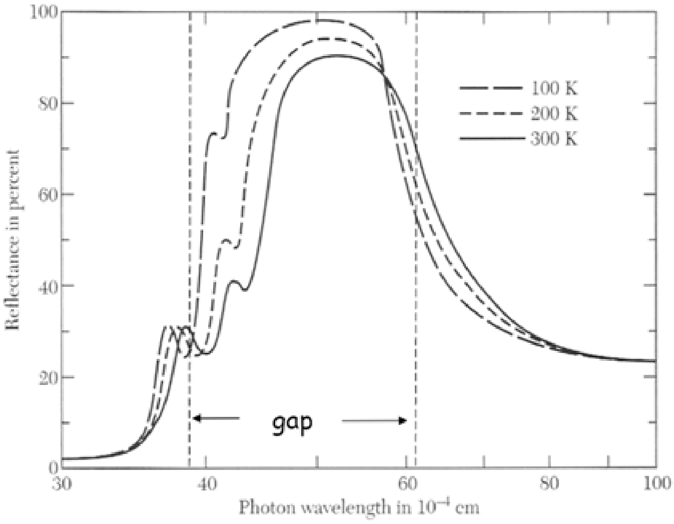

Figure 101: Reflectance of NaCl; gap = frequency gap of polaritons.

$$\varepsilon(\omega) = 1 + \frac{P}{\varepsilon_0 E} = 1 + \frac{Ne^2}{m(\omega_T^2 - \omega^2)} = \frac{\omega_T^2\varepsilon(0) - \omega^2\varepsilon(\text{inf})}{\omega_T^2 - \omega^2} \tag{193}$$

and at $\omega = \omega_T$ there is divergence as you can see in fig. 102. Therefore there is a region where the dielectric constant is negative which means that the wave vector k becomes imaginary. This indicates that waves decay exponentially and are reflected out of the material. So the region where $\varepsilon < 0$ corresponds to the frequency gap of the polaritons.

10.2.3 Magnons

Magnons are the low lying excitations of the ordered ferro- (or antiferro) magnetic state. The groundstate (zero temperature) of a ferromagnetic linear chain is visualized in figure 103 (a). Let us calculate the exchange energy in the Heisenberg model

$$\hat{H}_{exc} = -2J \sum_{k=1}^{N-1} \hat{\vec{S}}_k \cdot \hat{\vec{S}}_{k+1} \tag{194}$$

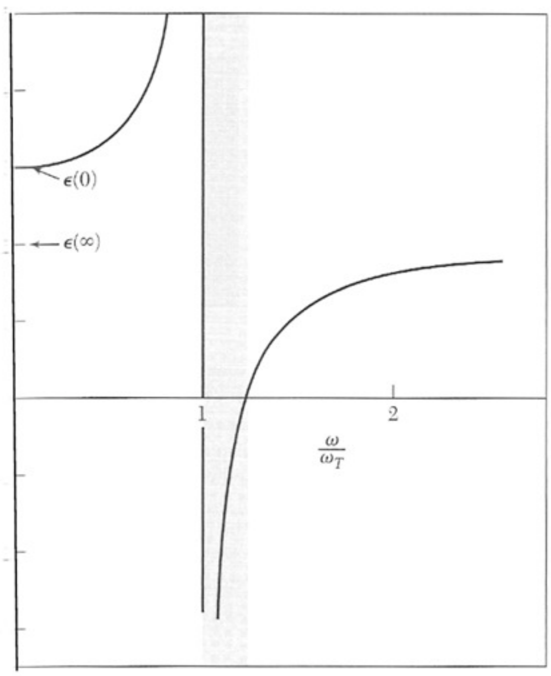

Figure 102: Dielectric constant as a function of $\frac{\omega}{\omega_T}$.

. Calculating the expectation value of this operator in the ground state of the linear spin chain

$$E_0 =< 0|\hat{H}_{exc}|0 > \text{, where } |0 >= |11...1 > \tag{195}$$

one arrives at

$$E_0 =< 0|\hat{H}_{exc}|0 >= -2JNS^2 \tag{196}$$

$\hbar$ was neglected here and also the fact that there are really N-1 interactions instead of N, the spin expectation value was calculated classically so $\sqrt{S(S+1)}$ is just S. Knowing the ground state energy E_0 we can ask the question what does an elementary excited state look like and what is its energy. For example we may be tempted to try a single spin flip like in figure 103 (b). Calculating its energy we see that two terms of equation 194 are affected. Their new energy is $+4JS^2$ while their old energy was $-4JS^2$. So we end up with a total energy increase of

$$E_1 = E_0 + 8JS^2 = -2JNS^2 + 8JS^2 \tag{197}$$

. There are excitations which have a much lower energy like the one drawn in figure 103 (c). Such an excited state may have an energy of the order of

$$E_1 \quad \propto \quad E_0 + (n_k + \frac{1}{2}) \cdot \hbar(2JSa^2)k^2, \text{ where } k <\approx \frac{\pi}{8a} \tag{198}$$

$$<\approx \quad E_0 + n_k \cdot \frac{JS^2}{4} \tag{199}$$

as we shall see later on.

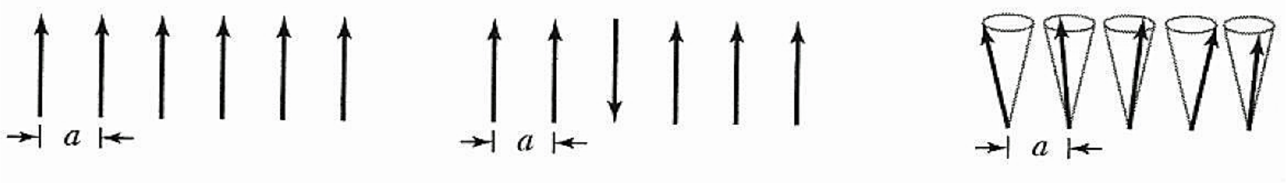

Figure 103: (a) Ground state of a linear ferromagnetic chain at zero temperature, (b) excited state where one spin is flipped, (c) excite state where the spin flip is equally distributet among all available spins resulting in a spin wave. [from Kittel]

To calculate the dispersion relation for Magnons we examine the k^{th} spin in equation 194

$$U_k = -2J\vec{S}_k \cdot (\vec{S}_{k-1} + \vec{S}_{k+1}) \tag{200}$$

. Inserting the relation between magnetic moment and spin $\vec{\mu} = \gamma\vec{S} = -g\mu_B\vec{S}$ into this relation we obtain

$$U_k = -\vec{\mu_k} \cdot (\frac{-2J}{g\mu_B}(\vec{S}_{k-1} + \vec{S}_{k+1})) \tag{201}$$

. Because the potential energy of a magnetic dipole is $U = -\vec{\mu} \cdot \vec{B}$ we may interpret

$$\vec{B}_k = \frac{-2J}{g\mu_B}(\vec{S}_{k-1} + \vec{S}_{k+1}) \tag{202}$$

as the effective magnetic field on spin k due to the nearest neighbors. The rate of change of angular momentum is the torque $\vec{T} = \frac{d\vec{S}}{dt} = \vec{\mu} \times \vec{B}$. Using the torque we set up equations of motion for the spin

$$\begin{aligned} \frac{d}{dt}\vec{S}_k &= \frac{-g\mu_B}{\hbar}\vec{S}_k \times \vec{B}_k & (203) \\ &= \frac{2J}{\hbar}(\vec{S}_k \times \vec{S}_{k-1} + \vec{S}_k \times \vec{S}_{k+1}) & (204) \end{aligned}$$

. The cartesian components of this relation are

$$\begin{aligned} \frac{d}{dt}\vec{S}_k^x &= \frac{2J}{\hbar}(S_k^y(S_{k-1}^z + S_{k+1}^z) - S_k^z(S_{k-1}^y + S_{k+1}^y)) & (205) \\ \frac{d}{dt}\vec{S}_k^y &= \frac{2J}{\hbar}(S_k^z(S_{k-1}^x + S_{k+1}^x) - S_k^x(S_{k-1}^z + S_{k+1}^z)) & (206) \\ \frac{d}{dt}\vec{S}_k^z &= \frac{2J}{\hbar}(S_k^x(S_{k-1}^y + S_{k+1}^y) - S_k^y(S_{k-1}^x + S_{k+1}^x)) & (207) \end{aligned}$$

. One way to solve these nonlinear set of equations it is to linearize them. This is valid in the low energy limit since we already know that low-lying excitations have a form of 103 (c) and therefore

$S^x, S^y << S^z$. It is now reasonable to neglect product terms of S^xS^x, S^yS^y and S^xS^y renaming S^z to S. This results in the linearized system valid in the low energy limit

$$\begin{aligned}\frac{d}{dt}\vec{S}_k^x &= \frac{2J}{\hbar}S(2S_k^y - S_{k-1}^y + -S_{k+1}^y) && (208)\\ \frac{d}{dt}\vec{S}_k^y &= -\frac{2J}{\hbar}S(2S_k^x - S_{k-1}^x + -S_{k+1}^x) && (209)\\ \frac{d}{dt}\vec{S}_k^z &= 0 && (210)\end{aligned}$$

. To solve this system we use plane wave solutions

$$\begin{aligned}S_p^x &= x_0 e^{i(pka-\omega t)} && (211)\\ S_p^y &= y_0 e^{i(pka-\omega t)} && (212)\end{aligned}$$

where p is a natural number and a is the lattice constant. Plugging in, the resulting equations are

$$\begin{aligned}-i\omega x_0 &= \frac{2JS}{\hbar}(2-e^{-ika}-e^{ika})y_0 = \frac{4JS}{\hbar}(1-cos(ka))y_0 && (213)\\ -i\omega y_0 &= -\frac{2JS}{\hbar}(2-e^{-ika}-e^{ika})x_0 = -\frac{4JS}{\hbar}(1-cos(ka))x_0 && (214)\end{aligned}$$

. The solution to this set of equations (setting the determinant to zero) is

$$\omega = \frac{4JS}{\hbar}(1-cos(ka)) \qquad (215)$$

which is the magnon dispersion relation in one dimension considering only nearest neighbor interaction. The eigenfunctions for the S components take the form

$$\begin{aligned}S_p^x &= \xi cos(pka-\omega t) && (216)\\ S_p^y &= \xi sin(pka-\omega t) && (217)\\ S_p^z &= \eta && (218)\end{aligned}$$

which is a spin precession around the z axis. Expanding the cosine in the dispersion relation one gets a $E \propto k^2$ behaveiour for long wavelengths (see figure 104).

To take a look at the thermal properties of such a system we consider the overall number of magnons which are excited at temperature T

$$N_{exc} = \sum_k n_k = \int_{1.BZ} D(\omega) < n(\omega) > \, d\omega \qquad (219)$$

where $< n(\omega) >$ is the Bose-Einstein statistics

$$< n(\omega) > = \frac{1}{e^{\frac{\hbar\omega}{k_B T}} - 1} \qquad (220)$$

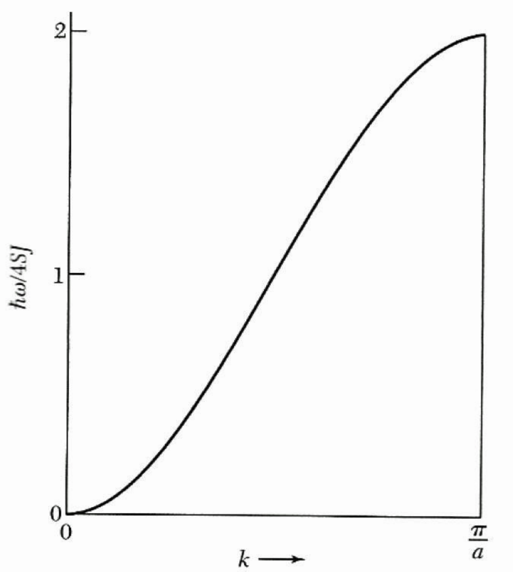

Figure 104: Magnon dispersion relation (1 dimensional, for nearest neighbor interaction). The slope for long wavelengths is proportional to k^2. [from Kittel]

. And the density of states in three dimensions $D(\omega)$ is

$$D(\omega)d\omega = \frac{1}{(2\pi)^3}4\pi k^2\frac{dk}{d\omega}d\omega \tag{221}$$

$$= \frac{1}{(2\pi)^3}4\pi k^2(2\sqrt{\omega}\cdot\sqrt{\frac{3JSa^2}{\hbar}})d\omega \tag{222}$$

$$= \frac{1}{4\pi^2}(\frac{\hbar}{2JSa^2})^{\frac{3}{2}}\sqrt{\omega} \tag{223}$$

where we used the dispersion relation $\omega \propto k^2$ obtained obove. Plugging these into the integral 219 we find for the total amount of magnons

$$N_{exc} = 0.0587\frac{k_B T}{2JSa^2}^{\frac{3}{2}} \tag{224}$$

Therefore the relative change in magnetization $\frac{\Delta M}{M(0)}$ is proportional to $T^{\frac{3}{2}}$.

10.2.4 Plasmons

Suppose you have some metal where you have a uniform distribution of the positive ions and a uniform distribution of the negative electrons as seen in fig. 105. We assume that the electrons are much lighter than the ions so that the ions don't move and are fixed. But the electrons can move. So if you pull them off to a side they are not uniformly distributed anymore but the ions still are. This causes a force on the electrons and if you let them go they will start to oscillate back and forth (the oscillation will of course decay after a certain time). These oscillations are called plasma oscillations, because they

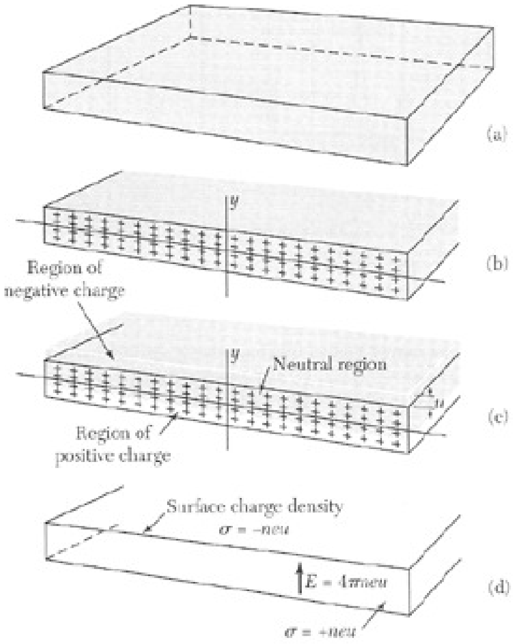

Figure 105: Charge density in a metal

are also seen in plasma. Plasma is a gas of positive and negative charges. If you move the electrons in the x-direction, the resulting force is the electric field that is caused by the protons. So Newton's law for a bunch of electrons in an electric field is

$$nm\frac{d^2x}{dt^2} = -neE \tag{225}$$

where the electric field E is determined by the following equation (out of Gauss law: $\nabla \cdot \mathbf{E} = \frac{\rho}{\epsilon_0}$, $\rho = ne$):

$$E = \frac{nex}{\epsilon_0}\ , \tag{226}$$

with n as the electron density. Now we plug eqn. (226) in eqn. (225) and we get a differential equation that just depends on x.

$$nm\frac{d^2x}{dt^2} = -\frac{n^2e^2x}{\epsilon_0} \tag{227}$$

$$\frac{d^2x}{dt^2} + \omega_p^2 x = 0 \tag{228}$$

The solution of this differential equation is the same like for a harmonic oscillator. The frequency ω_p is called Plasma frequency and it's defined by

$$\omega_p = \sqrt{\frac{ne^2}{m\epsilon_0}}\ . \tag{229}$$

For most metals this plasma frequency is up in the ultraviolet which means that in the visible spectrum they look shiny but in a frequency range above ω_p they are transparent (see chapter 7). Plasma waves can be quantized like any other waves and there is a quantum that equals $\hbar\omega_p$. This quantum is called plasmon, it describes oscillations of charges and can be measured with electron energy loss spectroscopy. Fig. 106 shows the results of an EELS measurement. The peaks correspond to plasma waves with a certain frequency and the spacing between the peaks is the quantum $\hbar\omega_p$. But there is a smaller second peak which is caused by surface plasmons whereas the dominant peak comes from the bulk plasmons.

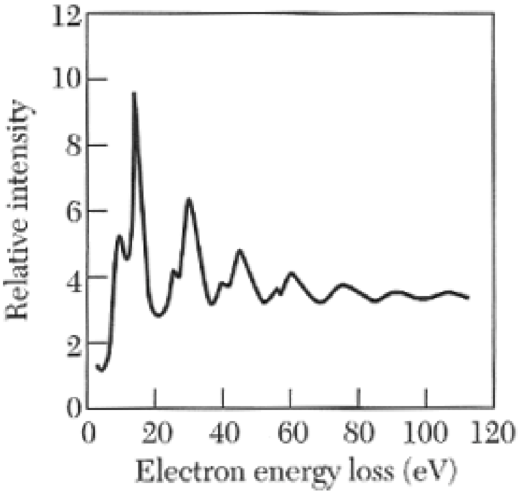

Figure 106: Results of an EELS measurement

10.2.5 Surface Plasmons

The charge could be non-uniform at the surface and electric fields then penetrate into the vacuum. In general, surface plasmons are waves in the electron density at the boundary of two materials.

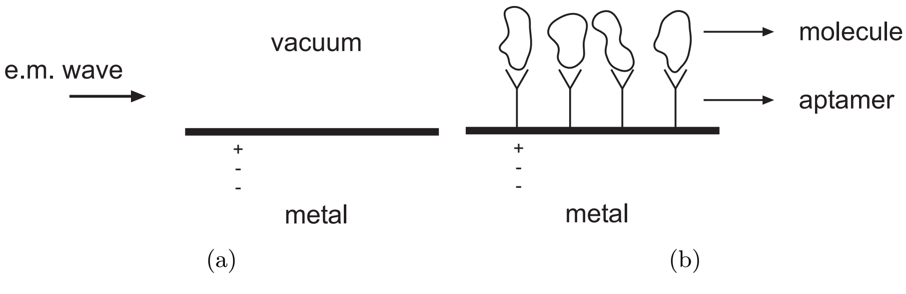

Figure 107: a) Surface plasmons; b) Biosensor.

Specifically, waves that propagate along the surface of a metal are a combination of a charge wave in the metal and an electromagnetic wave in the vacuum above (see fig. 107(a)). Due to that combination the surface plasmons tend to have a different (lower) frequency than the bulk plasmons. For example, this is used in stained glass[12]. In order to make red glass, gold particles are added during the production process. The surface plasma waves of these gold particles are down in the red so they have the right frequency to scatter red light and make the glass look red.

Surface plasmons are also used for biosensors. E.g. an organic light emitting diode is put on a gold layer and it emits light that excites surface plasmons on the gold structure. On this gold layer there are aptamers. Aptamers are molecules that stick with one side to a metal and with the other side to some chemical or biological material. If molecules are attached to the aptamers (see fig. 107(b)), the dielectric constant right at the interface changes and therefore the wavelength of the surface plasmons changes too (the frequency is bound to the OLED). This change can be detected.

10.3 Annotation: Translational Symmetry

Quasiparticles can be labeled with the symmetry label k. The translation operator T shifts a function one period (a...lattice constant):

$$Tf(x) = f(x+a) \tag{230}$$

Solutions of Bloch form are eigenfunctions of the translation operator.

$$\psi_k(x) \;=\; e^{ikx}u_k \tag{231}$$

$\Longrightarrow$

$$T\psi_k(x) \;=\; e^{ik(x+a)}u_k(x+a) \;=\; e^{ikx}e^{ika}u_k(x) \;=\; e^{ika}\psi_k(x) \tag{232}$$

u_k is a periodic function so $u_k(x) \;=\; u_k(x+a)$. It is easy to see that e^{ika} is the eigenvalue of the translation opertator.
The solution depends only on k (because a is always the same) so the labeling of the states happens only in terms of k.
The translation operator commutes with the Hamiltonian even when the interaction, the symmetry of the crystal, is the same. As a result it is possible to diagonalize the eigenfunctions of the Hamiltonian and the translation operator. Furthermore if you know the k you can also specify the eigenstates of the energy. So the **quantum numbers which are used, come from the symmetry** (e.g. Hydrogen atom).
Very important is that there isn't a good correspondence between the k and the momentum anymore, cause they don't describe the same.
One example of a quasiparticle system would be plasmons. Plasmons are oscillating electric charges which build a slow wave. In fact there are millions or billions of electrons which are involved in this wave, but (!) it's still a quasiparticle system with a specific k vector because millions of electrons making an interaction electron system.

---

[12] Buntglas

10.4 Experimental techniques

10.4.1 Raman spectroscopy

The principle of Raman spectroscopy is the inelastic scattering of light. Normally it is done with visible or infrared light. If the light is shined on the sample most of the light is scattered elastically, which means that the frequency and wavelength of the outgoing beam is the same as for the incoming beam. Some of the light is scattered inelastically, so a part of the energy is given to a phonon, a plasmon, a magnon, a polariton or to an exciton. Because of the conservation of charge, it is not allowed to emit an electron or a polaron. The outgoing light will have a lower frequency and a longer wavelength and this is called a stokes process in Raman spectroscopy. It could also happen that the incoming light absorbs a phonon or something like that and so the outcoming light has a higher frequency and a lower wavelength. This is called an anti-stokes process. This two situations are shown in fig. 108.

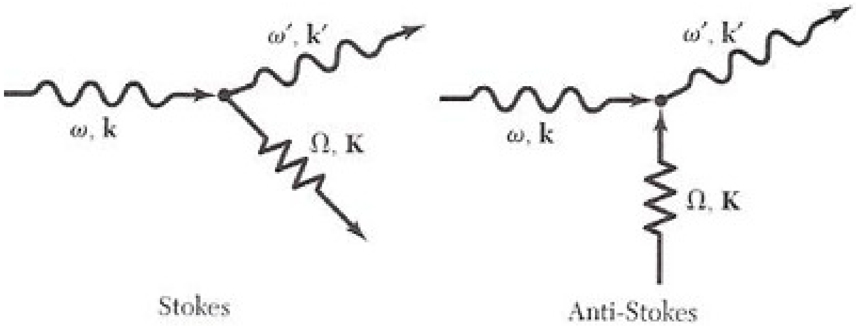

Figure 108: Stokes and anti-stokes process of Raman spectroscopy

The equations for the conservation of energy and momentum are:

$$\omega = \omega' \pm \Omega \tag{233}$$
$$\mathbf{k} = \mathbf{k}' \pm \mathbf{K} \pm \mathbf{G} \tag{234}$$

In the equation of the momentum conservation an additional term appears, which is a reciprocal lattice vector $\mathbf{G}$. Whenever a collision like this happens in a crystal, the crystal can give or absorb momentum with the reciprocal lattice vector, which is discrete.

Now we think of the problem in terms of waves and not particles. We start with a susceptibility that is constant over the time. The $\Delta\chi$ in fig. 109 stands for any kind of wave which comes along the crystal. For example, the wave belongs to a phonon, so the structure gets stretched locally and this has influence on the susceptibility and it gets modulated by the frequency of the phonon wave.

Mathematically this can be explained by an oscillating term in the formula of χ in eqn. (235). The result is that the polarization doesn't oscillate only with the frequency of the incoming light, but also

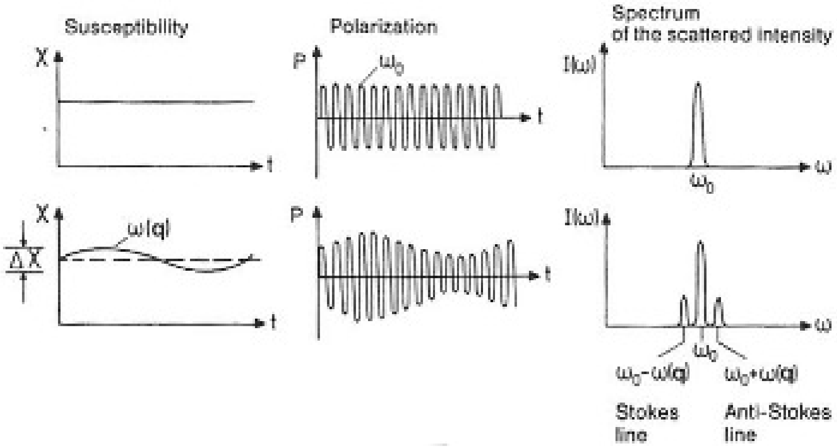

Figure 109: Modulation of susceptibility and the effect to the spectrum of the scattered intensity

with the additional term of the phonon wave. Some of the scattered phonons are forbidden by crystal symmetry and in this case, there are no peaks captured by the Raman spectroscopy.

$$\chi = \chi_0 + \frac{\partial \chi}{\partial X} X \cos(\Omega t) \tag{235}$$

$$\mathbf{P} = \epsilon_0 \chi \mathbf{E} \cos(\omega t) + \epsilon_0 \frac{\partial \chi}{\partial X} X \cos(\Omega t) \mathbf{E} \cos(\omega t) \tag{236}$$

In fig. 109 the stokes and anti-stokes peaks could be seen in the intensity-over-ω diagram. An interesting fact is, that the peaks of the stokes and anti-stokes process do not have exactly the same height. This has to do with the probability that a phonon would be absorbed or emitted. Equations (237) and (238) show the intensity of the peak in dependence of the number n_k of phonons in the state k.

$$\text{Stokes: } I(\omega - \Omega) \propto n_k + 1 \tag{237}$$

$$\text{Anti-Stokes: } I(\omega + \Omega) \propto n_k \tag{238}$$

If the temperature gets smaller, the ratio between the intensity of the stokes and anti-stokes peaks gets bigger and it is possible to calculate the probability that the state is occupied. The ratio of the heights at different temperatures can be seen in fig. 110.

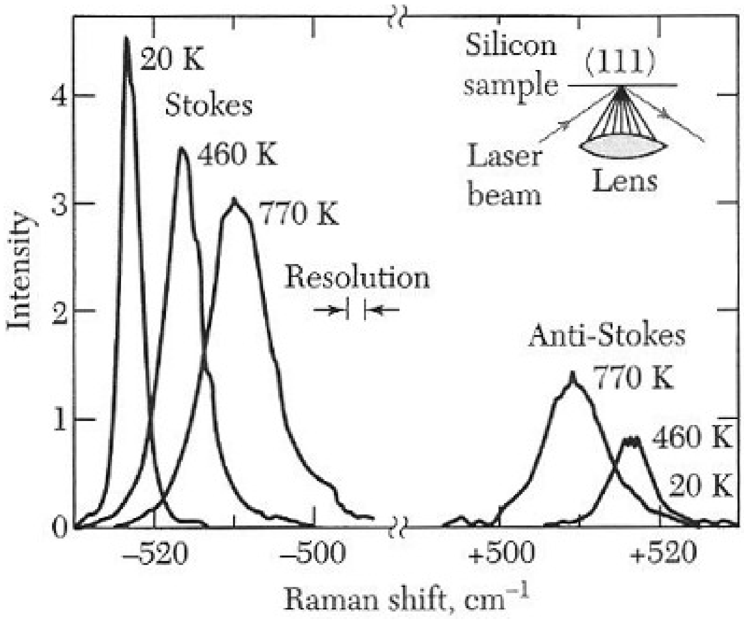

Figure 110: Different heights of stokes and anti-stokes peaks depending on the temperature

10.4.2 Ellipsometry (incomplete)

The incoming light gets polarized and the polarization of the outgoing light is measured. This is done for many different polarizations of the incoming light, so that one can get an impression of the dependence of the polarizations of the two light beams. The measured signal gives a lot of information about the thickness and the dielectric constant of the involved layers. For this technique to work, it is important that there are well defined homogenous layers in the crystal, so that one would be able to know of which layers the peaks are coming from. So ellipsometry is very surface sensitive because the light gets only a few atomic layers into the crystal before it will be sent out again.

The advantage of ellipsometry is that the ratio of the polarizations is independent of fluctuations of the air or of the light source.

10.4.3 EELS (missing)

10.4.4 Reflection electron energy loss spectroscopy

Instead of sending light to the crystal, electrons are used as incoming beam and the scattered electrons are measured. The fast moving electrons are creating a time dependent electric field and this field polarizes the material. The oscillating dipoles of the polarized sample are sending out radiation. If the polarization of the material moves out of phase with the electric field of the electrons, energy will be lost. This means that the energy of the reflected electrons must be less than the energy of the incoming ones. It is possible to calculate the dielectric constant with the informations collected by this experiment.

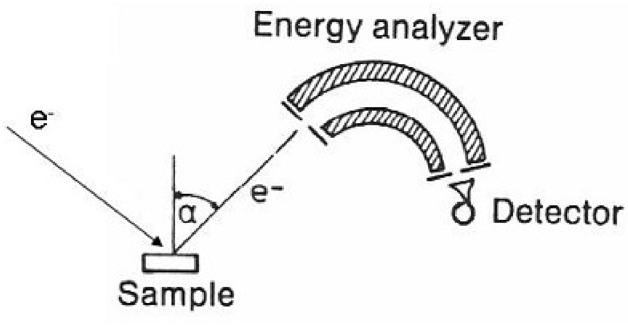

Figure 111: Principle of reflection electron energy loss spectroscopy

10.4.5 Photo emission spectroscopy

At this type of spectroscopy photons with high energy are shot against the sample and electrons are knocked out. When this is done with ultraviolet light, it is called UPS (ultraviolet photoemission spectroscopy). If x-rays are used as radiation source it is called XPS (x-ray photoemission spectroscopy). The amount of electrons at a certain energy gives information about the density of states of the material. As we already know, there are occupied states in the atom up to the fermi level. The incoming photon can hit an electron and puts it from the bounded level to the vacuum level. So the pattern which comes out of the energy analyzer is the same as the pattern of the density of states. Fig. 113 shows the measurement for silver and we can see that there are no occupied states after the fermi level.

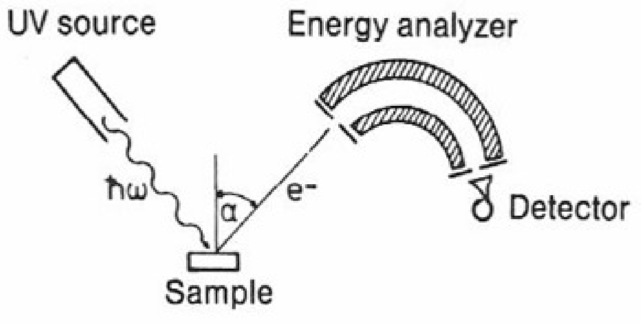

Figure 112: The principle of XPS and UPS

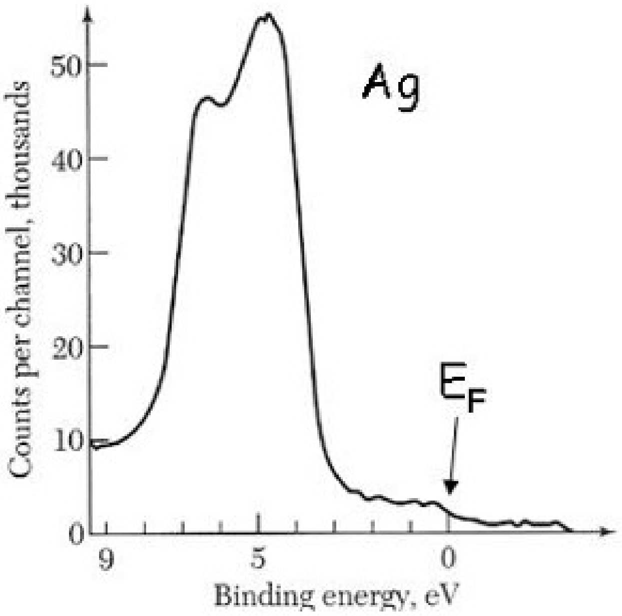

Figure 113: Photoemission spectroscopy for silver

10.4.6 ARPES

The ARPES (angle resolved photo emission spectroscopy) is an experimental method to get the dispersion relationship, which is needed to start the calculations. Here a photon (x-rays (XPS) or ultraviolet light (UPS)) comes in, hits the sample and shoots out an electron. An electron analyser finds out the energy of the electron. This is done just for a specific angle (angle resolved). The k-vector of the incoming photon and the k-vector of the outgoing electron are known, also the energy of the electron. From the variation of the energy of the incoming photon the dispersion relationship can be found. The idea is that you have a density of states and the incoming photons shift the whole thing up to free electrons. In the following figures 114 and 115 the principle of the arpes is shown.

10.4.7 IPES (missing)

10.4.8 KRIPES (missing)

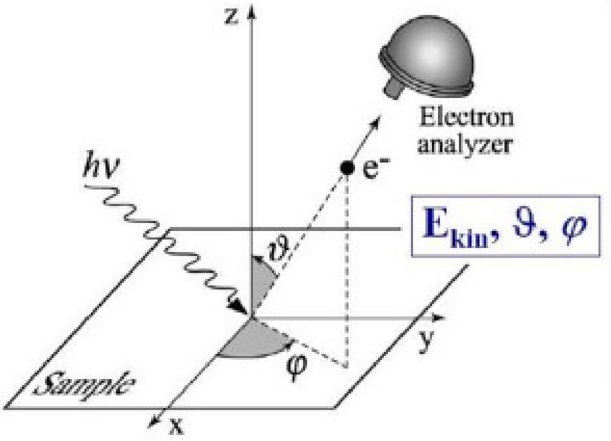

Figure 114: ARPES(Angle resolved photo emission spectroscopy)

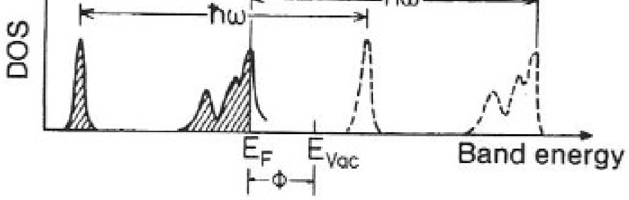

Figure 115: Shifting the electrons as the density of states over $\hbar\omega$ (energy of photons)

11 Structural phase transitions

This chapter is about structural phase transitions and the consequences to the dielectric constant. A structural phase transition is a transition from one crystal structure to another, for example from fcc to bcc. The stability of the crystal structure of a certain material is often dependent to the temperature. So it could happen, that the structure changes, if the temperature changes.

11.1 Example: Tin

A popular example for structural phase transitions is tin (Chemical symbol: Sn). This element has two forms:

- α-Sn: Gray tin, appears as a semiconductor, diamond crystal structure, stable below 13.2°C
- β-Sn: White tin, appears as a metal, tetragonal crystal structure, stable above 13.2°C

If tin is needed in applications where the temperature is colder than the transition temperature, it looses its good metal properties. To avoid the phase transition, some impurities have to be added to the pure metal. To understand the process of these transitions, we have to look at the free energy:

$$F = U - TS \tag{239}$$

The system tries to reduce its free energy F and so we can see, that the crystal structures must have different entropies. An easy model to explain the different entropies of the crystal structures is to think about the speed of sound, which has to be different, too. A lower speed of sound means softer phonon modes, which leads to more possible configurations, which means a higher entropy.

In order to calculate the entropy, we have to do some steps. First we need to measure or calculate the dispersion relationships of the two crystal structures. They are shown in fig. 116 for tin. When we have the dispersion relationships, we can calculate the density of states, which is plotted in fig. 117. With this we can write down the equation for the internal energy

$$U(\omega) = \int_0^\infty \underbrace{\hbar\omega}_{\text{Energy}} \underbrace{D(\omega)}_{\text{DoS}} \underbrace{\frac{1}{\exp(\frac{\hbar\omega}{k_B T}) - 1}}_{\text{Probability}} d\omega \tag{240}$$

and the integral for the entropy:

$$S = \int \frac{dU|_{V=const}}{T} = \int \frac{c_V}{T} dT \tag{241}$$

If this is done for both crystal structures, we should be able to predict where the structural phase transition will happen.

In the prior calculations, we said that the crystal tries to minimize the entropy, but at low temperatures often the enthalpy H is important for the choice of the crystal structure.

$$H = U + pV \tag{242}$$

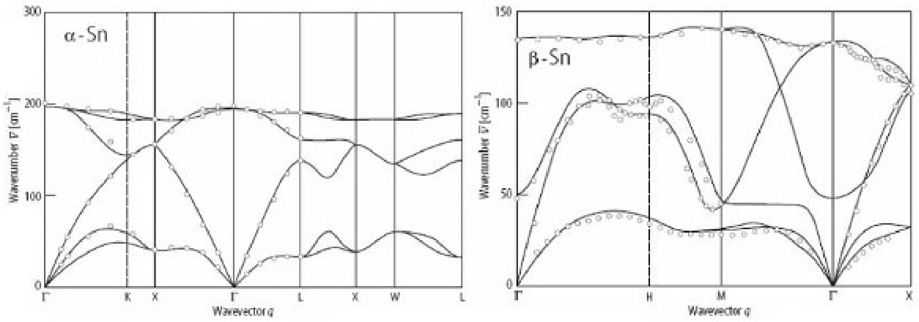

Figure 116: Dispersion relations for α-tin and β-tin

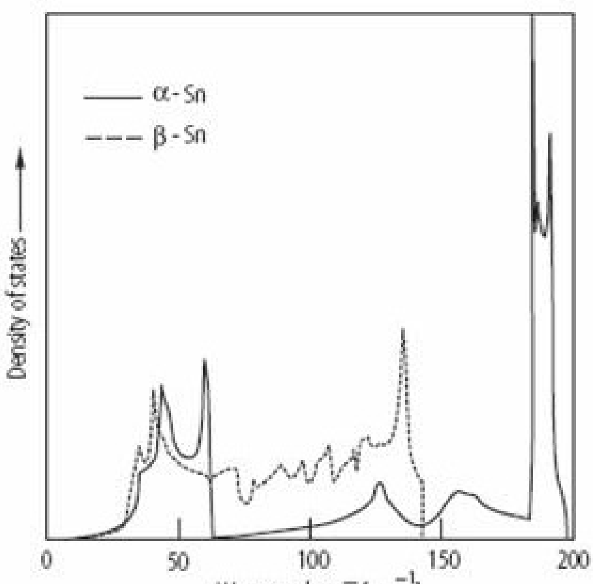

Figure 117: Density of states of α-tin and β-tin

At normal conditions the volume of a solid doesn't change very much, if the pressure is changed. So usually the enthalpy is almost the same as the free energy. In many experiments the controlled parameters are the temperature and the pressure. So we do two Legendre transformations and get the Gibbs free energy, which we have to minimize:

$$G = U + pV - TS \tag{243}$$

11.2 Example: Iron

Fig. 118 shows the phase diagram of iron with the specific heat in dependence of the temperature and the crystal structure. The low temperature phase is bcc. At higher temperatures it changes to a fcc structure, which is more tightly packed than the bcc structure. Normally, we expect the opposite, because tight packed structures are often dependent to low temperatures. This effect can be understood by considering the magnetic energy. At low temperatures the bcc phase is ferromagnetic, whereas the fcc phase is antiferromagnetic. Therefore, to create steel, which is not magnetic, impurities have to be added to the fcc phase at high temperatures to prevent the material of phase transitions to magnetic phases.

If the free energy including the magnet component is calculated, it turns out that the bcc phase has a lower energy than the fcc phase at low temperatures. In experiments it is always easy to measure the specific heat capacity, because that's just the energy you need to warm the material up. If we have a look at fig. 118, we can see that there is a jump from one phase to the other phase, where the solid line marks the stable phase. So the specific heat has a jump at the phase transition. When the fcc phase is stabilized by impurities, it is possible to measure the specific heat of this phase down close to zero degrees. What we see is a peak at about 15 K, which is called the Néel temperature. That's the temperature where an antiferromagnetic material becomes paramagnetic. The other big peak at about 1100 K coresponds to the Curie temperature, where a ferromagnet becomes a paramagnet. Because of its form, such peaks are called λ-points.

Remember that the two peaks correspond to electronic phase transitions, where the two jumps have to do with the structural phase transitions.

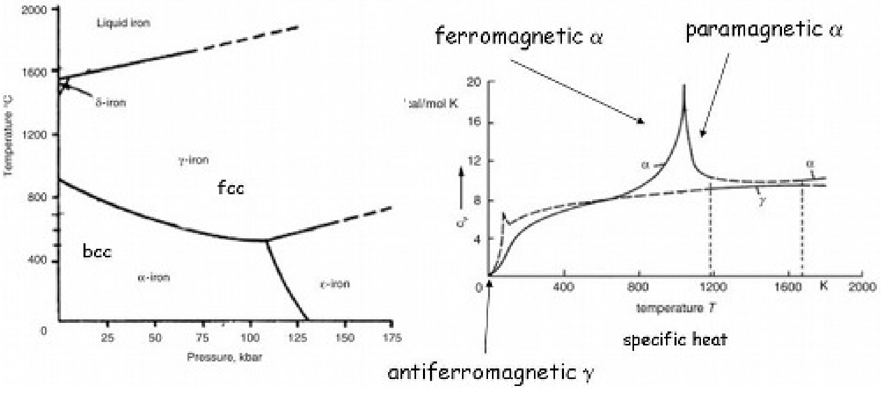

Figure 118: Phase diagram of iron with the specific heat in dependence of the temperature

11.3 Ferroelectricity

It turns out that interesting ferroelectric materials at room temperature are perovskits. The structure of a perovskit is shown in fig. 119, where we use $BaTiO_3$ as an example. The high temperature phase is cubic and there is no dipole moment. In the low temperature phase the positive charged ions (barium and titanium) move with respect to the oxygen, which is negative charged. So the unit cell gets a dipole moment and this effect is called ferroelectricity.

In fig. 120 we can see the spontaneous polarization of barium titanate as a function of temperature. The phase transition from tetragonal to cubic is not in the plot, but that will happen at about 120° C. In this case the spontaneous polarization will go to zero. In the specific heat-over-temperature diagram this transition again has the form of a λ.

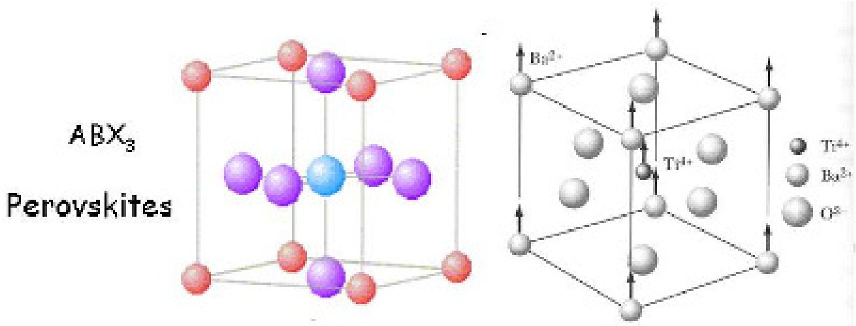

Figure 119: The structure of a perovskit with the example $BaTiO_3$

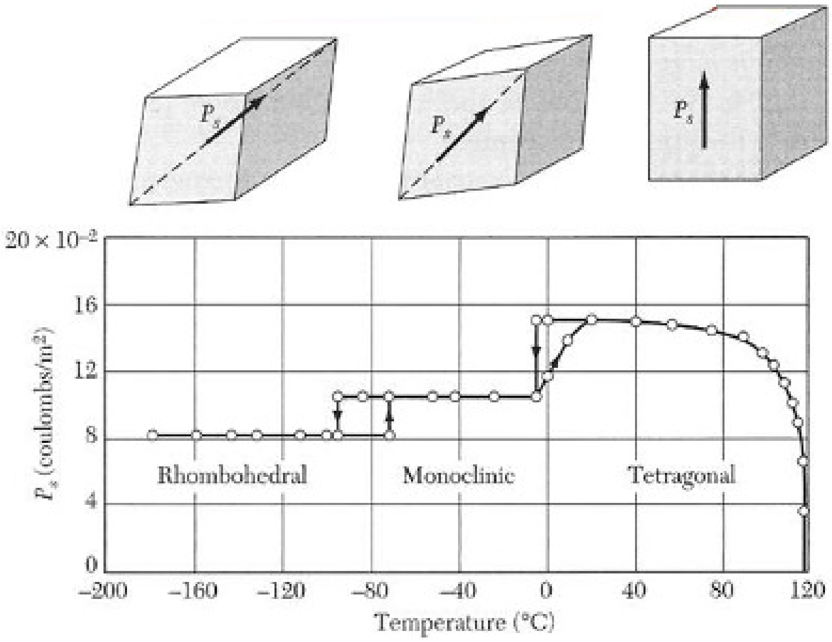

Figure 120: Spontaneous polarization of $BaTiO_3$ as a function of temperature

If we compare the dielectric constant of barium titanate (fig. 58) to the spontaneous polarization (fig. 120), we can see that the peaks are at the same temperatures. If the material is at a temperature near a phase transition (for example $-80°$) the energies of the two states are almost the same. So it easy for an electric field to switch between these two states, because of the nearly same free energies. That makes a high susceptibility and explains the peaks in the dielectric diagram. Above 120°C the material becomes paraelectric, which means that there is only polarization if an electric field is applied. This transition is similar to the ferromagnetic to paramagnetic transition. The susceptibility diverges like the Curie-Weiss law:

$$\chi = \frac{1}{T - T_C} \tag{244}$$

The fact that susceptibility and dielectric constant are related, causes the peak in the dielectric diagram with a $\frac{1}{T}$-decay. The peak in the diagram smears out because of impurities.

In such materials, domains with the same polarization direction are created. If higher electric fields are applied, the ferroelectric domains get smaller. Some domains will point in one direction and some in the other direction. This is done to minimize the electric energy, that's the same what happens in a ferromagnet. If a ferroelectric material is cooled down, the polarized domains will get very small but macroscopically there will be no polarization. But if the material is cooled down in a strong electric field, the domains will be pushed all in one direction, so the material will have a macroscopic polarization.

11.4 Pyroelectricity

Pyroelectricity is strongly related to ferroelectricity in the way that in both cases, one needs a material that consists of ions. At high temperatures, the crystal has a high symmetry crystal structure like a cubic structure and the centre of the positive charges in the unit cell is the same as for the negative charges and no spontaneous polarization can be observed. If this material is cooled down however, it will undergo a structural phase transition and end up in a lower symmetry crystal structure like a tetragonal structure, where the centres of the positive and the negative charges don't coincide anymore, which leads to a polarization. Generally speaking one can state, that all ferroelectrics go through a phase transition when they are cooled down, which leads to a change in the polarization.

Pyroelectric materials are used as sensors to detect heat for example and two of the most common pyroelectrics are ZnO and $LaTaO_3$

Fig. 121 shows the specific heat of $PbTiO_3$, a material that can be counted as a pyroelectric as well as a ferroelectric. The characteristic peak marks the point where the phase transition takes place. Above the transition temperature, there is no spontaneous polarization and because of that, the pyroelectric constant $\frac{\partial P}{\partial T}$, which is plotted as a function of the temperature in fig. 122(a) vanishes. Another interesting quantity to look at is the dielectric constant ϵ, which is proportional to $\frac{1}{T-T_C}$, where T_C is the critical temperature at which the phase transition occurs. This constant doesn't vanish for high temperatures, but it has also got a peak at the phase transition temperature. The dependence of ϵ on the temperature can be seen even better if one plots $\frac{1}{\epsilon}$ as a function of T, in which case it's just a linear function. (fig. 122(b))

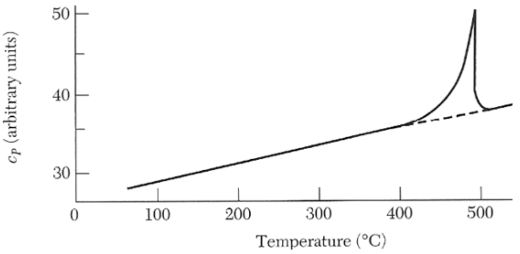

Figure 121: Specific heat of $PbTiO_3$

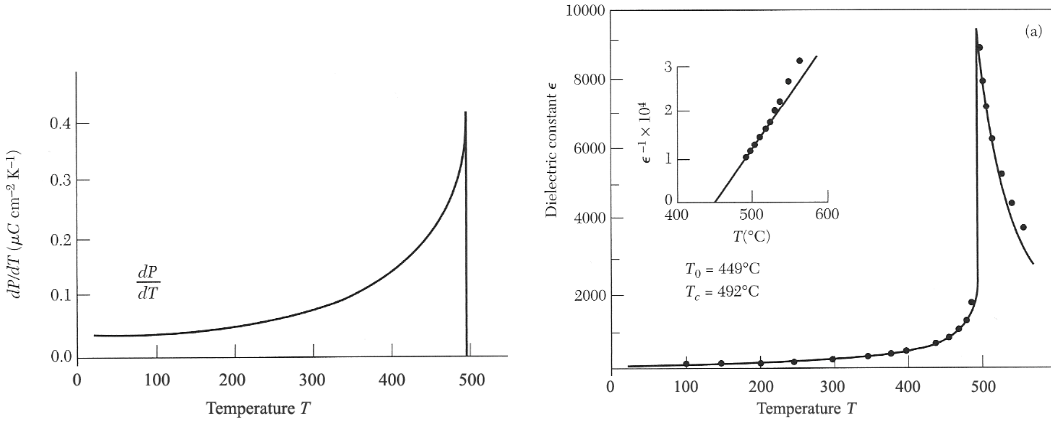

(a) (b)

Figure 122: a) Pyroelectric constant of $PbTiO_3$; b) Dielectric constant of $PbTiO_3$

11.5 Antiferroelectricity

Some structures, like $PbZrO_3$, also have a cubic structure at high temperatures and undergo a structural phase transition like pyroelectrics. But in contrast to pyroelectric materials antiferroelectrics don't have a macroscopic polarization, because the dipols in the unit cells arrange themselves antiparallel, hence the net polarization of the whole crystal vanishes.

Fig. 123 is a graphical summary of what was said in the last sections. As one can see, pyroelectrics and ferroelectrics behave the same at temperatures above and below the critical temperature. If an electric field at $T < T_C$ is applied however, the polarizations in the pyroelectric unit cells won't change, whereas the polarization in the ferroelectric unit cells amplifies the outer field by aligning parallel.

Antipolars and antiferroelectrics also behave the same without an electric field, but in contrast to pyroelectric and ferroelectric materials they don't exhibit a macroscopic polarization below T_C. By applying an electric field however, the antiferroelectric material behaves the same as the ferroelectric material below T_C, while the polarization of the antipolar material doesn't change at all.

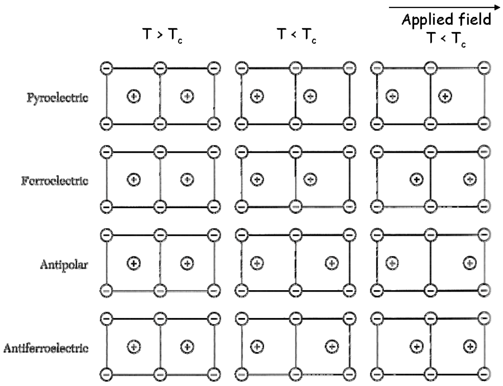

Figure 123: Graphical description for pyroelectricity, ferroelectricity, antipolarity and antiferroelectricity

11.6 Piezoelectricity

This material property is related to pyro- and ferroelectricity in a sense, that the crystal gets longer, when an electric field is applied. This happens, because the electric field couples with the polarization, which stretches the dipols apart and thus the material expands. Hence, in order to become piezoelectric, a material first has to show a spontaneous polarization.
The most commonly used piezoelectric materials are: $PZTs(Pb[Zr_xTi_{1-x}]O_3, 0 < x < 1)$, $BaTiO_3$, $PbTiO_3$, $KNbO_3$ and $LiNbO_3$.
Fig. 124 shows the phase diagram of PZT. The area labeled P_C means in there the crystal is paraelectric with a cubic crystal structure. FE_i labels areas with ferroelectric behaviour and a rhombohedral structure and F_T ferroelectric areas with tetragonal structure.

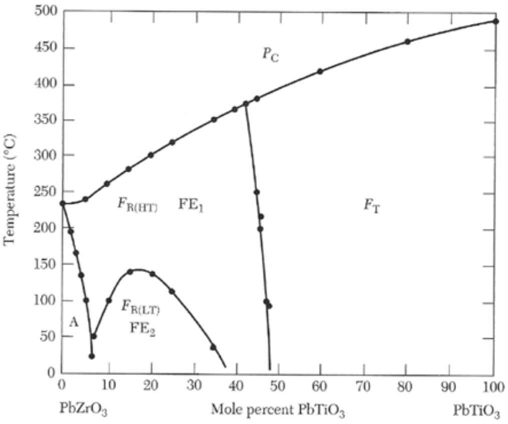

Figure 124: Phase diagram of PZT

11.7 Polarization

As one could see in the previous sections, all the mentioned material properties are in some sort related to each other and because of that we want to express the polarization in mathematical terms. Basically, the polarization can be computed by taking the derivative of the free energy G with respect to the electric field E_i (see chapter 8.2 Statistical Physics):

$$P_i = \frac{\partial G}{\partial E_i}$$

Now, one can build the total derivation of the polarization as follows:

$$dP_i = \frac{\partial P_i}{\partial \sigma_{kl}} d\sigma_{kl} + \frac{\partial P_i}{\partial E_k} dE_k + \frac{\partial P_i}{\partial H_k} dH_k + \frac{\partial P_i}{\partial T} dT \tag{245}$$

Here, σ_{kl} is one element of the strain tensor, H is the magnetic field and T the temperature. The first term describes the piezoelectric effect, the second term the electric polarization, the third the magneto-electric polarization and the fourth the pyroelectric effect.

The strain is also a very interesting property to look at, because as the polarization it also reveals much of a material's behaviour. Again, we compute the total derivation of the element i, j of the strain-tensor:

$$d\epsilon_{ij} = \frac{\partial \epsilon_{ij}}{\partial \sigma_{kl}} d\sigma_{kl} + \frac{\partial \epsilon_{ij}}{\partial E_k} dE_k + \frac{\partial \epsilon_{ij}}{\partial H_k} dH_k + \frac{\partial \epsilon_{ij}}{\partial T} dT \tag{246}$$

We identify the first term as the one ruling the elastic deformation, the second term describes the reciprocal piezoelectric effect, the third one the reciprocal piezomagnetic effect and the fourth the thermal expansion.

12 Landau Theory of Phase Transitions

Landau took a look at phase transitions and realized that each of these transitions is associated with a break in symmetry (except for infinite-order phase transitions, which will not be approached here). By cooling water to ice for example, there is a break in the translation symmetry, the transition of a material to superconductivity leads to a break in the gauge symmetry and so on. Therefore, Landau introduced an order parameter for each transition, which can be defined to be zero above the phase transition and nonzero below the transition. For ferromagnetism, this order parameter is the magnetization, for ferroelectricity the polarization, etc...

Phase transitions can be divided in first order and second order transitions. First order transitions exhibit a discontinuity in the first derivate of the free energy, e.g. a latent heat. The phase transition of water → ice is a typical example for a first order transition.
Second order phase transitions are continuous in the first derivate of the free energy but have a discontinuity in the second derivate of the free energy, thus they have no latent heat and the order parameter increases continuously. The transitions to ferromagnetism and ferroelectricity are second order transitions for example.

12.1 Second Order Phase Transitions

We will now take a closer look at the second order phase transitions, because they can be treated more easily with the Landau theory than first order transitions. Since the order parameter, in our specific case the magnetization, is zero above T_C and nonzero below T_C, it has to be small in the closer neighbourhood of T_C. Because of that, we can expand the free energy f in terms of the order parameter m.

$$f = f_0 + \alpha m^2 + \frac{1}{2}\beta m^4 + \dots \tag{247}$$

There are only even terms in this equation, because the odd ones cancel out for the magnetization due to reasons concerning the symmetry. By minimizing the free energy

$$\frac{df}{dm} = 2\alpha m + 2\beta m^3 + ...$$

we get two solutions for m:

$$m = \pm\sqrt{\frac{-\alpha}{\beta}} \quad at \;\; T < T_C \;\; and$$

$$m = 0 \quad at \;\; T > T_C$$

α must be temperature dependent too, because it's negative above T_C and positive below T_C, so we have another quantity that is small in the closer neighbourhood of T_C. Because of that, we rewrite $\alpha = \alpha_0(T - T_C)$ and are left with the following expressions for the free energy and the order parameter:

$$f = f_0 + \alpha_0(T - T_C)m^2 + \frac{1}{2}\beta m^4 + \dots \qquad , m = \pm\sqrt{\frac{-\alpha_0(T_C - T)}{\beta}} \quad at \;\; T < T_C$$

The free energy as a function of m is plotted in fig. 125. One can see, that the curvature of the free energy at the critical temperature is quite small, which leads to large fluctuations during the phase transition in a real material. (E.g. arising of steam bubbles while heating water to the boiling point) In our example of the magnetization there would be large areas in the material that are magnetized while other areas are still unordered at $T = T_C$.

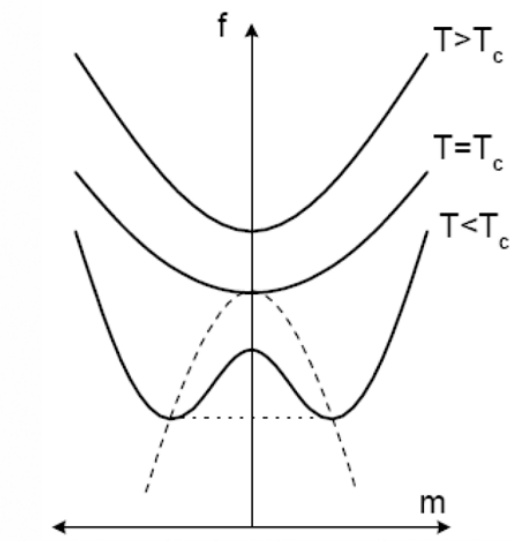

Figure 125: The free energy f as a function of the order parameter m for second order phase transitions

So in our case of ferromagnetism, the magnetization has to exhibit a square root dependence on the temperature, which coincides very well with experimental datas. (see fig. 126, the circles stand for experimental datas, the solid line for theoretical predictions)

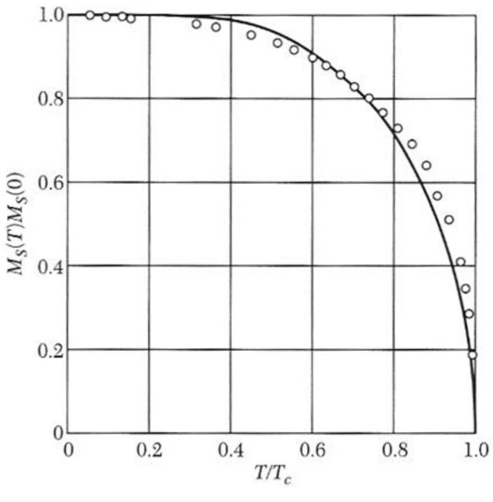

Figure 126: The magnetization as a function of temperature

For ferroelectricity, one gets the same dependence of the order parameter P on the temperature (fig. 127) and also the superconductivity exhibits a similar dependence (fig. 128)

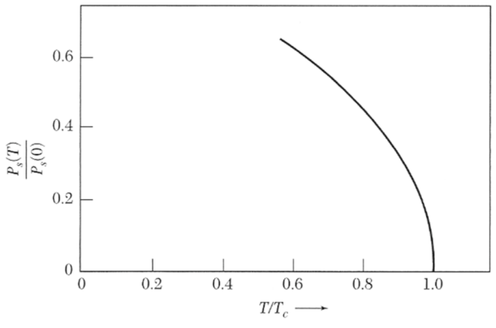

Figure 127: The polarization as a function of temperature

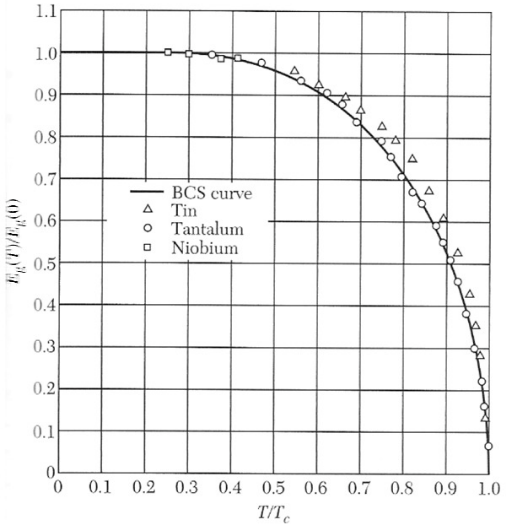

Figure 128: The superconductivity as a function of temperature

We now go back to the formula for the free energy and plug in our expression of the order parameter, to reveal the temperature dependence of the free energy at $T < T_C$:

$$f = f_0 - \frac{\alpha_0^2 (T - T_C)^2}{\beta} + \ldots \tag{248}$$

In many applications, the entropy S and the specific heat c_V are important quantities, so we also want to compute these at $T < T_C$ since we already know the free energy to test our theory.

$$s = -\frac{\partial f}{\partial T} = s_0 - \frac{2\alpha_0^2 (T - T_C)}{\beta} + \ldots$$

$$c_V = T\frac{\partial s}{\partial T} = c_0 - \frac{2\alpha_0^2 T}{\beta} + \ldots$$

These results are quite interesting, as one can see that the entropy changes slope at the phase transition and the specific heat is linear in temperature but exhibits a discontinuity at T_C (fig. 129). (These figures originally belong to a calculation about superconductivity, but they also hold true for our computations. The index n stands for "‘normal"’ and s for "‘superconducting"’, which is the material that undergoes the phase transition).

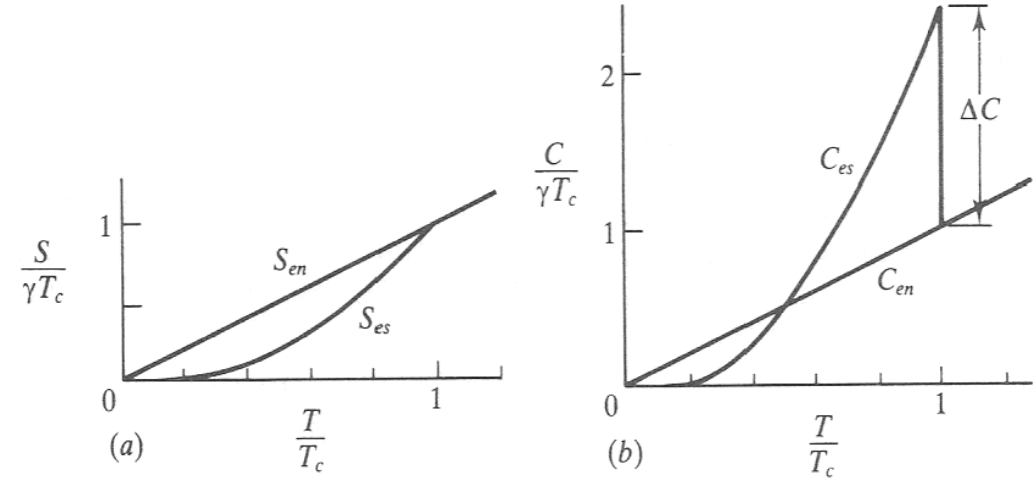

Figure 129: Entropy (a) and specific heat (b) as a function of temperature

We now want to take our calculations even further and include a magnetic field B, so the formula for the free energy becomes:

$$f = f_0 + \alpha_0(T - T_C)m^2 + \frac{1}{2}\beta m^4 - mB \tag{249}$$

By minimizing the free energy as before, one is left with an expression for small values of the order parameter m at $T > T_C$, which looks similar to the Curie-Weiss law:

$$m = \frac{B}{2\alpha_0(T - T_C)}$$

12.2 First Order Phase Transitions

First order phase transitions are very complicated to deal with, because the order parameter isn't necessarily small in the closer neighbourhood of T_C and even shows a discontinuity at T_C. There are many different ways to look at first order phase transitions and we want to take a closer look at the free energy f as before.

$$f = f_0 + \alpha_0(T - T_C)m^2 + \frac{1}{2}\beta m^4 + \frac{1}{3}\gamma m^6 + \dots \tag{250}$$

Here the first constant α_0 is positive, β is negative and γ keeps the free energy from diverging at extreme values for T. Fig. 130 shows a plot of the free energy as a function of the order paramter. At $T > T_C$, there is only one minimum at $m = 0$ but at $T = T_C$, there are three minima at different

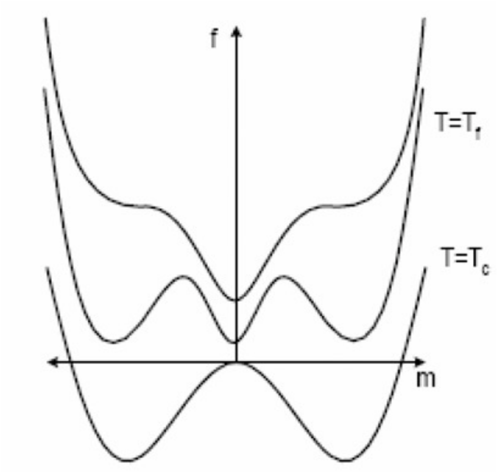

Figure 130: The free energy f as a function of the order parameter m for first order transitions

values for m. By cooling the material even further, the central minimum slowly vanishes while the outer minima become deeper. Because of that, processes like supercooling (lowering the temperature of a liquid or gas below its freezing point without becoming a solid) or superheating (heating a liquid above its boiling point without boiling) are possible, because the material is trapped in a metastable state, e.g. the local minimum at $m = 0$ of the free energy for some time.

Fig. 131 shows the polarization of $BaTiO_3$ as a function of the temperature, which is a typical example for a first order phase transitions.

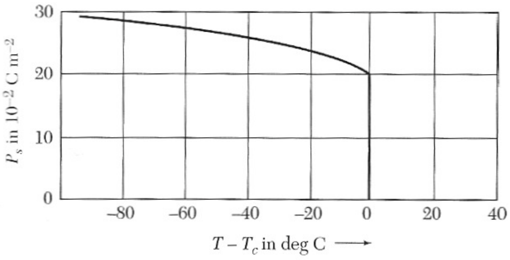

Figure 131: The polarization of $BaTiO_3$ as a function of temperature

We now minimize the free energy as in the last section and get the following solutions for m:

$$m = 0, \pm\sqrt{\frac{-\beta \pm \sqrt{\beta^2 - 4\alpha_0(T - T_C)\gamma}}{2\gamma}}$$

so far small values of the order parameter, the free energy is approximately:

$$f \approx f_0 + \alpha_0(T - T_C)\frac{-\beta \pm \sqrt{\beta^2 - 4\alpha_0(T - T_C)\gamma}}{2\gamma} \tag{251}$$

13 Superconductivity

Literature

- Rickayzen, *Theory of Superconductivity*, Interscience Publishers, 1965.
- Buckel, Kleiner, *Supraleitung - Grundlagen und Anwendungen*, Wiley, 2007.
- Ibach, Lüth, *Solid State Physics - An Introduction to Principles of Material Science*, Springer, 2002.
- Kittel, *Introduction to Solid State Physics*, Wiley, 2005.
- Lecture Notes by E. Schachinger and P. Hadley.

13.1 Introduction

Superconductivity is the phenomenon of unmeasurable low resistance below a critical (or transition) temperature T_c. It is observed in a wide class of materials, however, the theoretical description includes numerous subtleties. Today the phenomenon is (basically) well understood but the development of appropriate theoretical models and the corresponding experimental inspections display many aspects of the development of physics in the 20th century.

In 1911 Kamerlingh Onnes, three years after he first liquefied helium, observed that the electrical resistance of mercury drops to an unmeasurable low value below the critical temperature of $T_c \approx 4.2$ K. In fact it is fundamentally impossible to show that the resistance is exactly zero, but it is possible to give an upper limit. K. Onnes classified the first superconducting state with an upper limit to the resistance of 10^{-5} Ω. However, the more surprising fact was that the resistance did not increase with an increase of impurities in the mercury sample. Moreover, the resistance drops discontinuously within a temperature range of less than 0.01 K, see Fig. 132.

An elementary property of superconductivity as observed by K. Onnes is the experimental fact, that the superconducting state may be destroyed by placing the sample in a strong magnetic field. Furthermore, superconductivity reappears when the field is removed and the field strength required to destroy the superconducting state depends on the orientation of the specimen within the field. Nowadays, many different materials are known to show such behavior. Amongst non transition metals, such as Be or Al, the phenomenon is also observed in samples of transition metals, such as Nb, Mo or Zn, and even, when first exposed to high pressure (transition to the metallic phase) and then cooled to very low temperatures (transition to superconducting state), in semiconductors, such as Si, Ge, Se, Te. Typical transition temperatures for such materials are in the range of liquefied helium (~ 4 K). The transition temperature may depend on the crystal structure of the material, such as in Bi, where different modifications show different transition temperatures, but the crystal structure is not a necessary condition for superconductivity. Moreover, a wide range of alloys show superconducting behavior. For instance, the alloy $Nb_3Al_{0.75}Ge_{0.25}$ was for a long period the material with the highest yet observed transition temperature ($T_c = 20.3$ K). Amongst the most fascinating materials today are high temperature superconductors such as Y-Ba-Cu-O alloys with transition temperatures up to 100 K (e.g. $YBa_2Cu_3O_{7-x}$) or more exotic alloys, such as $(Sn_5In)Ba_4Ca_2Cu_{10}O_x$ with $T_c = 212$ K.

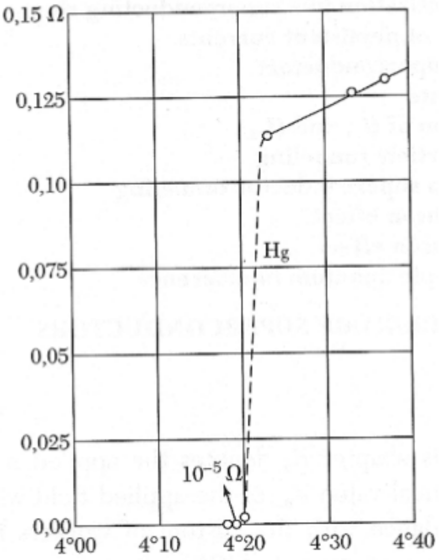

Figure 132: Resistance as a function of temperature for a mercury sample as investigated by K. Onnes.

The history of the theoretical investigation of superconductivity includes numerous aspects of 20th century theoretical physics. It took approximately 50 years until the first microscopic consistent explanation was presented by Bardeen, Cooper and Schrieffer, today known as the BCS theory of superconductivity. This theory required the development of quantum mechanics (1925), the discovery of quantum field theories in the late 1940s and finally the application of quantum field theoretical methods to solid state environments in the early 1950s. It turned out that the superconducting state is a quantum many particle effect of macroscopic size. Note that the effect of zero resistance is not describable within the framework of one electron dynamics. In a real crystal finite conductivity is the result of interactions of electrons (or holes) with crystal defects or phonons. Even if this interaction could be suppressed, electron-electron scattering would still cause a finite conductivity. In contrast to the simplified one electron picture, the BCS theory explains the superconducting state as a superfluid of Cooper pairs, which are quasiparticles consisting of two electrons which interact through phonons. The BCS theory was the basis for many different explanations of new phenomena in many particle systems.

Today's applications of superconductors range from superconducting magnets, used in NMR spectrometers, mass spectrometers or particle accelerators, to SQUIDs, which exploit the Josephson effect. Several researches were awarded the Nobel prize of Physics for achievements in the field of superconductivity: Onnes on *Matter at low temperature* (1913), Bardeen, Cooper and Schrieffer on *Theory of superconductivity* (1972), Esaki, Giaever and Josephson on *Tunneling in superconductors* (1973), Bednorz and Müller on *High-temperature superconductivity* (1987) and Abrikosov, Ginzburg and Leggett on *Pioneering contributions to the theory of superconductors and superfluids* (2003).

It is the aim of this section to give a brief introduction into some aspects of superconductivity. This short introductory subsection is followed by a review of the fundamental experimental observations in the second subsection. Phenomenological descriptions, i.e. thermodynamic considerations, the

Table 2: Transition temperatures T_c for some selected materials.

Material	T_c / K
Ti	0.4
Hg	4.2
C_{60}	19.2
Rb_2CsC_{60}	19.2
$YBa_2Cu_3O_{6.9}$	90.0
$(Sn_5In)Ba_4Ca_2Cu_{10}O_x$	212

London equations and the Ginzburg - Landau equations, are the topic of the third subsection. In the fourth subsection we will give a short introduction into some fundamental concepts of the BCS theory and discuss the flux quantization in this context. The Josephson effect will be topic of the fifth subsection.

13.2 Experimental Observations

13.2.1 Fundamentals

We already observed that superconductivity occurs in many metallic compounds, but also alloys, doped semiconductors and even organic molecules. The transition temperatures T_c range from $T_c = 0.001$ K for Rh up to $T_c = 212$ K for $(Sn_5In)Ba_4Ca_2Cu_{10}O_x$. Some materials reach the phase transition only under high pressure, for instance for Si $p = 165$ kbar and $T_c = 8.3$ K. In Tab. 2 the transition temperatures of some selected compounds are given. However, we can state that a material has to be nonmagnetic in order to become a superconductor under appropriate conditions (in particular, this statement is not true for high T_c superconductors, which are based on cuprates). The question whether every nonmagnetic material will become a superconductor at sufficiently low temperatures or not, can fundamentally not be answered.

One of the earliest observations was that strong magnetic fields destroy superconductivity. The critical field as a function of temperature, $H_c(T)$ where $H_c(T_c) = 0$, separates the normal from the superconducting state, see Fig. 133. Note that $H_c = \frac{1}{\mu_0}B_{ac}$, where B_{ac} is the critical magnetic field and μ_0 is the magnetic permeability of vacuum. The applied magnetic field will in the following be denoted by B_a.

Since the superconducting state is destroyed above the critical magnetic field, there exists a maximum current within the superconductor because a higher current would induce a magnetic field destroying superconductivity. This maximum current is called critical current J_c. It can be estimated by equating the energy of the critical magnetic field with kinetic energy of n electrons:

$$\mu_0 H_c^2 \approx \frac{1}{2} n m_e v^2, \tag{252}$$

where m_e is the electron mass and v the electron's velocity. Since the current density can be written as $J = -nqv$ (with q the elementary charge) we obtain an estimate for the critical current J_c as a

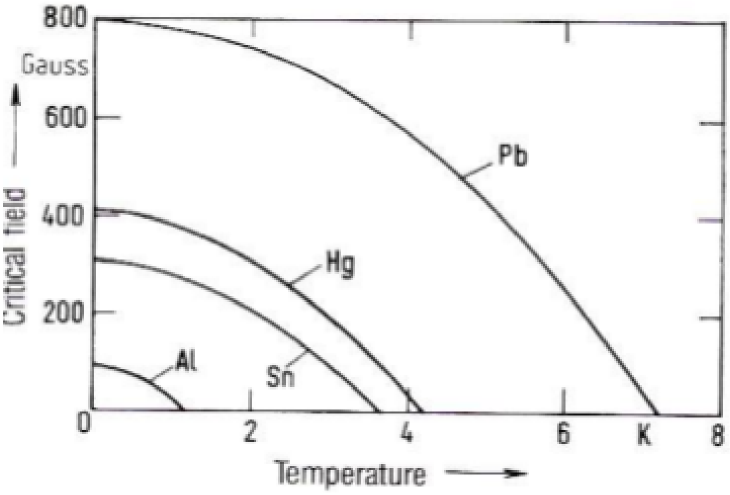

Figure 133: The critical magnetic field $H_c(T)$ as a function of temperature T. For $T = T_c$ we have $H_c(T_c) = 0$. $H_c(T)$ separates the normal (above the curve) from the superconducting (below the curve) state.

function of the critical magnetic field

$$J_c \approx \sqrt{\frac{2\mu_0}{q^2 n m_e}} H_c. \tag{253}$$

13.2.2 MEISSNER - OCHSENFELD **Effect**

In 1933 MEISSNER and OCHSENFELD observed that if a superconductor within an external magnetic field $\mathbf{B}$ is cooled below the transition temperature T_c, then the magnetic field is pushed out of the interior of the superconductor, i.e. $\mathbf{B} = \mathbf{0}$ within the superconductor. Note that this effect is reversible. This observation has several consequences. For instance, in case of a superconducting wire we can immediately deduce that current cannot flow within the superconductor due to AMPERE's law $\nabla \times \mathbf{B} = \boldsymbol{\mu_0}\mathbf{J}$. The current must therefore flow in the surface of the wire.

A second consequence is that a superconductor is not equal to an ideal conductor. For an ideal conductor we obtain from OHM's law $\mathbf{E} = \rho\mathbf{J}$, with $\mathbf{E}$ the electrical field and ρ the resistivity, that $\mathbf{E} \to \mathbf{0}$ in the limit $\rho \to 0$, since $\mathbf{J} < \infty$ within the superconductor. However, from MAXWELL's equations we now deduce that $\dot{\mathbf{B}} \sim \nabla \times \mathbf{E} = \mathbf{0}$. This is not equivalent to the observation by MEISSNER and OCHSENFELD since in the case of an ideal conductor we obtain that the magnetic field must not change on cooling through the transition temperature. Hence, we obtain that perfect diamagnetism is an essential property of the superconducting state.

We now explicitly write the magnetic field within the superconductor

$$\mathbf{B} = \mathbf{B_a} + \boldsymbol{\mu_0}\mathbf{M}, \tag{254}$$

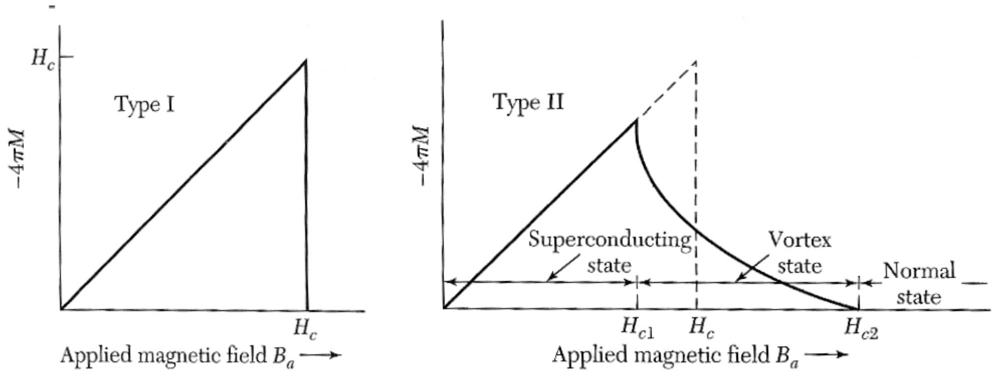

Figure 134: Illustration of the dependence of the magnetization on the applied magnetic field for type I and type II superconductors. In case of type I superconductors (complete MEISSNER - OCHSENFELD effect) the magnetization above the critical field (i.e. in the normal state) is too small to be resolved in this figure. In case of a type II superconductor (incomplete MEISSNER - OCHSENFELD effect) the magnetic field B starts to penetrate the superconductor at a critical value H_{c1} which is lower than the thermodynamic critical value H_c. Above the second critical point H_{c2} the compound is normal conducting, the state between H_{c1} and H_{c2} is called vortex state or SHUBNIKOV phase. Note that the area under both curves is the same.

where $\mathbf{M}$ is the magnetization. Since $\mathbf{B} = \mathbf{0}$ for $\mathbf{B_a} < \mathbf{B_{ac}}$ we have in the one-dimensional case

$$\frac{M}{B_a} = -\frac{1}{\mu_0} = -\varepsilon_0 c^2, \tag{255}$$

where ε_0 is the dielectric constant of vacuum and c is the vacuum speed of light. In Fig. 134(a) this relation is illustrated. Note that the superconductor undergoes a first order phase transition at H_c for $T \neq T_c$. However, such behavior is only observed in a a certain class of materials, which are nowadays known as type I superconductors. Type I superconductors are typically pure materials with low values of electrical resistance. For other materials, typically alloys or transition metals with a high electric resistance in the normal state, a different behavior is observed. These materials are referred to as type II superconductors since they undergo a second order phase transition at the critical magnetic field. Such a transition is depicted in Fig. 134(b). Type II superconductors posses two critical magnetic fields, H_{c1} and H_{c2}. Below H_{c1} the MEISSNER - OCHSENFELD effect is complete, while between H_{c1} and H_{c2} it is said to be incomplete. However, the sample is superconductive up to the second critical field H_{c2}. Between H_{c1} and H_{c2} the magnetic field within the superconductor is not equal to zero, $\mathbf{B} \neq \mathbf{0}$. I.e., the sample is threaded by flux lines. This state is referred to as the vortex state or SHUBNIKOV phase. Note that H_{c2} can be larger than H_c by orders of magnitude (which is in case of type II superconductors defined by the thermodynamics of the system).

13.2.3 Heat Capacity

Measurements show that for temperatures below the critical temperature, $T < T_c$, the entropy of the system is decreased, see Fig. 135. This contains the information that the superconducting state is

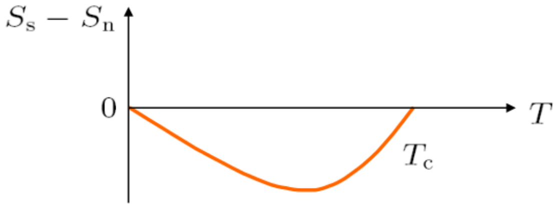

Figure 135: In the superconducting state the entropy is decreased with respect to the normal state.

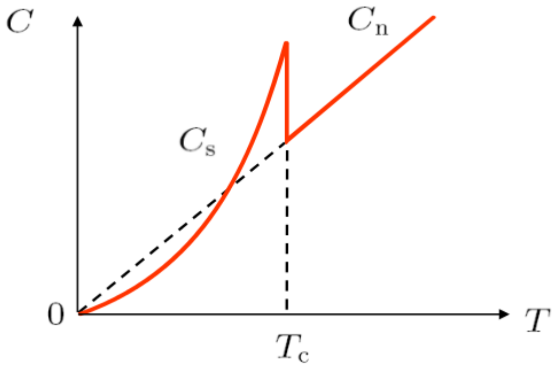

Figure 136: Schematic illustration of the dependence of the heat capacity on temperature in a superconductor.

more ordered than the normal state. This observation was of crucial importance for the development of microscopic theories. Since the change in entropy is very small, this must mean that only a small fraction of all conduction electrons participate in the transition to the superconducting state.

Furthermore, the heat capacity is discontinuous at the critical temperature for $B_a = 0$, see Fig. 136 and the observed form suggests an exponential form with argument proportional to $-\frac{1}{T}$, while in the normal state, the specific heat increases linearly with temperature. This allows the interpretation of excitations of electrons over an energy gap, see Fig. 136 and 137. The energy gap is well described within the BCS theory. In difference to normal insulators, the energy gap in superconductivity is not a result from electron-lattice interactions, but from electron-electron interactions.

13.2.4 Isotope Effect

The experimental observation that T_c varies with the isotopic mass is referred to as the isotope effect. For instance, in case of Hg one measures a change of T_c from 4.185 K to 4.146 K under a variation of the isotopic mass M from 199.5 to 203.4 atomic mass units. The experimentally observed relation between T_c and M reads

$$M^{\alpha} T_c = const., \tag{256}$$

where some selected values for α are given in Tab. 3. This observation includes a further, highly important information about the underlying physical processes: Since the transition temperature of

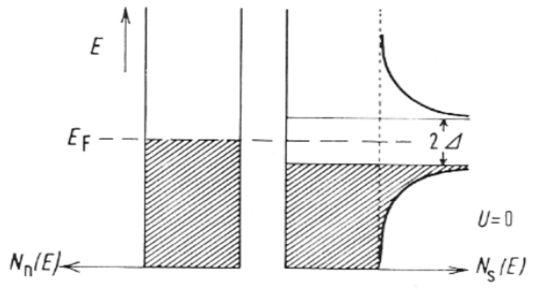

Figure 137: Schematic illustration of the energy gap in a superconductor.

Table 3: Some selected values of the exponent α related to the isotope effect. The vanishing value for some materials (such as Ru) was explained by means of its particular band structure.

Material	α
Ru	0.0
Mo	0.3
Hg	0.5
Sn	0.5

the superconductor varies with the atomic mass rather then with the electronic structure we can conclude that electron phonon interactions might play a crucial role.

13.3 Phenomenological Description

13.3.1 Thermodynamic Considerations

Since the transition between the superconducting and the normal state is reversible we can apply the basic concepts of thermodynamics in order to obtain an expression for the free energy F as a function of the critical field curve H_c and T. The work done on a type I (complete Meissner - Ochsenfeld effect) superconductor in an external magnetic field can be expressed by

$$W = \int_0^{\mathbf{B_a}} d\mathbf{B} \cdot \mathbf{M}. \tag{257}$$

Thus we identify the differential of the free energy as

$$dF = -\mathbf{M} \cdot d\mathbf{B}. \tag{258}$$

Since we deal with a type I superconductor we can exploit the known relationship between $\mathbf{M}$ and $\mathbf{B_a}$ in the superconducting state in order to obtain

$$dF_S = \frac{1}{\mu_0}\mathbf{B} \cdot d\mathbf{B}, \tag{259}$$

or in particular for $\mathbf{B} : \mathbf{0} \to \mathbf{B_a}$

$$F_S(\mathbf{B_a}) - F_S(\mathbf{0}) = \frac{1}{2\mu_0}\mathbf{B_a}^2. \tag{260}$$

If we consider a nonmagnetic metal in the normal state and neglect the magnetic susceptibility, then $\mathbf{M} = \mathbf{0}$ and accordingly

$$F_N(\mathbf{B_a}) = F_N(\mathbf{0}). \tag{261}$$

Now at $\mathbf{B_a} = \mathbf{B_{ac}}$ the energies are equal in the normal and in the superconducting state:

$$F_N(\mathbf{B_{ac}}) = F_S(\mathbf{B_{ac}}) = F_S(\mathbf{0}) + \frac{1}{2\mu_0}\mathbf{B_{ac}}^2. \tag{262}$$

Hence, at zero field, we have

$$\Delta F = F_N(\mathbf{0}) - F_S(\mathbf{0}) = \frac{1}{2\mu_0}\mathbf{B_{ac}}^2. \tag{263}$$

Here ΔF is the stabilization free energy of the superconducting state. Hence, at a temperature $T < T_c$, the superconducting state is more stable up to a critical magnetic field $\mathbf{B_{ac}}$. Above this field the normal state is more stable. The results for the stabilization energy are in excellent agreement with experimental results.

13.3.2 The London Equations

It is the aim of the following considerations to derive the Meissner - Ochsenfeld effect from a particular ansatz for the electrodynamic laws in the superconducting state. We write the equation of motion of a charged particle in an electrical field $\mathbf{E}$

$$m\dot{\mathbf{v}} = -q\mathbf{E}. \tag{264}$$

We now insert the current density $\mathbf{j_s} = -qn_s\mathbf{v}$, where n_s is the density of superconducting electrons, in order to obtain the first London equation

$$\dot{\mathbf{j}}_\mathbf{s} = \frac{n_s q^2}{m}\mathbf{E}. \tag{265}$$

From $\nabla \times \mathbf{E} = -\dot{\mathbf{B}}$ we obtain

$$\frac{\partial}{\partial t}\left(\frac{m}{n_s q^2}\nabla \times \mathbf{j_s} + \mathbf{B}\right) = \mathbf{0}. \tag{266}$$

This equation describes an ideal conductor, i.e. $\rho = 0$. However, the expulsion of the magnetic field in the Meissner - Ochsenfeld effect is not yet included. Integrating this equation with respect to time and neglecting the integration constant yields the second London equation, which already includes to correct physical description:

$$\nabla \times \mathbf{j_s} = -\frac{n_s q^2}{m}\mathbf{B}. \tag{267}$$

Note that since $\mathbf{B} = \nabla \times \mathbf{A}$ we can conclude that

$$\mathbf{j_s} = -\frac{n_s q^2}{m}\mathbf{A} \equiv -\frac{1}{\mu_0 \lambda_L^2}\mathbf{A}, \tag{268}$$

where we defined $\lambda_L = \sqrt{\frac{m}{n_s \mu_0 q^2}}$ with the dimension of length. Here, $\mathbf{A}$ has to be understood in the London gauge. For a simply connected superconductor it may be expressed by $\nabla \cdot \mathbf{A} = 0$ and $\mathbf{A_n} = \mathbf{0}$, where $\mathbf{A_n}$ is the normal component of $\mathbf{A}$ on an external surface, through which no current flows. The second London equation can be rewritten in the following way

$$\nabla \times \mathbf{j_s} = -\frac{1}{\mu_0 \lambda_L^2}\mathbf{B}. \tag{269}$$

Further, from Maxwell's equations

$$\nabla \times \mathbf{B} = \mu_0 \mathbf{j_s}, \tag{270}$$

we obtain

$$\nabla \times \nabla \times \mathbf{B} = -\nabla^2 \mathbf{B} = \mu_0 \nabla \times \mathbf{j}. \tag{271}$$

Combining Eqs. (269) and (271) yields

$$\nabla^2 \mathbf{B} - \frac{1}{\lambda_L^2}\mathbf{B} = \mathbf{0}. \tag{272}$$

Equivalently, we can combine Eqs. (267) and (271) in order to obtain

$$\nabla^2 \mathbf{j_s} - \frac{1}{\lambda_L^2}\mathbf{j_s} = \mathbf{0}. \tag{273}$$

We regard a semi-infinite superconductor ($z > 0$) in a magnetic field which is homogeneous in vacuum ($z < 0$), see Fig. 138. In case that $\mathbf{B} = B_x \mathbf{e_x}$ we obtain from Eq. (270) that $\mathbf{j_s}$ is of the form $\mathbf{j_s} = j_{sy}\mathbf{e_y}$. We can calculate the magnetic field and the current density in the superconductor from Eqs. (272) and (273):

$$B_x(z) = B_x^0 \exp\left(-\frac{z}{\lambda_L}\right), \tag{274}$$

and

$$j_{sy}(z) = j_{sy}^0 \exp\left(-\frac{z}{\lambda_L}\right). \tag{275}$$

This means that the magnetic field as well as the current decay exponentially with distance into the superconductor. Here, λ_L is referred to as the London penetration depth. For a typical superconductor such as Sn, its value is approximately 26 nm. Hence, the London equations describe the Meissner - Ochsenfeld effect particularly well.

13.3.3 Ginzburg - Landau Equations

In order to obtain the Ginzburg - Landau equations one introduces a complex valued order parameter φ where $|\varphi|^2 = n_s$ is the density of superconducting electrons. Based on Landau's theory

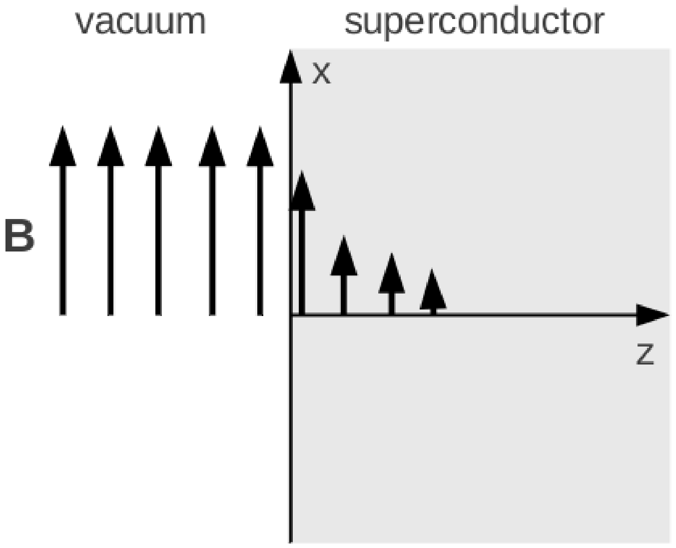

Figure 138: Illustration of the above example of a semi-infinite superconductor in a homogeneous magnetic field in vacuum.

of second order phase transitions, Ginzburg and Landau suggested that the free energy F_S in the superconducting state can be written in the following form

$$F_S = F_N - \alpha|\varphi|^2 + \frac{\beta}{2}|\varphi|^4 + \frac{1}{2m}\Big|\left(-i\hbar\nabla - q\mathbf{A}\right)\varphi\Big|^2 + \frac{1}{2\mu_0}\mathbf{B_a}^2, \tag{276}$$

where α and β are phenomenological constants and m is the quasiparticle's mass. Further, F_N denotes the free energy of the normal state. The equation can be interpreted in the following way: $\alpha|\varphi|^2 + \frac{\beta}{2}|\varphi|^4$ is a term of the typical form appearing in Landau's theory of second order phase transitions, $\frac{1}{2m}\Big|\left(-i\hbar\nabla - q\mathbf{A}\right)\varphi\Big|^2$ is an additional term which accounts for energy corrections due to spatial variations of the order parameter φ and the last term, $\frac{1}{2\mu_0}\mathbf{B_a}^2$ represents an additional contribution to the free energy according to Eq. (260). Minimizing the free energy F_S with respect φ yields the Ginzburg - Landau equations in terms of functional derivatives:

$$\delta F_S = \frac{\delta F_S}{\delta\varphi}\delta\varphi + \frac{\delta F_S}{\delta\varphi^*}\delta\varphi^*. \tag{277}$$

Note that $|\varphi| = \varphi\varphi^*$. We obtain

$$\begin{aligned} \delta F_S &= \left[-\alpha\varphi + \beta|\varphi|^2\varphi + \frac{1}{2m}\left(-i\hbar\nabla - q\mathbf{A}\right)\varphi \cdot \left(i\hbar\nabla - q\mathbf{A}\right)\right]\delta\varphi^* + \text{h.c.} \\ &= 0. \end{aligned} \tag{278}$$

In the kinetic term of the right hand side we have to deal with a term of the form $\nabla\varphi\cdot\nabla\delta\varphi^*$. We note that $\int d\mathbf{r}\nabla\varphi\cdot\nabla\delta\varphi^* = -\int d\mathbf{r}(\nabla^2\varphi)\delta\varphi^*$, where we assumed that $\delta\varphi^*$ vanishes at the integration boundaries. Conclusively we obtain

$$\int d\mathbf{r}\delta F_S = \int d\mathbf{r}\left[-\alpha\varphi + \beta|\varphi|^2\varphi + \frac{1}{2m}\left(-i\hbar\nabla - q\mathbf{A}\right)^2\varphi\right]\delta\varphi^* + \text{h.c.} \tag{279}$$

This is expression is equal to zero if

$$-\alpha\varphi + \beta|\varphi|^2\varphi + \frac{1}{2m}\left(-i\hbar\nabla - q\mathbf{A}\right)^2\varphi = 0. \tag{280}$$

This is the first GINZBURG - LANDAU equation. In order to obtain the second GINZBURG - LANDAU equation, one minimizes F_S, Eq. (276), with respect to the vector potential $\mathbf{A}$.

$$\frac{\delta F_S}{\delta\mathbf{A}} = \frac{q}{2m}\left[\varphi\left(-i\hbar\nabla + q\mathbf{A}\right)\varphi^* - \varphi^*\left(-i\hbar\nabla - q\mathbf{A}\right)\varphi\right] + \frac{1}{\mu_0}\nabla\times\nabla\times\mathbf{A}, \tag{281}$$

where we employed some rules of functional derivatives in the sense of distributions. In particular, we first define the functional $\mathbf{B_a}(\mathbf{r}) = F[\mathbf{A}] = \int d\mathbf{r}'[\nabla\times\mathbf{A}(\mathbf{r}')]^2\delta(\mathbf{r}-\mathbf{r}')$. We now write

$$\begin{aligned}\left\langle\frac{\delta F[\mathbf{A}]}{\delta\mathbf{A}},\mathbf{f}\right\rangle &= \frac{\mathrm{d}}{\mathrm{d}\varepsilon}F[\mathbf{A}+\varepsilon\mathbf{f}]\Big|_{\varepsilon=0} \\ &= 2\int d\mathbf{r}'\left(\nabla\times\mathbf{f}\right)\cdot\left(\nabla\times\mathbf{A}\right)\delta(\mathbf{r}-\mathbf{r}') \\ &= 2\int d\mathbf{r}'\mathbf{f}\cdot\nabla\times\nabla\times\mathbf{A}\delta(\mathbf{r}-\mathbf{r}'). \end{aligned} \tag{282}$$

In the last step (integration by parts) we used that $\mathbf{f}$ is some test function, i.e. it decays sufficiently fast for $|\mathbf{r}| \to \infty$. From the last line we deduce the desired result

$$\frac{\delta\mathbf{B_a}^2(\mathbf{r})}{\delta\mathbf{A}(\mathbf{r}')} = 2\nabla\times\nabla\times\mathbf{A}(\mathbf{r}')\delta(\mathbf{r}-\mathbf{r}'). \tag{283}$$

Using $\nabla\times\nabla\times\mathbf{A} = \nabla\times\mathbf{B_a} = \mu_0\mathbf{j_S}$ and $\frac{\delta F_S}{\delta\mathbf{A}} = 0$ we obtain the second GINZBURG - LANDAU equation as

$$\begin{aligned}\mathbf{j_S} &= -\frac{q}{2m}\left[\varphi\left(-i\hbar\nabla + q\mathbf{A}\right)\varphi^* - \varphi^*\left(-i\hbar\nabla - q\mathbf{A}\right)\varphi\right] \\ &= \frac{q}{m}\mathrm{Re}\left[\varphi^*\left(-i\hbar\nabla - q\mathbf{A}\right)\varphi\right]. \end{aligned} \tag{284}$$

where $\mathbf{j_S}$ is called the supercurrent.

We now regard several interesting outcomes of this model: Let $\mathbf{A} = \mathbf{0}$ and $\alpha \gg \beta|\varphi|^2$. Then we obtain in the one dimensional case from the first GINZBURG - LANDAU equation (280)

$$-\frac{\hbar^2}{2m}\frac{\mathrm{d}^2}{\mathrm{d}x^2}\varphi = \alpha\varphi \tag{285}$$

with the solution $\varphi(x) = \exp\left(ix/\xi\right)$ where $\xi = \hbar/\sqrt{2m\alpha}$. ξ may be interpreted as the intrinsic coherence length which will later turn out to be the average distance between the two electrons of a COOPER pair.

Another interesting case is obtained by regarding the situation of $\varphi = 0$ at $x = 0$ and $\varphi = \varphi_0$ as $x \to \infty$. This situation resembles a boundary between normal and superconducting state, i.e. there is a magnetic field H_c in the normal region. We regard an extreme type I superconductor, in particular the penetration depth satisfies $\lambda_L \ll \xi$. We have to solve

$$-\frac{\hbar^2}{2m}\frac{\mathrm{d}^2}{\mathrm{d}x^2}\varphi - \alpha\varphi + \beta|\varphi|^2\varphi = 0. \tag{286}$$

A proper solution satisfying the boundary conditions is

$$\varphi(x) = \sqrt{\frac{\alpha}{\beta}}\tanh\left(\frac{x}{\sqrt{2}\xi}\right). \tag{287}$$

Inside the superconductor we obtain $\varphi_0 = \sqrt{\frac{\alpha}{\beta}}$ as the solution of the minimization of $-\alpha|\varphi|^2 + \frac{1}{2}\beta|\varphi|^4$. Since inside the superconductor we have $F_S = F_N - \frac{\alpha^2}{2\beta} = F_N - \frac{1}{2\mu_0}B_{ac}^2$ we obtain

$$B_{ac} = \sqrt{\frac{\mu_0\alpha^2}{\beta}}. \tag{288}$$

For a small penetration length ($\varphi \approx \varphi_0$) we obtain from the second Ginzburg - Landau equation

$$\mathbf{js} = -\frac{q^2}{m}|\varphi_0|^2\mathbf{A}. \tag{289}$$

Comparison with the Eq. (268) yields

$$\lambda_L = \sqrt{\frac{m\beta}{\mu_0 q^2\alpha}}. \tag{290}$$

We now introduce the dimensionless parameter κ:

$$\kappa = \frac{\lambda_L}{\xi} \equiv \frac{m}{\hbar q}\sqrt{\frac{2\beta}{\mu_0}}. \tag{291}$$

We now show that this parameter characterizes the transition between type I and type II superconductors. We regard a type II superconductor exposed to a magnetic field which is slightly below the critical field H_{c2}. Accordingly, we can linearize the first Ginzburg - Landau equation:

$$\frac{1}{2m}\left(-i\hbar\nabla - q\mathbf{A}\right)^2\varphi = \alpha\varphi. \tag{292}$$

The vector potential is assumed to be of the form $\mathbf{A} = Bx\mathbf{e_y}$, i.e. $\mathbf{B} = B\mathbf{e_z}$. We obtain

$$-\frac{\hbar^2}{2m}\left(\frac{\partial^2}{\partial x^2} + \frac{\partial^2}{\partial y^2}\right)\varphi + \frac{1}{2m}\left(i\hbar\frac{\partial}{\partial y} + qBx\right)^2\varphi = \alpha\varphi. \tag{293}$$

We employ the ansatz $\varphi = \exp\left[i(k_y y + k_z z)\right]\chi(x)$ and obtain

$$\frac{1}{2m}\left[-\hbar^2\frac{\mathrm{d}^2}{\mathrm{d}x^2} + \hbar^2 k_z^2 + (\hbar k_y - qBx)^2\right]\chi = \alpha\chi. \tag{294}$$

Substituting $E = \alpha - \frac{\hbar^2 k_z^2}{2m}$ and $X = x - \frac{\hbar k_y q B}{2m}$ yields

$$-\frac{\hbar^2}{2m}\frac{\mathrm{d}^2}{\mathrm{d}X^2}\chi + \frac{q^2 B^2}{2m} X^2 \chi = E\chi \tag{295}$$

This is the equation of a harmonic oscillator with frequency $\omega = \frac{qB}{m}$ and eigenvalues $E_n = \left(n + \frac{1}{2}\right)\hbar\omega$. We note that the largest value of the magnetic field is given by the lowest energy eigenvalue $E_0 = \frac{1}{2}\hbar\omega = \alpha - \frac{\hbar^2 k_z^2}{2m}$, hence:

$$B_{max} = \mu_0 H_{c2} = \frac{2\alpha m}{q\hbar}. \tag{296}$$

By use of Eqs. (291) and (288) we obtain the interesting result

$$H_{c2} = \sqrt{2}\kappa H_c. \tag{297}$$

For $\kappa > 1/\sqrt{2}$ we have $H_{c2} > H_c$ and the superconductor is of type II.

13.4 Microscopic Theories

13.4.1 BCS Theory of Superconductivity

We briefly discuss the fundamental concepts of the BCS theory of superconductivity as developed by BARDEEN, COOPER and SCHRIEFFER in 1957. The applications of BCS theory range from the description of superfluidous He^3 to type I and type II metallic superconductors, and even some high-temperature superconductors. Moreover, the BCS theory proved to be very important for our modern understanding of theoretical solid state physics since many concepts appearing in the framework of this theory reappeared in the context of numerous further effects and phenomena, such as the fractional quantum Hall effect, topological insulators or even in nuclear physics.

The basic ingredient to a successful microscopic description is the realization that at sufficiently low temperatures two electrons form an energetically favored state through electron - phonon - electron interaction, called a COOPER pair. This attractive interaction between the electrons yields a ground state which is separated from the excited states by a band gap, as experimentally observed, see Sec. 13.2.3. Also the fact that phonons play a crucial role in the formation of this ground state was observed experimentally through the isotope effect, Sec. 13.2.4. Most of the thermodynamic properties of superconductors are a direct consequence of the occurrence of a band gap, thus a profound understanding of COOPER pairs is essential in a microscopic description of superconductivity.

13.4.2 Some BCS Results

We briefly summarize some of the most remarkable results from the BCS theory

(i) Attractive interaction between electrons leads to the formation of COOPER pairs. The ground-state is separated from the excited state by an energy gap. With the help of this energy gap one can explain phenomena such as the critical field, thermal properties and electromagnetic properties.

(ii) The electron - lattice - electron interaction can be understood in an intuitive way with the help of the following simplified picture: One electron interacts with the lattice and deforms it, the second electron is affected by the lattice deformation and moves therefore in the field of the first electron. In particular, the two electrons interact through the lattice deformation. In this attractive process the total energy is lowered.

(iii) The LONDON equations, and therefore also the penetration depth as well as the coherence length, are a direct consequence of the BCS theory. Since the LONDON equations account for the MEISSNER - OCHSENFELD effect, also this experimental fact is implicitly accounted for within the microscopic theory.

(iv) It is (correctly) predicted that the transition temperature is influenced by the electron density of the orbitals at the FERMI energy of one spin, $D(\varepsilon_F)$ and the electron lattice interaction parameter V which is connected to the electrical resistance at room temperature. In particular case $VD(\varepsilon_F) \ll 1$ (V attractive) the BCS theory predicts

$$T_c = 1.14\Theta \exp\left(-\frac{1}{VD(\varepsilon_F)}\right), \tag{298}$$

where Θ is the DEBYE temperature. This relation coincides qualitatively with experimental observations. Note that this means, the higher V (means large resistance at room temperature), the more likely the material will be superconductor when cooled below T_c.

(v) The magnetic flux through a superconducting ring is quantized (see Sec. 13.4.4) and since a COOPER pair consists of two electrons, the unit of charge is $2q$. This can be accounted for in the LONDON equations and in the GINZBURG - LANDAU equations when one replaces the quantities accordingly (n_s is now the density of COOPER pairs, $q \to 2q, \dots$).

(vi) There exists a BCS groundstate: In case of a non-interacting electron system one obtains the FERMI sea as the groundstate. Arbitrarily small excitations are possible. Within the framework of the BCS theory, one obtains, that for an appropriate attractive interaction potential a superconducting groundstate, which is separated from the excited states by an energy gap E_g, is formed. The most important property of the BCS groundstate is that orbitals are occupied in pairs: for every orbital with wavevector $\mathbf{k}$ and some spin occupied the orbital with opposite spin and wavevector $-\mathbf{k}$ is also occupied. These pairs are referred to as COOPER pairs; we give a short discussion below. COOPER pairs are bosons.

(vii) The BCS theory states that superconducting band gap $\Delta(T)$ as a function of temperature is implicitly given through the solution of the following equation:

$$\frac{\Delta(T)}{\Delta(0)} = \tanh\left[\frac{T_C}{T}\frac{\Delta(T)}{\Delta(0)}\right]. \tag{299}$$

Comparison with experimental data of Ta shows perfect agreement, see Fig. 139

13.4.3 COOPER Pairs

We regard a two electron system in a cube of volume 1 and periodic boundary conditions. We write the wave function in the basis of plane wave product state:

$$\psi(\mathbf{k_1}, \mathbf{k_2}; \mathbf{r_1}, \mathbf{r_2}) = \exp\left[i\left(\mathbf{k_1}\cdot\mathbf{r_1} + \mathbf{k_2}\cdot\mathbf{r_2}\right)\right]. \tag{300}$$

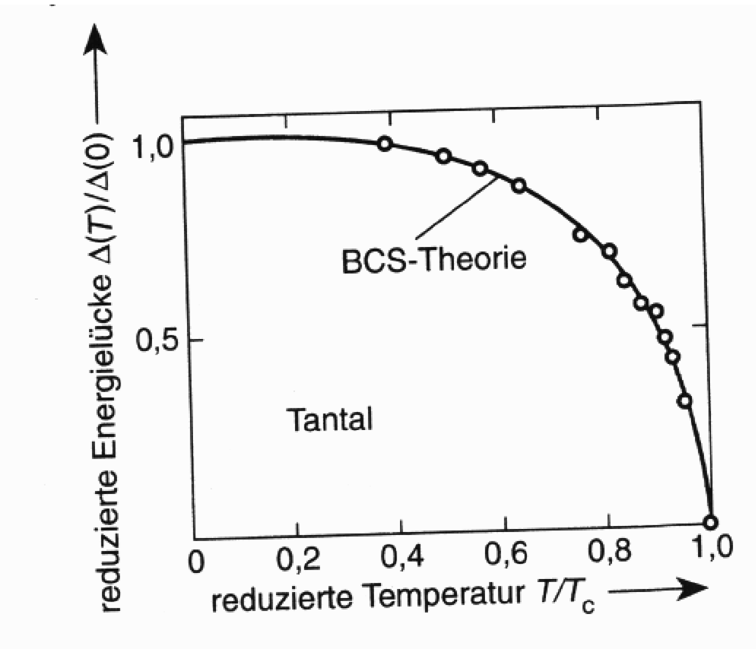

Figure 139: The superconducting band gap versus temperature. Comparison between theoretical (BCS) and experimental data for Ta.

Furthermore, we assume that the two electrons are of opposite spin. We perform a coordinate transformation according to

$$\mathbf{K} = \mathbf{k_1} + \mathbf{k_2}, \qquad \mathbf{k} = \frac{1}{2}\left(\mathbf{k_1} - \mathbf{k_2}\right) \tag{301}$$

and

$$\mathbf{R} = \frac{1}{2}\left(\mathbf{r_1} + \mathbf{r_2}\right), \qquad \mathbf{r} = \mathbf{r_1} - \mathbf{r_2}. \tag{302}$$

Consequently,

$$\psi(\mathbf{K}, \mathbf{k}; \mathbf{R}, \mathbf{r}) = \exp\left(i\mathbf{K} \cdot \mathbf{R}\right) \exp\left(i\mathbf{k} \cdot \mathbf{r}\right), \tag{303}$$

where the corresponding kinetic energy of the system is given by

$$\varepsilon_{\mathbf{K}} + E_{\mathbf{k}} = \frac{\hbar^2}{m}\left(\frac{1}{4}\mathbf{K}^2 + \mathbf{k}^2\right). \tag{304}$$

We now investigate the special case of $\mathbf{K} = \mathbf{0}$, i.e. $\mathbf{k_1} = -\mathbf{k_2}$ and expand the wave function in terms of the resulting basis functions:

$$\chi(\mathbf{r}) = \sum_{\mathbf{k}} g_{\mathbf{k}} \exp\left(i\mathbf{k} \cdot \mathbf{r}\right), \tag{305}$$

Let us introduce an interaction Hamiltonian H_I. The corresponding Schrödinger equation reads

$$\left(H_0 + H_I - \varepsilon\right)\chi(\mathbf{r}) = \sum_{\mathbf{k}'} \left[\left(E_{\mathbf{k}'} - \varepsilon\right) g_{\mathbf{k}'} + H_I g_{\mathbf{k}'}\right] \exp\left(i\mathbf{k}' \cdot \mathbf{r}\right) = 0. \tag{306}$$

Taking the scalar product with $\exp\left(i\mathbf{k}\cdot\mathbf{r}\right)$ yields

$$\left(E_{\mathbf{k}}-\varepsilon\right)g_{\mathbf{k}}+\sum_{\mathbf{k}'}g_{\mathbf{k}'}\langle\mathbf{k}\,|\,H_I\,|\,\mathbf{k}'\rangle=0. \tag{307}$$

Transforming the sum over $\mathbf{k}'$ into an integral over the energy E' gives

$$\left(E-\varepsilon\right)g(E)+\int dE'g(E')H_I(E,E')N(E')=0, \tag{308}$$

where $N(E)$ is the number of states with $\mathbf{K}=\mathbf{0}$ within the kinetic energy window of width dE' around E'. Detailed studies of the matrix elements $H_I(E,E')$ revealed that the contribution is most important in an energy range slightly above the (one electron) Fermi energy ε_F with thickness $\hbar\omega_D$, where ω_D is the Debye phonon cutoff frequency. We approximate $H(E,E')$ within this energy region by a constant, i.e.

$$H(E,E')=-V=const.\quad\text{for } E,E'\in[2\varepsilon_F,2\varepsilon_m]\quad\text{with } \varepsilon_m=\varepsilon_F+\hbar\omega_D. \tag{309}$$

Hence,

$$(E-\varepsilon)g(E)=V\int_{2\varepsilon_F}^{2\varepsilon_m}dE'g(E')N(E')=C, \tag{310}$$

with C a constant. We readily obtain

$$g(E)=\frac{C}{E-\varepsilon} \tag{311}$$

and

$$V\int_{2\varepsilon_F}^{2\varepsilon_m}dE'\frac{N(E')}{E'-\varepsilon}=1. \tag{312}$$

We now approximate $N(E')\approx N_F$ within this energy range and obtain the desired result

$$N_FV\int_{2\varepsilon_F}^{2\varepsilon_m}dE'\frac{1}{E'-\varepsilon}=N_FV\log\left(\frac{2\varepsilon_m-\varepsilon}{2\varepsilon_F-\varepsilon}\right)=1, \tag{313}$$

or with the help of $\varepsilon=2\varepsilon_F-\Delta$

$$\Delta=\frac{2\hbar\omega_D}{\exp\left(\frac{1}{N_FV}\right)-1}. \tag{314}$$

For $V>0$ (attractive interaction) the energy is lowered by excitation of a Cooper pair above the Fermi level. Here Δ is the binding energy of a Cooper pair. Within the framework of the BCS theory it is shown that this binding energy is closely related to energy gap of a superconductor.

13.4.4 Flux Quantization

In this section we aim to reproduce the result of flux quantization in a superconducting ring. Therefore we regard a gas of charged bosons (Cooper pairs). Let ψ be the pair wave function and $n = \psi\psi^* = const.$ the total number of pairs. We express ψ as

$$\psi = \sqrt{n}\exp(i\theta) \tag{315}$$

where the phase θ may be a function of local space. The particle velocity operator is given by

$$\mathbf{v} = \frac{1}{m}\left(-i\hbar\nabla - q\mathbf{A}\right) \tag{316}$$

and, consequently, the particle flux is given by

$$\psi^*\mathbf{v}\psi = \frac{n}{m}\left(\hbar\nabla\theta - q\mathbf{A}\right). \tag{317}$$

We can write the electric current density as

$$\mathbf{j} = q\psi^*\mathbf{v}\psi = \frac{qn}{m}\left(\hbar\nabla\theta - q\mathbf{A}\right). \tag{318}$$

Taking the curl of both sides of this equation yields the London equation:

$$\nabla\times\mathbf{j} = \frac{q^2n}{m}\nabla\times\mathbf{A}, \tag{319}$$

since $\nabla\times\nabla g = 0$ independent of the scalar function g. Due to the Meissner - Ochsenfeld effect we know that $\mathbf{B} = \mathbf{0}$ in the interior of the superconductor. Therefore, we have $\mathbf{j} = \mathbf{0}$ and it follows from (318) that

$$q\mathbf{A} = \hbar\nabla\theta. \tag{320}$$

We now select a closed path C through the interior of the superconductor and integrate the right hand side of (320):

$$\hbar\oint_C dl\ \nabla\theta = \hbar(\theta_2 - \theta_1), \tag{321}$$

i.e. $\hbar$ times the change of the phase when going once around the contour C. Since ψ must not change through the integration we obtain that

$$\theta_2 - \theta_1 \equiv 2\pi s, \tag{322}$$

with s some integer. For the left hand side of (320) we obtain through Stokes' theorem

$$q\oint_C dl\ \mathbf{A} = q\int_F d\mathbf{F}\cdot\nabla\times\mathbf{A} = q\int_F d\mathbf{F}\cdot\mathbf{B} = q\Phi, \tag{323}$$

the magnetic flux. Here, $d\mathbf{F}$ is an element of the area bounded by the contour C. Accordingly

$$\Phi = \frac{\hbar 2\pi s}{q} = \Phi_0 s, \tag{324}$$

with the flux quantum (referred to as fluxoid) Φ_0. Note that in the particular case of Cooper pairs we have to replace $q \to 2q$.

In type II superconductors one observes these quantized magnetic flux tubes in the Shubnikov phase. The magnetic field penetrates the superconductor and is organized in vortices. These vortices interact with each other and are rearranged in a periodic structure (like a lattice), see Fig. 140. The complete theory of type II superconductors was given by Ginzburg, Landau, Abrikosov and Gorkov.

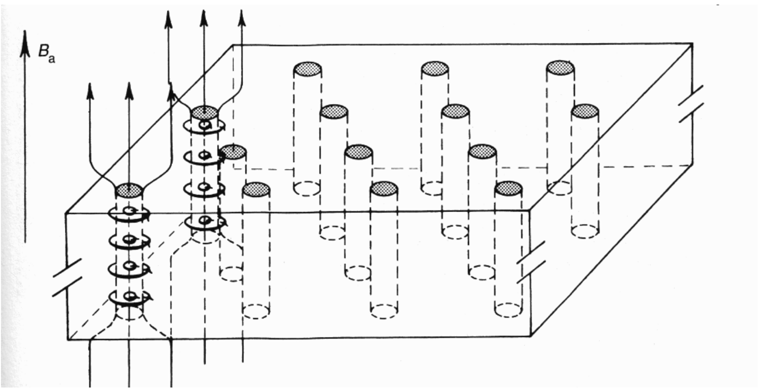

Figure 140: Schematic illustration of the flux penetration in the SHUBNIKOV phase.

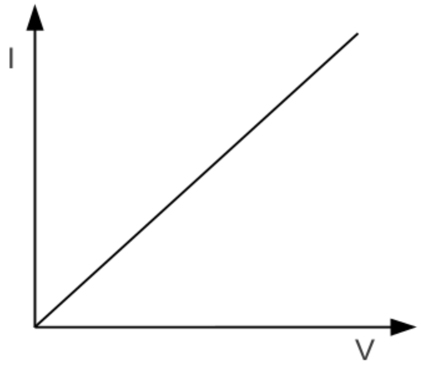

Figure 141: Schematic illustration of the IV characteristic of a tunnel barrier device, i.e. two metals separated by a thin insulator.

13.5 The JOSEPHSON Effect

13.5.1 Single Particle Tunneling

We regard the situation of two metals separated by a thin insulating layer. In the classical case, one observes tunneling through the barrier when a voltage is applied. The typical IV characteristic is of the form illustrated in Fig. 141, i.e. the current rises linearly with the applied voltage. The situation changes drastically if one of the metal plates is a superconductor, Fig. 142. This is due to the bandgap occurring in superconductors, Fig. 137. At $T = 0$ K, no current can flow until the applied voltage exceeds $V = \frac{E_g}{2q}$. At finite temperatures one observes a small current also at low temperatures due to thermal excitations of electron pairs across the bandgap.

13.5.2 The JOSEPHSON Effect

We regard two superconductors separated by a thin insulating layer. In the following ψ_1 denotes the probability amplitude on one side and ψ_2 on the other side of the insulator. We write the time

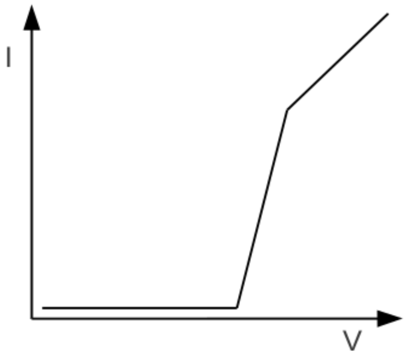

Figure 142: Schematic illustration of the IV characteristic of a superconducting tunnel barrier device, i.e. two metals separated by a thin insulator, where one of the metals is superconducting.

dependent SCHRÖDINGER equations for this problem

$$i\hbar\frac{\partial}{\partial t}\psi_1 = \hbar T\psi_2, \qquad i\hbar\frac{\partial}{\partial t}\psi_2 = \hbar T\psi_1, \tag{325}$$

where $\hbar T$ is the interaction rate between the electron pairs, referred to as electron pair coupling. Similar to Sec. 13.4.4 we write ψ_i as $\psi_i = \sqrt{n_i}\exp(i\theta_i)$. We now insert these expressions in the above equations, (325) and multiply the resulting equations with ψ_1^* and ψ_2^*, respectively. We obtain

$$\frac{1}{2}\frac{\partial}{\partial t}n_1 + in_1\frac{\partial}{\partial t}\theta_1 = -iT\sqrt{n_1n_2}\exp(i\delta) \tag{326}$$

and

$$\frac{1}{2}\frac{\partial}{\partial t}n_2 + in_2\frac{\partial}{\partial t}\theta_2 = -iT\sqrt{n_1n_2}\exp(i\delta) \tag{327}$$

where $\delta = \theta_2 - \theta_1$. We now equate the real and imaginary parts in order to obtain

$$\frac{\partial}{\partial t}n_1 = 2T\sqrt{n_1n_2}\sin(\delta) \qquad \frac{\partial}{\partial t}n_2 = -2T\sqrt{n_1n_2}\sin(\delta), \tag{328}$$

and

$$\frac{\partial}{\partial t}\theta_1 = -T\sqrt{\frac{n_1}{n_2}}\cos(\delta), \qquad \frac{\partial}{\partial t}\theta_2 = -T\sqrt{\frac{n_2}{n_1}}\cos(\delta). \tag{329}$$

In particular for $n_1 \approx n_2$, we have

$$\frac{\partial}{\partial t}(\theta_2 - \theta_1) = 0, \tag{330}$$

and

$$\frac{\partial}{\partial t}(n_2 + n_1) = 0. \tag{331}$$

Since the current is proportional to $\frac{\partial}{\partial t}n_2$ we obtain

$$J = J_0 \sin(\theta_2 - \theta_1) \tag{332}$$

where J_0 serves as a proportionality constant. Note that J_0 is also proportional to T. Hence, we obtained that there is a current flow according to the phase difference δ even if no external field is applied. This is the dc JOSEPHSON effect.

We now regard the case of an applied potential V. The equations (325) apply:

$$i\hbar\frac{\partial}{\partial t}\psi_1 = \hbar T\psi_2 - qV\psi_1, \qquad i\hbar\frac{\partial}{\partial t}\psi_2 = \hbar T\psi_1 + qV\psi_2. \tag{333}$$

We perform the same operations as above and we obtain

$$\frac{\partial}{\partial t}n_1 = 2T\sqrt{n_1 n_2}\sin(\delta) \qquad \frac{\partial}{\partial t}n_2 = -2T\sqrt{n_1 n_2}\sin(\delta), \tag{334}$$

and

$$\frac{\partial}{\partial t}\theta_1 = \frac{qV}{\hbar} - T\sqrt{\frac{n_1}{n_2}}\cos(\delta), \qquad \frac{\partial}{\partial t}\theta_2 = -\frac{qV}{\hbar} - T\sqrt{\frac{n_2}{n_1}}\cos(\delta). \tag{335}$$

Again, we assume $n_1 \approx n_2$ and obtain

$$\frac{\partial}{\partial t}(\theta_2 - \theta_1) = \frac{\partial}{\partial t}\delta = -\frac{2qV}{\hbar}, \tag{336}$$

or equivalently

$$\delta(t) = \delta(0) - \frac{2qVt}{\hbar}. \tag{337}$$

The superconducting current in this case is given by

$$J = J_0 \sin\left[\delta(0) - \frac{2qVt}{\hbar}\right]. \tag{338}$$

This is the ac JOSEPHSON effect. The current oscillates with a frequency given by $\omega = \frac{2qV}{\hbar}$. This is a very convenient method to determine ratio $\frac{e}{\hbar}$ by measuring the frequency and the voltage.

13.5.3 SQUID

A SQUID (superconducting quantum interference device) is a very precise magnetometer based on the JOSEPHSON effect. It consists of two JOSEPHSON junctions in parallel, see Fig. 143. We do not apply a voltage and we assume that a magnetic flux Φ passes through the interior of the circuit. From Sec. 13.4.4 we know that

$$\delta_a - \delta_b = \frac{2q}{\hbar}\Phi, \tag{339}$$

so that we can write

$$\delta_a = \delta_0 + \frac{q}{\hbar}\Phi, \tag{340}$$

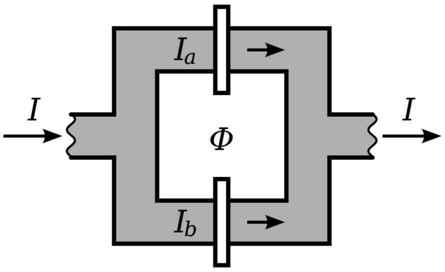

Figure 143: Schematic illustration of a SQUID.

and

$$\delta_b = \delta_0 - \frac{q}{\hbar}\Phi. \tag{341}$$

The total current in this case is given by

$$J = J_0 \left[\sin\left(\delta_0 + \frac{q}{\hbar}\Phi\right) + \sin\left(\delta_0 - \frac{q}{\hbar}\Phi\right)\right] = 2J_0 \sin(\delta_0) \cos\left(\frac{q}{\hbar}\Phi\right). \tag{342}$$

Since the current varies with the magnetic flux Φ, this is a very elegant method to measure the magnetic field.